Essays on Panel Data Prediction Models

Nandi, Shaoni

Awarding institution:
King's College London

Essays on Panel Data Prediction Models[1]

Shaoni Nandi

2023-12-19

[1]All views in this thesis belong to the author, and not to any institution she is affiliated to. All data are available in the public domain.

Abstract

Forward-looking analysis is valuable for policymakers as they need effective strategies to mitigate imminent risks and potential challenges. Panel data sets contain time series information over a number of cross-sectional units and are known to have superior predictive abilities in comparison to time series only models. This PhD thesis develops novel panel data methods to contribute to the advancement of short-term forecasting and nowcasting of macroeconomic and environmental variables. The two most important highlights of this thesis are the use of cross-sectional dependence in panel data forecasting and to allow for timely predictions and 'nowcasts'.

Although panel data models have been found to provide better predictions in many empirical scenarios, forecasting applications so far have not included cross-sectional dependence. On the other hand, cross-sectional dependence is well-recognised in large panels and has been explicitly modelled in previous causal studies. A substantial portion of this thesis is devoted to developing cross-sectional dependence in panel models suited to diverse empirical scenarios. The second important aspect of this work is to integrate the asynchronous release schedules of data within and across panel units into the panel models. Most of the thesis emphasises the pseudo-real-time predictions with efforts to estimate the model on the data that has been released at the time of predictions, thus trying to replicate the realistic circumstances of delayed data releases.

Linear, quantile and non-linear panel models are developed to predict a range of targets both in terms of their meaning and method of measurement. Linear models include panel mixed-frequency vector-autoregression and bridge equation set-ups which predict GDP growth, inflation and CO_2 emissions. Panel quantile regressions and

latent variable discrete choice models predict growth-at-risk and extreme episodes of cross-border capital flows, respectively. The datasets include both international cross-country panels as well as regional subnational panels. Depending on the nature of the model and the prediction targets, different precision criteria evaluate the accuracy of the models in out-of-sample settings. The generated predictions beat respective standard benchmarks in a more timely fashion.

Acknowledgements

I would like to express my sincere gratitude to all those who have supported me throughout my PhD journey.

First of all, I would like to extend my deepest gratitude to my primary supervisor Jack Fosten for his invaluable guidance and support during the four-year journey. His exceptional knowledge, patience, active listening, insightful comments, constructive criticism, encouragement and flexibility have shaped my research throughout my PhD journey. Some of his feedback prompted me to reflect on life as a whole and had a very profound impact on me. I am grateful that he agreed to be a co-author for the two chapters formed from parts of this thesis. I also extend my thanks to my second supervisor Martin Weale for guidance, encouragement, insightful discussions and helpful comments.

I am truly grateful to my thesis examiners, Anthony Garret and Stuart McIntyre, for dedicating their valuable time to carefully read my entire thesis. The insightful comments and stimulating discussions during the viva were truly enjoyable, and I am extremely thankful to both for their wholehearted participation and encouragement. Their comments played a significant role in improving the quality of my thesis.

I sincerely thank the Reserve Bank of India for allowing me to pursue this PhD and for providing financial support. The stimulating and challenging discussions, debates and assignments at the Bank have been the inspiration for the chapters in this thesis. I thank all of my colleagues who motivated me to embark on this journey. I very much look forward to resuming my services and serving the Bank in the near future.

I am grateful for the King's PGR International scholarship awarded by the King's

College London Centre for Doctoral Studies. I sincerely thank Goodenough College for the Barry Kanesu Memorial Scholarship during the academic year 2019–20. The scholarship was a great financial help and the vibrant community life in the college was crucial in those early days. Soon COVID19 emerged and life would have been immensely difficult without all the support, encouragement, guidance and pastoral care from Goodenough College. Thanks to Saeed Zeydabadi-Nejad for the pastoral care as warden during my stay in the International Halls.

This thesis has benefited from discussions in my upgrade viva and the following conferences and seminars: King's Business School PhD Symposia (2020,2021,2022), NBER-NSF Time Series Conference 2021, European Winter Meeting of the Econometric Society 2021, Econometric Society Winter School 2021, the International Association for Applied Econometrics Annual 2022 Conference, 42nd International Symposium on Forecasting 2022, Royal Economic Society PhD Conferences (2022 and 2023) and Money Macro and Finance Society PhD Conference 2023. I thank all the participants and the discussants for their insightful comments and interesting conversations.

I am very grateful to Christian Schumacher, Alexander Chudik, Eric Ghysels, Carlos Lamarche and Christian Brownlees for sharing the replication files for their chapters (Marcellino and Schumacher 2010; Chudik and Pesaran 2015a; Ghysels and Qian 2019; Harding et al. 2020; Brownlees and Souza 2021) which helped me to learn a lot.

My sincere thanks to Michele Piffer, Seyhun Sakalli and other participants of our Economics Reading Group for the many discussions on multiple chapters, each other's work and helpful guidance on writing and presenting. Special thanks to Anne Wilson for the writing groups and guidance.

I thank my teachers, Samarjit Das and Smarajit Bose from the Indian Statistical Institute and Biswajit Roy from Presidency College, Kolkata for their initial encouragement and enthusiasm which was crucial to starting my PhD.

I would also like take this opportunity to thank my colleagues and friends for the intellectual support and camaraderie that made the entire PhD journey enjoyable. I am particularly thankful to Linda Shuku, Richmond Egeyi and Siying Jia for the friendly

mentoring and willingness to share experiences with me. I would like to specially mention Valentina Chan and our virtual writing group with Susan Cooper, Taylor Annabell, Annelies Foccaert, Nayana Dhavan, Dushyanthy Pillai, Estelle Marie Broyer and Rendan Liu. It was such a great place for support and encouragement in this long journey. I also extend my gratitude to Catherine Lawton, Wendy Chan and Deema Aljaji. Moreover, I would also like to thank my colleagues from various U.K. universities, who enriched my journey. My thanks go to (in no particular order) Prajamitra Bhuyian, Anamitra Bhowmick, Sandipan Roy, Owen Maher, Soody Gholami, Chileshe Mabula, Carolyne M. Lunga, Fred Fischer, Ana Paola Ramos and María Soledad Larrea. Each one of them made the entire process a little bit easier and interesting. Finally I would like to specially thank Cláudia Fetter for our lovely study sessions at the Didcot library.

My heartfelt thanks to the warm and welcoming community of Didcot Parkway for accepting me into the town when I relocated from London in 2021. Throughout my stay in Didcot, I always felt at home and never alone. Whenever I encountered any problems, there was always someone to turn to. The stunning fields and natural surroundings kept me refreshed and focused on my research. As I prepare to leave Didcot and Oxfordshire, I will dearly miss this wonderful place.

My very special thanks to my dear colleague and friend Jayashree Kadkade as without her encouragement I could not have taken this giant step from Mumbai to London. Last but not the least, my deepest gratitude are with my family members, my husband Sourav and my daughter Sanchayita for their unconditional emotional support and boundless love.

Details of collaborations and publications

- Chapter 2 is a published chapter in Journal of Applied Econometrics (2023) https://doi.org/10.1002/jae.2980, jointly with Jack Fosten.
- Chapter 3 is a joint work with Jack Fosten (*submitted to the International Journal of Forecasting*).

Contents

List of Tables

List of Figures

Chapter 1

Introduction

Econometric data analysis has been historically used by policymakers to inform the decision-making process. The key aim of this PhD thesis is to understand and contribute to the advancement of research on econometric predictions useful for central banks and other policymakers focusing on issues such as monetary policy, financial stability or climate issues. The thesis focuses on two central ideas of econometric modelling: Cross-sectional Dependence (CSD) in panel data analysis and timely predictions accounting for delays in the publication of major time series. Based on the timing of prediction, we distinguish between the three terms: forecasting, nowcasting and backcasting and a substantial part of the thesis is devoted to nowcasting. The thesis is organised into six chapters: this introductory chapter is followed by four core chapters and the final sixth chapter concludes with some directions for related future research. The remainder of this chapter familiarise the reader with the main econometric concepts on which the thesis is based and then moves on to briefly introduce the core chapters.

The first main concept is panel data analysis – a growing field within econometrics with diverse applications. Panel data combines the advantages of time series and cross-sectional data and allows researchers to jointly investigate several cross-sectional units over time. A central concern of longer panels for a large number of cross-sectional units is CSD among the various units. As Chudik and Pesaran (2015b) and Pesaran (2016) describe, several real-life economic circumstances, such as omitted common effects,

spatial correlation or interactions between the panel units, may potentially cause CSD in panel datasets, even after explicitly modelling unit-specific regressors. The concept of CSD is becoming an increasingly important concern in modern macroeconometrics (see Breitung 2015) not only because of increased data availability but also due to greater economic transmission and spillovers beyond national boundaries. Some of the important examples of CSD in macroeconomics are: the impact of common shocks have been found to explain the Feldstein–Horoika puzzle (Bai 2009); the relationship between public debt expansion and economic growth (Chudik et al. 2017); propagation of global financial spillovers from Advanced Economy (AE) to Emerging Market Economy (EME) (Ahmed 2023), and so on. As the focus on regional economic data grows, econometric analysis of long panels of regional data (for example subnational data) also has received interest and it is important to account for CSD in such panels as well.

Turning now to the second principal issue – delayed release of important data series – the econometric nowcasting literature has always stressed the issue of publication lags in important data series and the consequent 'ragged edge' problem faced by policymakers. While in theory, the econometric models can be estimated with all data available, in reality, there are delays in data availability and policymakers often have to base their decisions on incomplete datasets. To illustrate the extent of lags, the advanced estimate of U.S. Gross Domestic Product (GDP) for Q2:2023 (April–June 2023) was released on 27 July,[1] the Harmonised Index of Consumer Prices (HICP) data for the EU for April 2023 was published on 17 May[2] and the data for Carbon Dioxide (CO_2) emissions for the U.S. states pertaining to the year 2018 were released at the beginning of March 2021.[3] This results in asynchronous release calendars and a 'ragged edge' in panel datasets.

Let us now turn to nowcasting. This is a term that originated in meteorological forecasting (WMO 2017) and then was adapted to economics. Historically, the term

[1] See https://www.bea.gov/news/schedule [Last accessed: 10/05/2023]

[2] See https://ec.europa.eu/eurostat/news/release-calendar?start=1684101600000&type=dayGridWeek [Last accessed: 10/05/2023]

[3] See https://www.eia.gov/environment/emissions/state/ [Last accessed: 11/11/2021]

nowcasting is used to define short-term and near-term weather predictions. In econometrics, nowcasting refers to the prediction of the variable in the current period, such as predicting the GDP of Q2:2023 while in Q2:2023, i.e. between the months of April and June of 2023. Forecasting specifically means predicting at a time prior to the target quarter – i.e., predicting Q2:2023 GDP growth in Q4:2022. Backcasting refers to predicting after the target quarter. Typically macroeconomic data have publication lags and are usually not released until a significant number of days have elapsed after the reference period. Therefore, predicting Q2:2023 GDP in July 2023 will be backcasting. Nowcasting and the staggered flow of macro data releases have gained ground in econometric literature due to their policy relevance. Policymakers need timely information which can be based only on the data that has been released and is available on the day of prediction.

Although panel data methods have been historically prevalent in the forecasting literature, they have found a place in the nowcasting and real-time econometric forecasting literature only recently. CSD, though recognised to be relevant and important has not yet been incorporated into the panel forecasting literature. This thesis contributes both to the CSD and the real-time prediction literature in the following ways. First, we develop a method to include CSD in linear Mixed-Frequency Panel Vector Autoregression (MF-PVAR) nowcasting models. Second, we extend a similar CSD framework to a panel bridge equation set-up. Subsequently, we turn our focus to panel quantile regression models and introduce CSD to a forward-looking panel quantile regression model. Finally, we propose a non-linear panel discrete choice model with a proxy to represent CSD and evaluate the model for real-time predictions. Our models target the prediction of a range of important macroeconomic and environmental variables. Specifically, we target GDP, inflation and Growth-at-Risk (GaR) which are of key importance to central banks and other economic policymakers. We also look into CO_2 emissions relevant to environmental policymakers to fulfil their carbon reduction plans. Finally, we target cross-border capital flows which are of central concern to a number of policies such as fiscal, monetary and macroprudential. In the following paragraphs,

we briefly introduce each model along with the corresponding target(s) of prediction and an indication of the key result from each of the subsequent chapters.

Chapter 2 builds a mixed-frequency panel data model for nowcasting economic variables across many countries. The model extends the MF-PVAR to allow for heterogeneous coefficients and a multi-factor error structure to model CSD. We propose a modified Common Correlated Effects (CCE) estimation technique to accommodate CSD and it performs well in simulations. The model is applied in two distinct settings: nowcasting GDP growth for a pool of advanced and emerging economies, and nowcasting inflation across many European countries. Our method is capable of beating standard benchmark models and can produce updated nowcasts whenever data releases occur in any country in the panel.

Chapter 3 proposes panel nowcasting methods to obtain timely predictions of CO_2 emissions and Energy Consumption (EC) growth across all U.S. states. This is of crucial importance not least because of the increasing role of sub-national low-carbon policies but also due to the very delayed publication of the data. Since the state-level CO_2 data are constructed from EC data, we propose a new panel bridge equation method. We use a mixed-frequency set-up where economic data are first used to predict EC growth. This is then used to predict CO_2 emissions growth while also allowing for CSD across states using estimated factors. We evaluate the model's performance using an out-of-sample forecasting study, finding gains in using timely economic data to nowcast and backcast state-level EC growth. These gains are sizeable in many states, even around two years before the data are eventually released. In predicting CO_2 emissions growth, nowcast accuracy gains are more focused on a few states although accurate nowcasts can be obtained across all states if they are made after the current year's EC data are released.

Chapter 4 re-examines the relationship between macro-financial vulnerability indicators and GaR – i.e., the tail quantiles of GDP growth and proposes an explicit incorporation of data-driven CSD using the CCE technique, with necessary modifications. Specifically, the model is an unobserved factor augmented multi-country panel

quantile regression framework. Thus, we directly account for the rising importance of international macroeconomic co-movements and commonalities. Using a long quarterly panel dataset for 24 countries, we find that including CSD enhances the model performance in both in-sample and out-of-sample evaluations. In a unique finding we note that in the presence of CSD, the indicators commonly associated with GDP catastrophes have limited significance on 5% GaR. Encouraged by superior out-of-sample performance, we analyse predicted GaR and estimate a range of measures to quantify risks. We find several meaningful signals of risk and GDP slowdowns which are relatable to observed data at various points in time. We additionally find that the factors which are used to represent the CSD determine the direction of GaR. Also, these factors have a time-varying impact – i.e., a positive role in normal times and exert further downward pull in times of distress.

Chapter 5 develops a new forecasting approach for the extreme episodes of cross-border capital flows and proposes a mixed-frequency binary choice model in a panel framework. The model predicts quarterly event probabilities using higher-frequency macro-financial predictors which are available daily and monthly. We generate a time series of out-of-sample predictions generated for each country and assess them using formal forecast verification techniques and statistical tests. We then construct a pseudo data release calendar and generate country-level sequences of predictions, each with an updated underlying information set incorporating a new data release into the mixed-frequency model. The panel model predicts with significant forecast skill [4] with respect to a random classifier – noticeably for two of the four episodes and marginally for the other two in the full information set-up. The pseudo-real-time analysis shows that the predictions can beat the random classifier and thus generate meaningful early warnings a quarter in advance of the target quarter. Accuracy remains stable as time elapses and more information becomes available.

Finally, Chapter 6 concludes the thesis with a summary of the findings and an

[4]The term forecast skill refers to accuracy of the forecasts of interest relative to suitable reference forecasts, common in the weather forecasting literature; see Murphy (1988).

exploration of potential related research ideas useful for future studies.

Chapter 2

Nowcasting from Cross-sectionally Dependent Panels

2.1 Introduction

Nowcasting has emerged as an important tool for timely policy-making, particularly by central banks who need to track key variables like GDP and inflation in real time. This is important as there is often a delay before the publication of economic data such as these. The main idea is to predict the variable of interest in a timely fashion leading up to its data release, using related available information from other higher-frequency variables. Nowcasting models have typically been developed and applied with single countries in mind using time series methods. On the other hand, this chapter builds a panel data nowcasting model when the aim is to produce nowcasts for many countries which may include both developed and emerging economies. The use of panel data can be very important in empirical settings where the number of time series observations is too low for a meaningful forecast evaluation exercise. It has also been argued that the use of pooled panel forecasts can provide accuracy gains over the use of individual time series forecasts (Baltagi 2008; Wang et al. 2019) which we look to develop in a nowcasting context.

The focus of this chapter is to develop tools for simultaneously making nowcasts of

economic series for as large a set of countries as possible, while allowing for potential heterogeneity as well as cross-country spillovers. In looking at large sets of different countries it is often necessary to focus attention on a handful of select predictor variables which are common across all countries, especially when including developing economies. Nevertheless, in our approach we can exploit the staggered flow of data releases (the 'ragged edge') across countries and across variables in updating our panel nowcasts. This differs from existing empirical nowcasting studies which have exploited the flow of data for a larger set of variables but only for an individual country or a very small number of similar countries (see Cascaldi-Garcia et al. 2023, and references therein). In making nowcasts for individual countries, our approach can also deliver more information than existing studies which have targeted global aggregate variables like GDP (Kindberg-Hanlon and Sokol 2018; Ferrara and Marsilli 2019). We can also model the inter-linkages across countries which builds on existing work which finds that international variables can improve nowcast accuracy (for example Bragoli and Fosten 2018).

We make three distinct contributions. First, we propose a mixed-frequency panel nowcasting set-up which is new to the literature and allows for errors to be dependent over the individuals in the panel. We address the mixed-frequency issue using a Mixed Data Sampling (MIDAS) approach, particularly the Unrestricted Mixed Data Sampling (UMIDAS) model (Foroni et al. 2015). We adapt this model to a potentially heterogeneous and CSD panel framework with a multi-factor error structure (Chudik and Pesaran 2015a), while also allowing for different lag structures across countries based on their ragged edge of data availability. Our method allows for full parameter heterogeneity across cross-sectional units but we can also shut down heterogeneity and pool across the panel dimension which can yield improvements in nowcast accuracy as we display in our empirical application. Among the prevalent mixed-frequency nowcasting methods (see Ghysels 2018, for a recent review), we focus on MIDAS-type nowcasting models as they have already been extended to a panel framework with encouraging results (Babii et al. 2020; Fosten and Greenaway-McGrevy 2022). We

build upon these studies by further allowing for heterogeneous parameters to reflect diverse macro-dynamics, and a factor error structure to account for CSD. The resultant model is a panel extension of the observation-driven Vector Autoregression (MFVAR) model of Ghysels (2016).

Secondly, we propose a method for obtaining feasible nowcasts given the unknown factor error structure, by suggesting a novel modification of the CCE factor estimation technique of Chudik and Pesaran (2015a) which allows it to be used for nowcasting. We use a lagged CCE approach which estimates the factors only based on the data available at the time of making the nowcast. This moves away from the original CCE method, developed with the use of contemporaneous variables in estimating the factors, which is widely used in applied causal studies but cannot be used for forecasting or nowcasting applications. The method is simple to implement using least squares estimation, and can be adapted to pooled panel least squares in cases where coefficient heterogeneity is not permitted. Simulation studies find that the Lagged Common Correlated Effects (LCCE) method performs well in terms of estimation accuracy and out-of-sample prediction, which motivates its use for estimating Panel Mixed Data Sampling (PMIDAS) nowcasting models with different lag structures determined by the ragged edge.

The third contribution is to apply our method in two distinct empirical settings: nowcasting the real GDP growth of a large set of developed and emerging economies, and nowcasting the inflation rate of European countries. In the first application we construct a panel dataset of more than 30 countries' real GDP as well as some key predictors like business surveys (manufacturing and services) and Industrial Production (IP). To assess how nowcasts evolve as we add information from across the panel, we perform a pseudo out-of-sample experiment making use of a doubly asynchronous calendar of macroeconomic releases: the data releases are staggered both across variables and across countries. This means that we end up with more nowcast updates than in many studies with single countries or only a few countries. The out-of-sample analysis uses a relatively short initial estimation time span which further motivates the panel

approach over time series methods. We make several interesting findings. Firstly, we find that our proposed PMIDAS model performs better than a simple time series autoregressive benchmark when we pool the coefficients across countries and only allow heterogeneity through fixed effects. Secondly, we find that a single business survey variable is able to deliver as good a nowcast as when using one or more other predictors. This is potentially due to their timeliness and providing good economic signal (see also Bańbura et al. 2013; Cascaldi-Garcia et al. 2023). Finally, we find that nowcasts monotonically improve across the panel as we add information across countries and variables. This shows that findings of nowcast monotonicity also hold in the panel data context in a similar way to those seen in the time series nowcasting literature (Giannone et al. 2008; Aastveit et al. 2014; Marcellino et al. 2016; Fosten and Gutknecht 2018). Our results also hold after investigating their robustness to the choice of evaluation sample and the addition of extra predictor variables.

Our second contrasting empirical application assesses how the PMIDAS model performs in nowcasting monthly inflation across a large set of European countries. We use weekly energy prices to provide a timely signal for tracking movements in inflation as in Modugno (2011, 2013). We therefore offer a new approach by nowcasting a panel of countries' inflation instead of single countries. This study is a useful contrast to the global GDP example as in this case the nowcast updating does not come from the staggered release of information across countries, it only comes from the higher frequency of the predictor. This demonstrates how our method can be applied in a variety of settings. Our findings mirror those of the GDP application, showing that our proposed method is capable of nowcasting inflation well, beating a benchmark model on average across all countries in the sample.

In relating this chapter more widely to the literature, the PMIDAS model we propose brings together two distinct strands of literature: mixed-frequency methods and panel data models with CSD. Mixed-frequency methods are widely used in macroeconometrics with various models and estimation techniques proposed (Kuzin et al. 2011; Schorfheide and Song 2015; Ghysels 2016). The literature on panel data methods has also grown

significantly over time. In particular, the large heterogeneous panel data model with a CSD multi-factor error structure has become an important tool. Pesaran (2006) introduced the CCE method of factor estimation, further developed by Chudik and Pesaran (2015a) for dynamic panel models which allows for: heterogeneous coefficients, CSD, factor error structure, and feedback between target and predictor variables. We bring these aspects together in our mixed-frequency panel nowcasting model with CSD.

This chapter also connects two related empirical strands of literature, namely cross-country macroeconomic forecasting and nowcasting. Inter-country linkages have been admitted in the forecasting literature for the past few decades; see, for instance, Canova and Ciccarelli (2004), Gavin and Theodorou (2005), Chen and Ranciere (2019) and Garnitz et al. (2019) for panel data; Chudik et al. (2016) for Global Vector Autoregression (GVAR); and Caselli et al. (2020) for density forecasting. Additionally, the recent empirical nowcasting literature has also recognised the importance of international data. Several studies find that the inclusion of international macro-data improves accuracy, for instance Schumacher (2010), Eickmeier and Ng (2011), Bragoli and Fosten (2018) and Cepni et al. (2019). Separately, inter-linkages have been incorporated into New Keynesian type macroeconomic models, which are now used extensively by policy-makers and private institutions for nowcasting as well (Hantzsche et al. 2018). The prevalence of these studies all highlight the importance of using cross-country effects in our panel nowcasting model.

The rest of the chapter is organised as follows. Section 2.2 introduces the main nowcasting model and the estimation technique. The Monte Carlo simulation is presented in Section 2.3. Sections 2.4 and 2.5 display the two different empirical applications to GDP nowcasting and inflation nowcasting. Section 2.6 concludes the chapter. Appendix A contains some of the simulation results, other charts, various additional technical details as well as and empirical results which are not included in the main chapter.

2.2 Set-up

In this section, we introduce the PMIDAS set-up for panel nowcasting allowing for heterogeneity and CCE, using mixed-frequency data with a ragged edge. We base the model on the dynamic CSD panel data model of Chudik and Pesaran (2015a) with crucial modifications for the nowcasting case as we outline below. As the model is based on unknown factors, we then set out how to obtain a feasible model which can be estimated and used for nowcasting.

2.2.1 The Nowcasting Model

We will set up the model using the case of a quarterly target variable with monthly predictors as is the case with real GDP nowcasting. However, as we show in our simulations and empirical illustrations, our set-up can easily be generalised to allow for other mixed-frequency combinations such as annual to quarterly, or monthly to weekly. Suppose we have data on the quarterly target variable of interest $y_{i,t}$ for cross-sectional units $i = 1, 2, \ldots, N$ and quarters $t = 1, 2, \ldots, T$. We also have a vector of k predictor variables measured at a higher monthly frequency which we denote $x_{i,t}^M$. We follow Ghysels (2016) and stack the three months of quarter t into the following vector for each i:

$$X_{i,t}^M = \begin{pmatrix} x_{i,t}^M \\ x_{i,t-\frac{1}{3}}^M \\ x_{i,t-\frac{2}{3}}^M \end{pmatrix} \tag{2.1}$$

which will allow us to combine the quarterly and monthly data in a MIDAS-type model. When other frequency combinations are considered, one can modify the notation and the stacked vector in equation (2.1) accordingly.

In nowcasting it is of crucial importance to take account of the ragged edge, in other words using only the recent observations available at the time of making the nowcast, which may differ across individual units, i, and across variables. Suppose we

are making a nowcast on day v of the nowcast period.[1] Then we denote d_{iv} to be the latest available quarterly lag of the target variable $y_{i,t}$ for the cross-section i on the v^{th} day of the nowcast quarter.[2] Similarly, we denote m_{iv} as the latest available monthly lag (relative to the last month of quarter t) for $x_{i,t}^M$ for cross-section i on the v^{th} day of the nowcast quarter. The value $m_{iv} = 0$ corresponds to the case where all three months of the quarter are available for the predictor variable. In other words, the date v is varied at a daily frequency in order to capture the staggered release of new monthly and quarterly information which can be used to update the nowcasts. We therefore use this notation to allow for a fully asynchronous calendar of data releases across all entities in the cross section. We also allow for the release to be staggered across the k variables in $x_{i,t}$ though we suppress this additional dependence of the lags on k to avoid notational clutter.

The main nowcasting model we consider uses this lag structure in a PMIDAS model with a multi-factor error assumption:

$$y_{i,t} = c_{vi} + \phi_{vi} y_{i,t-d_{iv}} + \beta_{vi}' X_{i,t-\frac{m_{iv}}{3}} + u_{v,i,t} \tag{2.2a}$$

$$u_{v,i,t} = \gamma_{vi}' f_t + \varepsilon_{v,i,t} \tag{2.2b}$$

where c_{vi} are individual fixed effects, ϕ_{vi} is the coefficient on the autoregressive lag, and in this quarterly to monthly example β_{vi} is a $3k \times 1$ vector of individual-specific slope coefficients on the lag of the vector described in equation (2.1).[3] The term f_t is an $m \times 1$ vector of unobserved common factors which are used to model the CSD in the error term $u_{v,i,t}$ and has loadings γ_{vi}. The parameters and error terms of the model depend on nowcast date v as the model variables are dependent on the lag structure determined by v. We specify the model with full heterogeneity of coefficients (across i)

[1] For more details on the notation used for nowcast updating, see Bańbura et al. (2013).

[2] As an example with two countries $i = 1, 2$, if $d_{1,25} = 1$ and $d_{2,25} = 2$, this implies that on day 25 of the nowcast period, the previous quarter's observation for $y_{i,t}$ has already been released for country 1 but not yet for country 2.

[3] We could, of course, include more lags of $y_{i,t}$ and more than three monthly lags of $x_{i,t}$ by adding additional terms to the right hand side of equation (2.2a). We do not write this down here to save introducing additional notation.

and note that, even with fully heterogeneous coefficients, the model still retains a panel structure through the assumed error dependence.[4] The model can be modified to have homogeneous coefficients which do not change across i. This would reduce the number of parameters to estimate and can yield forecast accuracy gains in certain scenarios (see Wang et al. 2019). This is something we will consider in our empirical study.

The model in equation (2.2a) therefore builds on the original model of Chudik and Pesaran (2015a) in two distinct ways. We firstly build in the mixed-frequency aspect which results in the panel equivalent of an unrestricted MIDAS model. This choice of model is motivated by Foroni et al. (2015) who conclude that UMIDAS performs better as compared to more complex nonlinear MIDAS models in the case that the difference in frequencies is not too high. The second key difference is the lag structure which is determined by the availability of the data, or the ragged edge. In Appendix A we provide step-by-step detail on how these modifications are made to the original set-up of Chudik and Pesaran (2015a).

Our model choice is targeted towards situations in which a relatively small number of k predictors are available in making the nowcasts. As mentioned before, this is the main focus of our first empirical application where we aim to have a large coverage of global economies for which only a few common predictors are available for a reasonable time span. Other examples of the applicability of this model include GDP nowcasting at the sub-national level where relatively few usable regional predictors are typically available (see for example Fosten and Greenaway-McGrevy 2022). Our methods therefore align more closely with the small-dimensional nowcasting literature such as bridge and MIDAS models, see Schumacher (2016) for a survey. This is in contrast to studies where a larger number of predictors are available for an individual country or a handful of developed countries (see, for instance, Cascaldi-Garcia et al. 2023) where it has become common to extract factors from those variables. This may soon

[4]These heterogeneous coefficients are assumed in Chudik and Pesaran (2015a) to follow a random coefficient model with independently and indentically distributed (i.i.d.) errors when they derive the theoretical properties of the model. In practice, we estimate these heterogeneous coefficients using an Ordinary Least Squares (OLS) regression for each cross-sectional unit.

become applicable in our context once harmonised macro datasets become available for a large range of developed and developing countries. Additionally, the modification of heterogeneous panel data models with CSD to allow for high-dimensional predictors requires theoretical development and is something which we leave for further study.

2.2.2 Estimation and Nowcasting

We firstly note that equations (2.2a) and (2.2b) can be combined to write down a model for $y_{i,t}$ as follows:

$$y_{i,t} = c_{vi} + \phi_{vi} y_{i,t-d_{iv}} + \beta'_{vi} X^M_{i,t-\frac{m_{iv}}{3}} + \gamma'_{vi} f_t + \varepsilon_{v,i,t} \tag{2.3}$$

However, we do not directly use equation (2.3) for nowcasting due to the presence of the unobserved factors f_t which we must estimate. To do so, we propose a lagged version of the CCE estimation technique of Chudik and Pesaran (2015a). We specify that the predictor variable $X_{i,t-\frac{m_{iv}}{3}}$ is also influenced by the common factor and lags of $y_{i,t}$:

$$X^M_{i,t-\frac{m_{iv}}{3}} = \kappa_{vi} + \alpha_{vi} y_{i,t-d_{iv}} + \Gamma'_{vi} f_t + \epsilon_{v,i,t} \tag{2.4}$$

where, recalling from before, a value of $m_{iv} = 0$ corresponds to the last month of the current quarter. The terms κ_{vi}, α_{vi} and $\epsilon_{v,i,t}$ are vectors and Γ_{vi} is a matrix to match the dimensions of $X^M_{i,t}$.

The role of equation (2.4) is not for use in nowcasting, as it models the high-frequency variable as a function of the low-frequency variable. Instead, it is used as a device to cast equation (2.3) into a Vector Autoregression (VAR) form based on a stacked vector:

$$z^M_{i,t,v} = \begin{pmatrix} y_{i,t-d_{iv}} \\ X^M_{i,t-\frac{m_{iv}}{3}} \end{pmatrix} \tag{2.5}$$

which resembles the approach of Ghysels (2016) where low-frequency and high-frequency

variables are stacked together. In most applications, the primary focus is on the equation for the low-frequency variable which matches what is already done in traditional single-equation MIDAS models.

Once the mixed-frequency and ragged edge are accounted for in the stacked vector in equation (2.5), the set-up becomes similar to the original Chudik and Pesaran (2015a) which also stacks the target variable with a vector of predictors. The full steps of this procedure are given in Section A.1 of Appendix A and mirror those of Chudik and Pesaran (2015a), which we omit here for the sake of brevity. Intuitively, the steps start by writing down a VAR for $z_{i,t,v}^{M}$ as a function of the unknown factors f_t. This VAR can be averaged cross sectionally and inverted to move between the factors themselves and cross-sectional averages of the $z_{i,t,v}^{M}$ variable. We show how this is done below, after making some important comments about $z_{i,t,v}^{M}$.

We note that the vector $z_{i,t,v}^{M}$ in equation (2.5) resembles the vector $z_{i,t}$ used in the CCE estimation method of Chudik and Pesaran (2015a) except for a very important difference. In our case, $z_{i,t,v}^{M}$ only includes the lags of the target and predictor variables which are actually available at nowcast date v. This means that $z_{i,t,v}^{M}$ can be used to estimate the factors in a way which is feasible on the day the nowcast is made. The original paper of Chudik and Pesaran (2015a) used contemporaneous $y_{i,t}$ and $x_{i,t}$ variables in estimating the factors which is not suitable for prediction. We therefore refer to this as lagged CCE (LCCE) estimation.

In obtaining the feasible nowcasting model for $y_{i,t}$, we use a cross-sectional (weighted) average of $z_{i,t,v}^{M}$ using a weight vector $w = (\omega_1, \omega_2, \ldots, \omega_N)'$. We define the cross-sectionally weighted average of equation (2.5) as:

$$\overline{z}_{t,v}^{M} = \sum_{i=1}^{N} \omega_i z_{i,t,v}^{M} \tag{2.6}$$

and we can use the following representation of equation (2.3):

$$y_{i,t} = c_{vi}^{*} + \phi_{vi} y_{i,t-d_{iv}} + \beta_{vi}' X_{i,t-\frac{m_{iv}}{3}}^{M} + \delta_{vi}'(L)\overline{z}_{t,v}^{M} + \varepsilon_{v,i,t} + O_p(N^{-1/2}) \tag{2.7}$$

where $\delta_{vi}(L)$ is an infinite-order lag polynomial with a form depending on the parameters of equations (2.3) and (2.4), and the $O_p(N^{-1/2})$ term is an asymptotically negligible remainder term resulting from using $\overline{z}_{t,v}^M$ in place of the factors.[5]

The final feasible nowcasting equation is based on a finite approximation of the infinite number of lags of $\overline{z}_{t,v}^M$ used in equation (2.7):

$$y_{i,t} = c_{vi}^* + \phi_{vi} y_{i,t-d_{iv}} + \beta_{vi}' X_{i,t-\frac{m_{iv}}{3}}^M + \sum_{l=0}^{p_T} \delta_{vil}' \overline{z}_{t-l,v}^M + e_{v,i,t} \tag{2.8}$$

where the overall error term $e_{v,i,t}$ in this feasible nowcasting equation contains the approximation from the lag truncation as well as from replacing the factors with $\overline{z}_{t,v}^M$.[6] The choice of the lag truncation is suggested to be $p_T = T^{1/3}$ by Chudik and Pesaran (2015a).

We finally have a model for $y_{i,t}$ which is linear in variables which are available on day v of the nowcast period. The model can be estimated by OLS and nowcasts can be feasibly obtained using the estimated coefficients and the latest available data. In the most general model described earlier with full parameter heterogeneity, OLS estimation amounts to performing one regression per cross-sectional unit. However, researchers may wish to restrict the amount of allowed heterogeneity, in which case the model can be estimated by pooled panel OLS.[7] We explore this in the empirical applications where we first obtain results under full heterogeneity using equation-by-equation OLS and then we shut down all heterogeneity except for individual-specific constants and use pooled OLS for estimation.

We can use the OLS parameter estimates to obtain a nowcast of quarter T for every cross-sectional unit i on day v of the nowcast period by estimating the conditional

[5] We note that the main interest of Chudik and Pesaran (2015a) is in demonstrating the equivalence of equations (2.3) and (2.8) and they are not *per se* concerned with consistency in estimating the 'true' factors as in studies like Bai and Ng (2002) and Stock and Watson (2002).

[6] The use of $\overline{z}_{t,v}^M$ in equation (2.8) bears resemblance to 'factor-augmented' type models, where in our case the factors are estimated across countries.

[7] In the full heterogeneity case when the number of lags is large, or if we use very high-frequency data for $x_{i,t}$, one may consider using a shrinkage estimator like ridge or Least Absolute Shrinkage and Selection Operator (LASSO) in obtaining the nowcasts.

mean of $y_{i,t}$ given all available information on day v as:

$$\widehat{y}_{i,T,v} = \widehat{c}^{*}_{vi} + \widehat{\phi}_{vi} y_{i,T-d_{iv}} + \widehat{\beta}'_{vi} X^{M}_{i,T-\frac{m_{iv}}{3}} + \sum_{l=0}^{p_T} \widehat{\delta}'_{vil} \overline{z}^{M}_{T-l,v} \tag{2.9}$$

where, as written here, if one decides to impose some homogeneity on the coefficients and pool the model, then pooled panel OLS estimates can be used in equation (2.9) to obtain the nowcasts.

2.3 Monte Carlo Simulations

In this section, we carry out Monte Carlo simulations using the model described so far to assess the performance of our LCCE estimation strategy where we modify the CCE estimation approach of Chudik and Pesaran (2015a) for use in nowcasting. Our simulations are based on the model described in equations (2.3) and (2.4). However, for simplicity and tractability in the simulations, we ignore the presence of the ragged edge in the data and assume there is only a single nowcast date for which the available lags are $d_{iv} = 1$ and $m_{iv} = 0$. In other words, we assume that the previous lag is available for the target variable along with the current period for the higher frequency predictor. We will maintain the quarterly-to-monthly frequency mix (we denote the ratio of high to low frequency as $q = 3$) in the baseline simulations but we will also check how the results hold with a frequency mix of $q = 4$ which could represent an annual-to-quarterly or monthly-to-weekly frequency mix.

2.3.1 Set-up

We generate a panel dataset of dimensions $N \times T$ from model equations (2.3) and (2.4) with $d_{iv} = 1$ and $m_{iv} = 0$.[8] We choose the parameter values to make the simulated series resemble macroeconomic growth rates, as well as being guided by the parameter

[8]Equations (2.3) and (2.4) with $d_{iv} = 1$ and $m_{iv} = 0$ in fact match equations (A.1a), (A.1b) and A.1c in Appendix A where we abstract from the ragged edge.

choices used by Chudik and Pesaran (2015a). We fix the number of regressors to be $k = 1$ and let the regression coefficients in β_i be i.i.d.$U[0, 0.4]$ across i. The fixed-effects terms c_i and κ_i are assumed to be i.i.d.$U[-1, 1]$. The values of ϕ_i and α_i are chosen as i.i.d.$U[0, 0.4]$ and i.i.d.$U[0, 0.25]$ respectively. The error component $\varepsilon_{i,t}$ in equation (2.3) (now without a v subscript due to the absence of the ragged edge in the simulations) is generated as i.i.d.$N(0, 1)$ and the unobserved common factors f_t are generated as independent stationary Autoregressive (AR)(1) processes as below:

$$f_{tl} = \rho_f f_{t-1,l} + \xi_{tl}, \tag{2.10}$$

where $\rho_f = 0.25$, $\xi_{tl} \sim N(0, 1)$ for $l = 1, 2, \ldots, m$ and $t = 1, 2, \ldots, T$ and we consider $m = 2$ factors here. The loadings on both factors are generated as i.i.d.$N(0.25, 0.1)$ for y and i.i.d.$N(-1, 0.1)$ and i.i.d.$N(1, 0.1)$ for x for the first and second factor respectively. The error component $\epsilon_{i,t}$ in equation (2.4) is also generated as a stationary AR(1) process as:

$$\epsilon_{i,t} = \rho_\varepsilon \epsilon_{i,t-\frac{1}{q}} + \eta_{i,t}, \tag{2.11}$$

where $\rho_\epsilon = 0.22$ and $\eta_{i,t}$ is i.i.d.$N(0, 1)$. We use an initial 100 observations as burn-in. The value of p_T, the lag truncation parameter is selected at $T^{\frac{1}{3}}$, as recommended by Chudik and Pesaran (2015a). We will look at results over a variety of sample sizes $N, T \in \{50, 100, 150, 200\}$. We let M denote the number of Monte Carlo replications, which is set at $M = 1000$.

We focus on two different aspects of results based on this data generating process. We firstly assess the estimation of the parameters in the main nowcasting equation (in other words ϕ_i and β_i), where we compare our LCCE method to the original CCE method where contemporaneous $y_{i,t}$ is used in estimating the factors. This is to verify that we do not lose a lot of estimation accuracy by using LCCE rather than CCE, which we have to do in order to make nowcasting feasible. Since we allow heterogeneity

in the parameters across i, we first define the following mean group parameters:

$$\phi = \frac{1}{N}\sum_{i=1}^{N}\phi_i \, , \beta^{(j)} = \frac{1}{N}\sum_{i=1}^{N}\beta_i^{(j)} \tag{2.12}$$

where the superscript j on $\beta_i^{(j)}$ indexes the element of the vector β_i and we recall that the parameters no longer depend on v as we abstract from the ragged edge here. We will analyse the average (over the replications) absolute deviation of the estimated mean group parameters from the actual parameter value. The use of the absolute bias is slightly different to the criterion used in the literature on CCE estimation (see Pesaran 2006; Chudik and Pesaran 2015a), where the actual value of the bias is used and the exact sign is analysed. However, in this chapter the main focus is on nowcasting, so the forecast efficiency is of primary interest and the sign of any bias is not important.

The second aspect of the results we focus on is the out-of-sample performance of the PMIDAS model. In this regard, we wish to see if the additional complexity of the PMIDAS model (in terms of parameters and factors to estimate) introduces unwarranted forecast uncertainty over a simpler benchmark time series AR(1) model which may also be a good approximation for the serially dependent data we generate. To analyse out-of-sample performance we split the dataset into two parts in the time dimension, the first being used for model estimation and the latter for out-of-sample forecasting. Let R and P denote the window length for estimation and evaluation samples respectively. The entire time period covered by the panel is therefore split as $T = R + P$. We use a recursive window starting with R estimation observations, producing the nowcast and then increasing the estimation window by one observation at a time (see West 1996). As in Hansen and Timmermann (2012), the split point can sometimes affect the out-of-sample results. To mitigate the issue, three different splits are considered: $P = 0.2T$, $P = 0.3T$ and $P = 0.5T$. Thus, we ensure that our forecast evaluation results are not dependent on the choice of split points.

The measure of accuracy we use is the Root Mean Square Forecast Error (RMSFE)

as defined below:

$$RMSFE = \frac{1}{N}\sum_{i=1}^{N}\sqrt{\frac{1}{P}\sum_{t=R}^{T}\hat{e}_{i,t}^{2}} \tag{2.13}$$

where the forecast error $\hat{e}_{i,t}$ is the difference between $y_{i,t}$ and the forecast defined in equation (2.9). The statistic in equation (2.13) used in this panel setting gives us a single statistic for the average RMSFE across all individuals in the panel.

2.3.2 Results

Table 2.1 summarises the results for the absolute bias for the two estimation techniques under consideration. The figures represent the mean absolute bias. The panels from top to bottom summarise the results for ϕ followed by the individual parameters in the vector β. The results show that absolute biases in both the CCE and LCCE estimates are very small and diminish further towards zero at higher panel dimensions. For smaller panels, the bias in the autoregressive parameter ϕ is marginally higher in both CCE and LCCE when compared with those of the β coefficients.[9]

The difference in bias from the two estimation methods is negligible for all panel dimensions and converges to zero for larger panels. This is confirmed graphically by Figures A.1 to A.4 in Appendix A.2 which depict the distribution of the difference in the bias between the two methods, showing that it vanishes to zero with the panel size. Overall this means that the modification to use LCCE estimation does not have a substantial impact on the parameter estimates in the model, while the advantage of the lag structure we deploy in LCCE is that it can be used for forecasting and nowcasting. The bias results remain similar when we move from the frequency mix $q = 3$ to $q = 4$ which can be seen from Table A.1 and Figures A.5 to A.9 in Appendix A.

Turning now to the forecast performance of the PMIDAS model estimated by LCCE. Here our aim is to verify that the estimation of the additional factors and parameters

[9]We note that the bias in ϕ does not improve substantially with N, only with T, which mirrors the findings of Chudik and Pesaran (2015a).

Table 2.1: Simulation Results – Absolute Bias in LCCE and CCE – $q = 3$

	CCE				LCCE			
N/T	**50**	**100**	**150**	**200**	**50**	**100**	**150**	**200**
				ϕ				
50	0.0589	0.0266	0.0179	0.0127	0.0519	0.0243	0.0167	0.0118
100	0.0607	0.0255	0.0168	0.0120	0.0534	0.0238	0.0155	0.0112
150	0.0612	0.0272	0.0172	0.0122	0.0548	0.0251	0.0161	0.0114
200	0.0598	0.0265	0.0173	0.0121	0.0533	0.0245	0.0162	0.0113
				$\beta^{(0)}$				
50	0.0217	0.0134	0.0106	0.0085	0.0215	0.0148	0.0128	0.0109
100	0.0155	0.0093	0.0072	0.0063	0.0159	0.0108	0.0087	0.0081
150	0.0128	0.0073	0.0061	0.0049	0.0126	0.0082	0.0076	0.0062
200	0.0111	0.0067	0.0054	0.0043	0.0113	0.0072	0.0064	0.0056
				$\beta^{(1)}$				
50	0.0229	0.0136	0.0108	0.0092	0.0227	0.0156	0.0132	0.0114
100	0.0160	0.0096	0.0075	0.0065	0.0161	0.0107	0.0092	0.0082
150	0.0133	0.0080	0.0061	0.0051	0.0135	0.0090	0.0074	0.0068
200	0.0121	0.0067	0.0053	0.0045	0.0121	0.0074	0.0065	0.0058
				$\beta^{(2)}$				
50	0.0226	0.0136	0.0108	0.0087	0.0227	0.0148	0.0133	0.0113
100	0.0164	0.0096	0.0077	0.0063	0.0166	0.0109	0.0092	0.0083
150	0.0129	0.0075	0.0061	0.0051	0.0129	0.0086	0.0072	0.0065
200	0.0109	0.0069	0.0054	0.0044	0.0111	0.0078	0.0065	0.0057

Notes: The numbers in this table are the absolute biases in the estimates of the key model parameters estimated using two methods, LCCE and CCE, across different sample sizes.

in our panel nowcasting model does not harm forecast performance relative to a smaller naïve time series AR(1) model in this simulated set-up. The results are summarised in Table 2.2 which displays the RMSFE of the PMIDAS model relative to the time series AR(1) benchmark. Figures less than one indicate superior forecast performance of the PMIDAS model. Here we present results for the frequency mix $q = 3$ which represents the most common scenario of GDP nowcasting, as in our first empirical application, where the objective is to nowcast quarterly GDP using monthly information. However we also have results for $q = 4$ in Appendix A, which is the frequency mix we use in our second empirical application on monthly inflation nowcasting using weekly data.

The main conclusion is that the out-of-sample RMSFE is of our PMIDAS model is clearly lower than that of the time series AR(1) benchmark across sample sizes and

sample splits. We also see that the gain against the benchmark grows with the sample size T, even in fairly modest sample sizes. This indicates that the estimation of the factors and additional parameters does not harm the predictions relative to a simple time series AR(1) model which might be considered a good approximation in settings such as these with serial dependence. The findings remain very similar across the different sample splits we consider, with the exception of the lowest sample size $T = 50$ and a sample split of 50% where the AR(1) has similar RMSFE, which is due to the very low number of in-sample periods used for model estimation. We also show that the results are similar when we change the frequency mix from $q = 3$ to $q = 4$ which can be seen in Table A.2 in Appendix A.

Table 2.2: Simulation Results – Forecast Accuracy of PMIDAS Relative to AR(1) Benchmark – $q = 3$

	20%				**30%**				**50%**			
N/T	**50**	**100**	**150**	**200**	**50**	**100**	**150**	**200**	**50**	**100**	**150**	**200**
50	0.9143	0.8156	0.7877	0.7688	0.9442	0.8249	0.7884	0.7738	0.9864	0.8318	0.7931	0.7773
100	0.9172	0.8144	0.7854	0.7687	0.9446	0.8248	0.7875	0.7718	0.9875	0.8328	0.7922	0.7762
150	0.9216	0.8158	0.7878	0.7693	0.9489	0.8250	0.7886	0.7733	0.9911	0.8310	0.7925	0.7769
200	0.9166	0.8135	0.7866	0.7673	0.9445	0.8231	0.7883	0.7715	0.9882	0.8305	0.7926	0.7763

Notes: This table represents the relative RMSFE of PMIDAS with mixed-frequency data, resembling a monthly to quarterly frequency mix. Figures less than one indicate superior performance of the PMIDAS model as compared to a time series AR(1) model. Results are shown for sample split ratios for P equal to 20, 30 and 50% of the total sample.

2.4 Empirical Application I: Global GDP Nowcasting

In this section, we apply the panel nowcasting techniques developed in this chapter to predict the quarterly real GDP growth rate of a large panel of advanced and emerging economies using timelier monthly economic activity. The main advantage of our study relative to the existing literature is that we make nowcasts for a large number of individual countries and not just of aggregate global GDP as in studies such as Ferrara and Marsilli (2019). Our study also looks at a wider spread of countries than the related study of Cascaldi-Garcia et al. (2023) which focusses on a handful of European countries.

2.4.1 Data and Set-up

Data

The target variable is the annual year-on-year (y-o-y) growth rate of quarterly GDP in constant national prices. The y-o-y growth rate is widely used by many policymakers both in developed and emerging economies and is also useful for those countries which do not report seasonally adjusted quarterly figures. However we will also compare our results when using quarter-on-quarter (q-o-q) growth rates which are widely used in academic studies. We predict real GDP growth using a business survey (manufacturing) index in our baseline model, and will also explore the results using various combinations of other predictors including business survey (services) and an IP index. The focus on survey indicators is important due to their timeliness in capturing near-term economic outlook. These types of predictors are commonly used in existing nowcasting studies (for instance Marcellino and Schumacher 2010; and Schumacher 2016, for MIDAS and bridge equation models; and Giannone et al. 2008, for dynamic factor models). These particular series are also chosen for their availability for a large number of countries.

The dataset is sourced from the Organisation of Economic Co-operation and

Development (OECD) Main Economic Indicators (MEI), covering 37 member countries and selected non-member partners. We consider the final vintage for the historical data as the real time data are not available for most of the countries we consider. The dataset covers a large share of global GDP, with member countries accounting for almost 50% (OECD 2020) and includes some emerging economies with large global GDP shares such as India and China. The list of countries included in our sample can be found in Table 2.3.

There is some variation in the availability of data series across countries. The balanced panel database for GDP with manufacturing business surveys starts from January 2001 and ends in March 2020, which totals $T = 77$ quarters, i.e. 231 months of data. There are 34 available countries consisting of 23 AEs and 11 EMEs.[10] The business survey for services, however, is only available for 21 European economies (including the the U.K.) which starts in 2003 as this enables the inclusion of 8 additional countries into the panel. Other components of the business surveys have even lower availability.[11] For IP there are 35 countries, with 22 AEs and 13 EMEs. After examining all series for stationarity, the business survey variables are left in levels and IP is transformed using growth rates.[12]

Figure 2.1 summarises the distribution in GDP growth and the monthly predictors across the OECD countries for the last two decades. There is evidence of a broad common time pattern as well as some variation across countries. The dispersion of growth rates among countries increased during the Global Financial Crisis (GFC) years (2008–10) and continued for some time. This was followed by a period of very low variation in growth among countries. For the monthly predictors IP and business surveys also we notice a dispersion within the countries along with a broadly common

[10]The classification of AE and EME is as per IMF (2021).

[11]It is challenging to obtain other high-frequency indicators harmonised across countries that are available in a timely fashion. Other variables such as building permits and commercial vehicle sales were explored. However, there are significant publication lags of more than a year in many countries and so we focus our attention on the series mentioned previously.

[12]Until December 2018, the OECD used to publish seasonally adjusted figures for all series and countries. Most of the series are taken directly into the final dataset, as they are seasonally adjusted from the source entirely. IP data for India and Chile are adjusted using the X-13 algorithm.

Table 2.3: Country Coverage

Variable	***N***	**Country Names**
Business Surveys – Manufacturing	34	Australia, Austria, Belgium, Canada, Czech Republic, Denmark, Finland, France, Germany, Greece, Hungary, Ireland, Italy, Japan, Luxembourg, Mexico, Netherlands, New Zealand, Norway, Poland, Portugal, Spain, Sweden, Switzerland, Turkey, United Kingdom, United States, Brazil, Estonia, India, Israel, Slovenia, Latvia, Lithuania
Business Surveys – Services	21	Austria, Belgium, Czech Republic, Denmark, Finland, France, Germany, Greece, Hungary, Ireland, Italy, Netherlands, Poland, Portugal, Spain, Sweden, United Kingdom, Estonia, Slovenia, Latvia, Lithuania
Industrial Production	35	Austria, Belgium, Canada, Czech Republic, Denmark, Finland, France, Germany, Greece, Hungary, Ireland, Italy, Japan, Korea, Luxembourg, Mexico, Netherlands, Norway, Poland, Portugal, Slovak Republic, Spain, Sweden, Turkey, United Kingdom, United States, Brazil, Chile, Estonia, India, Israel, Slovenia, Latvia, Lithuania, Costa Rica

Notes: The table lists the countries taken in the sample for each predictor variable.

time path. These monthly variables seem to track the time path of GDP, which reinforces their suitability as GDP predictors.

Pseudo Out-of-Sample Set-up

To evaluate the performance of the PMIDAS model using real GDP and the monthly predictors detailed earlier, we perform a pseudo out-of-sample experiment using a recursive estimation scheme. As in the simulation section, we split the full sample into $T = R + P$ where the evaluation window, P, is set to be equal to $P = 0.3T$ so that 30% of the available sample is retained for evaluation. For each quarter in the evaluation sample, the nowcasts are computed for each day during a time window of 155 days from the start of the nowcast quarter. Consequently, this includes backcasting from the 91st day of the quarter onward. By the end of the window of 155 days, official GDP figures are available for the majority of the countries under consideration.

We construct a pseudo-calendar to track the releases for all variables in the dataset. For the GDP and IP variables, this is constructed by replication of the average release day in the four quarters of 2018. Similarly, for the survey data the approximate release

Figure 2.1: Cross-country Distribution of Real GDP Growth and Predictors Across Time

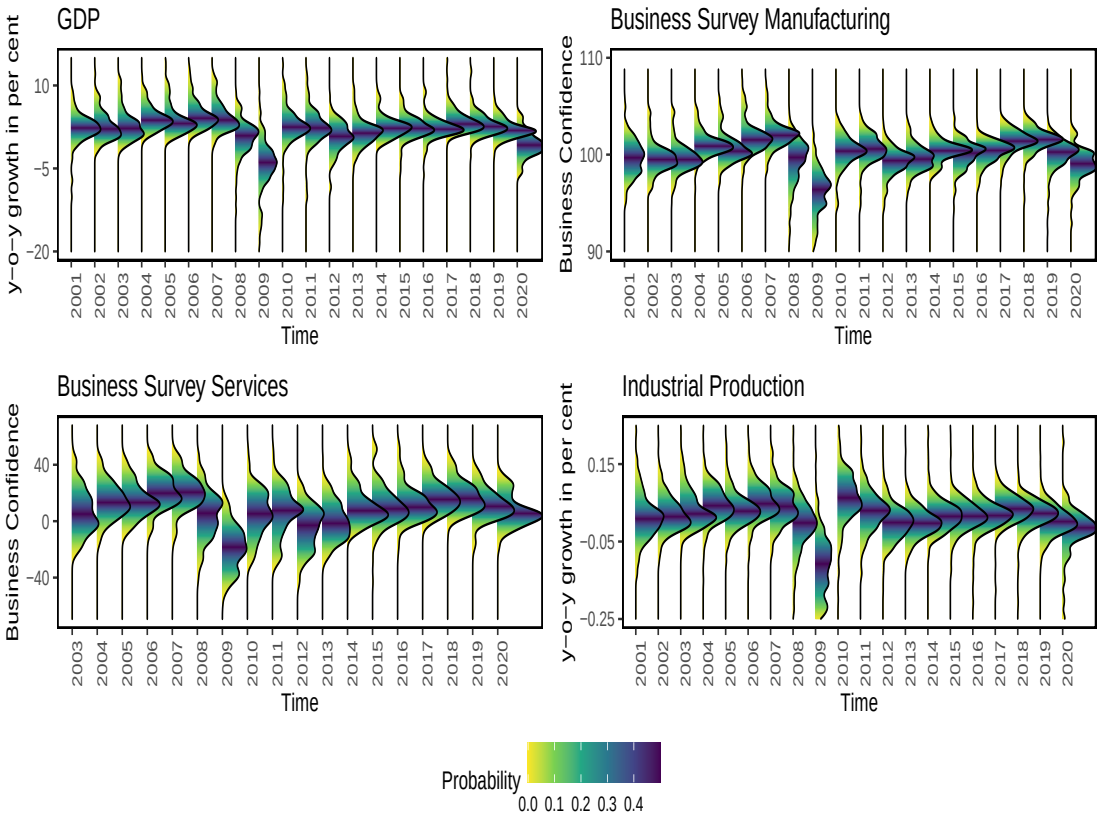

Notes: For each year on the horizontal axis, the cross-country distribution is displayed, with colours shaded from yellow to blue in order of low to high occurrence probability.

date was analysed at the end of the sample and replicated for all of the years in the evaluation window. All months are assumed to have 30 days and accordingly the quarters consist of 90 days uniformly. Figures A.10a, A.10b and A.10c in Appendix A.4 present the average lags considered for GDP, Business Survey Manufacturing (BSM) and IP respectively. The services survey data are assumed to be available uniformly on day 21 of the previous month.

At each period in the nowcast evaluation exercise, we first use the pseudo-calendar to assess which lags are available for every country. This determines the exact lag specification of the nowcasting model in equation (2.8).[13] Then the model is estimated

[13]The number of lags is also as in equation (2.8) where we do not consider further lags of $y_{i,t-d_{iv}}$

and the nowcasts are obtained for every country. This is done for each of the 155 days of the nowcast and backcast period, for each of the P evaluation quarters we consider. For every day v in the nowcast period, we can obtain the RMSFE by individual country i as follows:

$$RMSFE_{v,i} = \sqrt{\frac{1}{P}\sum_{t=R}^{T} \hat{e}_{v,i,t}^2} \tag{2.14}$$

where $\hat{e}_{v,i,t}$ denotes the prediction error from the PMIDAS model on nowcast day v for country i in quarter t (with a similar statistic being used for the benchmark model). We will assess the distribution of these individual RMSFEs as well as using the average across all countries in a similar way to equation (2.13) from the simulation section.

2.4.2 Main Results

In this section, we present the nowcast performance of the PMIDAS model for both the y-o-y and q-o-q target variables using the BSM variable as the baseline case. Although we allow for possibly heterogeneous coefficients in the nowcasting model in equation (2.8), an interesting empirical question is whether pooling can produce better nowcasts. We therefore also produce results where we impose homogeneity on all of the slope coefficients in equation (2.8) while we still have individual-specific fixed effects to allow heterogeneity. We will compare the results of these methods to the time series AR(1) benchmark model. As mentioned, we compute the nowcasts on a daily basis for 155 days from the beginning of the nowcast period and we will track how the model performance changes as we add new information.

The main results using the BSM data are presented in Tables 2.4 and 2.5 which

and $X^M_{i,t-\frac{m_{iv}}{3}}$ and where the lag truncation of the factors is $p_T = T^{1/3}$ as detailed before. Although some methods have proposed panel forecast lag selection methods in the presence of fixed effects nuisance parameters (Lee and Phillips 2015) and CSD (Greenaway-McGrevy 2019), these are not applicable in the current context with potential parameter heterogeneity and factors. In previous versions of the chapter we also experimented with the use of machine learning methods like LASSO and the Elastic Net in order to perform shrinkage and lag selection, motivated by other studies using this in the MIDAS context (Siliverstovs 2017; Xu et al. 2018; Babii et al. 2020).

display the y-o-y and q-o-q results. The numbers represent the quantiles (across countries) of the RMSFE of each model on different nowcast days. Starting with the y-o-y results in Table 2.4, the most striking finding is that the model which has uniformly lowest RMSFE across all nowcast dates is the proposed PMIDAS model when pooling is used with equal slopes across countries. In particular, we see gains relative to the time series AR model, which holds across the 25%, 50% and 75% quantiles. On the other hand, the fully heterogeneous model does not perform as well as the AR model. This indicates that the question of to 'pool or not to pool', as put by Wang et al. (2019), is that nowcast performance is improved when pooling across this sample of global economies. This result is mirrored when looking at the q-o-q results in Table 2.5 where we see that the best method across nowcast days and quantiles is the pooled PMIDAS model, whereas allowing full parameter heterogeneity leads to worsening even relative to an AR benchmark. Overall, these results lend evidence in favour of the mixed-frequency panel data approach, in a similar way to findings of Fosten and Greenaway-McGrevy (2022) and Babii et al. (2020) although with different applications. The findings are also in favour of the use of panel models for forecasting in general, see Baltagi (2008), where in this case the panel dimension is especially useful when the model is pooled across countries.

Table 2.4: GDP Nowcast RMSFE by Quantile – y-o-y

	PMIDAS						Benchmark (BM)		
	Pooled			Not Pooled			Time Series AR		
Days	**25%**	**50%**	**75%**	**25%**	**50%**	**75%**	**25%**	**50%**	**75%**
1	0.7850	1.0568	1.3127	1.0785	1.3658	1.6879	0.9865	1.1307	1.4636
16	0.7956	1.0440	1.3373	1.0785	1.3658	1.6879	0.9865	1.1307	1.4636
31	0.7265	1.0124	1.3647	1.0657	1.3525	1.5683	0.9082	1.0642	1.3018
46	0.6570	0.9127	1.1834	1.0088	1.2610	1.4927	0.8866	1.0487	1.2867
61	0.6146	0.8146	1.0767	0.9293	1.1573	1.4804	0.8115	0.9249	1.2867
76	0.5597	0.7427	1.0269	0.7460	0.9618	1.2776	0.7627	0.9077	1.2550
91	0.5512	0.7323	1.0013	0.7376	1.0246	1.2659	0.7327	0.8952	1.2550
106	0.5443	0.7293	1.0273	0.7376	1.0246	1.2659	0.7327	0.8952	1.2550
121	0.4043	0.6249	0.9947	0.4600	0.7054	1.0614	0.4745	0.7627	1.0487
136	0.0000	0.0000	0.7990	0.0000	0.0000	1.0470	0.0000	0.0000	0.8324
151	0.0000	0.0000	0.0000	0.0000	0.0000	0.0000	0.0000	0.0000	0.0000

Notes: The table reports the quantiles across countries of RMSFE for each method. We display two nowcasts per month of the nowcast period. The single predictor variable used is the BSM indicator. The RMSFE drops to zero after a country's GDP data are released, so all displayed quantiles have a value of zero on day 151 of the nowcast period.

Table 2.5: GDP Nowcast RMSFE by Quantile – q-o-q

	PMIDAS						BM		
	Pooled			Not Pooled			Time Series AR		
Days	**25%**	**50%**	**75%**	**25%**	**50%**	**75%**	**25%**	**50%**	**75%**
1	0.4310	0.5448	0.7014	0.7127	0.8975	1.2539	0.5950	0.7355	1.0317
16	0.4386	0.5425	0.7223	0.7127	0.8975	1.2539	0.5950	0.7355	1.0317
31	0.4457	0.5446	0.7284	0.7317	0.8897	1.2474	0.5950	0.7323	1.0317
46	0.3966	0.5494	0.6674	0.6824	0.8863	1.2466	0.5885	0.7323	0.9823
61	0.4006	0.5463	0.6619	0.7200	0.9313	1.2460	0.5885	0.7394	0.9823
76	0.3816	0.5416	0.6728	0.6466	0.7207	1.1244	0.5885	0.7416	0.9823
91	0.4215	0.5777	0.7000	0.6327	0.7477	1.0849	0.5885	0.7416	0.9823
106	0.4239	0.5713	0.7007	0.6327	0.7477	1.0849	0.5885	0.7416	0.9823
121	0.3166	0.5137	0.6673	0.3224	0.6433	0.8061	0.3797	0.6138	0.8046
136	0.0000	0.0000	0.5729	0.0000	0.0000	0.7314	0.0000	0.0000	0.7416
151	0.0000	0.0000	0.0000	0.0000	0.0000	0.0000	0.0000	0.0000	0.0000

Notes: See notes for Table 2.4.

In order to visualise the behaviour of the RMSFE across all days of the nowcast period, Figures 2.2 and 2.3 plot the mean of the RMSFE across all countries for each of the 155 nowcast days, for the same models as in Table 2.5. These results confirm that, on average, the pooled version of the PMIDAS model has better performance than the AR model and the version of the model with fully heterogeneous coefficients. Importantly, the plots help to reveal how the methods behave as we sequentially add more information across countries and variables. Indeed, from Figure 2.2 it seems that the average RMSFE for the y-o-y GDP growth target is monotonically falling as we add information. Therefore this panel model, like with the time series studies mentioned before, improves as we take into account more information as it becomes available during and beyond the nowcast quarter. For the q-o-q target, the results are slightly weaker, showing only moderate improvements in the pooled PMIDAS approach at the beginning of the nowcast period before RMSFE flattens until near the end of the nowcast period.

Figure 2.2: GDP Nowcast Average RMSFE – y-o-y

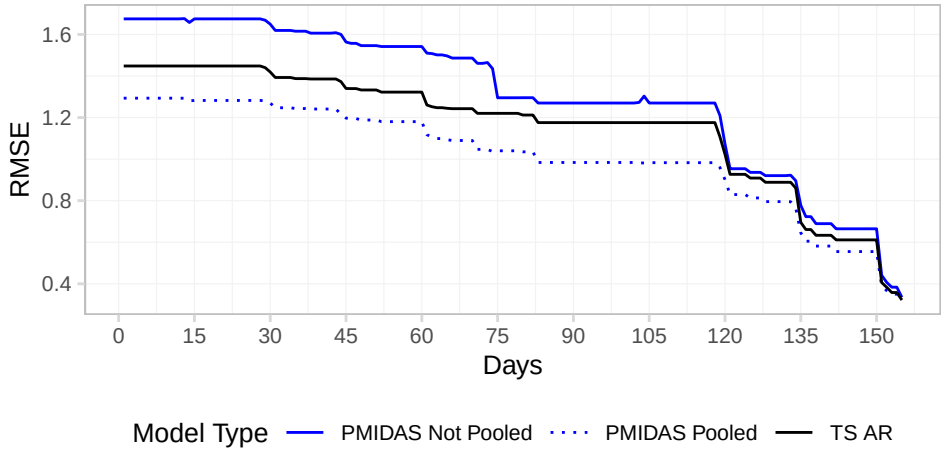

Notes: The figure plots the mean of RMSFE across all countries on each of the 155 days in the nowcast period. The single predictor variable used is the BSM indicator.

Figure 2.3: GDP Nowcast Average RMSFE – q-o-q

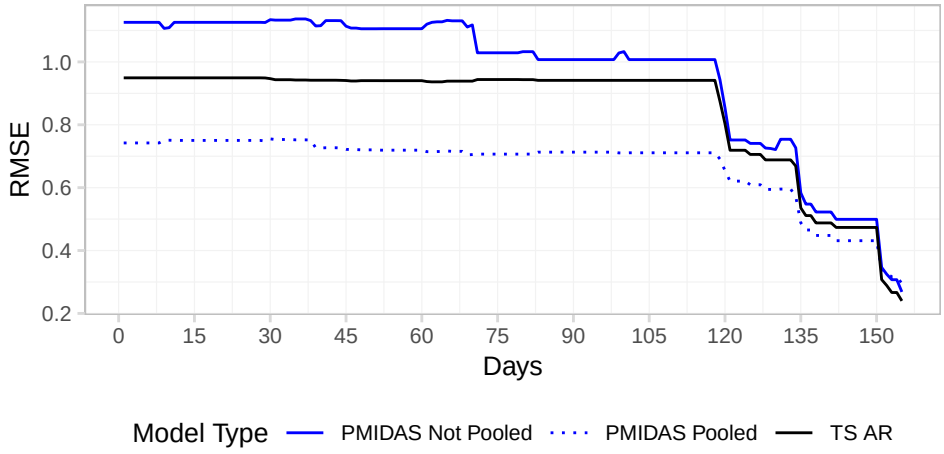

Notes: See notes for Figure 2.2.

2.4.3 Further Results

The results in the previous section focussed on the PMIDAS model when using the BSM variable as the sole predictor. It is important to assess how the PMIDAS model performs when changing to use other monthly predictors, and to allow for multiple predictor variables. To do this we employ the two other variables mentioned earlier:

Business Survey Services (BSS) and IP. In order to obtain a common sample across all variables we have to drop the number of countries to 19 so the results are based on a smaller sample than those in the previous section. We obtain results for the single-variable models as well as the other combinations of two and three variables. Figures 2.4 and 2.5 display the RMSFE for the pooled PMIDAS model across the various combinations of variables in the model. The results show that, while the three single-variable models all perform quite similarly, as soon as the number of variables included in the model increases the nowcast performance worsens.[14] This is likely due to the additional burden of parameter estimation.

Figure 2.4: GDP Nowcast Average RMSFE, y-o-y – Additional Predictors

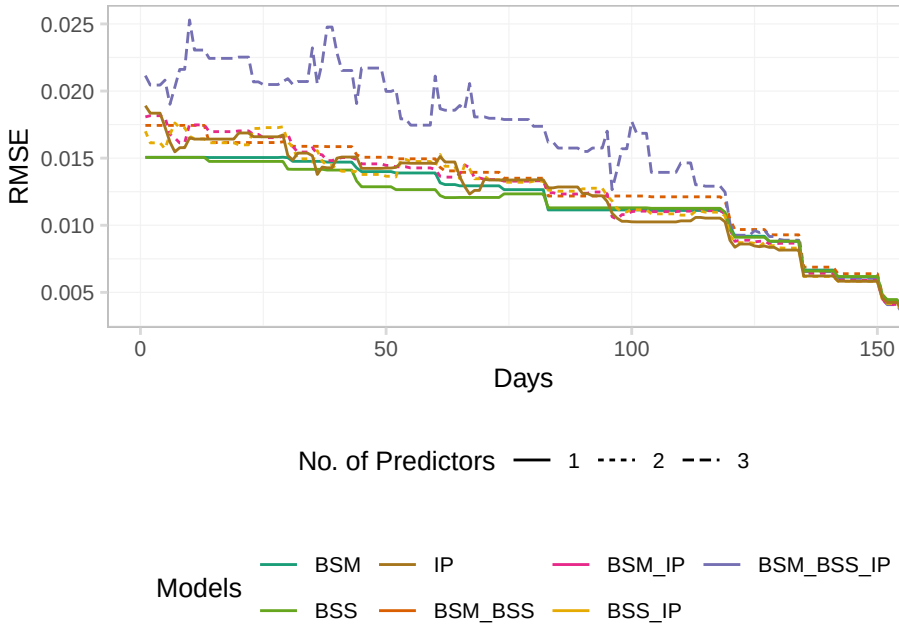

Notes: The figure plots the mean of RMSFE across all countries on each of the 155 days in the nowcast period. The pooled PMIDAS model results are displayed for various combinations of 'BSM', 'BSS' and 'IP'.

To further explore the robustness of the results to our chosen set of predictor

[14]When looking at individual countries there is some evidence that the performance does change with different predictors. The fact that there is some difference in accuracy gains of MIDAS models when using different variables has also been documented in earlier studies (see Clements et al. 2008; Clements and Galvão 2009; Foroni et al. 2015; Schumacher 2016).

Figure 2.5: GDP Nowcast Average RMSFE, q-o-q – Additional Predictors

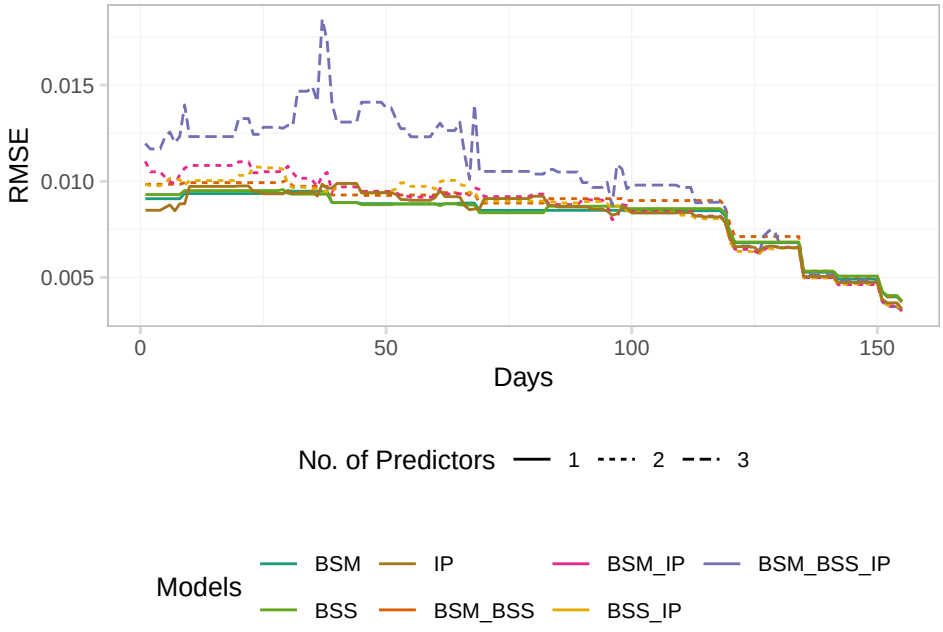

Notes: See notes for Figure 2.4.

variables, we also experimented with adding further surveys available in the OECD MEI database (additional business surveys from retail, trade and construction as well as a consumer confidence survey). This further reduces the number of countries in the sample to 18. However, in searching over many possible combinations of models up to three variables, we find that it is always the case that RMSFE is increasing in the number of variables. The results can be found in Figures A.11 and A.12 in Appendix A. We therefore conclude that a single well-chosen predictor variable can dominate larger models in this PMIDAS context.[15]

We also explore the robustness to the choice of sample split in terms of the in-sample and out-of-sample observations. The results in Figures A.13 to A.16 in Appendix A show that the results are qualitatively similar when we vary the sample split from $P = 0.2T$ to $P = 0.4T$. While the magnitude of the RMSFE changes slightly as we alter the split fraction, the ranking of the models remains very stable across all of the

[15]An alternative way to include additional predictors would be to use a dynamic factor model as in Cascaldi-Garcia et al. (2023) which we do not explore in this chapter.

nowcast dates. We therefore believe the results are not affected by this choice.

2.5 Empirical Application II: Euro Area Inflation Nowcasting

In this section, we present an additional contrasting empirical application to the previous one, where we predict the monthly inflation rate of a set of European countries. Although inflation data are monthly, they are published with a two to three week delay which makes timely nowcasts important to short-term policymakers and market participants. We will exploit data from weekly energy prices which follows the approach of Modugno (2013).[16] The set-up differs from the previous section on global GDP nowcasting as here the data are released at the same time across countries with the timeliness coming from the use of high-frequency weekly data, whereas in the GDP context the data releases were staggered across countries. There are few, if any, studies looking to use panel approaches to nowcast inflation so this application may be of stand-alone interest.

2.5.1 Data and Set-up

We will target the annual (y-o-y) growth rate of inflation as this is what tends to be monitored most closely by market participants and news agencies. However, as in the previous section, we will also present results for the month-on-month (m-o-m) inflation target which is also of interest. The data we use are the Eurostat HICP for which monthly data are available around three weeks after the end of the reference month. We transform the HICP data as annual and monthly log differences (for y-o-y and m-o-m respectively). As a predictor variable we use consumer prices of petroleum products, net of duties and taxes, which are taken from the European Commission's Weekly Oil Bulletin (WOB). We use data for automotive gas oil, heating gas oil and

[16]The earlier version of the paper (Modugno 2011) analysed both U.S. and Euro area inflation whereas Modugno (2013) focusses only on U.S. inflation.

Euro Super 95 gasoline, which we average together as in Modugno (2011). We use the same transformations as in the case of inflation, i.e. the annual (52 week) and weekly log differences (for y-o-y and m-o-m respectively).

Our dataset runs from July 2004 and ends in December 2019 which gives us a total of $T = 186$ months and 812 weeks of data. The dataset covers all major countries in the European Union, including the largest Euro area countries Germany, France and Italy.[17] In performing the out-of-sample evaluation, as in the previous empirical application, we will retain 30% of the sample for evaluating the nowcasts, so $P = 0.3T$. This means that we start nowcasting in May 2015 and continue until we reach the end of the sample. We will evaluate the performance of the PMIDAS model with four weekly lags (both with pooled and non-pooled coefficients) and compare the performance to a time series AR benchmark.

We will make a sequence of inflation nowcasts on different dates, v, throughout the month. We start on day one of the reference month and then make four subsequent nowcasts on days 7, 14, 21 and 28. Using information on the HICP release schedule, we always attribute the inflation release to occur when we update the model on nowcast day 21. This means that at the beginning of the nowcast month, we do not have the past month's inflation data; this only becomes available when we update the model on day 21. Regarding the weekly WOB data, on each nowcast date we will use the most recent weekly data point which has been released before the nowcast date. We always use the four most recent weeks' data to make the nowcast. In the same way as the previous empirical application, we will summarise the nowcast performance for each of the countries on each nowcast date using the quantiles and average of the $RMSFEa_{v,i}$ statistic described in equation (2.14).

[17]The full set of countries is: Austria, Belgium, Cyprus, Denmark, Estonia, Finland, France, Germany, Hungary, Ireland, Italy, Latvia, Lithuania, Luxembourg, Malta, Netherlands, Poland, Portugal, Slovenia, Spain and Sweden.

2.5.2 Results

We now present the nowcast evaluation results for the y-o-y and m-o-m inflation nowcasting exercise. In a similar way as before, Tables 2.6 and 2.7 display the quantiles of the RMSFE across countries, for the pooled and non-pooled PMIDAS model and the time series AR benchmark. The results are similar to the previous empirical application in the sense that we find the pooled-PMIDAS model outperforms the time series AR benchmark for the reported quantiles for both y-o-y and m-o-m targets.

Table 2.6: Inflation Nowcast RMSFE by Quantile – y-o-y

	PMIDAS						BM		
	Pooled			Not Pooled			Time Series AR		
Days	**25%**	**50%**	**75%**	**25%**	**50%**	**75%**	**25%**	**50%**	**75%**
1	0.3684	0.3920	0.4424	0.3657	0.4912	0.6628	0.3552	0.4272	0.5734
7	0.3436	0.3841	0.4428	0.3602	0.4789	0.6702	0.3552	0.4272	0.5734
14	0.3090	0.3706	0.4198	0.3699	0.4540	0.6094	0.3552	0.4272	0.5734
21	0.2149	0.2721	0.3297	0.2900	0.3576	0.4286	0.2645	0.3277	0.4013
28	0.2103	0.2830	0.3366	0.2762	0.3446	0.4819	0.2645	0.3277	0.4013

Notes: The table reports the quantiles across countries of RMSFE for each method, for each of the five nowcast days under consideration. The RMSFEs have been scaled up by 100 from the log-difference transformation.

Table 2.7: Inflation Nowcast RMSFE by Quantile – m-o-m

	PMIDAS						BM		
	Pooled			Not Pooled			Time Series AR		
Days	**25%**	**50%**	**75%**	**25%**	**50%**	**75%**	**25%**	**50%**	**75%**
1	0.0756	0.0828	0.1178	0.0869	0.1212	0.1556	0.0781	0.0886	0.1256
7	0.0697	0.0795	0.1083	0.0826	0.1085	0.1390	0.0781	0.0886	0.1256
14	0.0688	0.0804	0.1039	0.0844	0.1122	0.1434	0.0781	0.0886	0.1256
21	0.0451	0.0514	0.0644	0.0405	0.0676	0.1169	0.0474	0.0556	0.0747
28	0.0430	0.0502	0.0663	0.0433	0.0757	0.1078	0.0474	0.0556	0.0747

Notes: Please see the notes for Table 2.6.

Figures 2.6 and 2.7 graphically display the nowcast performance on average throughout the nowcast period on the five different nowcast dates. Likewise from the figures we can again validate the superiority of the pooled PMIDAS model relative to the benchmark. We also see that the nowcasts tend to improve as the weekly information

is added, especially when we nowcast the y-o-y inflation rate. We note that, as is common in nowcasting studies involving an autoregressive term, there is a sharper drop in the RMSFE on the date when the previous period's inflation is released, in other words on day 21 of the nowcast period.

Overall, we find encouraging results for the use of PMIDAS type models in the context of nowcasting a panel of European countries' inflation. Coupled with the previous section's results on global GDP nowcasting, there is evidence that this method can usefully be applied in a variety of different settings.

Figure 2.6: Inflation Nowcast Average RMSFE - y-o-y

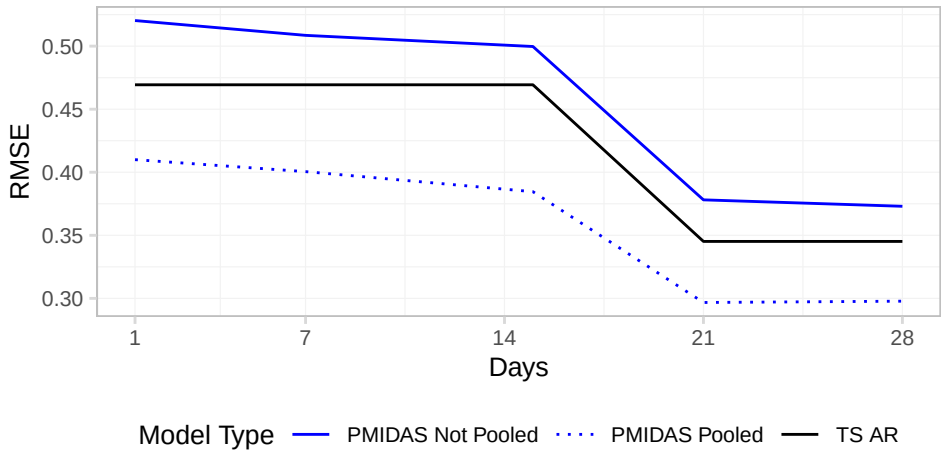

Notes: The figure plots the mean of RMSFE across all countries on each of the 5 dates in the nowcast period. The single predictor variable used is the oil price.

Figure 2.7: Inflation Nowcast Average RMSFE - m-o-m

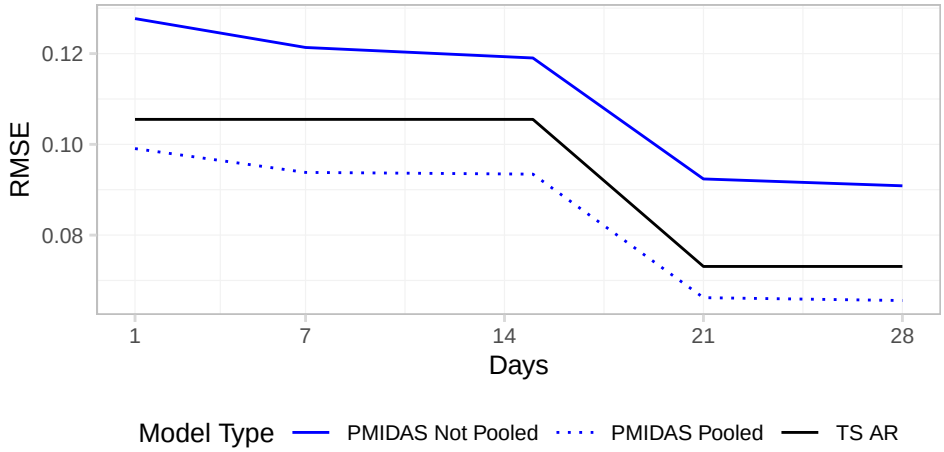

Notes: See notes for Figure 2.6.

2.6 Conclusion

In this chapter, we build a mixed-frequency panel data nowcasting model that can simultaneously make predictions of a large number of countries, regions or sectors. Our approach is based on a panel version of a UMIDAS type nowcasting model, which we extend to allow for heterogeneous coefficients and cross-sectionally dependent errors with a factor structure. We base our estimation approach on the CCE estimation method of Chudik and Pesaran (2015a), which must be adapted to the nowcasting setting. This requires us to use only the lags of the data which are available on the date which we make the nowcast, unlike existing CCE approaches which use contemporaneous variable for estimation which is suitable for causal studies but not for forecasting.

We provide two contrasting empirical applications of our methodology: nowcasting a large amount of global countries' GDP, and nowcasting European countries' inflation. The first main conclusion from both of our empirical studies is that our proposed PMIDAS approach is capable of beating a simple benchmark model, when we switch off heterogeneity and pool the coefficients of the model with heterogeneity only coming through the fixed effects. The results imply evidence in favour of pooling in the

debate of whether 'to pool or not to pool' (Wang et al. 2019), though our model can flexibly allow for more heterogeneity if required in other empirical settings. From the contrasting nature of our applications, we conclude that our method has the potential to work well in nowcasting other types of economic variables. Finally, our results also show that adding new releases of data across variables and countries is able to improve nowcast accuracy in a roughly monotonic fashion. From this we conclude that, although existing studies typically assess nowcast performance as new data arrives for a single country across several variables, there is also benefit in incorporating timely data releases which occur across different countries in a panel data context.

Chapter 3

Nowcasting U.S. State-Level CO_2 Emissions and EC

3.1 Introduction

The growing climate emergency has rapidly expanded the need for policies on abating CO_2 emissions due to fossil fuel energy production and consumption. The importance of using environmental variables in economic modelling is now well accepted since the seminal Dynamic Integrated Climate-Economy model (DICE) model of Nordhaus (1992). This has led to significant recent debate amongst economic policymakers on tracking the social cost of carbon (Rennert et al. 2021) as well as the widespread use of environment-economic models by international institutions such as the OECD and the United Nations.[1] In turn, this has placed increasing importance on the ability to forecast and monitor both short-term and long-term EC and CO_2 emissions. Our focus will be on near-term prediction, or 'nowcasting' of these environmental variables, which has only recently received attention by Bennedsen et al. (2021) in the context of nowcasting national U.S. CO_2 emissions.

[1] See: https://www.oecd.org/environment/indicators-modelling-outlooks/modelling.htm and https://www.unep.org/explore-topics/green-economy/what-we-do/economic-and-trade-policy/green-economy-modelling [Last accessed: 01/09/2022]

In this chapter, we propose new models for jointly nowcasting multiple regions' EC and CO_2 emissions, specifically for states in the U.S., which has not yet been studied in the existing literature. This improves upon studies which look only at the national context by allowing a more granular overview of regional environmental degradation. The focus on sub-national variables is important for several reasons. Firstly, there is growing evidence that sub-national efforts to reduce emissions can accelerate the achievement of national abatement targets (see Hultman et al. 2020, and the references therein). Secondly, the discussion of local-level environmental action has gained a stage in the largest climate meetings, such as the dedicated *'Cities, Regions and the Built Environment'* day at Conference of Parties (COP)26. Finally, there are already many sub-national environmental initiatives in the U.S., where around half of all U.S. states currently have greenhouse gas emissions targets,[2] and more than ten states which participate in the Regional Greenhouse Gas Initiative (RGGI), a market-based program to reduce emissions. For these reasons, it is crucial that policymakers have access to up-to-date data on regional CO_2 emissions and EC. However, it is very challenging to monitor the movements in these variables in real time as the data are only available annually and with very long publication lags. This challenge has not been addressed by existing academic studies.

This chapter aims to fill this gap in the literature by providing a novel nowcasting methodology for U.S. state-level EC and CO_2 emissions growth. This allows us to obtain timely predictions of these variables before the data are published. This builds on existing academic studies in several ways. Firstly, our study is unique in nowcasting state-level EC and CO_2 emissions, where only the recent study of Bennedsen et al. (2021) looks at nowcasting national CO_2 emissions and not at state level. Secondly, our chapter provides a novel application of recently-emerging panel data nowcasting methods which have typically been used only for predicting macroeconomic variables like real GDP (Fosten and Greenaway-McGrevy 2022) and not environmental variables. More broadly, panel data nowcasting is a relatively new and increasing field (Babii

[2]See: https://www.c2es.org/content/state-climate-policy/ [Last accessed: 29/03/2022]

et al. 2020; Koop et al. 2020; Larson and Sinclair 2022) relative to the long history of time series nowcasting (see the surveys of Bańbura et al. 2013; Bok et al. 2018). Finally, our chapter is different from traditional nowcasting studies of real GDP where publication lags may be only one or two months. In our setting, there is even stronger motivation for the use of nowcasting due to the annual frequency and the abnormally large publication lags in the U.S. state-level EC and emissions data. The CO_2 data are only available over two years after the end of the relevant year, while EC data have a delay of around a year and a half. These publication lags make the problem more interesting than existing studies and require methods which are capable not just of nowcasting but also backcasting.

The first contribution of the chapter is to propose a panel data nowcasting methodology for state-level EC and CO_2 emissions growth. Motivated by the fact that the emissions data are calculated directly from EC data, we propose a two-step bridge equation approach adapted to the case of panel data. We first use a mixed-frequency panel MIDAS model to obtain nowcasts of annual state-level EC growth using higher frequency quarterly economic activity data. This model we use is adapted from the mixed-frequency approach of Ghysels (2016), which we extend from the time series to the panel data context, and the model's predictions can be updated every time new information arrives. We then employ a panel bridge equation approach to transform the nowcasts of EC growth into nowcasts of CO_2 emissions growth. In doing so, we use a multi-factor error structure to allow for CSD across states in the style of Chudik and Pesaran (2015a). Our panel bridge equation model is similar to the well-known time series bridge equation approach (see for example Baffigi et al. 2004; Foroni and Marcellino 2014; Schumacher 2016) with the difference that we extend this to allow the modelling of panel data, which is an improvement in contexts where regional data are available. The CSD structure we use is similar to the panel nowcasting approach of Chapter 2, which in this chapter we adapt to the case of bridge equation models.

The second contribution of the chapter is the empirical part where we perform a detailed pseudo out-of-sample forecasting study using our models to predict EC

and CO_2 emissions growth over a period of history. We mimic the release schedule of the variables in real time and make multiple nowcasts and backcasts for every period under consideration. This allows us to assess how the performance of these methods changes as we add new information into the nowcasting model, as is commonly done in empirical nowcasting studies (see, for instance, Giannone et al. 2008; Bańbura et al. 2013; Bok et al. 2018). For the predictions of EC growth, we use real GDP or real personal income growth. Since these economic series have a much lower publication lag, we first of all consider restricting the data flow to only use the year-end annual growth rate of these series in predicting annual EC growth, before turning to assess whether incorporating the mixed-frequency quarterly data can make further improvements. We finally use the bridge equation method to feed in these EC predictions and arrive at predictions of CO_2 emissions growth.

We make several interesting findings. We find that the predictions of EC growth improve across states when current economic data are used for nowcasting and backcasting, relative to a naïve benchmark. There are particularly sizeable gains in several states, which we assess by looking at the across-state distribution of the gain in predictive accuracy of our model relative to the benchmark. Even when using the economic data at the annual frequency, gains in predictive accuracy occur around a year ahead of the release of the EC data. This highlights the gain from using timely information in prediction, even if there is no difference in the frequency of the series. Furthermore, when we increase the frequency to use quarterly economic data we find that nowcast improvements are possible even within the nowcast year itself, around two years before the release of the data for the target variable. With regard to the CO_2 predictions, the gains are less notable when adding economic data although still sizeable in some states, and the biggest gains come when we add in the current year's EC. This is still important as these accurate predictions come many months before the release of the data by the statistical authorities, and we use a much simpler methodology than that used in constructing the data. We find some additional but marginal gain from using factors estimated to pick up common correlated effects in the CO_2 bridge equation

method. We also provide various robustness checks such as the use of per capita EC and emissions growth as target variables.

Our empirical study builds on an increasing body of empirical work in nowcasting. While only the aforementioned study of Bennedsen et al. (2021) looks at nowcasting environmental variables, there have been a vast amount of studies using nowcasting for macroeconomic monitoring. The majority of studies look at nowcasting real GDP and have done so in a variety of different contexts: developed economies (Bok et al. 2018; Anesti et al. 2022), EMEs (Dahlhaus et al. 2017; Bragoli and Fosten 2018) global GDP (Ferrara and Marsilli 2019) and so on. Nowcasting has also been applied to several other macroeconomic series such as the GDP components (Fosten and Gutknecht 2018), inflation (Modugno 2013; Knotek and Zaman 2017) and unemployment claims (Larson and Sinclair 2022). Our chapter helps to shift this focus from macroeconomic to environmental nowcasting, which we believe will be a fruitful area of future research.

The rest of the chapter is organised as follows. Section 3.2 describes the data sources used in the study. Section 3.3 contains the models we propose and Section 3.4 details the pseudo out-of-sample methodology we use in evaluating these models. Section 3.5 discusses the results of the pseudo out-of-sample experiment and Section 3.6 concludes the chapter. Appendix B houses additional sets of results not included in the main text.

3.2 Data

3.2.1 CO_2 Emissions

State-Level CO_2 emissions data are available from the U.S. Energy Information Administration (EIA).[3] The data are available on an annual basis with observations from 1980 onwards. The data cover the CO_2 emissions from direct fuel use across various sectors: commercial, industrial, residential and transportation. We focus on the total emissions

[3]See: https://www.eia.gov/environment/emissions/state/ [Last accessed: 11/11/2021]

by state but we will also consider per-capita CO_2 emissions as this has been the target variable of other studies (Bennedsen et al. 2021). Of crucial importance to this study is that the publication lag for the CO_2 emissions data is very large, around two years and three months after the end of the reference year. For instance, the data for 2018 were released at the beginning of March 2021. This lag is considerably larger than other types of state-level data such as the economic variables mentioned below. This lack of timeliness will mean that both nowcasting and backcasting are appropriate.

In producing the data, the EIA estimate state-level CO_2 emissions based on underlying EC data from the State Energy Data System (SEDS).[4] Knowing this aspect of the data construction is what motivates the use of a bridge equation where total state-level CO_2 emissions data are directly linked to total state-level EC data.[5] We note that this approach will be like an approximation to the more disaggregated way in which the EIA computes the state-level CO_2 data. To be more precise, according to the EIA's methodology documentation,[6] the conversion to CO_2 emissions from EC is first made at a very granular level by fuel type and sector, using different emissions factors and proportions of fuel used in fuel combustion. After conversion, the total CO_2 emissions are summed up from the disaggregates. An alternative approach to ours would be a bottom-up approach to mimic the EIA's calculation by nowcasting the disaggregate EC series, converting them and then aggregating them afterwards. However, we do not pursue this approach as it would entail a large amount of additional nowcast uncertainty: (i) the nowcast errors from a large number of individual disaggregates summed up to get the total, (ii) the errors from predicting the emissions factors which are themselves estimated and would require nowcasting, (iii) some estimation of the proportions of each fuel type that is used in combustion, which the EIA bases on various sources. We prefer a direct top-level approach, much in the same way that GDP

[4] See: https://www.eia.gov/state/seds/ [Last accessed: 11/11/2021]

[5] This is instead of modelling CO_2 emissions directly as a function of, say, economic variables. We tried this latter approach in our empirical investigations but found it to perform worse than modelling using EC.

[6] See: https://www.eia.gov/environment/emissions/state/pdf/statemethod.pdf [Last accessed: 31/08/22]

nowcasters target the aggregate GDP series and not the very granular disaggregated output series which are also available.

3.2.2 EC

The data for state-level EC are also available on an annual basis. The data are available from the SEDS, mentioned earlier, also produced by the EIA. The annual time series for each state are available from 1960 onwards. As with CO_2 emissions, we will consider both the raw and per-capita EC in our analysis. Regarding the timeliness of the data, although the data frequency is the same as that of CO_2 emissions, the SEDS data are published in a more timely fashion. Here, the publication lag is around one year and six months, which is roughly nine months quicker than for the CO_2 data. For instance, the data for 2019 were published at the end of June 2021. Although the data are more timely, if we want to use the current year's EC in predicting CO_2 emissions, this would constitute a backcast and not a nowcast. In order to obtain nowcasts of EC and therefore CO_2 emissions, we require data which are available in a much more timely fashion, such as the economic indicators outlined next.

3.2.3 Economic Indicators

Since the aim is to produce state-level EC nowcasts, it is natural to use state-level economic indicators. We consider two different variables: real GDP and real Personal Income (PI). Both of these series are available from the Bureau of Economic Analysis (BEA).[7] The quarterly PI data are available at a quarterly frequency for all states from 1950 onwards, which we deflate by the GDP deflator for the U.S. to obtain real figures. The real GDP data have a much shorter history than PI. Annual data are available from 1997, and are published separately from the quarterly data which are only available from 2005. We will therefore consider both annual and quarterly versions so that we can compare GDP and PI as predictors in the annual case. In the quarterly

[7] See: https://www.bea.gov/data/gdp/gdp-state and https://www.bea.gov/data/income-saving/personal-income-by-state [Last accessed: 12/02/2022]

case we will focus on PI data only as the time span of the quarterly GDP data is not long enough for a meaningful pseudo out-of-sample reconstruction.

There are two factors which make these economic series appropriate for nowcasting EC and therefore CO_2 emissions. Firstly, their quarterly frequency makes them anyway more timely than the annual data. Secondly, for both PI and GDP, the publication lag is around three months after the end of the reference quarter.[8] This implies that already in the middle of the nowcast year, the first quarter of that year's economic data are available for making predictions of EC for that same year.

It is difficult to expand on the set of economic predictor variables we use due to the limited availability of state-level data. For instance, Bennedsen et al. (2021) note that the IP index is useful in nowcasting national CO_2, but IP data are not available by state. However, we will instead show some additional results using the Philly Fed's State Coincident Indices.[9] These indices are available in a timely fashion at the monthly level and are constructed using a dynamic factor model on four state-level employment type series, which bears resemblance to the factor model methods used in nowcasting with many predictors.

3.3 PMIDAS and Bridge Equation Methodology

In this section we describe the models we use to predict the annual growth of EC and subsequently of CO_2 emissions growth.[10] As mentioned earlier, the CO_2 data are released in March over two years after the reference year, whereas the EC data are published in June each year, a year and a half after the reference year. The economic

[8] We will assume the same publication lags for GDP and PI, as these data are generally released in the same month, often on the same date. See: https://www.bea.gov/news/schedule/full [Last accessed: 12/02/2022]

[9] See: https://www.philadelphiafed.org/surveys-and-data/regional-economic-analysis/state-coincident-indexes [Last accessed: 12/02/2022]

[10] We focus on the growth rates of these series as is standard in the macroeconomic nowcasting literature when analysing trending unit root processes. Since there is little existing evidence on unit roots in the state-level EC and CO_2 emissions data we performed a battery of panel unit root tests (the Levin et al. (2002) (LLC) test, the Im et al. (2003) test (IPS) and the Choi (2001) test). As expected, these tests confirm non-stationarity in levels and stationarity in growth rates. We do not present the results in the text for the sake of brevity.

data are available in a more timely fashion. Our approach is therefore to use a bridge equation to compute predictions of CO_2 emissions growth for the target year by first obtaining predictions of EC using economic indicators. Therefore, while CO_2 emissions are the 'target' variable of the bridge equation, we also obtain timely predictions of EC which is of separate interest in itself.

We differ from the prevalent bridge equation models (see Foroni and Marcellino 2014; Schumacher 2016, and the references therein) in several important ways. Firstly, we use a panel data set-up instead of a time-series approach that is common in economic nowcasting. Secondly, the EC variable we predict in the first step is not available at a higher frequency but has lesser publication lags as compared to our final target variable, CO_2 emissions. Lastly, we do not restrict ourselves to AR models for predicting EC as is typical of economic bridge equation set-ups. Instead, we also use panel data models and incorporate mixed-frequencies to use higher frequency quarterly PI or real GDP growth.

3.3.1 PMIDAS Model for EC

We now describe the panel model for nowcasting EC growth using economic data. Since the economic data are both more timely and available at a higher frequency, we will try out two different approaches. In the first approach we simply use annual data for both the EC and economic variables, in order to assess whether the timeliness of economic data is useful even when using annual data. In the second approach we check whether inserting quarterly economic data in a mixed-frequency approach brings further benefits. This is also motivated by the data constraint mentioned earlier, that the quarterly real GDP figures do not have sufficient history to be used in a pseudo out-of-sample experiment whereas the annual GDP data do have sufficient history. The annual version will therefore give results both when using GDP and PI whereas the quarterly version will only yield results when using PI.

Annual Frequency Model

We start out with the model which predicts EC using the available autoregressive lags on day v of the nowcast period as well as the annual lags of the economic indicator:

$$c_{i,t} = \alpha_{vi} + \phi_v c_{i,t-d_{cv}} + \beta_v X_{i,t-d_{Xv}} + u_{v,i,t} \tag{3.1}$$

where t denotes the annual time index and $c_{i,t}$ is a generic notation indicating the annual growth rate in EC. In the main results this is simply the percentage change in actual EC for state i in year t, in other words the growth rate of $EC_{i,t}$. Alternatively, we also explore the results where $c_{i,t}$ is the growth rate of per capita consumption, in other words the growth rate of $\frac{EC_{i,t}}{pop_{i,t}}$, where $pop_{i,t}$ is the state population. In a similar way, $X_{i,t}$ is a generic notation for the annual growth rate of the economic indicator, either GDP or PI, and could be actual or per-capita according to the target variable.

The model in equation (3.1) takes account of the ragged edge problem in the following way. Denoting v to be the date of prediction, we define d_{cv} as the available lag of $c_{i,t}$ at the time of prediction, based on its publication lag. Similarly, d_{Xv} is used to denote the available lag of $X_{i,t}$ used in the model at time v. As we change the nowcast date v, the available lags of each variable may change and the model lag structure is updated to accommodate new information. Since the model variables change on each date, v, the parameters of the model and the error term are also indexed by v. To give an example, in nowcasting year t, if v is the start of year t, based on the data flow described in Section 3.2 earlier, the model will use $c_{i,t-3}$ and $X_{i,t-2}$. After March of year t, the economic data are updated and $X_{i,t-2}$ is replaced with $X_{i,t-1}$ and so on. The full updating procedure will be described later when we introduce the pseudo out-of-sample set-up.

Mixed-Frequency Model with Quarterly Data

We now re-state equation (3.1) so that the quarterly frequency of the economic data is fully utilised in a mixed-frequency model. This model is a panel version of the UMIDAS

model (see Foroni et al. 2015; Schumacher 2016) which takes on the following form:

$$c_{i,t} = \alpha_{vi} + \phi_v c_{i,t-d_{cv}} + \beta_v^{(m)\prime} \boldsymbol{x}_{i,t-\frac{q_v}{4}} + u_{v,i,t} \tag{3.2}$$

where $\boldsymbol{x}_{i,t-\frac{q_v}{4}} = (x_{i,t-q_v/4}, x_{i,t-(q_v-1)/4}, x_{i,t-(q_v-2)/4}, x_{i,t-(q_v-3)/4})'$ denotes the generic stacked skip-sampled PI or GDP growth which is inserted into the model with a quarterly lag of q_v at nowcast date v. Note that a lag of one quarter is denoted in annual terms as $t - \frac{1}{4}$. In equation (3.2), the slope coefficient $\beta_v^{(m)}$ is a vector of length four, corresponding to the stacked skip-sampled process $\boldsymbol{x}_{i,t-\frac{q}{4}}$ consisting of the four quarters in a year. The nowcast updating works in the same way as for equation (3.1). When we change the nowcast date, v, we update the lag structure to incorporate any newly-available annual data for $c_{i,t}$ and quarterly data for $\boldsymbol{x}_{i,t}$.

Equations (3.1) and (3.2) are panel versions of the Autoregressive with an exogenous regressor (ARX) model and we refer to it as the ARX model subsequently. We will also use a naïve benchmark method to compare with the predictions from the panel ARX model. For this benchmark we will use a simple historic mean prediction using all available data at the time of making the nowcast.[11] Later on, we use the EC predictions from both the panel ARX and the benchmark model to predict CO_2 emissions and compare the results.

3.3.2 Bridge Equation for CO_2 Emissions

Here we describe the main nowcasting bridge equation for CO_2 emissions growth, where we plug in the predictions for EC obtained from the previous equations (3.1) or (3.2). We define $\hat{c}_{v,i,t}$ generically as the predicted value of $c_{i,t}$ on day v of the nowcast period. The main equation is a panel bridge equation model with a multi-factor error structure:

$$e_{i,t} = \theta_{vi} + \rho_v e_{i,t-d_{ev}} + \delta_v \hat{c}_{v,i,t} + \lambda_v f_t + \varepsilon_{v,i,t} \tag{3.3}$$

[11] In previous version of the chapter we also considered using an autoregressive benchmark but the results are qualitatively similar.

where we define emissions growth, $e_{i,t}$, which either represents the growth of $CO2_{i,t}$, the CO_2 emissions in state i in year t, or the growth of per-capita emissions $E_{i,t} = \frac{CO2_{i,t}}{pop_{i,t}}$. In a similar way to before, the autoregressive lags included in the model depend on the publication lag, which at prediction time v is denoted by d_{ev}. As earlier, the parameters and error term in equation (3.3) also depend on v as the model variables change with v.

The variable f_t denotes unknown factors with loadings λ_v which are common across all states and are used to model the CSD in the error terms. In order to estimate these factors, in a similar way to Chudik and Pesaran (2015a) they are also assumed to influence the $\hat{c}_{v,i,t}$ in the following way:

$$\hat{c}_{v,i,t} = \zeta_{vi} + \kappa_v e_{i,t-d_{ev}} + \Gamma_v f_t + \epsilon_{v,i,t} \tag{3.4}$$

We note that equations (3.3) and (3.4) assume away heterogeneity (across i) in the factor loadings λ and Γ, which was permitted in the original paper of Chudik and Pesaran (2015a). This is partly because pooling coefficients is often seen to be preferable to heterogeneous coefficients in panel forecasting (Wang et al. 2019), and also because our relatively small number of annual time periods makes it less desirable to add coefficient heterogeneity. Thus, the common factors f_t could also be regarded as time fixed-effects; see Pesaran (2016, Ch. 31, p. 833).

Equations (3.3) and (3.4) jointly create a set-up that can be estimated through the CCE method. Since the original method of Chudik and Pesaran (2015a) was not designed to use for forecasting, we use the LCCE approach developed in Chapter 2 which ensures that only the available lags of the predictor variables are used in estimating the factors. In this way, the final prediction equation replaces the unknown factors in equation (3.3) as follows:

$$e_{i,t} = \theta_{vi} + \rho_v e_{i,t-d_{ev}} + \delta_v \hat{c}_{v,i,t} + \sum_{l=0}^{p_T} \gamma'_{vl} \overline{z}_{v,i,t-l} + \varepsilon_{v,i,t} + O_p(N^{-\frac{1}{2}}) \tag{3.5}$$

where $\overline{z}_{v,i,t}$ are the factor estimates used to pick up CCE in the errors and p_T is a lag truncation parameter. The factor estimates are obtained by taking a state-weighted

average of the vector $z_{v,i,t} = [e_{i,t-d_{ev}}, \hat{c}_{v,i,t}]'$. Chudik and Pesaran (2015a) and Chapter 2 discuss the equivalence of least squares estimation of equation (3.5) and the system of equations (3.3) and (3.4). We therefore use panel least squares estimation of equation (3.5) in our out-of-sample forecasting exercise.

We will compare the results with those from a simple panel ARX model, where we simply estimate equation (3.3) without the factors f_t. This will allows us to observe any effects from allowing CSD. As a naïve benchmark, in the same way as earlier, we will use the historic mean using the data available at the time of making the nowcast.

3.4 Pseudo Out-of-Sample Set-up

We perform pseudo-out-of-sample experiments for nowcasting annual EC and CO_2 emissions growth across the $N = 51$ individual states plus the District of Columbia. We start our out-of-sample nowcasts in 2009 and finish in 2018. As is common in the nowcasting literature (dating back to Giannone et al. 2008) we will make multiple nowcast and backcast updates at different dates, v, for every year in the out-of-sample evaluation period. We do this to replicate the ragged edge in the data using a calendar of releases as they would have occurred in real time. This allows us to see how the nowcasts and backcasts behave, on average, as we add more information whenever it becomes available. For every data release we take into account the new lag of data available, adjust the model lag structure as detailed earlier, re-estimate the models and obtain first the EC predictions and then the CO_2 predictions from the bridge equation in equation (3.5). Once we have finished making nowcasts and backcasts of a given year, we move on to the next year by expanding the information set as in the recursive out-of-sample scheme of West (1996).

To be more specific on the nowcast updating procedure, we will start by making a nowcast at the beginning of the reference year, at the end of January. This can be seen as the first date in Tables 3.1 and 3.2 which detail the release calendar in the annual and quarterly data set-up. We then move through the nowcast year, updating in March

and then June in both the annual and quarterly set-ups. In the quarterly set-up, there are two further releases in the nowcast year in September and December as additional quarterly lags of the economic data become available as seen in Table 3.2. This gives a total of three nowcasts in the annual set-up and five in the quarterly set-up. We then move into the next year and start backcasting. For EC this gives a further two updates in both the annual and quarterly set-ups, as we stop updating the economic data after the observation for the target nowcast year has been released (in other words we do not use 'future' economic data to predict current EC). This gives a total of five predictions (three nowcasts and two backcasts) for EC in the annual set-up and seven (five nowcasts and two backcasts) in the quarterly set-up. When it comes to making the CO_2 predictions, we have the same number of predictions made as in the case of EC but there are two additional updates: in March of the second backcast year when the first lag of CO_2 data is released, and in June when the current year's EC data is released. In other words, the last bridge equation nowcast we make of CO_2 will replace the predicted EC with its actual realised value.

Table 3.1: Release Calendar for the Annual Set-up

		Month	**Year**	EC	**GDP/PI**	**CO_2**
Nowcast	1	January	0	3	2	4
	2	March	0	3	1	3
	3	June	0	2	1	3
Backcast	4	March	1	2	0	2
	5	June	1	1	0	2
	6	March	2	1	0	1
	7	June	2	0	0	1

Notes: Month and Year denote when the prediction is made, with Year being the number of years after the nowcast year (so Year 0 is the nowcast year itself).
The columns EC, GDP/PI and CO_2 display the available lags of that variable in years, relative to the nowcast year. The horizontal line after release 5 denotes the point at which we stop predicting EC in the annual set-up. Releases 6 and 7 are only used for predicting CO_2.

We will therefore have multiple nowcasts and backcasts made per year for a total of nine evaluation years from 2009 to 2018. Since all of the data series have slightly

Table 3.2: Release Calendar for the Quarterly Set-up

		Month	Year	EC	GDP/PI	CO_2
Nowcast	1	January	0	3	5*	4
	2	March	0	3	4*	3
	3	June	0	2	3*	3
	4	September	0	2	2*	3
	5	December	0	2	1*	3
Backcast	6	March	1	2	0*	2
	7	June	1	1	0*	2
	8	March	2	1	0*	1
	9	June	2	0	0*	1

Notes: The same as for Table 3.1 except the publication lags for GDP/PI (*) are in quarters relative to the last quarter of the nowcast year. A value of 0* means that all quarters of the nowcast year are already available).
The horizontal line after release 7 denotes the point at which we stop predicting EC in the quarterly set-up. Releases 8 and 9 are only used for predicting CO_2.

different sample sizes, it is useful to consider the proportion of the sample which is being used for evaluation. In predicting EC, given that annual state-level GDP data begins only in 1997, starting our evaluation in 2009 implies we use around a half of the sample for evaluation of the EC predictions using GDP. Since the data span for PI is much longer we use about 17% of the sample for evaluating the EC predictions using PI. In predicting CO_2, given that the data runs from 1980 to 2018, we assess the accuracy of our predictions for about a quarter of the total length of our time sample.

To compare the accuracy of the predictions from the various competing methods, we will use the average RMSFE as the criterion. This will be the square root of the time-averaged squared prediction errors, averaged across all states $i = 1, ..., N$. The RMSFE will be tracked across multiple nowcast dates, v, and is defined as follows, denoting that T is the last year in the sample and we have P out-of-sample predictions made:

$$RMSFE_v = \frac{1}{N}\sum_{i=1}^{N}\sqrt{\frac{1}{P}\sum_{t=T-P+1}^{T}\widehat{\varepsilon}_{v,i,t}^2} \tag{3.6}$$

where $\widehat{\varepsilon}_{v,i,t}$ generically stands for the prediction error of a model on nowcast date v for

state i and year t.

We will also perform some analysis of the RMSFE for each state, where we do not average over the states. In other words we take the RMSFE for state i on nowcast date v as:

$$RMSFE_{vi} = \sqrt{\frac{1}{P}\sum_{t=T-P+1}^{T}\widehat{\varepsilon}_{v,i,t}^{2}} \tag{3.7}$$

where, of course, these results are only indicative as they are based on rather a small time series sample size and will be treated with some caution.

3.5 Results

In this section, we discuss the results of the pseudo-out-of-sample experiment described in the previous section. We first discuss the accuracy of the EC predictions before then turning to the accuracy of the bridge equation method results for CO_2 emissions. For these accuracy assessments for EC and CO_2, we analyse both the annual data set-up and the quarterly data set-up as described earlier. We present results only for the original EC and CO_2 growth series, with the per-capita growth being reported in Appendix B.[12] The findings are very similar between the main results and the per-capita results.

3.5.1 EC Results

EC Predictions with the Annual Data Flow

Figure 3.1 displays the RMSFEs obtained from predicting the growth rates of EC according to the release schedule in Table 3.1, where the economic data are used at the annual frequency. In all figures, the RMSFEs have been normalised by the RMSFE of the benchmark in the first nowcast period so that any figures lower than 1 are gains

[12] In arriving at the per-capita figures for the quarterly series, the population is assumed to remain constant for all four quarters of any year and is equal to the annual number.

relative to the benchmark in the first period. These results show that, on average across all states, there is a drop in the RMSFE from the ARX model when the model also includes current economic data, both for GDP and PI. From Table 3.1, we noted earlier that there are only two annual economic data releases, which occur in releases two and four. While release two, corresponding to the year lagged economic data, is not able to improve the RMSFE of the ARX model in comparison to the benchmark, release four shows that the ARX model improves over the benchmark on the release of the up-to-date economic data. We see a sharper drop in the RMSFE based on the PI data relative to the GDP data. We note that the GDP data only have a relatively short history, starting in 1997, so the results based on PI appear to be more reliable.

Figure 3.1: RMSFE – EC, Annual Data Flow

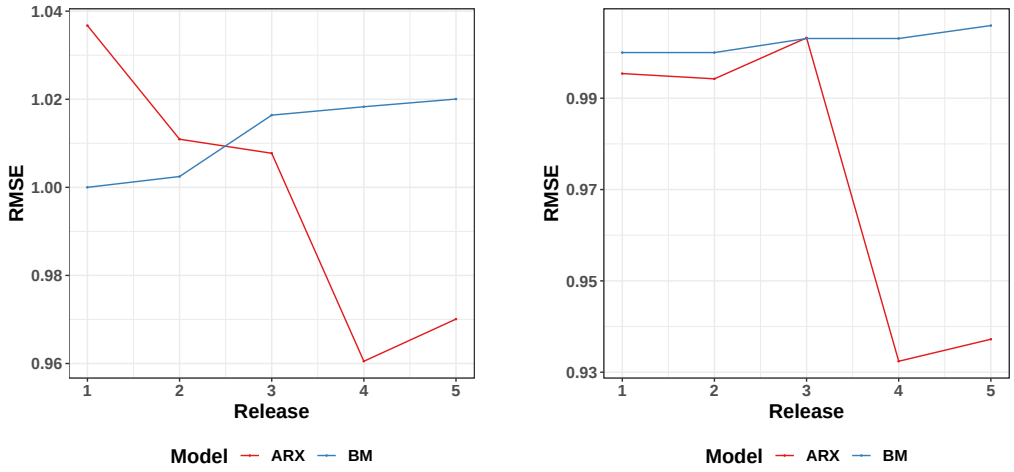

(a) Predictor: GDP (b) Predictor: PI

Notes: The RMSFE figures are normalised by the BM at the first release date. Therefore any points below 1 indicate that the RMSFE is lower than that of the benchmark in the first nowcast period.

While the average RMSFE results across states show a quantitatively modest improvement over the benchmark after economic data have been released (gains of 5-6% in both cases), when we dig into the individual states we see much more substantial improvements of our method in some of the larger states such as Florida, with gains of up to 30%. To summarise the results across states, Table 3.3 presents the quantiles of

the state-specific RMSFEs for the ARX model relative to the benchmark model. In general the table confirms what is seen in Figure 3.1 and we see that at releases 4 and 5 there are gains from the ARX model relative to the benchmark across the majority of states. Additionally, we see that gains at the later nowcast updates are as large as 20% over the benchmark in several states at the 10^{th} percentile, both for the GDP and PI models. The gain is in the region of 10% to 15% at the 25^{th} percentile.

Table 3.3: Distribution of Relative RMSFE Across States – EC – Annual Data Flow

Release	10%	25%	50%	75%	90%
1	0.9918	1.0128	1.0332	1.0590	1.0949
2	0.9499	0.9880	1.0056	1.0336	1.0582
3	0.9419	0.9609	0.9927	1.0245	1.0552
4	0.8476	0.8872	0.9365	0.9882	1.0488
5	0.8337	0.8854	0.9418	0.9974	1.0833

(a) Predictor – GDP

Release	10%	25%	50%	75%	90%
1	0.9810	0.9879	0.9961	1.0058	1.0142
2	0.9185	0.9790	1.0007	1.0233	1.0531
3	0.9392	0.9826	1.0088	1.0310	1.0495
4	0.7974	0.8757	0.9331	0.9969	1.0163
5	0.7999	0.8806	0.9351	0.9979	1.0195

(b) Predictor – PI

Notes: The numbers represent the quantiles of the distribution of relative RMSFE across states, where we take the RMSFE of the ARX model relative to the benchmark. Figures lower than 1 indicate that the RMSFE of the ARX model was lower than that of the benchmark for all of the countries below the relevant quantile.

The naïve benchmark method, on the other hand, does not improve even as newer relevant information is added in calculating the historic mean. If anything, the results seem to worsen as the data for EC gets released and is included in the predictions. This is more evident from Figure 3.1b where we use the entire available history of EC growth rates since 1961.

In summary, we find that releases of current economic data yield improvements in predicting growth rates of EC. The improvement is modest on average across all states, and rather large in some of the most energy-consuming states. Looking at the performance across all states indicates that the proposed method is capable of delivering nowcast accuracy gains in a non-trivial number of states once relevant economic data are included in the model. We find that the backcast made in March of the year after the reference year (release four) is of particular use. This is available well over a year in advance of the release of the EC data, and so we are able to make timeliness gains even using this example with annual economic data.

EC Predictions with the Quarterly Data Flow

Now we present an assessment of the nowcast and backcast predictions of EC growth using the mixed-frequency version of the model in equation (3.2). In this case we update the dataset following Table 3.2 using quarterly frequency PI data. The quarterly state-level GDP data starts only in 2005 and hence leaves us with too few observations for estimating and evaluating the models. Therefore, we do not include state-level GDP in the mixed-frequency analysis.

Figure 3.2 shows the average RMSFE across states from the mixed-frequency panel ARX model, in contrast to the naïve benchmark. As in the annual case earlier, we find a noteworthy drop in RMSFE once the PI data for successive quarters of the target year starts to get released and is included in the model. The RMSFE gains relative to the benchmark are as much as 10% on average across states, which is somewhat larger than that when using annual data. Furthermore, in the annual model the drop in RMSFE could be observed only after all four quarter's data have been released. In the mixed-frequency case we notice falling RMSFE right from the release of the first quarter of data (release date 3 in Table 3.2). By the end of the prediction period, while the benchmark does not improve at all, the mixed-frequency ARX model has shown improvements using economic data.

As with the annual results, we also display the distribution of the relative RMSFE

Figure 3.2: Average RMSFE Across States – EC – Quarterly Data Flow

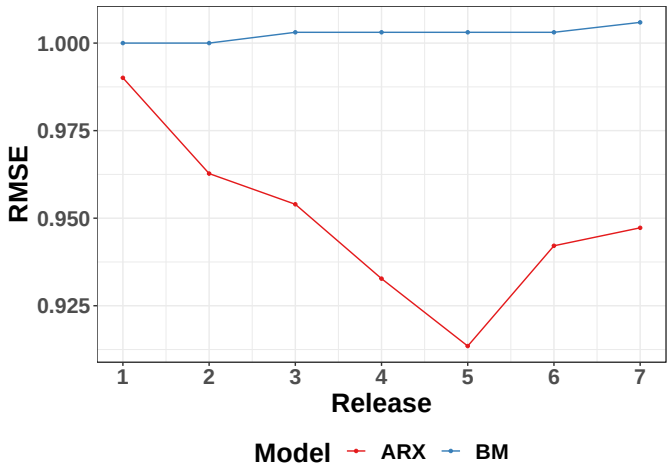

Notes: The same as Figure 3.1 but we note that only PI data are used in the quarterly data flow set-up due to the short time span of quarterly state-level GDP data.

Table 3.4: Distribution of Relative RMSFE Across States – EC – Quarterly Data Flow

Release	10%	25%	50%	75%	90%
1	0.9227	0.9556	0.9841	1.0133	1.0643
2	0.8808	0.9218	0.9705	1.0010	1.0568
3	0.8527	0.8997	0.9605	0.9930	1.0422
4	0.7896	0.8746	0.9315	0.9845	1.0316
5	0.7839	0.8681	0.9033	0.9616	1.0392
6	0.8128	0.8946	0.9568	0.9892	1.0363
7	0.8138	0.8945	0.9619	0.9916	1.0224

Notes: The same as for Table 3.3.

across quantiles, which can be seen in Table 3.4. Here we see that there are nowcast accuracy gains of up to 20% in the best 10^{th} percentile of states, which is even larger that in the annual case, with the added benefit that the quarterly predictions can be derived in a more timely fashion. Even at the 25^{th} percentile, there are gains of around 15% from using the ARX model relative to the benchmark, once sufficient data have been added into the model.

Overall, these quarterly results show an improvement over the annual results both in terms of the relative gain of the ARX compared to the benchmark, but especially due to their additional timeliness. Since we start to get the quarterly information on

the nowcast year in around June of the same year, we can see improvements in RMSFE around two years before the EC data are published.

3.5.2 CO_2 Emissions Results

Now having the predictions of the EC for the target year, we can proceed to predict the CO_2 emissions growth rate using the bridge equation model in equation (3.3). We do this in two parts as earlier, first evaluating the nowcasts when only the annual economic data are incorporated into the EC nowcasts, and then allowing for quarterly economic data to be used. As before, both PI and GDP are used in the annual frequency results whereas only PI is used in the quarterly results.

CO_2 Emissions Predictions with the Annual Data Flow

Figure 3.3 displays the results of the bridge equation method based on EC nowcasts from either the ARX or benchmark method (as in Figure 3.1). In a similar way to before, there is improvement in predictive accuracy from the fourth data release onwards, in other words when the economic data for the target year is released. However, these gains are less obvious than in the case of EC. Some gains of up to 10% on average can be seen when bridging using the predictions of EC including GDP data ('EC.GDP') which improves more than when predicting EC with the benchmark method ('EC.BM') and no economic data. We note that the addition of factors in the bridge equation model (displayed with dashed lines) does yield some minor improvements but these are somewhat marginal.

The most striking finding is the very sharp drop of almost 75% at the final release date when we incorporate the actual observed EC data into the bridge equation model. This clearly makes sense as the CO_2 data are derived from EC, however it is noteworthy that we are able to generate good predictions many months before the CO_2 data are released, even when using a simple panel data regression model which is far simpler than the methodology used to construct the actual CO_2 data.

Figure 3.3: Average RMSFE Across States – CO_2 Emissions – Annual Data Flow

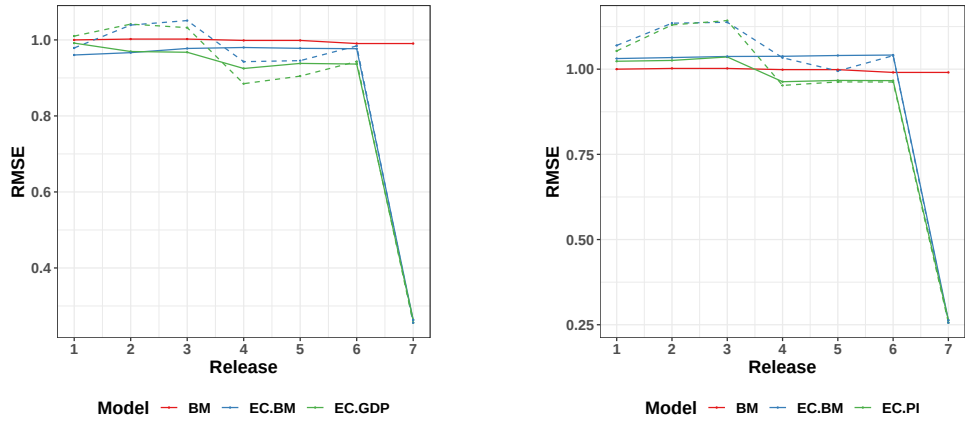

(a) Predictor: State-Level GDP (b) Predictor: State-Level PI

Notes: Dashed lines indicate that factors were used in the CO_2 model. EC.BM: bridge equation predictions for CO_2, benchmark model for EC; EC.GDP/EC.PI: bridge equation predictions for CO_2, GDP/PI model for EC. The RMSFE is normalised on the benchmark in the first nowcast period as in previous figures.

Tables 3.5 and 3.6 present the relative RMSFE distributions across states, for all of the models considered in Figure 3.3. As before, these tables reveal more information about the performance of the bridge equation method than looking at the average across all states. For instance, in the case where the EC nowcasts used in the bridge equation have been derived from GDP data (Tables 3.5a and 3.5b), we see gains of around 20% relative to the benchmark in the top 10^{th} percentile at nowcast point four when recent economic data are available. We also notice a similar pattern to the average results before when looking across all percentiles, with a sudden drop in the RMSFE of the bridge equation method (relative to the benchmark) at the end of the prediction period when the current year's EC data are released.

CO_2 Emissions Predictions with the Quarterly Data Flow

Finally, we perform the evaluation of the CO_2 predictions where the quarterly data were used in the EC predictions. These are, again, only performed with PI as the economic indicator as in Figure 3.2. The results of the pseudo-out-of-sample experiment

Table 3.5: Distribution of Relative RMSFE Across States – CO_2 Emissions – Annual Data Flow (Predictor: GDP)

Release	**10%**	**25%**	**50%**	**75%**	**90%**
1	0.9168	0.9694	1.0000	1.0286	1.0579
2	0.8763	0.9242	0.9744	1.0118	1.0641
3	0.8706	0.9349	0.9625	0.9980	1.0273
4	0.8277	0.8804	0.9186	0.9650	1.0481
5	0.8266	0.8733	0.9300	1.0038	1.0949
6	0.8526	0.8790	0.9413	0.9960	1.0766
7	0.1732	0.2101	0.2704	0.3241	0.3958

(a) Model: EC.GDP

Release	**10%**	**25%**	**50%**	**75%**	**90%**
1	0.9034	0.9720	1.0143	1.0481	1.1228
2	0.9520	1.0073	1.0483	1.0979	1.1239
3	0.9251	0.9956	1.0311	1.0755	1.1119
4	0.7765	0.8298	0.8743	0.9371	1.0394
5	0.7715	0.8127	0.8933	1.0009	1.1013
6	0.8439	0.8846	0.9381	0.9985	1.1116
7	0.1757	0.2003	0.2470	0.3114	0.3955

(b) Model: EC.GDP with Factors

Table 3.5: (cont'd...)Distribution of Relative RMSFE Across States – CO_2 Emissions – Annual Data Flow (Predictor: GDP)

Release	10%	25%	50%	75%	90%
1	0.9038	0.9305	0.9572	1.0023	1.0237
2	0.9167	0.9438	0.9646	0.9953	1.0220
3	0.8903	0.9479	0.9812	1.0097	1.0486
4	0.9400	0.9645	0.9861	1.0062	1.0418
5	0.9309	0.9597	0.9816	1.0097	1.0311
6	0.9376	0.9777	0.9941	1.0129	1.0305
7	0.1732	0.2101	0.2704	0.3241	0.3958

(c) Model: EC.BM

Release	10%	25%	50%	75%	90%
1	0.8929	0.9428	0.9766	1.0138	1.0882
2	0.9622	1.0093	1.0439	1.0829	1.1180
3	0.9653	1.0048	1.0643	1.1019	1.1253
4	0.8890	0.9151	0.9411	0.9788	1.0364
5	0.8656	0.8939	0.9618	1.0095	1.0403
6	0.9479	0.9787	0.9923	1.0252	1.0633
7	0.1757	0.2003	0.2470	0.3114	0.3955

(d) Model: EC.BM with Factors

Notes: The numbers represent the quantiles of the distribution of relative RMSFE across states, where we take the RMSFE of the bridge equation model relative to the benchmark. Figures lower than 1 indicate that the RMSFE of the bridge equation model was lower than that of the benchmark for all of the countries below the relevant quantile. Results are presented for different methods of computing the EC forecasts (EC.GDP and EC.BM) as well as with and without factors.

Table 3.6: Distribution of Relative RMSFE Across States – CO_2 Emissions – Annual Data Flow (Predictor: PI)

Release	10%	25%	50%	75%	90%
1	0.9656	0.9817	1.0097	1.0516	1.0992
2	0.9598	0.9887	1.0184	1.0400	1.1080
3	0.9487	0.9961	1.0310	1.0542	1.1459
4	0.8608	0.9257	0.9648	1.0172	1.0416
5	0.8710	0.9281	0.9742	1.0201	1.0443
6	0.8963	0.9482	0.9843	1.0196	1.0455
7	0.1732	0.2101	0.2704	0.3241	0.3958

(a) Model: EC.PI

Release	10%	25%	50%	75%	90%
1	0.9862	1.0067	1.0363	1.0818	1.1786
2	1.0157	1.0630	1.1330	1.1867	1.2624
3	1.0003	1.0826	1.1457	1.2005	1.2699
4	0.8231	0.9067	0.9496	1.0154	1.1015
5	0.8430	0.8827	0.9751	1.0322	1.1459
6	0.8901	0.9449	0.9821	1.0124	1.0389
7	0.1757	0.2003	0.2470	0.3114	0.3955

(b) Model: EC.PI with Factors

Release	10%	25%	50%	75%	90%
1	0.9765	0.9918	1.0095	1.0394	1.1251
2	0.9774	0.9906	1.0071	1.0503	1.1216
3	0.9787	0.9972	1.0108	1.0526	1.1242
4	0.9903	1.0019	1.0154	1.0648	1.1165
5	0.9935	1.0052	1.0178	1.0600	1.1245
6	0.9962	1.0026	1.0320	1.0767	1.1570
7	0.1732	0.2101	0.2704	0.3241	0.3958

(c) Model: EC.BM

Release	10%	25%	50%	75%	90%
1	1.0005	1.0198	1.0487	1.1041	1.1710
2	1.0421	1.0792	1.1285	1.1959	1.2561
3	1.0367	1.0795	1.1327	1.1872	1.2777
4	0.9499	0.9747	1.0062	1.0908	1.1965
5	0.9102	0.9488	0.9733	1.0475	1.0966
6	0.9988	1.0126	1.0327	1.0694	1.1337
7	0.1757	0.2003	0.2470	0.3114	0.3955

(d) Model: EC.BM with Factors

Notes: The same as Table 3.5 but with EC.PI instead of EC.GDP. The estimation sample is larger for the PI results compared with the GDP results due to the data availability. See text for further details.

(Figure 3.4) are comparable to those of the annual results discussed earlier. As with the annual CO_2 results using the PI model for the EC nowcasts, the gains on average are not very large until the release of the current year's EC data which improves the predictive accuracy remarkably.

Figure 3.4: Average RMSFE Across States – CO_2 Emissions – Quarterly Data Flow

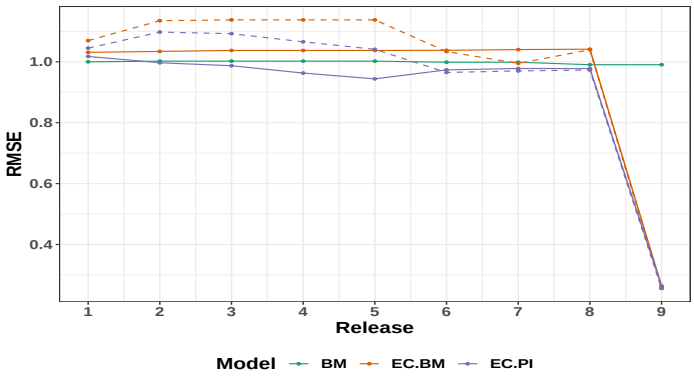

Notes: The same as for Figure 3.3.

Table 3.8 shows, in a similar way to earlier results, that if we dig down into the quantiles of the relative RMSFE across states, then there are some sizeable RMSFE gains relative to the benchmark even when quite early on in the nowcast period. These gains are as large as 15% in the case where the EC.PI bridge model is used with factors 3.8b. However, in general the findings tend to show that is fairly difficult to improve much over the benchmark in predicting CO_2 emissions until the point at which EC data become available.[13] As mentioned before, this still presents an opportunity to obtain reliable CO_2 nowcasts several months before the statistical authority releases the actual data. The numbers represent the quantiles of the distribution of relative RMSFE across states, where we take the RMSFE of the bridge equation model relative to the benchmark. Figures lower than 1 indicate that the RMSFE of the bridge equation model was lower than that of the benchmark for all of the countries below the relevant quantile. Results are presented for different methods of computing the EC forecasts

[13]We note that formal statistical testing of the relative predictive accuracy is not available in our context with only 10 out-of-sample observations, where the power of Diebold–Mariano type tests will be very low.

(EC.GDP and EC.BM) as well as with and without factors.

Table 3.8: Distribution of Relative RMSFE Across States – CO_2 Emissions – Quarterly Data Flow

Release	10%	25%	50%	75%	90%
1	0.9477	0.9795	1.0014	1.0494	1.0961
2	0.8998	0.9433	0.9880	1.0356	1.0777
3	0.8912	0.9402	0.9803	1.0179	1.0770
4	0.8654	0.9111	0.9603	1.0092	1.0427
5	0.8470	0.8974	0.9431	0.9841	1.0141
6	0.8708	0.9463	0.9857	1.0188	1.0500
7	0.8907	0.9361	0.9920	1.0231	1.0471
8	0.9101	0.9644	0.9962	1.0234	1.0481
9	0.1732	0.2101	0.2704	0.3241	0.3958

(a) Model: EC.PI

Release	10%	25%	50%	75%	90%
1	0.9671	0.9939	1.0302	1.0840	1.1427
2	0.9790	1.0340	1.1034	1.1570	1.2390
3	0.9779	1.0260	1.0803	1.1478	1.2663
4	0.9424	0.9967	1.0873	1.1245	1.1594
5	0.9308	0.9905	1.0430	1.0916	1.1287
6	0.8472	0.9299	0.9666	1.0135	1.0966
7	0.8461	0.9094	0.9818	1.0265	1.1407
8	0.8955	0.9631	0.9895	1.0148	1.0351
9	0.1757	0.2003	0.2470	0.3114	0.3955

(b) Model: EC.PI with Factors

3.5.3 Further Results

We also explored the robustness of these empirical results to a number of additional checks, the results of which we display in Appendix B. Firstly, we re-ran all results of the chapter using the per capita EC and CO_2 data. The results in Appendix B.1 and B.2 demonstrate very little difference to the results reported in the main text which indicates that the same results hold if we use the per capita or level figures when computing the growth rates. Secondly, we performed an additional set of results to explore the robustness to the sample split used in generating the out-of-sample predictions. In Figure B.5 in Appendix B.3, the evaluation sample 2000–2018 is

Table 3.8: (cont'd...) Distribution of Relative RMSFE Across States – CO_2 Emissions – Quarterly Data Flow

Release	**10%**	**25%**	**50%**	**75%**	**90%**
1	0.9765	0.9918	1.0095	1.0394	1.1251
2	0.9774	0.9906	1.0071	1.0503	1.1216
3	0.9787	0.9972	1.0108	1.0526	1.1242
4	0.9787	0.9972	1.0108	1.0526	1.1242
5	0.9787	0.9972	1.0108	1.0526	1.1242
6	0.9903	1.0019	1.0154	1.0648	1.1165
7	0.9935	1.0052	1.0178	1.0600	1.1245
8	0.9962	1.0026	1.0320	1.0767	1.1570
9	0.1732	0.2101	0.2704	0.3241	0.3958

(c) Model: EC.BM

Release	**10%**	**25%**	**50%**	**75%**	**90%**
1	1.0005	1.0198	1.0487	1.1041	1.1710
2	1.0421	1.0792	1.1285	1.1959	1.2561
3	1.0367	1.0795	1.1327	1.1872	1.2777
4	1.0367	1.0795	1.1327	1.1872	1.2777
5	1.0367	1.0795	1.1327	1.1872	1.2777
6	0.9499	0.9747	1.0062	1.0908	1.1965
7	0.9102	0.9488	0.9733	1.0475	1.0966
8	0.9988	1.0126	1.0327	1.0694	1.1337
9	0.1757	0.2003	0.2470	0.3114	0.3955

(d) Model: EC.BM with Factors

Notes: The same as Table 3.5.

compared to that of 2009–2018, showing that the results are indeed stable over time. In terms of the models we run and the variables used, we attempted several additional checks. Figure B.6 displays results using the Philly Fed's state coincident index which is like a principal component from a set of state-level employment series. The results are no better than the main results where we use GDP or PI as predictors. Figure B.7 shows that the CO_2 nowcasts are worse when we use the economic variables directly instead of through the EC bridging variable, and this direct model cannot pick up the large drop in RMSFE we see at the end of the sample on the release of the EC data. Finally, Figure B.8 shows that the results are not improved by combining both GDP and PI in the same model instead of using them individually.

3.6 Conclusion

This chapter has proposed methods for obtaining timely predictions of U.S. state-level EC and CO_2 emissions growth. Motivated by the very long publication lags for these variables, we use the flow of more timely economic data to make nowcasts and backcasts. Our contribution is a first step in the direction of making real time predictions of sub-national variables related to environmental degradation. We have moved the focus of existing panel nowcasting studies away from the classic GDP and macroeconomic nowcasting setting.

Our empirical study produces historic out-of-sample nowcasts of state-level EC growth and CO_2 emissions growth, from which we draw the following conclusions. Firstly, we conclude that the use of timely economic data can give important improvements in predicting EC growth on average across all states, and can deliver especially large gains in a smaller group of states including larger ones such as Florida. These predictive gains can occur almost two years before the EC data are released. On the other hand, we conclude that the CO_2 predictions are less affected by the release of economic data and that it is better to wait until the release of the current year's EC data, at which point a very accurate prediction can be made. This is, nevertheless,

able to produce a reliable CO_2 prediction many months before the statistical authority releases the data and using a method which is far simpler.

There is still much more work to be done on state-level energy and CO_2 nowcasting. With the 'big data' revolution increasing the granularity of available data, it would be useful to see our method perform with a more complete dataset. An interesting example would be to assess whether firm-level emissions data can be aggregated in a timely fashion for the purpose of predicting state-level emissions.

Chapter 4

Cross-sectional Dependence in Growth-at-Risk

4.1 Introduction

Monetary policy remained accommodative after the GFC, to revive growth and restore the financial systems. Continuation of such policy support confronted policymakers with a key challenge – the build-up of financial vulnerabilities and consequent worsening of the medium term risks. Highlighting this inter-temporal trade-off, the International Monetary Fund (IMF), introduced the concept of GaR as a surveillance tool (IMF 2017). GaR quantifies downside risks to GDP growth and is measured as the lower quantiles of the GDP growth distribution.

This chapter re-examines the relationship of GaR for 24 countries with seven macro-financial and uncertainty indicators in a multi-country panel quantile regression framework. A growing range of papers contribute to the understanding of the relationship of financial conditions and the tail quantiles of GDP growth, and two main perspectives emerge. One set of papers finds that financial conditions play a critical role in the future distribution of GDP growth and particularly influence the lower quantiles (Adrian et al. 2019a; Aikman et al. 2019; Carriero et al. 2020; Adrian et al. 2022; Iseringhausen 2023). On the other hand, Plagborg-Moller et al. (2020) find

that financial variables have no additional predictive information for the distributional forecasts of GDP growth. Brownlees and Souza (2021) find that models using vulnerability indicators rank low in terms of out-of-sample forecast performance. Reichlin et al. (2020) show that among financial condition indicators, price variables such as spreads have limited advanced information on growth vulnerability, while non-financial leverage provides leading signals for the left tail of the GDP distribution.

In an interlinked global economy, increased trade and financial integration with time and the strong co-movement of key macroeconomic indicators across countries are recognised as stylised facts (Ca' Zorzi et al. 2020). Foreign financial conditions have been found to have important contributions to domestic financial conditions over the last two decades and the speedy transmission of spillover impacts challenges timely policy action to control the domestic financial conditions (Arregui et al. 2018). While spillovers may arise from multiple sources, our framework allows natural data-driven spillovers in the form of CSD. Therefore, we do not need to assume any specific source, channel or structure of the spillover effects. Among the GaR studies to date, Lloyd et al. (2023) explicitly include foreign variables and find significant impact and improved model performance.

We differ in our method from the existing panel quantile models (for instance Aikman et al. 2019; Adrian et al. 2022; Iseringhausen 2023; Lloyd et al. 2023) and incorporate the CSD panel framework. To construct the CSD panel quantile model for GaR, the closest related study is that of Harding et al. (2020), which extends the CCE technique of Pesaran (2006) and Chudik and Pesaran (2015a) to quantile regressions. The CCE approach has the unique advantage that it simplifies the entire estimation process and enables direct estimation of the factor-augmented panel model, without the requirement to explicitly estimate any additional quantities, such as, the number of factors, the factors themselves or their loadings. Despite using a long enough panel dataset, there are constraints as the GDP is measured at most quarterly. We address this issue by allowing heterogeneity through the country specific fixed effects and pooling the regression coefficients and factor loadings. The homogeneous loadings

allow us to include 'time-effects' in addition to cross-sectional fixed effects, which have not so far been included in panel quantile models due to complications in estimation and asymptotics (Chernozhukov et al. 2020).

From a forecasting perspective, we also implement another important modification in the factor estimation technique. Harding et al. (2020) estimate the factors using the CCE method in a panel quantile setting, which is based on contemporaneous cross-sectional averages of the variables. In a purely forecasting scenario, the contemporaneous GDP growth is not available. So, we use the LCCE estimation technique, developed in the previous chapter, extended to the panel quantile regression framework. This is our main panel quantile model with CSD. A panel fixed-effects model not including the CSD component (no-CSD) (as in Aikman et al. 2019; Adrian et al. 2022) and unconditional quantiles (as in Brownlees and Souza 2021) are the benchmarks.

We estimate projected GaR up to 12 quarters using the local projections method of Jordà (2005), and subsequently evaluate the models in-sample and recursive out-of-sample set-ups for each vulnerability indicator. A graphical analysis of a time series of predicted GaR from each model follows. A fitted skew-t distribution (Azzalini and Capitanio 2003) in turn generates four time-varying conditional moments and the entire predictive distribution. Finally, a decomposition of the predicted GaR from the CSD panel model separates the two components – the panel component consisting of the fixed-effects and the effect of the vulnerability indicator, and the combined effect of the factor and the loadings.

We emphasise four main findings. Firstly, in the presence of the factors characterising CSD, all the seven indicators have a limited impact on the 5% GaR for almost all horizons up to 12 quarters. However, certain predictors, such as Term Spread (TS), Credit to GDP Gap (CG) and Economic and Polictical Uncertainty (EPU), have significant and interpretable impact in the medium term for higher GaR thresholds (10–15%). The factors have dual interpretation as proxies for unobserved common shocks and international inter-linkages. We conclude that the commonly accepted vulnerability indicators associated with crisis, do not have any significant marginal

predictive power for the lower quantiles of GDP growth. This relates to the findings of Plagborg-Moller et al. (2020) and Brownlees and Souza (2021). Alternatively, exclusion of the factors makes all the vulnerability indicators significant as documented in other GaR studies such as Adrian et al. (2022).

Our second key finding is the superior performance of the CSD panel model in both in-sample and out-of-sample evaluations, using Tick-Loss (TL), also known as the quantile score function. Our findings are robust in different sub-samples, including and excluding the GFC of 2007–09.

In the third main finding, we note that out-of-sample GaR predictions from the CSD panel model have interpretable economic patterns over time for most countries. The predicted higher moments, especially variance and kurtosis, provide important early warning signals for volatility and tail–risks. From the moment analysis, we conclude that the risk emanates from a combination of a leftward shift of the entire distribution and rising tail–risks. We complement the findings from the moments and the predictive density by Expected Shortfall (ES) – another well-accepted measure of tail–risk.

Finally, our results demonstrate that the unobserved factors have a strong influence and a mitigating role in normal economic times, whereas in times of economic distress the factors further worsen the situation.

This chapter relates to three important strands of literature. Firstly, and most directly, it relates to the GaR literature. Although the term GaR was originated by the IMF (2017), the use of quantile regressions for GDP growth existed even before (Manzan 2015). GaR is studied in the context of individual countries or regions (Adrian et al. 2019a; Ferrara et al. 2022) and multi-country frameworks (Aikman et al. 2019; Brownlees and Souza 2021; Adrian et al. 2022; Iseringhausen 2023; Lloyd et al. 2023). This chapter is closer to the latter strand of literature. The closest to this chapter is that of Lloyd et al. (2023) who, in a panel framework, establish the significant impact of international inter-linkages and GDP tail–risks. Carriero et al. (2020), Plagborg-Moller et al. (2020) and Ferrara et al. (2022) estimate GaR in a Bayesian framework. The quantile regression framework to identify tail–risks has also been

applied to other important macro-financial variables, such as unemployment, inflation (Adams et al. 2021), exchange rates (Eguren-Martin and Sokol 2022), house prices (Alter and Mahoney 2020) and capital flows (Martin et al. 2020; Gelos et al. 2022).

Secondly, this chapter relates to the literature on CSD in panel quantile regressions. CSD has been established as an important characteristic of panels. It can be estimated with the CCE technique of Pesaran (2006), which was further developed for dynamic heterogeneous panels by Chudik and Pesaran (2015a). An alternative estimation technique is that of Bai (2009). Quantile regression was introduced by the seminal work of Koenker and Bassett (1978). The first panel quantile model was that with fixed-effects of Koenker (2004), and the literature expanded thereafter (Lamarche 2010; Canay 2011; Galvao and Wang 2015). Harding and Lamarche (2014) first introduced the interactive fixed-effects (CSD) in panel quantile models. This has been further developed for dynamic heterogeneous panels by Harding et al. (2020). Ando and Bai (2020) provide an alternative iterative estimation technique similar to Bai (2009).

Thirdly, this chapter relates to GDP catastrophe and early warning literature, as we include four vulnerability indicators in addition to the aggregate financial conditions index which is commonly used in GaR literature. We mention papers that link various indicators to recession: credit boom (Schularick and Taylor 2012; Jordà et al. 2013, 2015, 2016; Krishnamurthy and Muir 2017, and others); TS (Rudebusch and Williams 2009; Garcia Alvarado 2020, and others), CG (Drehmann and Juselius 2014) and uncertainty (Bloom 2014; Ahir et al. 2018).

The rest of the chapter is organised as follows. Section 4.2 describes the econometric framework of cross-sectionally dependent panel quantile regressions we use to model and predict GaR. Section 4.3 presents the empirical application – i.e., assess the significance of the predictors, quality of fit and analyses the time series of predicted GaR in an out-of-sample setting. Section 4.4 concludes the chapter.

4.2 Econometric Framework

In this section, we describe the quantile regressions used to model the distribution of real GDP growth and its relationship with different vulnerability indicators. With the quantile regression technique of Koenker and Bassett (1978), we can analyse the impact of changes in a set of conditioning variables on the entire conditional distribution of the dependent variable, i.e. GDP growth. Optimal estimates of a range of conditional quantiles are obtained instead of estimating only the mean.

We denote $Y_{i,t}$ as the quarterly growth rates of seasonally adjusted GDP and $x_{i,t}$ as the selected indicator from the set of the different vulnerability indicators detailed in Section 4.3. Time is denoted by $t = 1, 2, \ldots, T$ and the countries for which we estimate the GaR – i.e., the cross-sectional units are labelled with $i = 1, 2, \ldots, N$.

We develop our panel framework for the conditional quantiles of GDP growth following Harding et al. (2020) and adapt it to the specifics of our data-set. First, let us consider the following panel data model for the forecast horizon of h quarters:

$$Y_{i,t+h} = \alpha_i + \beta^h x_{i,t} + \epsilon_{i,t} \tag{4.1a}$$

$$\epsilon_{i,t} = \lambda f_t + \zeta_{i,t} \tag{4.1b}$$

$$x_{i,t} = \alpha_{xi} + \gamma f_t + v_{i,t} \tag{4.1c}$$

The CSD represented by the factor error structure of equation (4.1b) is estimated by the CCE method of Chudik and Pesaran (2015a) and adapted to quantile regressions by Harding et al. (2020). We want to estimate the factor-augmented panel quantile regression in equation (4.2) which is obtained by combining equations (4.1a) and (4.1b). The primary role of equation (4.1c) is to estimate the factors using the CCE technique and has no direct role in predictions.

$$Q_{Y_{i,t+h}}(\tau|x_{i,t}) = \alpha_i(\tau) + \beta^h(\tau)x_{i,t} + \lambda(\tau)f_t \tag{4.2}$$

where τ is the quantile in the interval $(0, 1)$ and:

$$\theta_i(\tau) = \left(\alpha_i(\tau), \beta^h(\tau)\right) \text{ is the set of parameters to be estimated and,} \quad (4.3)$$

$$Q_{Y_{i,t+h}}(\tau|x_{i,t}) = \inf\{y : P(Y_{i,t+h} \leq y|x_{i,t})\} \quad (4.4)$$

We use LCCE with lagged dependent variables in the cross-sectional averages as the LCCE technique has been shown to be consistent and asymptotically unbiased in panel regressions (Chapter 2). This is a necessary modification for a forward-looking analysis where we do not assume the knowledge of the target quarter GDP growth. Thus, we define our vector of cross-sectional averages as in equation (4.5) and minimise the asymmetric quantile loss function given by equation (4.6):

$$\overline{z}_t = \begin{pmatrix} \overline{Y}_{t-1} \\ \overline{x}_t \end{pmatrix} \quad (4.5)$$

where

$$\overline{Y}_t = \frac{1}{N}\sum_{i=1}^{N} Y_{i,t},\ \overline{x}_t = \frac{1}{N}\sum_{i=1}^{N} x_{i,t},$$

$$\rho_\tau(u) = u\left[\tau - I(u \leq 0)\right] \quad (4.6)$$

where I(.) is the indicator function – i.e.,

$$I(u \leq 0) = \begin{cases} 1, & \text{if } u \leq 0 \\ 0, & \text{otherwise} \end{cases}$$

Hence, the final equation we estimate is:

$$Q_{Y_{i,t+h}}(\tau|x_{i,t}) = \alpha(\tau) + x_{i,t}\beta^h(\tau) + \sum_{l=0}^{p_T} \overline{z}_{t-l}\Delta_l(\tau) \quad (4.7)$$

Harding et al. (2020) demonstrate the asymptotic equivalence of the two optimization problems – i.e., the one with unknown factors as in equation (4.2) and the one where the factors are substituted by cross-sectional averages. The CCE approach has the unique advantage that it simplifies the entire estimation process and enables direct estimation of the factor-augmented panel model, without the requirement to explicitly estimate any additional quantities, for example, the number of factors, the factors or their loadings.

The data set we use is large. However, with the highest frequency of GDP growth being quarterly, we still face data limitations. Accordingly, we allow heterogeneity through country-specific fixed-effects coefficients and pool the other parameters. In addition to the advantages of pooling in panel model, the homogeneous factor loadings also, in a way, let us include time fixed effects, which have not so far been included in panel quantile models due to complications in estimation and asymptotic (Chernozhukov et al. 2020).

We benchmark the performance of the CSD panel model against the panel model which does not incorporate CSD. This is similar to the model implemented in a number of recent GaR and other 'at-risk' papers (for instance Aikman et al. 2019; Adrian et al. 2022):

$$Q_{Y_{i,t+h}} = \alpha_i(\tau) + \beta^h(\tau)x_{i,t} \tag{4.8}$$

All models are estimated for up to 12 quarters ahead using local projections (Jordà 2005) which gives us the estimated quantile of GDP growth distribution for the specified horizon. This enables us to understand how the left tail of the GDP develops over the forecast horizons. For inference we use bootstrap. Various forms of block bootstrap and tapered block bootstrap (Gregory et al. 2018) were tried, but they failed to improve results. For that reason, we keep to i.i.d. bootstrap. The coefficients $\beta^h(\tau)$ quantifies the association between the vulnerability indicator and the quantiles τ of the predicted GDP growth distribution at horizon h.

4.3 Empirical Application

In the empirical application, we estimate the LCCE panel quantile model as described in Section 4.2. We then assess the fit of the model, evaluate the significance of several vulnerability indicators and establish prediction accuracy. Thereafter, we recover the entire predicted density by fitting a skew-t density and arrive at an estimated time series of risk-quantification measures.

4.3.1 Data

Our empirical application is based on the cross-country data-set of Brownlees and Souza (2021) consisting of 24 OECD countries covering largely the period Q1:1973 to Q4:2016. We use seven indicators as predictors. These broadly belong to two groups – macro-financial and uncertainty indicators. Five of our macro-financial indicators used in modelling GDP catastrophes could be further grouped into financial conditions and macro-financial imbalance indicators as per the practical guidance on GaR by Prasad et al. (2019). Representing financial conditions, we have the National Financial Conditions Index (NFCI) and TS indicating the price of risks embedded in asset prices; CG and Credit to GDP Growth (CR) represent macro-financial imbalances due to credit boom–bust cycles. We also include House Prices (HP) representing both macro-financial imbalances through housing market disequilibrium and financial conditions as HP also reflect ease of obtaining finance.

Although NFCI has received the maximum attention in GaR studies, the other predictors also have a long history of association with economic downturns. The predictive content of TS for future growth and recession is known for a long time (see Rudebusch and Williams 2009; Garcia Alvarado 2020, and others). The forecasting power of TS for future GDP is one of the most robust stylised facts in macroeconomics (Adrian et al. 2019b). Measured by the deviation of credit to GDP ratio from its long-run trend, CG is often associated with leverage and financial cycles. It measures the build-up of systemic leverage that poses risk to the banking sector (Drehmann

et al. 2011). The Basel Committee of Banking Supervision (BCBS) recommends its use to track excess credit and vulnerability to the banking sector (BIS 2010). A series of empirical studies document the link between HP and the real economy. Claessens et al. (2012) find that recessions following housing busts are weaker and recoveries associated with rapid growth in credit and housing tend to be stronger. Movements in both HP and CR are jointly noted to precede crisis and are important as early warning indicators (see Aikman et al. 2019, and the references therein).

Additionally, we also model GaR on two indicators of uncertainty – EPU and World Uncertainty Index (WUI).[1] The literature examining the relationship between uncertainty and real economic activity has expanded rapidly after the GFC (see Jo and Sekkel 2019, and the references therein). Ahir et al. (2018) define WUI using the frequency of the word 'uncertainty' in the quarterly Economist Intelligence Unit country reports. The index generally spikes around the occurrences of major disruptions originating from economic, political or health issues. Baker et al. (2016) develop the EPU index as a text-based indicator capturing general uncertainty based on newspapers. WUI and EPU are conceptually different yet have a lot in common and co-move over time (Ahir et al. 2018) and tend to precede declines in growth. While the previously stated macro-financial group of indicators has already been studied in the context of GaR, the uncertainty indicators have only very recently been studied by Brownlees and Souza (2021).

The importance of modelling CSD is already evident from the literature and stylised facts. Further from our data, Figure 4.1 shows the results of a systematic examination of international macro-financial synchronisation using correlations patterns over time. We study the degree of co-movement between the different indicators within countries using simple pair-wise correlations. We compare the distribution of the bilateral correlations for all possible country pairs for each indicator, over two different sub-periods, to identify the changes in the nature of association among countries. The first sub-period ends in Q4:1999 and the second sub-period starts at Q1:2000.

[1]The uncertainty indices have a relatively shorter time-span starting on 1985 and 1996 respectively.

Figure 4.1: Distribution of Bilateral Correlations

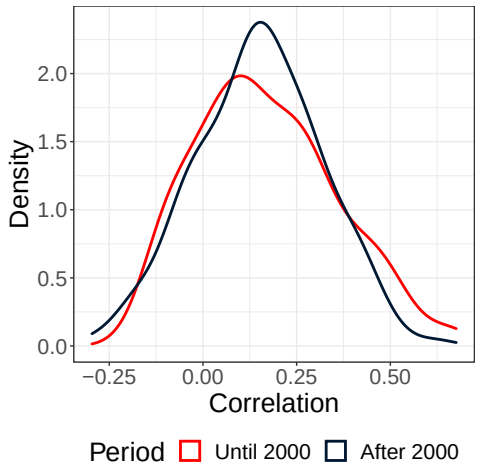

(a) CG

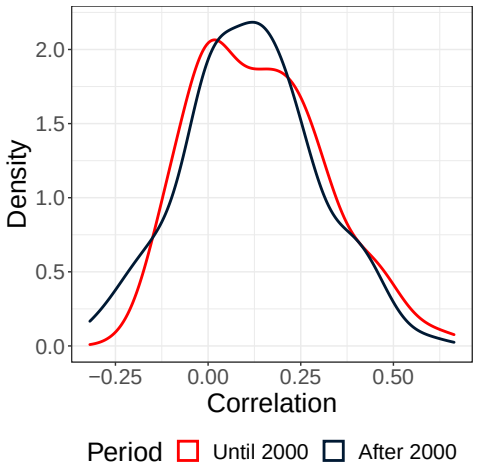

(b) CR

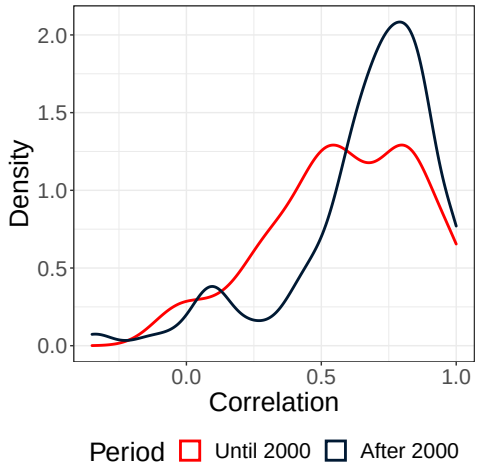

(c) EPU

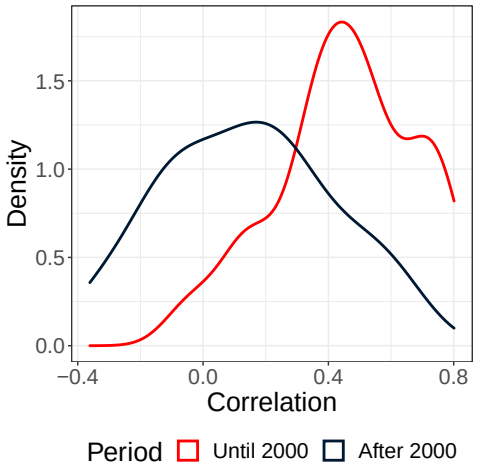

(d) HP

Figure 4.1: (cont'd...) Distribution of Bilateral Correlations

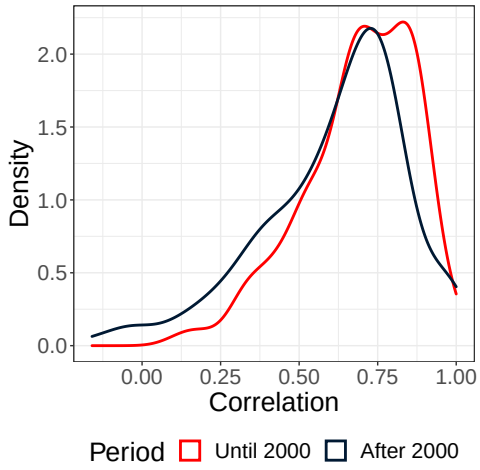

(e) TS

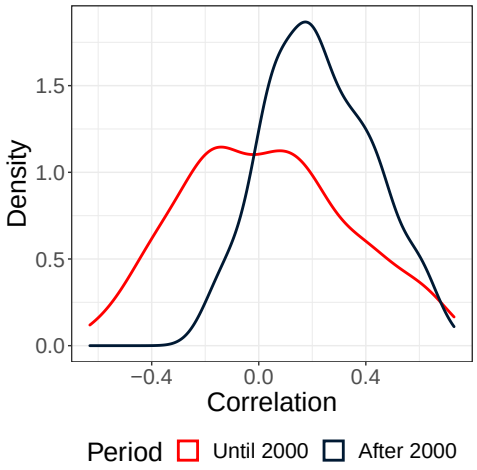

(f) WUI

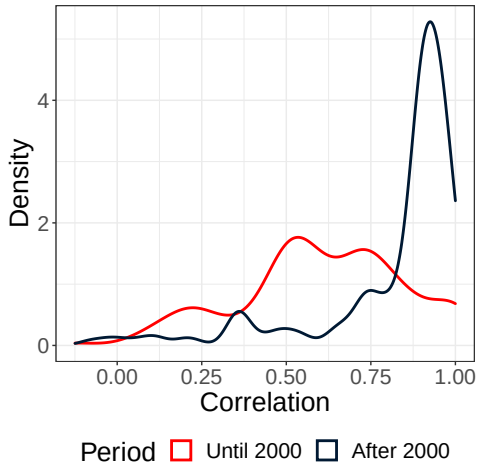

(g) NFCI

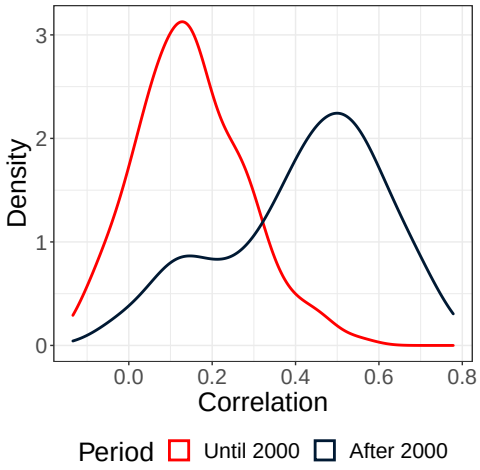

(h) GDP Growth

Notes: The figures show the distribution of all possible pairwise correlations among countries for the selected indicator over time. We split the time series into two parts to identify the changing nature of synchronisation among the countries. Excluding Greece, Israel, Portugal, Ireland and Belgium. Figure 4.1d is based on 12 countries for which long time-series data were available.

The plots (Figure 4.1) reveal a general shift of the distribution towards the right. This is most striking for the NFCI (Figure 4.1g) and is also very distinct for GDP growth (Figure 4.1h). Especially from 2003 onwards, we see that the financial condition indices of all the countries move remarkably along the same path, excepting a few countries. The credit variables do not show a rightward shift in distribution but show a higher peakedness of the density function around the positive modal values (Figures 4.1a and 4.1b). TS remain equally synchronised before and after 2000. Surprisingly, the pair-wise correlation for HP seems to have declined indicating less synchronisation post-2000 (Figures 4.1d and 4.1e). These initial indications of increased synchronisation of macro-financial data in recent times suggest a greater impact of spillovers and common shocks in recent times. We now proceed to the actual estimation of the CSD panel models in the subsequent sections.

4.3.2 In-Sample Results

The results of the in-sample analysis of the different models are presented in this section in two parts. Firstly, we assess the significance of the various vulnerability indicators and identify the determinants of GaR at different forecast horizons. Subsequently, we evaluate the quality of fit of the benchmark models stated in Section 4.2.

We begin by reporting the estimation results of a set of quantile regressions used to gauge the explanatory power of each predictor. For each country, forecast horizon $h = 1, 2, 3, \ldots, 12$ and predictor, we estimate the 5% quantile regression for the equations (4.2) and (4.8) – i.e., the panel with and without CSD respectively. We estimate the GaR up to 12 quarters ahead as this is the time range considered by Adrian et al. (2022) as it is common while framing policies. Models with and without CSD are presented in Figure 4.2, where we show the relationship between the 5% GaR and different vulnerability indicators across horizons.

We also use additional GaR levels: 10 and 15%. Most of the GaR literature mentions a 5% worst-case scenario. But 5% GaR leaves very few actual occurrences of such events, even with advanced economies which have a large history of macroeconomic

data. The size of the testing window must increase as we increase the severity of the GaR measure. With quarterly GDP being the dependent variable, there is limited scope to increase the number of observations. While it is important for policymakers to know and possibly influence the conditional response of the 5% GaR, modelling higher levels of GaR can also provide useful signals. Thus, to ensure the dual objectives of the robust analysis and usefulness to policy, we use several levels of GaR.

We focus on the impact of each vulnerability indicator on GaR estimated from the quantile regressions. We examine the relationship between one standard deviation change in the vulnerability indicator and the corresponding adjustment in GaR at different horizons (Adrian et al. 2018; Aikman et al. 2019; Lloyd et al. 2023, and others). The coefficients are interpreted as impact on estimated GaR, due to one standard deviation change in the vulnerability indicator. Since we directly model the quantiles of quarterly percentage changes in GDP, the figures directly correspond to the quarterly changes in GaR for the respective horizon. We also look at the one standard deviation bootstrap confidence bands of the estimated coefficients.

Surprisingly, from the CSD panel model (Figure 4.2), we see very little impact of any of the seven vulnerability indicators on 5% GaR. There is an initial negative impact of tightening financial conditions, which ease out and become insignificant as we increase the forecast horizon. This finding is contrary to the observations from cross-sectionally independent panels. The no-CSD panel corroborates the earlier findings of Adrian et al. (2022), who note that financial conditions have a negative impact on GaR in the near term and have a positive impact on farther horizons. The 5% GaR from the no-CSD panel seems to benefit from tighter financial conditions in the longer term. This effect disappears once we account for the CSD in panels.

At higher GaR levels (results in Appendix C.1.1), we find TS, CG and EPU to be significant in the medium term. Brownlees and Souza (2021) also find TS to be the second most important variable in predicting GaR in the in-sample analysis of up to four quarters prediction horizon for half of the sample of countries. The significance of TS is in line with the literature on early warning signals and the yield curve inversion

Figure 4.2: Impact of Variables on 5% GaR

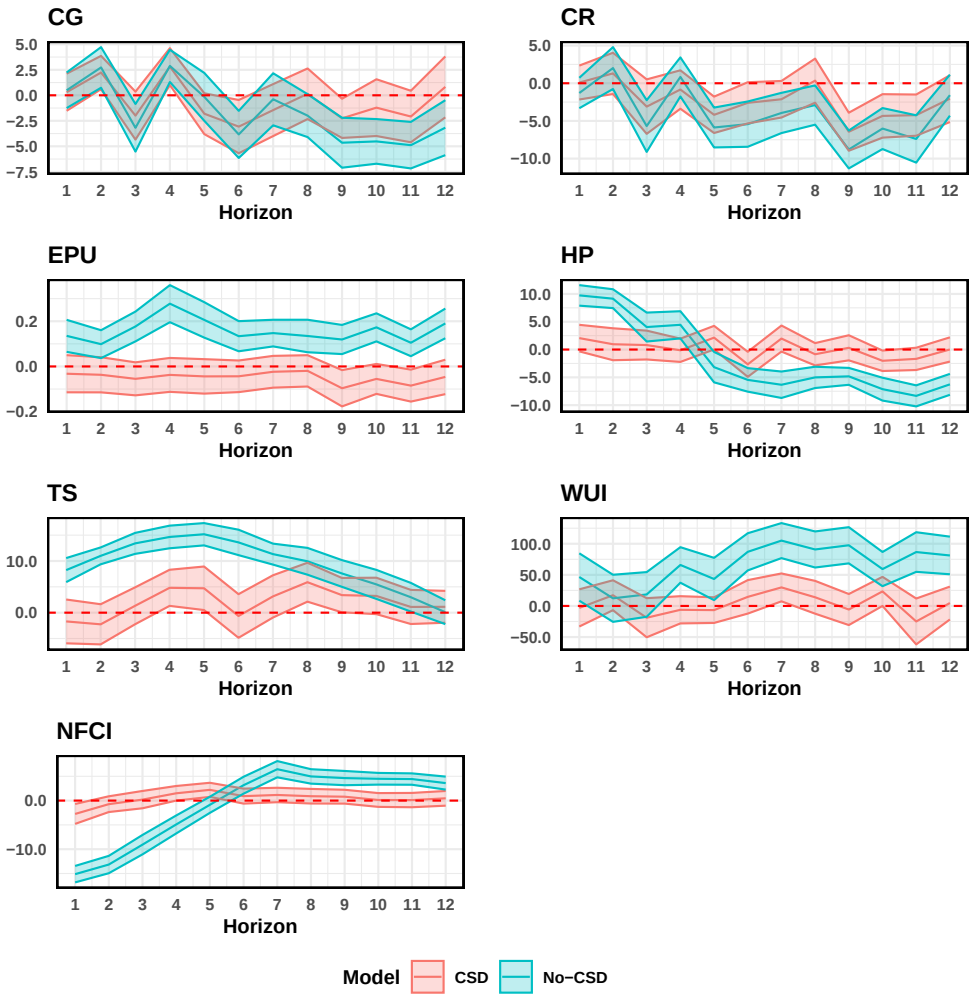

Notes: These figures compares the significance of the predictor over various prediction horizons for the two panel models. Shaded areas represent one standard deviation bootstrap confidence intervals.

phenomenon. The inverse relationship, i.e. association of larger CG with declining GaR, is consistent with Drehmann and Juselius (2014) who establish CG as an important early warning indicator up to five years preceding a crisis. Other variables we consider remain insignificant for all GaR levels.

These results partially corroborate the findings of Aikman et al. (2019), who find financial conditions insignificant in the medium term and in the presence of other determinants of GaR. The findings also resonate with those of Reichlin et al. (2020) who conclude that there is limited value in financial variables for detecting GDP risk in advance and that of Plagborg-Moller et al. (2020) who find no marginal power of financial variables to predict GaR, in addition to macroeconomic data. In general, therefore, it seems that the strength of the relationship between GaR with the NFCI as revealed by a panel model without CSD is overstated. The reason for the difference in results may be inferred from the interpretation of the CSD factor error structure. The multi-factor error structure could be interpreted as natural data-dependent cross-country spillover impacts. These could also be regarded as proxies for common shocks not directly observed. While each of the seven vulnerability indicators has been known to forewarn of a crisis, our findings suggests that there are common underlying factors that contribute to GaR projections and these variables do not have any noteworthy predictive content beyond the aforementioned common factors.

Next, we compare the in-sample goodness-of-fit measure for the panel models, one with the CSD and one without CSD. We use the metric developed by Koenker and Machado (1999), which is a quantile-specific relative measure of the goodness-of-fit of two conditional quantile functions. This measure of in-sample fit has been recently used in 'at-risk' studies by Eguren-Martin and Sokol (2022) and Lloyd et al. (2023). We define the goodness-of-fit measure R^1 for GaR level τ and forecast horizon h as:

$$R_h^1(\tau) = 1 - \frac{\hat{V}(\tau)}{\tilde{V}(\tau)} \tag{4.9}$$

where $\hat{V}(\tau)$ denotes the sum of weighted absolute residuals from the respective model

that we are trying to evaluate. $\tilde{V}(\tau)$ denotes the sum of weighted absolute residuals of the historical unconditional quantiles. The interpretation is similar to the standard R^2 in linear regression. We can therefore attribute any difference in $R^1(\tau)$ estimated from the CSD and no-CSD panels as the incremental contribution of the multi-factor error structure to the goodness-of-fit of the estimated τ^{th} quantile of the h–quarter-ahead real GDP growth.

The results in Table 4.1 reveal an improved in-sample fit from the CSD panel models as compared to the ones without CSD for 5% GaR. Similar results for other GaR levels are presented in Appendix C.1.2. The measures are comparable to that of Lloyd et al. (2023). $R^1(\tau)$ nearly doubles due to the inclusion of the CSD. Also, $R^1(\tau)$ remains at similar levels across all horizons and is elevated in the CSD models for all the vulnerability indicators. The improvement in goodness-of-fit further strengthens the importance of modelling CSD.

4.3.3 Out-of-Sample Assessment

In this section, we back-test the proposed CSD panel model and assess it relative to the benchmark models in a pseudo-out-of-sample framework. We generate out-of-sample GaR forecasts in an h–step-ahead recursive window scheme. The time dimensions of the panel are split up into estimation and evaluation windows. If we denote the total number of periods by T, then T is split as $T = R + P$ where we estimate the model using the first R periods and evaluate the model by computing the recursive predictions for the following P periods. For the out-of-sample analysis presented below, we consider $R = 0.25T$.

Coverage

We define the average empirical coverage for the predicted GaRs as the mean (over time and cross-sections) number of realisations of GDP growth that are higher than the predicted GaR – equation (4.10a). Coverage of accurate GaR predictions is expected not

Table 4.1: In-Sample Goodness-of-Fit: 5% GaR

Indicator	Horizon 1	2	3	4	5	6	7	8	9	10	11	12
						CSD						
CG	0.0298	0.0304	0.0290	0.0309	0.0340	0.0346	0.0357	0.0344	0.0335	0.0298	0.0259	0.0275
CR	0.0284	0.0283	0.0291	0.0294	0.0307	0.0305	0.0316	0.0308	0.0321	0.0305	0.0314	0.0351
EPU	0.0556	0.0538	0.0554	0.0569	0.0555	0.0509	0.0530	0.0510	0.0486	0.0462	0.0460	0.0423
HP	0.0266	0.0240	0.0242	0.0241	0.0253	0.0262	0.0273	0.0273	0.0274	0.0264	0.0269	0.0282
TS	0.0380	0.0380	0.0375	0.0379	0.0364	0.0357	0.0335	0.0309	0.0300	0.0288	0.0257	0.0275
WUI	0.0493	0.0427	0.0427	0.0413	0.0426	0.0449	0.0445	0.0423	0.0287	0.0229	0.0202	0.0215
NFCI	0.0600	0.0525	0.0539	0.0538	0.0540	0.0502	0.0479	0.0381	0.0326	0.0317	0.0296	0.0305
						No-CSD						
CG	0.0005	0.0001	0.0001	0.0006	0.0000	0.0000	0.0010	0.0006	0.0002	0.0001	0.0001	0.0005
CG	0.0000	0.0001	0.0003	0.0002	0.0010	0.0002	0.0016	0.0000	0.0012	0.0002	0.0003	0.0005
EPU	0.0232	0.0175	0.0212	0.0198	0.0183	0.0154	0.0165	0.0105	0.0116	0.0119	0.0145	0.0078
HP	0.0014	0.0021	0.0027	0.0002	0.0003	0.0008	0.0002	0.0000	0.0000	0.0004	0.0015	0.0013
TS	0.0012	0.0003	0.0000	0.0000	0.0006	0.0019	0.0010	0.0005	0.0016	0.0013	0.0000	0.0000
WUI	0.0063	0.0054	0.0009	0.0005	0.0020	0.0005	0.0003	0.0017	0.0010	0.0010	0.0001	0.0012
NFCI	0.0002	0.0014	0.0038	0.0053	0.0094	0.0103	0.0091	0.0069	0.0055	0.0050	0.0059	0.0044

Notes: The table compares the in-sample goodness-of-fit measure for the two panel models across forecast horizons. The goodness-of-fit is measured relative to unconditional quantiles.

to deviate very far from the nominal coverage. If $GaR_{i,t|t-h}$ denotes the h–quarter-ahead $100 \times \tau\%$ GaR, then its coverage can be expressed as:

$$C_{\tau,h} = \frac{1}{N}\sum_{i=1}^{N}\left[\frac{1}{T}\sum_{t=h+1}^{T} 1_{Y_{i,t}>GaR_{i,t|t-h}}\right] \tag{4.10a}$$

Figure 4.3 and Appendix C.2.1 contain the plots of average empirical coverages across various quantile levels. We find that the coverage is quite close to the nominal expected coverage for the majority of the CSD models[2] as compared with the benchmark or no-CSD panel model. It is hard to arrive at the best performing model based on coverage alone, therefore we substantiate these findings with additional out-of-sample performance indicators below.

Figure 4.3: Coverage

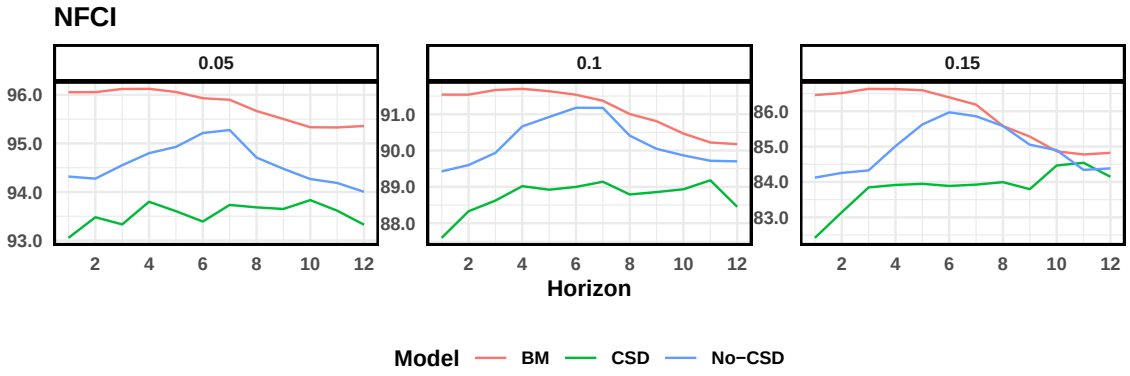

Notes: These figures plot the coverage for the different models with NFCI as predictor considered over different prediction horizons. The GaR levels are indicated in the panel headers. The other predictors can be found in Appendix C.2.1.

DQ Test

Dynamic Quantile (DQ) of Engle and Manganelli (2004) tests ascertain the optimality of the estimated conditional quantiles and hence the underlying model by testing the predictability of the hit sequence using specific regressors. We define the hit sequences

[2]The coverage does not appear adequate for the EPU and WUI models which are estimated on shorter data spans.

as the series of binary variables equalling $1-p$, when we observe a violation of the $p\%$ GaR and $-p$ otherwise as:

$$H_{i,t} = 1_{Y_{i,t}<GaR_{i,t|t-h}} - p \tag{4.10b}$$

We report two versions of the DQ tests of Engle and Manganelli (2004). First we present unconditional tests with no auxiliary predictors. The second one tests optimality in the presence of lagged hit sequences as regressors. We consider a suitably tailored Wald test statistic as in Brownlees and Souza (2021). We define the DQ regressions as:

$$H_{t+h} = c_0 + \sum_{k=1}^{K} c_k W_{kt} + u_{t+h} \tag{4.10c}$$

W_{kt} is assumed to be constant and lagged hits respectively for DQ_{unc} and DQ_{hits}. We test the following null hypothesis:

$$H_0 : c_0 = c_1 = \cdots = c_k = 0 \tag{4.10d}$$

Finally, we report the number of countries for which we fail to reject the null hypothesis at the 5% level of significance – i.e., the countries for which the hit sequences of the violations of predicted GaR are optimal. We consider the DQ tests for 12 horizons. Table 4.2 shows that the panel models using NFCI as predictor can generate optimal sequences of predicted GaR for majority of the countries in our sample. The unconditional quantile benchmark shows a minor improvement in the conditional DQ test results in Table 4.2b but the same does not hold when we run the robustness results in Appendix C.2.4 Table C.5. The DQ tests for other models using different indicators are placed in Appendix C.2. Appendix C.2.4 contains the results for DQ tests excluding the GFC. These conclusions remain unchanged.

Table 4.2: DQ Tests – NFCI

GaR	5%			10%			15%		
Horizon	BM	CSD	No-CSD	BM	CSD	No-CSD	BM	CSD	No-CSD
1	18	14	16	12	16	15	14	17	12
2	18	20	20	14	19	19	14	17	17
3	18	21	20	14	18	20	14	18	16
4	17	20	20	14	18	20	14	20	18
5	18	19	20	14	17	20	14	16	18
6	18	18	21	14	19	19	15	17	17
7	18	18	22	15	19	20	16	17	17
8	17	19	21	16	18	20	16	17	19
9	18	19	21	17	19	19	16	17	18
10	18	19	20	18	19	19	15	18	19
11	18	20	20	18	18	19	14	18	18
12	18	19	20	18	17	19	14	17	18

(a) Unconditional

GaR	5%			10%			15%		
Horizon	BM	CSD	No-CSD	BM	CSD	No-CSD	BM	CSD	No-CSD
1	8	13	8	6	11	5	6	10	6
2	18	18	15	15	18	13	7	12	12
3	21	20	20	13	15	13	13	17	11
4	21	20	20	18	18	17	13	18	16
5	21	20	21	18	19	18	17	14	18
6	20	19	21	20	14	19	17	11	18
7	21	19	23	19	17	21	17	15	18
8	22	22	20	19	17	20	17	18	18
9	19	22	20	21	17	20	14	17	17
10	19	20	22	22	19	18	21	18	17
11	19	19	20	20	19	21	17	18	20
12	19	18	20	21	20	20	18	18	19

Notes: These tables compare the results of the DQ tests across the three different panel models under consideration. The figures count the countries (out of 24) for which we are not able to reject the null hypothesis, i.e. we have an optimal predicted GaR sequence at 5% level of significance.

(b) Hit

TL

TL, also referred to as the quantile score, is a standard loss function to formally evaluate the conditional quantile estimates and is used in several recent GaR and density prediction studies (see Manzan 2015; Carriero et al. 2020; Brownlees and Souza 2021; Iseringhausen 2023). It is the asymmetrically weighted average of the difference between observed and h–quarter-ahead predicted quantile (the GaR). equation (4.10f) is the sample estimate of the expected h-step ahead loss defined as (see Clements and Galvão 2008):

$$TL_{\tau,h} = E\left[\rho_\tau\left(Y_{i,t} - GaR_{i,t\|t-h}\right)\right] \tag{4.10e}$$

We compare the performance of each model by TL. We define the out-of-sample average TL for a forecast horizon of h quarters as:

$$TL_{\tau,h} = \frac{1}{N}\sum_{i=1}^{N}\left[\frac{1}{T}\sum_{t=h+1}^{T}\rho_\tau\left(Y_{i,t} - GaR_{i,t|t-h}\right)\right] \tag{4.10f}$$

$$\text{where } \rho_\tau(u) = u(\tau - 1_{u\leq 0}) \tag{4.10g}$$

Table 4.3 displays the TL and shows that the CSD panel model stands out in terms of larger gains in TL against the benchmarks. For lower quantiles (5, 10 and 15%) that are considered as measures of GaR, the CSD panel model emerges as the best-performing model, across all the 12 horizons under consideration. We show only NFCI here and to complete the analysis, TL with all other predictors are presented in Appendix C.2.3. The same results hold for other indicators as well, except WUI.

We ensure robust out-of-sample performance by repeating with other GaR levels and different sub-sample, excluding the GFC around 2008 (see Appendix C.2.4)[3]. Our conclusions about the superior performance of the CSD panel model remains unchanged for NFCI and HP as predictors.

[3]We had to exclude WUI and EPU due to shorter data spans

Table 4.3: TL – NFCI

	5%		10%		15%	
Horizon	**CSD**	**No-CSD**	**CSD**	**No-CSD**	**CSD**	**No-CSD**
1	11.66	7.48	8.02	4.92	5.35	3.05
2	9.92	5.19	6.36	3.27	3.37	1.98
3	6.94	3.88	4.82	2.46	3.35	1.37
4	5.00	3.27	4.29	1.82	2.92	1.02
5	4.71	2.88	4.07	1.46	2.93	0.97
6	3.69	2.46	3.87	1.63	2.50	1.42
7	3.16	2.17	3.16	1.03	1.90	1.08
8	3.44	2.08	3.71	1.53	2.64	1.24
9	2.58	2.48	3.42	1.59	2.34	1.11
10	2.13	2.36	3.21	1.62	2.29	1.30
11	0.67	2.22	2.54	1.68	1.93	1.24
12	-0.07	1.46	1.31	1.22	1.84	0.60

Notes: This table compares the out-of-sample prediction accuracy for the two panel models across forecast horizons. The figures show relative gain in TL with respect to the unconditional quantiles BM. NFCI is the predictor here. Similar tables for other predictors can be found in Appendix C.2.3.

Combining the findings of the in-sample and out-of-sample performance, our results are generally in line with Brownlees and Souza (2021) – i.e., the models that generate superior out-of-sample forecast performance, are not able to establish a direct relationship of GaR with financial conditions, or other vulnerability indicators, at least for the 5% GaR. However, we differ in our findings as the predictors have an indirect role through the unobserved factors – i.e., the CSD.

4.3.4 Estimated GaR

Having established the out-of-sample accuracy of the CSD panel model, in this subsection we analyse the time series characteristics of projected GaR for individual countries in our panel. Figure 4.4 compares the estimated GaR at 12 quarter horizons for six major countries in our sample – i.e., Australia, Japan, South Korea, Germany, the the U.K. and the U.S.. We illustrate the GaR with NFCI as the vulnerability indicator. Other forecast horizons are presented in Appendix 5.

Figure 4.4: Estimated GaR (5%) at 12 Quarter Horizons, Predictor – NFCI

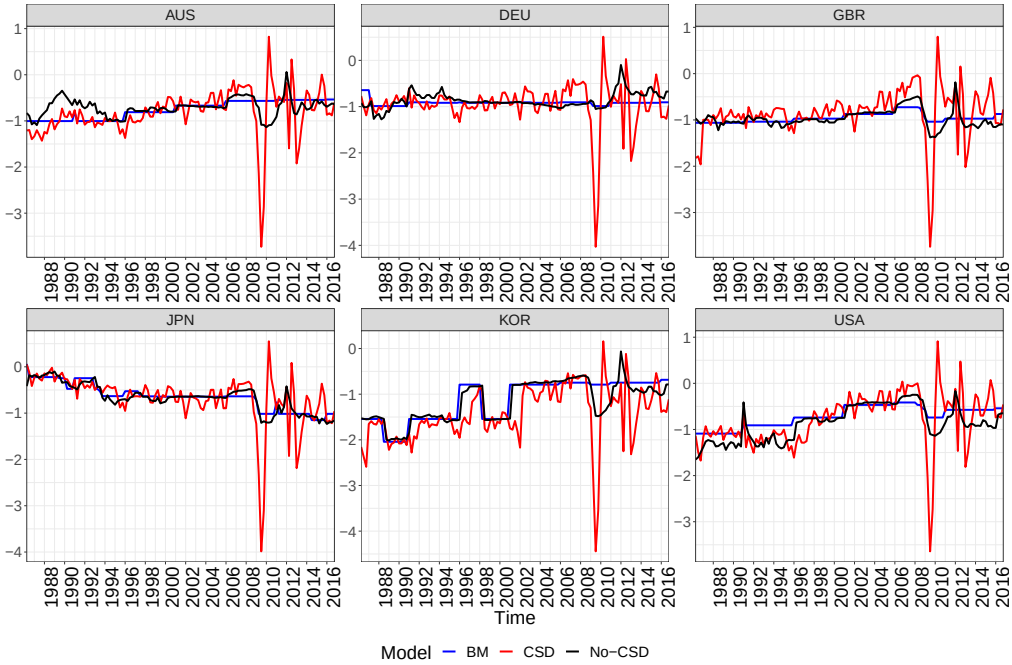

Notes: These figures compare the time series of out-of-sample GaR predictions from the two panel models and the unconditional quantiles benchmark. We display six major countries from our sample of 24, i.e. Australia, Germany, the the U.K., Japan, South Korea and the U.S. respectively.

The GaR predictions from different models turn out to be quite distinct. The CSD panel model has sharper characteristics and is able to provide more distinct signals as compared to the no-CSD panel model. The no-CSD panel model, although replicates most of the directions, is not able to capture the magnitude as well as the CSD panel model. This is due to the better explanatory power we saw in the in-sample analysis and improved out-of-sample predictive accuracy in terms of TL. As a result, we see distinct and meaningful characteristics in the series of estimated GaR from the CSD panel.

With the CSD model, we are able to reproduce distinct patterns for different countries. Japan displays a decline in pattern while Korea shows an increase. The U.S., the the U.K., and Germany exhibit an upward trend until the GFC. We see a sharp fall around the GFC and the sharpest decline is for Korea, among the six countries. Post GFC, there is stronger co-movement. In the following sections, we explore further

the properties of the out-of-sample forecasts of the GaR.

4.3.5 Risk and Higher Moments

In addition to the GaR analysis, several studies (Adrian et al. 2019a; Plagborg-Moller et al. 2020; Lloyd et al. 2023) predict higher moments of GDP. But there is no consensus on the findings. While Plagborg-Moller et al. (2020) do not find any meaningful interpretation of moments other than the conditional mean, Lloyd et al. (2023) find that quantiles conditioned on additional foreign variables are able to generate relatable patterns of time-varying higher-order moments. Adrian et al. (2019a) find that higher moments of GDP growth are correlated with financial conditions. Delle-Monache et al. (2020) also find that conditional on large financial information sets, there is marked negative skewness and downside risk in the recovery path, in the past decade. In this section, we explore the conditional moments using the estimated panel quantile models considered in this chapter.

To arrive at the time-varying moments, we follow the method of Adrian et al. (2019a), by smoothing the predicted quantiles using the skew-t distribution of Azzalini and Capitanio (2003). Hence, we arrive at the entire conditional distribution of future GDP growth. The skew-t probability density function takes the following functional form:

$$f(y;\mu,\sigma,\alpha,\nu) = \frac{2}{\sigma} t\left(\frac{y-\mu}{\sigma};v\right) T\left(\alpha\frac{y-\mu}{\sigma}\sqrt{\frac{\nu+1}{\nu+\left(\frac{y-\mu}{\sigma}\right)^2}};\nu+1\right) \tag{4.11}$$

where $t(.)$ and $T(.)$ respectively denote the probability density function (pdf) and cumulative density function (cdf) of the Student t-distribution. The distribution is characterised by four parameters: the location μ, scale σ, fatness ν and shape α. For each quarter, we choose these parameters to minimise the squared distance between our estimated conditional quantiles (5^{th}, 25^{th}, 75^{th} and 95^{th}) and the quantiles of the

skewed t-distribution. This is a non-linear least-squares problem as follows:

$$\{\hat{\mu}_{t=h}, \hat{\sigma}_{t=h}, \hat{\alpha}_{t=h}, \hat{\nu}_{t=h}\} = \underset{\mu,\sigma,\alpha,\nu}{\arg\min} \sum_{\tau} \left[\hat{Q}_{y_{t+h}|x_t}(\tau|x_t) F^{-1}(\tau; \mu, \sigma, \alpha, \nu)\right] \tag{4.12}$$

The estimated smooth quantiles from the models have very distinct features. This is also evident in the moments computed. We generate the moments of all orders for all countries to analyse risk signals. Here we exclusively focus on one country, i.e. the U.S. only (Figure 4.5) for brevity. Moments of six major countries are in Appendix C.5.

Figure 4.5: Moments of U.S. GDP, Conditional on NFCI

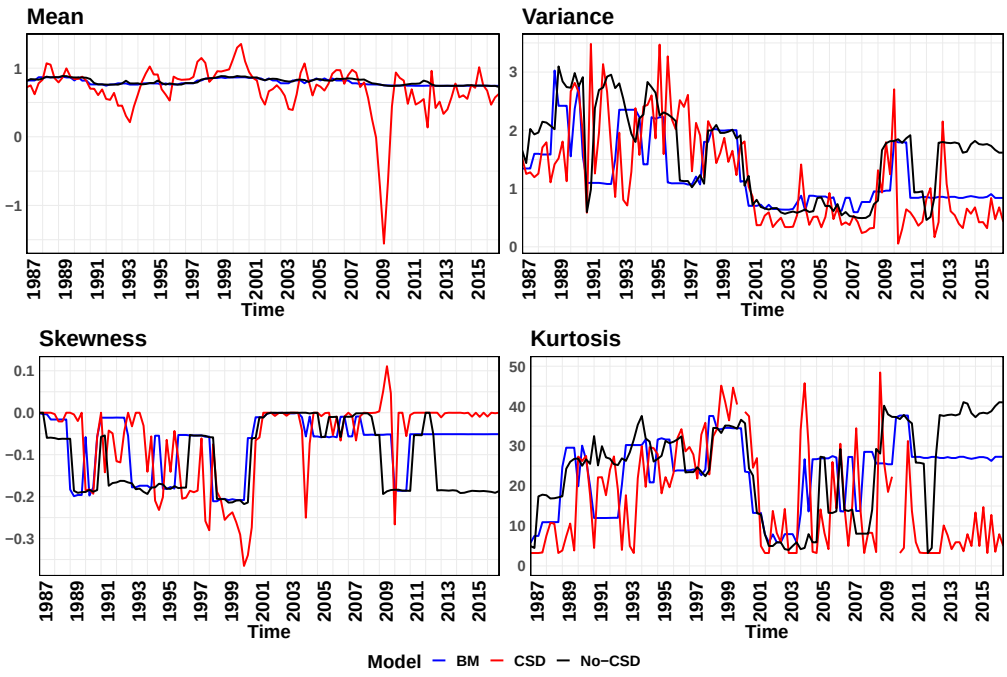

Notes: The figures compare the time series of conditional moments from the two panel models and the unconditional quantiles benchmark. We display the moments for the U.S. here and five other major countries in Appendix C.5.

The moment analysis indicates the GFC 2008–09 with higher variance and spiking kurtosis. Additionally, we are able to identify from the moments other known episodes of macroeconomic risk. For example, for the U.S., we can relate to the end of 1980s' and the early 1990s' recession, characterised by the then rapid growth in the U.S. credit and HP, accompanied by weak bank capital and further enhanced by monetary policy

tightening in the late 1980ss (Aikman et al. 2019). This is followed by a few years of relatively lower risk. Subsequently, we can identify the period in the late 1990's decade, when the U.S. experienced a series of macro-financial challenges – i.e., the telecom-media-technology (TMT) bubble and the onset of a recession, worsened further by the terrorist attacks of September 2001 (IMF 2002).

Although both panel models are able to indicate risk, signals from the CSD panel are sharper, specifically in the latter part of our sample. For instance, the post-GFC restoration of the financial systems and the consequent low-risk period is captured only by the time-varying moments of the CSD panel model. Further analysis of the entire predictive density (Appendix C.4) and skewness of the CSD panel model indicates that the risks emanate not from the negative skewness, but more from a shift of the entire distribution to the left and higher variance due to fatter tails.

We compute ES as an additional measure of tail–risk quantification, to quantify the signals generated by the higher moments. ES is a classic quantification of tail–risk, measuring the expected value, conditional on violation of a threshold. It is the officially endorsed measure of risk by the Basel Committee and has renewed emphasis in the Third Basel Accord (Patton et al. 2019). GaR studies (Adrian et al. 2019a; Reichlin et al. 2020; Iseringhausen 2023) have also computed and compared ES. In this context, ES is the expected GDP growth conditional on the violation of GaR.

For a chosen target probability π, ES is defined for the i^{th} cross-section as:

$$SF_{i,t+h} = E(Y_{i,t+h}|Y_{i,t+h} \leq GaR_{\pi}) \tag{4.13}$$

Figure 4.6, shows the estimated ES measures from the different models using the NFCI as the vulnerability indicator. We note the flexibility of the ES measure constructed from the CCE panel models, in terms of the strength of the signals in times of distress. The lowest estimated ES is during the GFC. In addition to the periods of risk we identified in the moment analysis, we see a low ES around 2013, when the

Figure 4.6: ES Conditional on NFCI

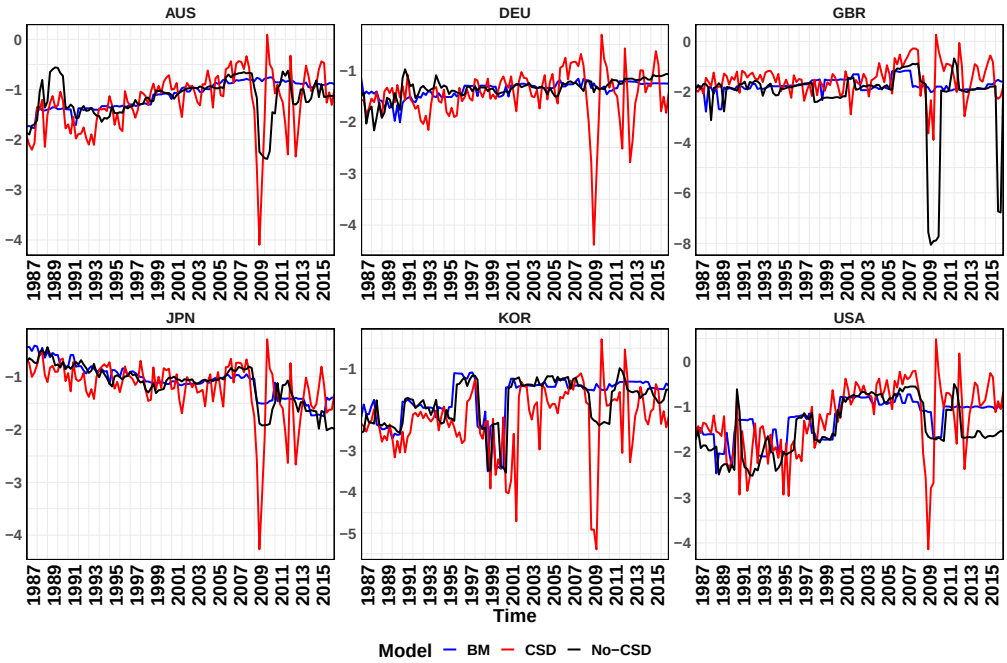

Notes: The figures compare the time series of conditional ES from the two panel models and the unconditional quantiles benchmark. We display six major countries from our sample of 24, i.e. Australia, Germany, the the U.K., Japan, South Korea and the U.S. respectively.

growth outlook was bleak, with the recovery from the financial crisis slowing down. The important attributed reasons were weaker demand due to fiscal consolidation and weak financial systems. Apart from these, a general sentiment of uncertainty and the then ongoing European turmoil were some of the key factors that exerted a downward pull on the GDP growth of the major advanced economies (IMF 2012). As the outlook on growth gradually improved thereafter (IMF 2013a,b), we see a corresponding movement in ES too. As in predicted GaR, we recognise distinct ES time series for the different countries.

4.3.6 Forecast Decomposition

The results so far indicate superior in-sample and out-of-sample performance when we include the multi-factor error structure in the panel model. In this section, we try to understand the contribution of the different components to the total predicted

GaR by the CSD panel model only (we do not compare models in this section). We decompose the predicted GaR and segregate the role played by the global factors. A similar breakdown of estimated GaR into different sub-components has been done by Aikman et al. (2019) to identify the drivers of GaR and create a risk monitoring tool.

Figure 4.7: Decomposition of Predicted GaR (5%) – Predictor: NFCI

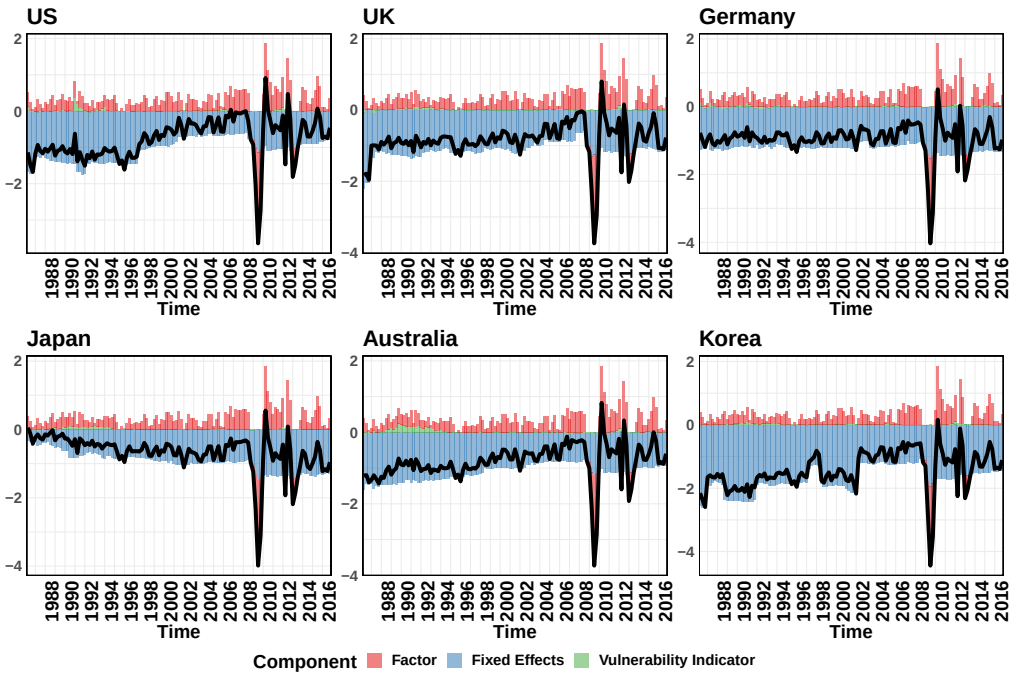

Notes: The figures explicitly decompose the predicted GaR into two components, the CSD and the rest. We display six major countries from our sample of 24, i.e. Australia, Germany, the the U.K., Japan, South Korea and the U.S. respectively. Prediction horizon is 12 quarters ahead.

The black solid line in Figure 4.7 represents the predicted GaR (5%), 12 quarters ahead with NFCI as the vulnerability indicator. Although the magnitude of GaR is driven by the panel components, the direction is influenced by the CSD. The panel components (excluding the multi-factor error structure) have a negative impact and lower GaR. The common factors have a mitigating effect and generally pull up GaR. However, in times of extreme distress, for example, around the GFC, we see that both the panel components and the global factors together pull GaR down. The country-specific dynamics are quite distinct. The non-inclusion of these mitigating global factors in the no-CSD panel may be the reason for signalling elevated risks in

terms of higher kurtosis post-GFC in the period 2013–2016. Similar findings for other forecast horizons are displayed in Appendix C.6.

4.4 Conclusion

In this chapter, we provide evidence that modelling CSD is important and useful to forecast GaR in a multi-country panel quantile set-up. The factors used to model the CSD, have dual interpretations as common shocks or as international spillover impacts. When augmented with CSD, the results of our panel quantile regressions suggest that important vulnerability indicators are rendered insignificant for 5% GaR, up to a forecast horizon of 12 quarters. However, we find that three indicators namely CG, TS and EPU are significant in the medium term for higher GaR levels. These conclusions were obtained using a panel of 24 countries. We also find that the CSD panel models have superior out-of-sample performance in terms of TL. Thus, though the CSD models have the best in-sample fit and out-of-sample accuracy, cannot relate 5% GaR with macro-financial vulnerability indicators. We demonstrate the practical relevance of CSD panel models by generating out-of-sample GaR, complete predictive distribution and its moments. We quantify tail–risk by ES. The analysis suggests signals obtained from these are able to replicate the state of the economy at various low points in time and is consistent with the published IMF outlooks around similar times. In addition, a breakdown of the forecasts into the panel components and the interactive fixed-effect terms indicate that the CSD part of the panel has a mitigating effect in normal times and exerts a further downward pull at crisis times.

Chapter 5

Timely Predictions of Capital Flow Episodes

5.1 Introduction

Cross-border capital flows are recognised to be highly episodic and the episodes often turn out to be disruptive to the concerned economies. Such episodes attract a lot of policy-attention as they can impact economies through multiple channels, such, as substantial fluctuations in the asset markets or the exchange rate or high inflation rates (Ghosh et al. 2016). Therefore, understanding and anticipating such episodes is of importance to policymakers so as to put effective measures (monetary, fiscal or macro-prudential) in place, in a timely fashion, to mitigate the adverse consequences. IMF (2020) recommended several crisis-specific measures, including foreign currency interventions, capital flow management, sovereign debt management and macro-prudential policies. Further, international coordination, global safety nets, and IMF policies can also aid to alleviate the impact of these events (Scheubel et al. 2019). For more information on policy measures, we refer to BIS (2021).

In this chapter, we develop a panel model that uses higher frequency data to produce and update the real-time predictions of the probabilities of extreme episodes in cross-border capital flows and also provide techniques to assess the quality of the

predictions in an out-of-sample context. We find that our model can beat a random classifier and produce better quality projections than a naïve benchmark. There is no material difference between the three link functions that we compare. The quality of predictions remains steady, as we update the model in real-time as new data are released. Thus, we obtain stable satisfactory performance right from a quarter in advance of the target quarter.

This adds to the existing body of literature which focusses on identifying the various drivers of capital flow episodes and corresponding mitigating measures. Given the high level of global financial integration, the transmission of shocks through cross-border capital flows can be particularly quick. A very recent example is COVID-19-triggered disruptions (IMF 2020). However, it is surprising that studies to date did not focus at all on the timeliness of predictions. Further, there is no assessment of the effectiveness of identified factors in terms of out-of-sample accuracy of the predicted event probabilities. Also, though the literature has identified daily and monthly variables that impact the quarterly episodes, all studies to date temporally aggregate the higher frequency data to quarterly frequency, thus potentially missing out on important information that could have been obtained from direct modelling of the higher frequency data.

In this chapter, we address these gaps with three main contributions. The first of our main contribution is the mixed-frequency discrete choice panel model, which is novel to capital flows context. We introduce country-specific fixed effects and cross-sectional averages in this model, which has not been considered in the closely related literature (Forbes and Warnock 2012; Ghosh et al. 2016; Forbes and Warnock 2021). Our empirical model brings together three different frequencies – quarterly, monthly and daily. Therefore, we use daily and monthly data to arrive at high-frequency predictions of important extreme events. Additionally in a pseudo-real-time framework, we also take into account the publication delays in the capital flows data and the monthly macro-financial series. We use MIDAS techniques building on the recent studies by Audrino et al. (2019) and Galvão and Owyang (2022). We compare three link functions: the logit, probit and the complementary log–log; instead of a predetermined link

function that is most commonly used in the capital flows literature. We estimate the model using maximum likelihood. Our model can be updated on real-time basis as and when new data are released.

Our second contribution is the empirical application where we obtain simultaneous pseudo-real-time predictions for 27 countries in mixed-frequencies. Closely mimicked versions of the release calendar of the IMF Balance of Payments (BoP) database and the high-frequency indicators give us a pseudo-real-time capital flow database, which is the first one of its kind to be used in episode predictions, to the best of our knowledge. Our redefined episodes reflect the 'ripples' instead of 'waves' as found by Forbes and Warnock (2021). Although the predictions can be updated daily, for brevity we update on major monthly data releases.

The BoP database of the IMF provides a long time series of relevant data with comprehensive coverage of countries. The data are published at annual and quarterly frequencies. However, as with most macro data, it has significant publication lags. There are higher–frequency proxy databases like that from the Emerging Portfolio Fund Research (EPFR) and the Institute of International Finance (IIF). Although several studies have analysed these data, there are important differences when compared to the IMF BoP database and a list of caveats is needed (Koepke and Paetzold 2022). Besides, these databases largely proxy the portfolio flows and investment funds. Although the importance of portfolio flows has generally increased over time, as Forbes and Warnock (2021) demonstrate, bank-debt-flows led about half and a third of the surges and stops during the pre- and post-GFC periods respectively while the bank flows led around 41% and 36% of the retrenchments in their pre- and post-crisis samples. Also, these databases are expensive to obtain, which precludes their widespread use and the replication of empirical results. Thus, we focus directly on high-frequency modelling of the quarterly IMF BoP database using publicly available macro-financial indicators, and therefore our results are directly interpretable and replicable.

Our third contribution is a rigorous out-of-sample prediction accuracy assessment framework using a number of forecast verification techniques. We use the Receiver

Operating Characteristic Curve (ROC), and the Area Under Receiver Operating Characteristic Curve (AUROC) to compare predictions from different model specifications at various points in time. The bootstrapped distribution is used in formally testing for statistical significance. The results are also substantiated by the Brier Score (BS) and the Kuiper's Score (KS) which have a very long history in forecast verification.

Following are our three main findings. Firstly, we find that all predictions are significantly better than the random classifier. Therefore, our mixed-frequency predictors have statistically significant forecasting skills.[1] Secondly, we find that there is no significantly quantifiable difference between the various link functions and all link functions for all episodes can produce skilled predictions. Thirdly, in our pseudo-real-time exercise, which is perhaps the most relevant in terms of decision-making, we find the prediction accuracy remains steady and robust to the flow of new information that is absorbed by the model. The AUROC measures in the pseudo-real-time assessment turn out to be significantly skilled as early as 90 days prior to the start of target quarter. The subsequent sequence of predictions reveals a steady performance, as newer data are added to the model.

This chapter brings together various strands of literature. First and most directly, we relate to the capital flows literature. Their episodic nature, volatility and adverse consequences are all well-studied. So far, there are two approaches. The first one is to discretise the flows into binary events and to study their probabilities, causal factors and consequences (see Forbes and Warnock 2012; Ghosh et al. 2016; Forbes and Warnock 2021). The second approach is to model the tail quantiles as in IMF (2020), Martin et al. (2020) and Gelos et al. (2022) in line with the seminal paper of Adrian et al. (2019a) on GDP GaR. The push and pull factors of capital flows have been investigated and identified (see Koepke 2019, for a comprehensive survey; also see Kaminsky 2019, for an extensive survey on latest trends and directions on capital flows research). Recent literature has also recognised the issue of publication lags in

[1] As in the meteorological literature, the term skilled forecasts indicate predictions that outperform the random classifier.

the official IMF BoP database and tried several higher frequency proxies (for example Friedrich and Guérin 2020; Crescenzio and Lepers 2021).

We also directly relate to and extend the nowcasting literature. Particularly, we relate to the two very new strands of nowcasting. Firstly, the approach of this chapter is in similar spirit as that of event probability nowcasting studies such as that of bank defaults in Audrino et al. (2019) or recession probabilities in Galvão and Owyang (2022). Secondly, we also take forward the panel data nowcasting (Babii et al. 2020; Fosten and Greenaway-McGrevy 2022) literature. Thus, we relate closely to mixed-frequency modelling, which goes hand in hand with the nowcasting literature. Specifically, we relate to the MIDAS methods (see Clements and Galvão 2008; Schumacher 2016; Ghysels 2018; Ghysels and Qian 2019). Additionally, we also link with the long thread of literature on discrete choice modelling and forecast verification techniques (see Mason and Graham 2002; Bouallègue et al. 2018). These approaches are increasingly getting used in macroeconomics as well – (for example, Berge and Jordà 2011; Liu and Moench 2016; Galvão and Owyang 2022; Garratt and Petrella 2022; McCracken et al. 2022).

The rest of the chapter is organised as follows. Section 5.2 introduces the data along with the event definitions and constructions for our target events. Section 5.3 details our empirical framework by introducing our mixed-frequency model and the pseudo-out-of-sample set-ups and the accuracy assessment framework. Section 5.4 presents the main empirical application and Section 5.5 concludes.

5.2 Data and Definitions

5.2.1 Capital Flows

There has been several shifts in the pattern of capital flows over time and these have been particularly noted and discussed post GFC. As highlighted Figure 5.1 from BIS (2021) some of the key changes are: i) gross capital flows shifted towards lower levels that is yet to recover; ii) flows to AE has remained below 7% of GDP ever since;

iii) flows to EME were relatively more resilient, although with temporary slowdowns; iv) emerging Asia maintained a steady rising trend of capital flows. We source our

Figure 5.1: Capital Flows by Type and Region

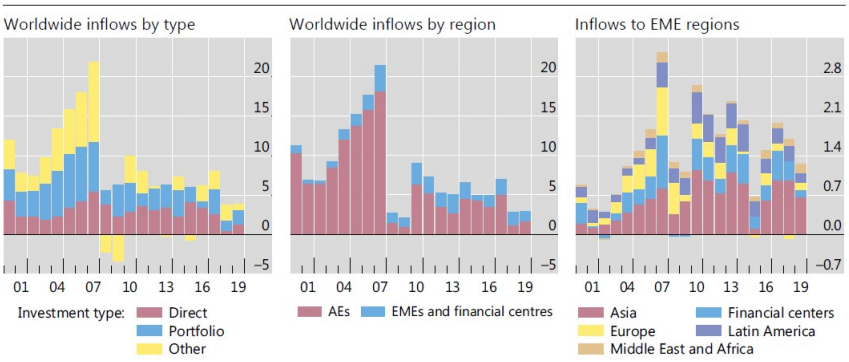

Notes: This figure is sourced from BIS (2021) and highlights some of the important changes in pattern of capital flows.

data from the comprehensive database created by Forbes and Warnock (2021) as it is updated until 2020 and takes into account the recent shift in focus from net to gross capital flows. We construct a balanced panel of 27 countries for 136 quarters (Q1:1985: to Q4:2019). Although the Forbes and Warnock (2021) database consists of 59 countries, only 28 of them start in Q2:1978, while other countries are added to the database at later starting dates (see Table 5.1). We keep all of the countries starting in Q1:1978 in our final balanced panel[2]. Hence, we have a panel of 27 countries and Figure 5.2 shows that this panel still retains most of the features of the entire data set.

5.2.2 Re-defining Capital Flow Episodes

The capital flow episodes considered in this chapter are based on now nearly standardised definitions from the seminal paper of Forbes and Warnock (2012), where they made the classic move from net to gross capital flows, primarily because a focus on gross flows allows to distinguish between foreign and domestic origins of the flows. This differentiation is important because of several reasons: (i) Domestic investors have

[2]except Argentina which did not have complete data in the original database

Table 5.1: Starting Dates and Countries of Forbes and Warnock (2021) Database

Starting Point	**Count**	**Names of Countries**
1978 Q2	28	U.S., U.K., Austria, BelLux, Denmark, France, Germany, Italy, Netherlands, Norway, Sweden, Canada, Japan, Finland, Iceland, Portugal, Spain, Australia, Argentina, Brazil, Guatemala, Israel, Bangladesh, Sri Lanka, India, Korea, Philippines, Thailand
1979 Q1	1	Mexico
1980 Q1	1	New Zealand
1981 Q1	2	Ireland, Indonesia
1984 Q1	2	Turkey, Taiwan
1985 Q1	2	South Africa, Poland
1988 Q1	1	Bolivia
1989 Q4	1	Hungary
1991 Q1	3	Chile, Peru, Romania
1992 Q1	2	Estonia, Slovenia
1993 Q1	5	Czech Republic, Slovak Rep, Latvia, Lithuania, Croatia
1994 Q1	2	Venezuela, Russia
1995 Q1	1	Singapore
1996 Q1	1	Colombia
1998 Q1	2	Panama, China
1999 Q1	5	Switzerland, Greece, Costa Rica, HongKong, Malaysia

Notes: The table shows the starting dates for the different countries in the Forbes and Warnock (2021) capital flows database.
BelLux: Belgium and Luxembourg combined, as in Forbes and Warnock (2021).

gained importance over time, and therefore unlike historically, gross and net flows no longer mimic each other (ii) In the recent decades, gross flows have been much more volatile than net flows (iii) Foreign and domestic investors have distinct motivations for the investments they make and consequently do not react in the same way to shocks and policy measures (iv) Different policy actions might be effective in mitigating the impacts of extreme capital flows originating from domestic and foreign investors.

There are four types of extreme episodes defined as sudden and sharp increases or declines in inflows and outflows respectively and Table 5.2 presents a condensed representation. Sharp increases in inflows are defined as surges whereas sharp declines are defined as stop episodes. Similarly, rises and falls in outflows are classified as flight and retrenchment episodes respectively.

Further, Forbes and Warnock (2021) find important shifts in the nature of capital

Figure 5.2: Total Flows

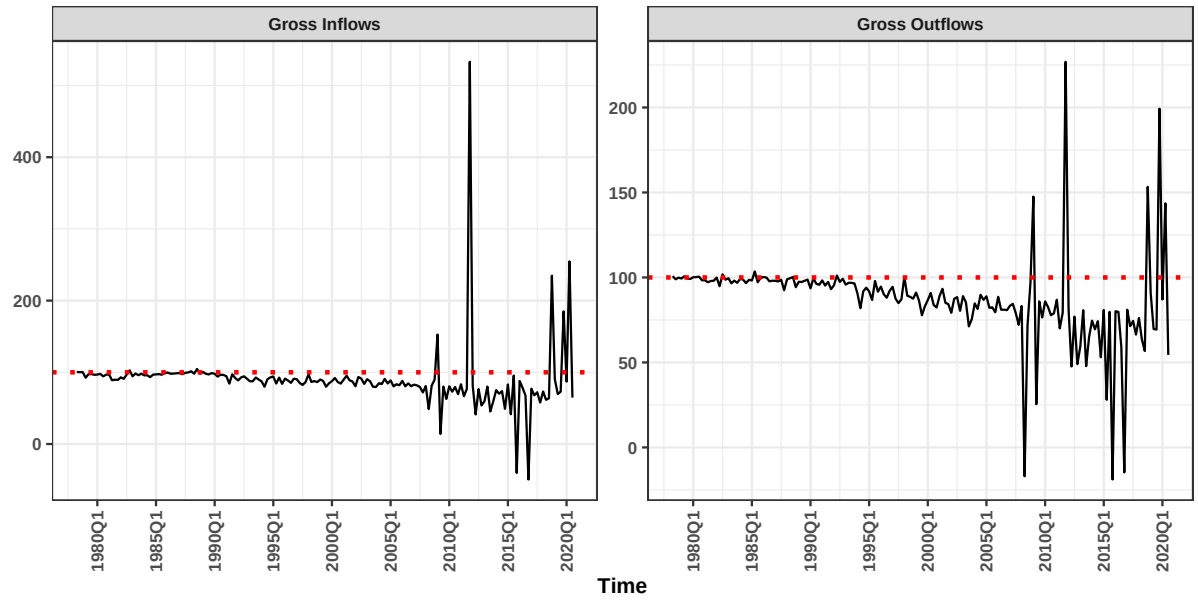

Notes: This figure compares the total gross flows by category for the countries selected in our panel viz all in the database of Forbes and Warnock (2021). The black lines display the flows of the selected countries as a percentage of all countries in the database. The red dotted line is the 100% mark.

Table 5.2: Classification Capital Flows Episodes

Event	Inflow (foreigners)	Outflow (domestic)
Sharp Increase	Surge	Flight
Sharp Decrease	Stop	Retrenchment

Notes: The table shows the categorisation of different types of capital flows into four extreme episodes

flows and also their drivers after the GFC. In a key finding, they record that the incidence rates of capital flow episodes have declined post-GFC. Before the crisis, the capital flow episodes impacted a large number of countries. For instance, they find that pre-GFC, around 80% and 63% of countries experienced retrenchments and stop episodes respectively. In contrast, the corresponding post-GFC incidence rates were found to be substantially lower at 27% and 22% respectively. The fall in the incidence rates is particularly prominent for the AEs. The EMEs, however, continued witnessing higher incidence rates, especially during the uncertain times around 2015 that are more commonly known as the 'taper tantrum' following the announcement of reduction of the quantitative easing programme of the U.S. Federal Reserve. Considering this important transition in the pattern of capital flows, we redefine the episodes as described below. Let us introduce some notation now. Let:

$$K_{,i,t} = \text{Capital Inflow/Outflow} \tag{5.1}$$

$$C_{i,t} = \sum_{l=0}^{3} K_{i,t-l} \tag{5.2}$$

$$\Delta C_{i,t} = C_{i,t} - C_{i,t-4} \tag{5.3}$$

We recognise an episode when $\Delta C_{i,t}$ exceeds (or falls short of) its five-year rolling mean by one standard deviation (five-year rolling). The method remains the same for other countries. To compute five-year rolling means and standard deviations, we lose some data points at the start of the sample. Our final data set thus starts at Q1:1985. Figures 5.3a and 5.3b illustrate the process graphically for four sample countries. Thus, our redefined episodes relax two of the original identification criteria of Forbes and Warnock (2021) i.e, we do not require any violation of the two-standard deviation bands of the rolling means and the episodes need not last for any minimum period. Besides illustrating the identification of episodes, Figures 5.3a and 5.3b can also validate the stylised fact of expanding volatility, recorded earlier by Broner et al. (2013). Table 5.3

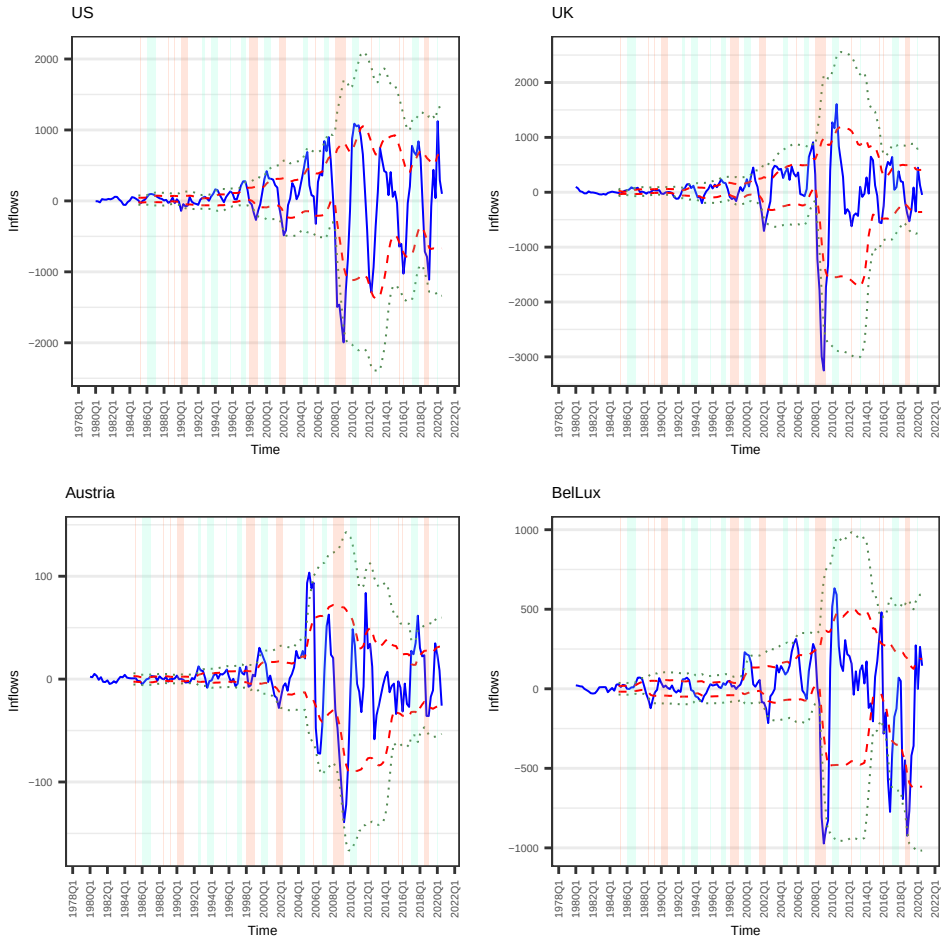

(a) Changes in 4-qtr MA of capital inflows

Notes: The blue line plots the $\Delta C_{i,t}$. The red dotted line shows the one-standard-deviation bands. The green dotted line shows the two-standard-deviation bands. The orange shaded bands indicate stops and the blue bands show the surge episodes. There are similar figures for other 23 countries.

Figure 5.3: Construction of Capital Flow Episodes

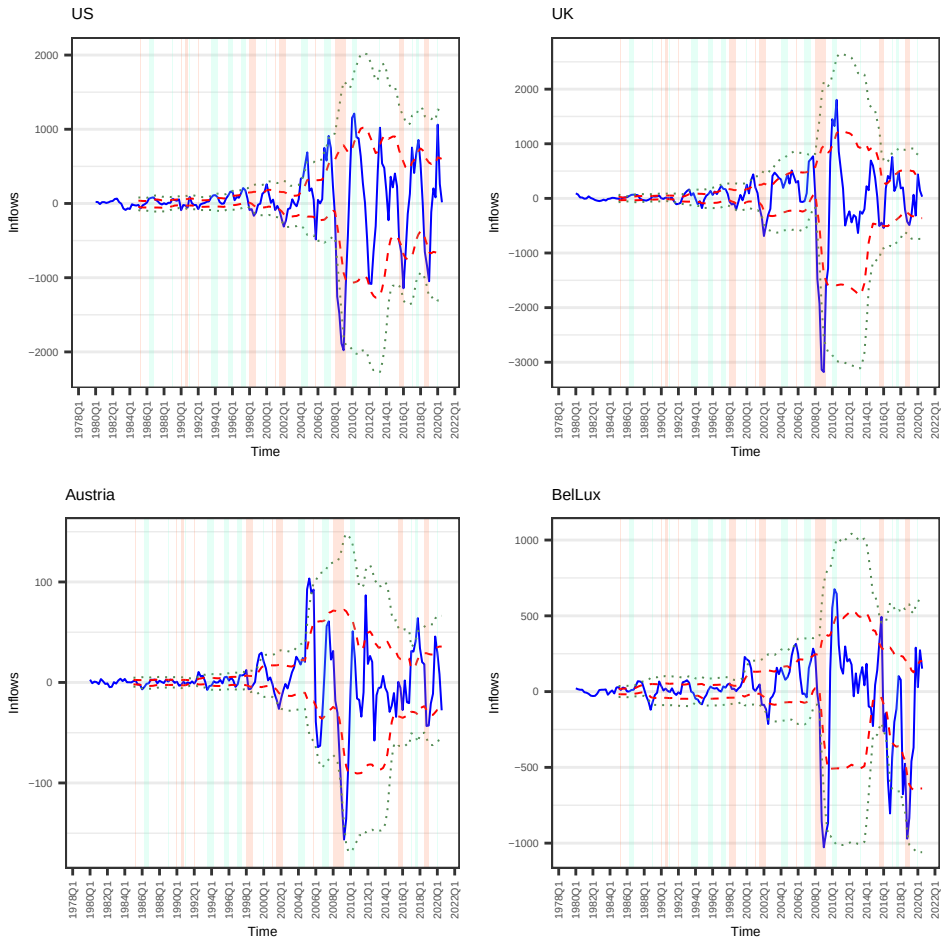

(b) Changes in 4-qtr MA of capital outflows

Notes: The orange shaded bands indicate retrenchment and the blue bands show the flight episodes. The rest are same as in Figure 5.3a.

summarises the data and presents the incidence rates for each type of episode and country during the entire period under consideration.

Table 5.3: Count of Episodes

Country	Surge	Stop	Retrench	Flight
U.S.	35	29	27	32
U.K.	37	27	25	35
Austria	28	29	25	33
Belgium-Luxembourg	33	28	28	31
Denmark	35	35	28	38
France	36	26	24	33
Germany	32	24	33	33
Italy	28	32	31	32
Netherlands	37	26	29	41
Norway	33	27	30	35
Sweden	35	23	27	42
Canada	29	28	22	31
Japan	33	31	32	30
Finland	38	30	31	32
Iceland	39	29	27	42
Portugal	32	27	24	27
Spain	35	27	27	37
Australia	30	30	29	25
Brazil	28	25	27	30
Guatemala	26	29	25	27
Israel	25	27	30	37
Bangladesh	30	28	32	40
Sri Lanka	27	26	33	25
India	36	29	26	34
Korea	32	28	29	41
Philippines	34	19	18	29
Thailand	32	29	35	36

Notes: This table shows country-specific counts of different episodes across 27 countries for 143 quarters (Q1:1985 to Q3:2020). In this table we have additional data for the first three quarters of 2020 which were not used in modelling as the data for Q4:2020 were not available.

5.2.3 Predictors

Following Forbes and Warnock (2012, 2021), our predictors can be broadly classified into three groups: global, contagion and domestic. The predictors are, however, suitably

modified. The old VXO (Volatility Index) calculated by the Chicago Board Options Exchange (CBOE) measures global risk.[3]Following the stationarity transformations that are standard in the GDP nowcasting literature (see Giannone et al. 2008; Bańbura et al. 2012, and others), we calculate global money supply as the average of M2 in the U.S., EU, Japan and M4 for the U.K., converted to U.S. dollars and then transformed to y-o-y log differences. The average of the daily m-o-m differences from the U.S., the U.K., Japan and Germany indicate global interest rates. Our metric for measuring global growth is the monthly global economic activity index, first proposed by Kilian (2009) and further developed by Kilian and Zhou (2018). This is a more timely measure of economic activity compared to the quarterly global GDP growth, which was previously used in studies on capital flow episodes. Besides being available monthly, Kilian's index has a number of other advantages such as a long history, global coverage and is also robust to structural change (Kilian and Zhou 2018). Recognising the significance of oil prices as found by Forbes and Warnock (2021), we include daily global crude oil prices by transforming the West Texas Intermediate (WTI) crude prices as m-o-m log differences. The non-oil commodity prices are constructed as the m-o-m log differences of monthly non-energy commodity price series published by the World Bank. Table 5.4 presents the summary of all data series along with their frequencies and transformations. Figure 5.4 displays the time series of our transformed high-frequency data.

The contagion variable remains the same regional binary indicator indicating the occurrence or absence of an episode in a geographical region as defined by Forbes and Warnock (2012, 2021). In the pseudo-real-time exercise instead of assuming the availability of full information, we compute a real-time[4] version of the contagion variable, considering the pseudo-calendar of capital flow data releases.

Additionally, we introduce a new variable which we construct as the cross-sectional averages of lagged capital flows along with its pseudo-real-time version. It is an average

[3]Old VXO is highly correlated with the current index CBOE Volatility Index (VIX). We retain old VXO as a measure of risk in line with Forbes and Warnock (2021).

[4]We have used final vintages as we have sourced our data from https://www.dropbox.com/s/hcwz96okzpem8nl/ForbesWarnock_flows_dataset.dta?dl=1[Last accessed:20/07/2022]

Figure 5.4: High-Frequency Data

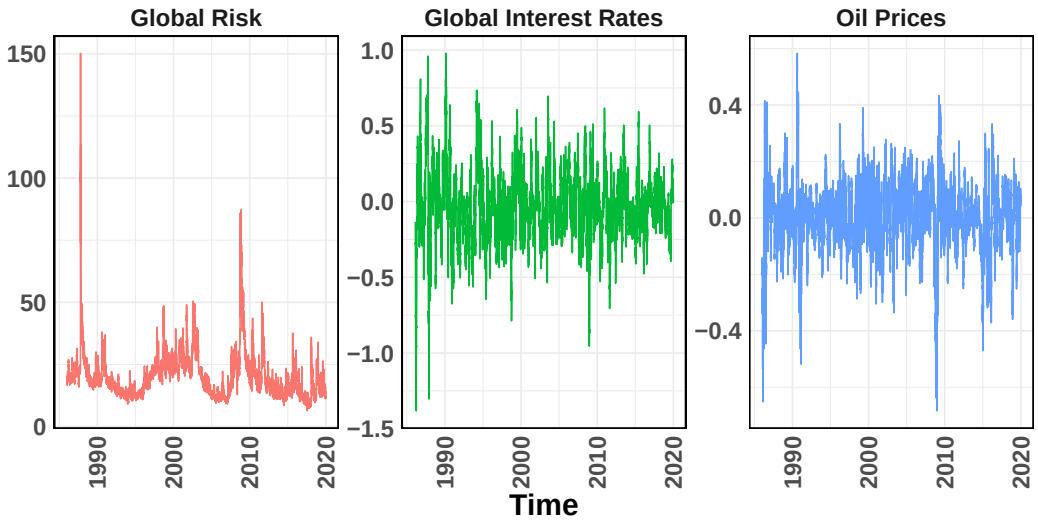

(a) Daily Data

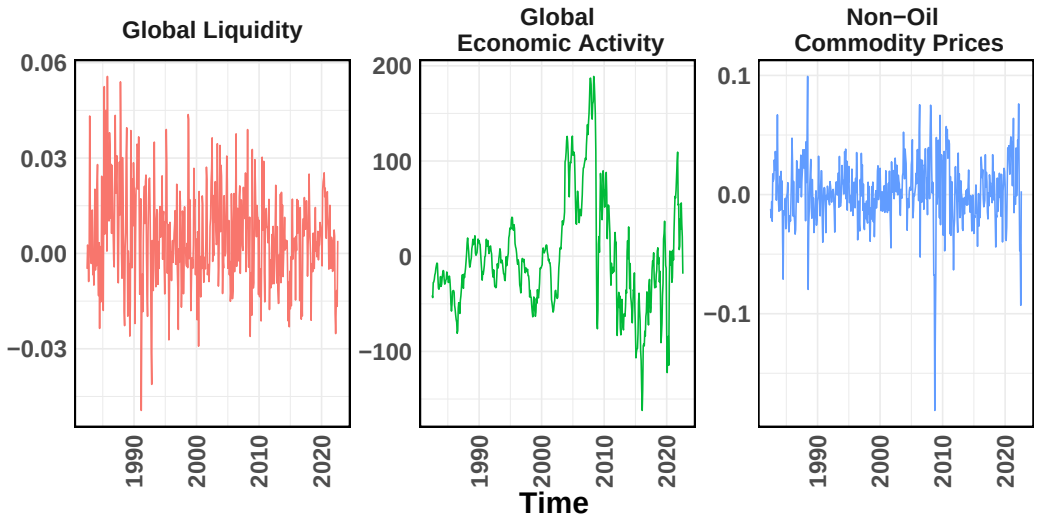

(b) Monthly Data

Notes: These figures display the time series of the high-frequency predictors after suitable stationarity transformation as in Table 5.4. The high-frequency predictors are taken up to December 2019.

of the inflows for the surges and stops and an average outflows when modelling the flights and retrenchments. This is expected to proxy the international transmission of shocks across countries as well as account for the possible interdependence of the events. It is worth noting that while our model explicitly includes the global 'push' factors, the novel fixed effects parsimoniously proxy the country-specific 'pull' factors.

Table 5.4: Data Details

Sl No	Series	Frequency	Transformation
1	VXO[a]	Daily	Replace NA with the last available
2	M2	Monthly	$\Delta(log)$ in USD
3	10Y Gsec Yields	Daily	Daily m-o-m
4	Global Economic Activity[b]	Monthly	Nil
5	Crude Oil (WTI Spot)	Daily	$\Delta(log)$
6	Commodity Prices (Non-Energy)[c]	Monthly	$\Delta(log)$
7	Capital Flows Episodes	Quarterly	Forbes and Warnock (2021)

Notes: This table shows the frequencies and the transformations of all variables in the mixed-frequency panel database. All data are sourced from Macrobond, unless indicated otherwise below

[a] Sourced from https://fred.stlouisfed.org/series/VXOCLS [Last accessed: 28–11-2022]. Assumed to start on Jan 1, 1986, with the same value as on Jan 2, 1986.

[b] See https://www.dallasfed.org/research/igrea [Last accessed: 02–5-2023]

[c] See https://thedocs.worldbank.org/en/doc/5d903e848db1d1b83e0ec8f744e55570-0350012021/related/CMO-Historical-Data-Monthly.xlsx [Last accessed: 28–11-2022]

5.3 Empirical Approach

5.3.1 A Mixed-Frequency Panel Binary-Choice Model

The mixed-frequency model considered in this chapter is based on the standard binary-choice models where the target of prediction can take two discrete values only. Since some macroeconomic time series, for example capital flows, in this context, are available only at a quarterly frequency and the predictors are available at higher frequencies, we extend the binary choice model to incorporate mixed-frequencies. To cope with the mixed-frequencies, we use MIDAS methods.

Throughout this chapter, the quarterly events of interest are denoted by binary

variable $E_{i,t}^{(e)}$; $E_{i,t}^{(e)} = 1$ indicates a realisation of the event e - a surge, stop, flight or retrenchment – for the i^{th} cross-sectional unit and the t^{th} time-point; conversely, $E_{i,t}^{(e)} = 0$ indicates the non-realisation of the event. Assume $\pi_{i,t}^{(e)}$ denotes the corresponding probability. To express as the analogous latent variable threshold model, let $Y_{i,t}^{*(e)} = \eta_{i,t}^{(e)} + \epsilon_{i,t}^{(e)}$ denote the underlying unobserved latent variable such that when $Y_{i,t}^{*(e)} \geq 0$, we realise the event – i.e., $E_{i,t}^{(e)} = 1$ and vice versa. $\epsilon_{i,t}^{(e)}$ are independent observations from the cdf F. Therefore, for prediction horizon h and given information set Ω_t, we have the following prediction equation:

$$\pi_{i,t+h}^{(e)} = Pr\left[E_{i,t+h}^{(e)} = 1|\Omega_t\right] = Pr\left[Y_{i,t+h}^{*(e)} \geq 0|\Omega_t\right] = F\left[\eta_{i,t+h}^{(e)}|\Omega_t\right] \tag{5.4}$$

We let F, i.e. the cdf, assume the following functional forms:

$$F(z) = \begin{cases} 1 - exp\left[-exp\left(z\right)\right], & \text{clog–log} \\ \Phi(z) & \text{probit} \\ \frac{1}{1+exp(-z)}, & \text{logit} \end{cases} \tag{5.5}$$

Let us assume that the high-frequency variables are sampled M_k times more frequently than the events $E_{i,t}^{(e)}$, where $k = 1, 2$. For the empirical application, there are two distinct high-frequency predictors – daily and monthly; the main events are quarterly. The predictions are performed on day v, which is crucial to determine data availability. We assume the monthly data are available with a lead of w_v, quarterly data are available with lag d_v and the daily data are published on the day of prediction without any lag.

Following is the main model we estimate[5]:

$$\begin{aligned}\pi^{(e)}_{i,t_v+h} &= Prob(E^{(e)}_{i,t_v+h} = 1|\Omega_{t_v}) \\ &= F\left[\alpha_i + \sum_{j=1}^{J} \beta_{M_1,j} B_j^{(M_1)}\left(L^{\frac{1}{M_1}}, \theta_{M_1,j}\right) g^{(M_1)}_{t_v,j}\right. \\ &\left. + \sum_{k=1}^{K} \beta_{M_2,k} B_k^{(M_2)}\left(L^{\frac{1}{M_2}}, \theta_{M_2,k}\right) g^{(M_2)}_{t_v+w_v,k} + \gamma c_{i,t_v-d_v} + \delta \overline{g}_{t_v-d_v}\right]\end{aligned} \tag{5.6a}$$

that is:

$$\begin{aligned}\eta^{(e)}_{i,t_v} &= \alpha_i + \sum_{j=1}^{J} \beta_{M_1,j} B_j^{(M_1)}\left(L^{\frac{1}{M_1}}, \theta_{M_1,j}\right) g^{(M_1)}_{t_v,j} + \sum_{k=1}^{K} \beta_{M_2,k} B_k^{(M_2)}\left(L^{\frac{1}{M_2}}, \theta_{M_2,k}\right) g^{(M_2)}_{t_v+w_v,k} \\ &+ \gamma c_{i,t_v-d_v} + \delta \overline{g}_{t_v-d_v}\end{aligned} \tag{5.6b}$$

The α_i are the country-specific fixed effects. $B_j^{(M_k)}$ are the exponential Almon MIDAS polynomials with the following generalised functional form:

$$B(L^{\frac{1}{m}}, \theta) = \sum_{q=1}^{K} b(q;\theta) L^{\frac{q-1}{M}} \tag{5.7a}$$

$$L^{\frac{s}{M}} x_t = x_{t-\frac{s}{M}} \tag{5.7b}$$

$$b(q,\theta) = \frac{exp(\theta_1 q + \theta_2 q^2)}{exp(\sum_{q=1}^{Q} \theta_1 q + \theta_2 q^2)} \tag{5.7c}$$

where $g^{(M_1)}_{t,j}$ denotes the daily variables; $g^{(M_2)}_{t+w_m}$ denotes the monthly variables, $c_{i,t-d_v}$ denotes the contagion variables and $\overline{g}_{t-d_v}$ denotes the global cross-sectional averages of capital flows generically – i.e., it represents the global average inflows when predicting the surges and stops whereas it indicates average outflows when predicting flights and retrenchments. The model can be easily further generalised to include other frequency mixes or other variables.

Estimation is carried out by the maximum likelihood method using numerical

[5]Regression coefficients depend on the day of prediction, denoted as v. It's not explicitly stated to avoid clutter in notation.

techniques. We use the Nelder–Mead algorithm and iterate until convergence. As demonstrated by Ghysels and Qian (2019) with the beta lag polynomial, we find that even with one parameter fixed, the Almon polynomial in equation (5.7c) still can assume different shapes (see Figure 5.5) to suit empirical applications. This can partially reduce the number of parameters to estimate and thereby bring down the computational process. Therefore, we fix the second parameter of the Almon-lag polynomial – i.e., equation (5.7c) – and estimate the other.

Figure 5.5: Shapes of the Almon Polynomial

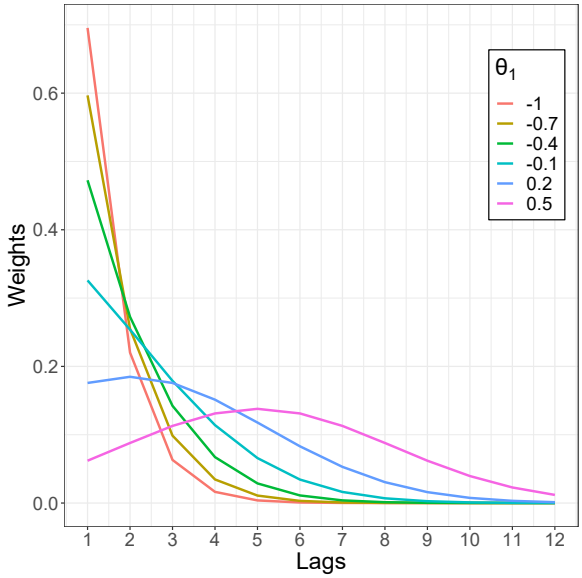

Notes: This figure plots the different shapes of the Almon polynomial in equation (5.7c) when we keep $\theta_2 = 0.05$ and vary θ_1 as in equation (5.7c).

5.3.2 Out-of-Sample Accuracy Measures

AUROC

We use AUROC to measure prediction accuracy. The term ROC originated in the field of radar signal-detection theory (Peterson et al. 1954) and has been extensively used in medical sciences, meteorology and psychology. The ROC is now a standard measure of evaluating binary predictions and has been considered in recent macroeconometrics,

particularly in the last decade, mostly to evaluate recession probabilities (see Berge and Jordà 2011; Liu and Moench 2016; Galvão and Owyang 2022; McCracken et al. 2022).

Very briefly, the ROC curve is a forecast verification tool that characterises the accuracy of the forecasting system in anticipating the event under consideration. To construct ROC curves, the predicted event probabilities are converted to binary form, i.e. when they exceed or fall short of a chosen threshold the event is to occur or not to occur. The correspondence between a series of such transformed binary predictions and actual event realisations can be summarised using two metrics – hit rates and false alarms. The hit rates are also known as sensitivities and the false alarms as 1− *specificity*. Specifically, for one sample contingency table as in Table 5.5, we define hit rates and false alarms as in equations (5.8). We construct several such contingency tables for each point in a grid of cut-off points. Given a set of event realisations, predicted probabilities and a grid of cut-off values, the ROC curve traces out the locus of all possible hit and false alarm rates[6].

Table 5.5: Sample Contingency Table

		Observed	
		Yes	No
Predicted	Yes	a	b
	No	c	d

Notes: This table is an illustration of a hypothetical contingency table in a binary classification problem

$$\text{Hit Rate/Sensitivity} = \frac{a}{a+c} \tag{5.8a}$$

$$\text{False Alarm} = \frac{b}{b+d} \tag{5.8b}$$

[6]We refer to Robin et al. (2011) for computational details.

Therefore, if we have an ideal model which always classifies correctly, we can expect all hit rates to be one and all false alarms to be zero. In contrast, if we have a model which is no better than a simple random guess, we expect all hit rates and false alarms to be around 0.5. The AUROC is a standard measure to summarise and compare ROC curves. In the case of an ideal perfect prediction, the AUROC measure should be equal to one. The closer it is to one, the better the predictions are. If the predictions have some skill (accuracy) with respect to a random classifier, we expect the AUROC to be greater than 0.5. Thus we borrow the term 'forecast skill' from Murphy (1988) to indicate such AUROC scores. Formal testing methods, based on the standard asymptotic normality property of the AUROC, assess if the forecast skills exceed 0.5 using and distinguish between different ROC curves.

We use bootstrapped distributions as standard in the forecast verification literature and also used in macroeconometrics, for instance, Liu and Moench (2016). The bootstrap method consists of cross-sectional and temporal block resampling (such as that suggested in Kapetanios 2008) to account for autocorrelation in time and across countries. The block length (b) are selected as $N^{\frac{1}{3}}$ and $T^{\frac{1}{3}}$ for the time-series and the cross-sectional dimensions respectively. The resampled panel dimensions are ensured to be equal to that of the original panel dataset.

BS

We corroborate the results obtained from AUROC with BS (Brier 1950), the most commonly used scalar summary performance measure of probabilistic predictions (Wilks 2010). As defined in equation (5.9), BS is computed as the mean square probability forecast error and is closely relatable to the RMSFE used in other chapters of this thesis.

$$BS = \frac{1}{NT} \sum_{i=1}^{N} \sum_{t=1}^{T} [E_{i,t} - \pi_{i,t}]^2 \tag{5.9}$$

BS is a negatively oriented score, ranging from zero to one – i.e., BS declines with improvement in prediction accuracy.

KS

The results are further substantiated with KS, also known as Peirce Skill Score, which is widely used for contingency tables and has been prevalent as a measure of forecast verification since 1884 (Wilks 2019). It is calculated as the difference between hit rates and false alarms. Unlike AUROC and BS used so far, KS applies to deterministic predictions and is specific to contingency tables. Therefore, we convert our probabilistic predictions to deterministic event predictions by recognising the occurrence of an event if the predicted probabilities exceed a chosen threshold. Instead of restricting the analysis to a specific threshold, we select a range of thresholds at various points of the distribution of the predicted probabilities, in such a way that we cover their entire distribution.

5.4 Results

The empirical application proceeds in two parts as we present the out-of-sample prediction results on the actual capital flow data using the high-frequency macro-financial data we described earlier. First, we will focus on the hypothetical full-information scenario. Then we will turn our attention to the pseudo-real-time application.

5.4.1 Full-Information Results

Our first set of results aims to examine the performance of the mixed-frequency models in an out-of-sample context. Here, we assume that at the time of prediction, all relevant information is accessible to the forecaster. Thus, we do not account for the data publication lags and assume that the IMF BoP data are available to the forecaster for all countries in the panel until a quarter before our target quarter. In our mixed-frequency approach, all the relevant higher–frequency (i.e., daily and monthly) data

are also taken to be at our disposal at the time of prediction. We choose $J = 40$ daily and $K = 3$ monthly lags. Therefore, we extend the current related (Forbes and Warnock 2012; Ghosh et al. 2016; Forbes and Warnock 2021) literature to out-of-sample mixed-frequency analysis, from the present temporally aggregated in-sample analysis and thus can investigate important aspects of the model performance.

AUROC

We adopt the following approach for accuracy assessment. Our targets are one-quarter-ahead probabilities for the four possible extreme episodes defined earlier – i.e., surge, stop, flight and retrenchment. We model each one of the episodes separately. The cross-sectional averages of the respective capital flows (i.e., inflows for surges and stops, and outflows for flights and retrenchments) act as a link between episodes. The pseudo-out-of-sample design splits the time dimension into two halves – i.e., $T = R + P$ observations. We estimate the model parameters using the first R quarters and predict one step at a time using the subsequent P quarters using a recursive estimation scheme – i.e., an expanding sequence of estimation samples. Hence, our evaluation sample starts in Q3:2002 and ends in Q4:2019 – a total of 69 quarters. The ROC diagram shows the correspondence between the predictions and the actual event occurrences. The combined AUROC score summarises the performance by pooling together all countries in the panel. Subsequently, we also turn our focus to the AUROCs for individual countries in our panel.

Figure 5.6 presents the overview of assessment in the form of the ROC curves for different episodes and the three link functions – clog–log, probit and logit. Generally, the predictions from our models are better than random classifier lines. For each episode and link function, Figure 5.7 presents the mean and 95% Confidence Interval (CI) of the bootstrapped AUROC distribution and the results differ across episodes. Although the ROC curves of flights and surges outperform the random classifier universally across link functions, the performance of stop and retrenchment episodes are weaker at overall level. However as Figure 5.8 demonstrates, stops and the retrenchment predictions are

relatively better when we analyse the AUROC scores for countries separately. The CIs in Figure 5.7 show that almost all of the link functions generate significantly better results than the random classifier for flights and surges, whereas the differences are only marginally significant different from a random classifier for the other two episodes – namely, stops and retrenchments. It is further evident from the overlapping CIs in Figure 5.7 that the differences between the three link functions are statistically indistinguishable.

Figure 5.6: AUROC for the Full-Sample Full-Information Model

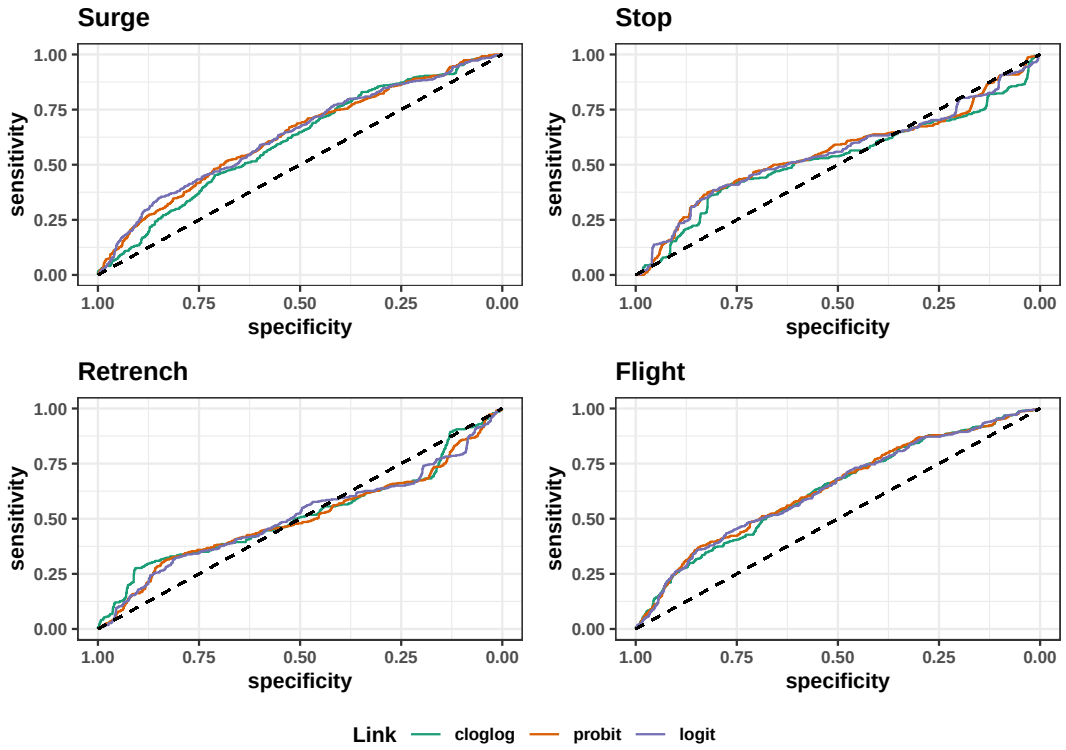

Notes: ROC curves for the different combinations of episodes and link functions. The ROC curves are computed after pooling the predictions and the observed across all countries. The 45°dotted black line represents a random classifier – the benchmark.

Figure D.1 in the Appendix plots the AUROC scores for a intercept only benchmark model, i.e. for each country we model the latent variable by historical means and then apply the appropriate link function. A comparison of Figures 5.7 and D.1 clearly reveals distinguishable gains in prediction accuracy from our mixed-frequency panel

models, while the benchmark model appears inseparable from the random classifier.

Figure 5.8 shows that there is variation in the quality of estimation across the 27 countries in the panel. The cloglog link outperforms for the flights and the retrenchment episodes at a country-level. Generally, the model predictions are better than the random classifier and there are some countries with excellent AUROC scores, around 0.8. Most countries have an AUROC between 0.6 and 0.7, across episodes and link functions. Countries such as Sweden, the Netherlands, Iceland, the U.S., the U.K. and India have better overall AUROC scores. In contrast, Finland, Japan, Portugal, Bangladesh, and Australia have the lowest prediction accuracy across episodes, in that order.

Differences in the quality of predictions can be noted among the four episodes, within each country. With the cloglog link function, 44% of countries show the best prediction accuracy for the retrenchment episodes followed by 41% of countries exhibiting the most accurate results for the stop episodes; further, in 11% of the countries flights are predicted with the highest accuracy while in only 4%[7] of countries, predictions for surges are the most precise. The U.K., BelLux[8], Korea, Italy and India show the highest variation in accuracy among the different episodes. For example, predictions for the U.K. are extremely precise for retrenchments and stops, while they are distinctly worse for flights and surges. On the other hand, we notice a very high accuracy for flights and stops in India and weaker performances for retrenchments and stops. Similarly, there are disparities when we focus on other link functions and into countries.

Robustness to different modelling choices is established from Figures D.2 and D.3 in the Appendix, with a few alternatives such as excluding the cross-sectional averages and including dummy for the GFC. Our conclusions remain unchanged.

BS

The figures in Table 5.6 show the BS for the full-information analysis. We find that the scores are closer to the perfect BS of zero and farther away from the worst BS of

[7]This is actually only one country, Norway, where a high level of precision is observed for all four episodes.

[8]Belgium and Luxembourg combined

Figure 5.7: 95% CI for AUROC

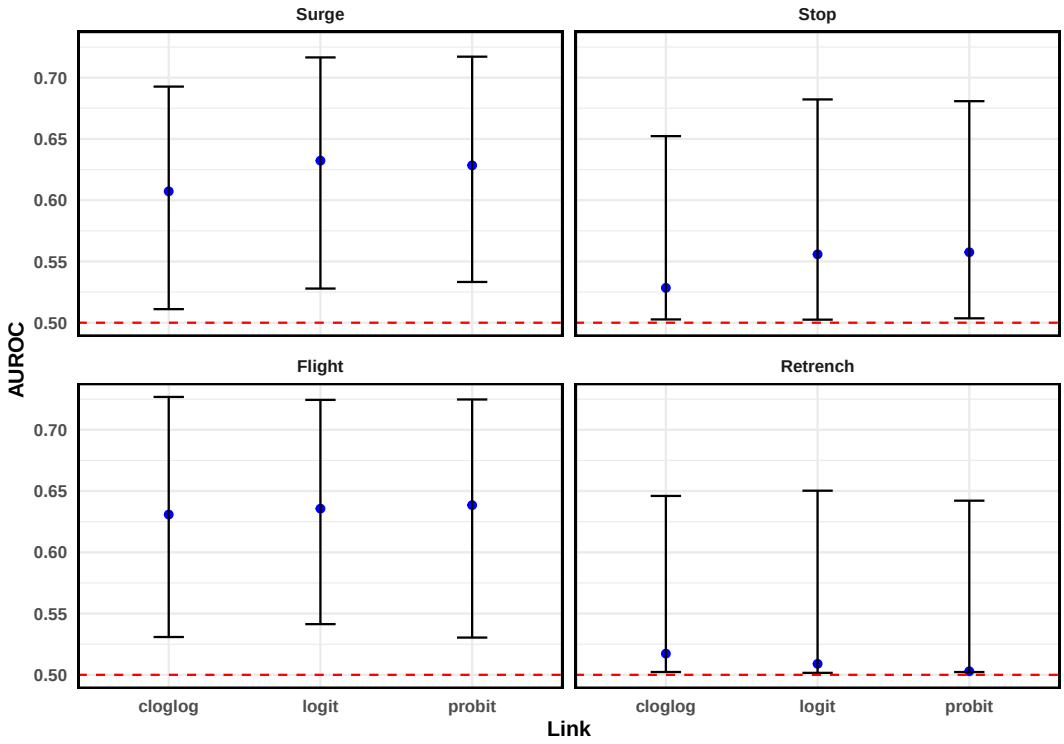

Notes: AUROC for the different episodes and link functions. The blue dots indicate the point estimate of the AUROC and the whiskers indicate the 95% CI obtained from 1,000 block bootstrap replications.

Figure 5.8: Distribution of AUROC Across Countries

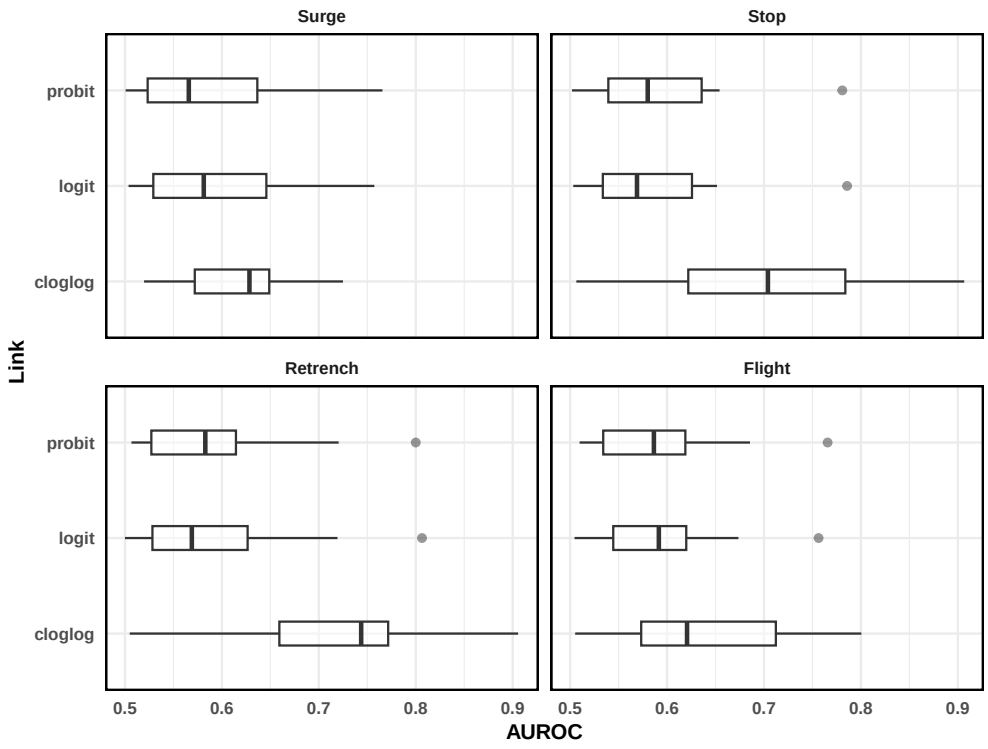

Notes: These figures show the distribution of AUROC scores across the 27 countries of the panel for the full-information set-up.

one. There is no quantifiable difference noted among the episodes and link functions. Improvements are evident when compared to similar BS reported for the benchmark model in Table D.1 of Appendix D.1.1. Therefore, these complement the findings of the AUROC scores earlier.

Table 5.6: BS - Full Sample Assessment

Episodes	cloglog	probit	logit
Surge	0.1629	0.1616	0.1616
Stop	0.1592	0.1515	0.1515
Retrench	0.1624	0.1558	0.1555
Flight	0.1692	0.1682	0.1672

Notes: This table shows the Brier Scores for the different events and link functions for the full sample assessment.

KS

The results displayed in Table 5.7 demonstrate improved KS from the full-information mixed frequency set-up than those from the benchmark model, as reported in Table D.2 of Appendix D.1.1. KS are generally higher when the threshold is set at either the 50^{th} or 75^{th} percentiles of the predicted probability distribution, compared to higher or lower percentiles.

5.4.2 Pseudo-Real-Time Application

In this section, as prevalent in the nowcasting literature, we will make multiple predictions, while continuously updating our information set to reflect new data releases. This is achieved in two steps. We first construct a pseudo-calendar mimicking the actual data release schedule for the different series under consideration. Then we generate a sequence of predictions consisting of forecasts, nowcasts and backcasts. Finally, we assess the predictions using the same verification framework as earlier. We also examine the monotonicity of the scores – i.e., whether the scores improve over time as more recent data are absorbed by the model.

Table 5.7: KS for the full-information analysis

		Thresholds				
Episodes	**Link**	**5%**	**25%**	**50%**	**75%**	**95%**
Surge	cloglog	0.0409	0.1385	0.1496	0.1130	0.0259
Stop	cloglog	-0.0851	-0.0606	0.0463	0.1747	-0.0005
Retrench	cloglog	-0.0637	-0.1141	-0.0071	0.1034	0.0173
Flight	cloglog	0.0334	0.1550	0.1811	0.1611	0.0495
Surge	probit	0.0409	0.1289	0.1846	0.1576	0.0641
Stop	probit	-0.0351	-0.0642	0.0962	0.1782	0.0209
Retrench	probit	-0.0245	-0.1212	0.0250	0.0998	0.0316
Flight	probit	0.0303	0.1581	0.1749	0.1949	0.0495
Surge	logit	0.0346	0.1321	0.1846	0.1830	0.0514
Stop	logit	-0.0280	-0.0499	0.0642	0.1854	0.0565
Retrench	logit	-0.0316	-0.1141	0.0285	0.1069	0.0351
Flight	logit	0.0334	0.1550	0.1719	0.1887	0.0464

Notes: This table displays the KS for the full-information results over a range of thresholds covering the entire distribution of probabilistic predictions across episodes and different link functions.

Data Releases and Calendar

The IMF BoP data archives[9] preserve the actual country-level release dates for the quarterly capital flows. Typically, the data are released on Wednesdays of the last whole week of the month. The pseudo-calendar averages the publication lags in days from the quarter-end-date for each country over a period of 20 quarters during the five years spanning from Q2:2017 to Q2:2022. Table 5.8 and Figure 5.9 present the summary statistics of the publication lag for the 27 countries we consider. Publication lags are enormous, with the minimum being 86 days and many countries having publication lags of more than 100 days. The shortest average publication lags are for Brazil, followed by Turkey and Indonesia.

We have daily and monthly data as high-frequency predictors. The daily data are assumed to be available on the day of prediction with no lags. Table 5.9 presents the exact lags for the several monthly series we consider. Among these, the shortest lag is for the M2 series in Japan, which is available after 14 days. and other monthly series

[9]See https://data.imf.org/?sk=7a51304b-6426-40c0-83dd-ca473ca1fd52&sid=1542634807764 [Last accessed: 15-11-2022].

are usually published within 30 days. We assume that there is a 30-day lag for all monthly series.

Table 5.8: Summary of Publication Lags Across Countries

No. of Countries	Min	Q1	Median	Mean	Q3	Max
27	86	138	146	157	153	346

Notes: This table shows the distribution of publication lags for the capital flows data in the IMF BoP database. The average (from Q2:2017 until Q2:2022) of publication lags presented as the difference in days from the quarter end date until the date of data release.

Figure 5.9: Publication Lags Across Countries

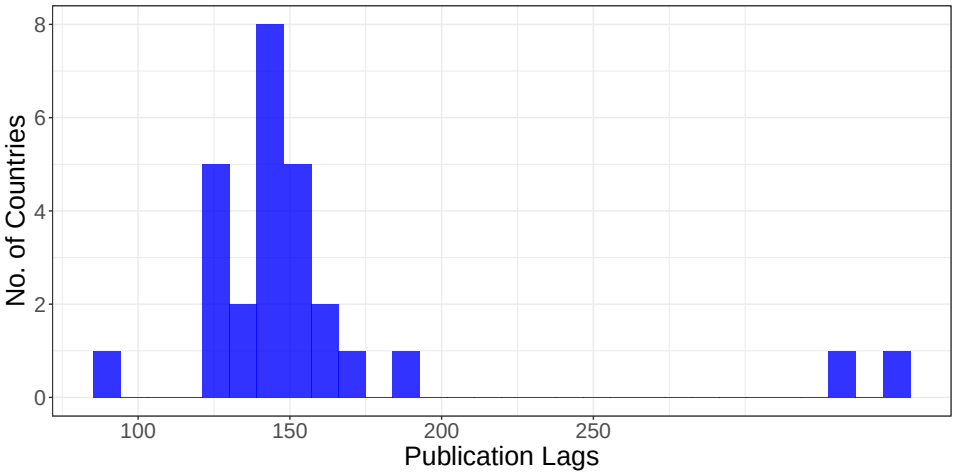

Notes: See Table 5.8

Table 5.9: Monthly Data Release Calendar

No.	Series	Publication Lags[a]	Source
1	M2 (EUR)	30	European Central Bank
2	M2 (U.S.)	30	The Federal Reserve
3	M4 (U.K.)	30	Bank of England
4	M2 (Japan)	14	Bank of Japan
5	World Economic Activity	30	Federal Reserve bank of Dallas
6	Commodity Prices	30	World Bank

Notes: This table shows the publication lags in days and the sources of the monthly data.

[a] In days, approx.

Prediction Sequences and Monotonicity Assessment

For each episode, we consider monthly updates of predictions. The sequence of out-of-sample predictions consists of 10 updates, starting at the beginning of the quarter preceding the target quarter and ending 90 days after the end of the quarter. Every update of the predictions incorporates new releases of the monthly series and includes the latest daily data. Even after 90 days, all of the countries in our panel, except Brazil, await the release of the BoP actual data, as seen earlier in Table 5.8. By the end of the quarter, the first lags are usually available for all except Guatemala, Sri Lanka and Thailand. Thus, the chain of prediction consists of three forecasts, four nowcasts and three backcasts. The actuals for the accuracy assessment are constructed from the latest available vintage of the IMF BoP database.

AUROC

Figure 5.10 shows the AUROC scores for the different prediction days for each of the three link functions and the four episodes. The AUROC from the panel models beat the random classifier from the starting point of our prediction sequence. Also, the results are distinctly better than a naïve constant-only benchmark (see Figure D.4) The AUROC scores are comparable to the full-sample results presented earlier in Figure 5.7. Therefore, the predictions from our mixed-frequency model display forecast skills as early as the beginning of the quarter before the target quarter. Thereafter, the accuracy of the predictions as measured by the AUROC remains steady with fluctuations in a low band as new information becomes available and are passed on to the model.

We formally test the sequence of AUROC scores to identify if there is any significant gain from additional information being absorbed by the model. For every prediction date, starting from the second date, we test if the current AUROC is different from the previous AUROC – i.e., if AUC_i denotes the AUROC for the i^{th} prediction date, we test for $H_0 : AUC_i = AUC_{i-1}$ vs $H_0 : AUC_i \neq AUC_{i-1}$ for $i = 2, 3, \ldots 10$[10]. Table 5.10

[10]We assume normality of the AUROC scores and compute the standard deviation using bootstrap.

Figure 5.10: AUROC at Different Prediction Dates

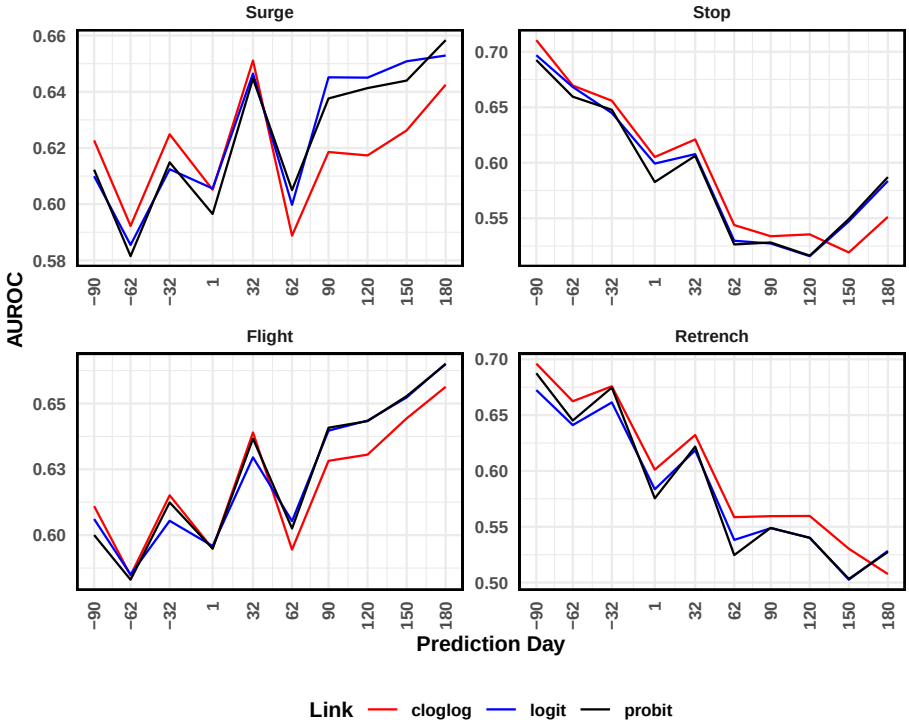

Notes: This figure shows the sequence of AUROC scores for different episodes and link functions. Prediction days are referenced from the start of quarter. Therefore, minus 90 means the starting day of the previous quarter.

displays the p-values for the sequences of these tests. We find that excepting a few prediction dates towards the end of our sequence, the majority of the AUROC scores are statistically significantly different from the AUROC scores of the previous prediction date. Thus, although our AUROC sequences display a variation in a low range and do not exhibit monotonicity, they can significantly absorb new information. These results further strengthen the finding that the sequence of AUROC are stable and indicate satisfactory performance of our model up to two quarters ahead of the target quarter end.

Table 5.10: Tests of Significance of AUROC sequences

Prediction Day	Surge	Stop	Retrench	Flight
		cloglog		
2	0.0029	0.0002	0.0036	0.0116
3	0.0040	0.3680	0.3153	0.0109
4	0.1093	0.0001	0.0000	0.0841
5	0.0000	0.0283	0.0000	0.0000
6	0.0000	0.0000	0.0001	0.0006
7	0.0019	0.0935	0.8932	0.0003
8	0.7159	0.6493	0.9561	0.2517
9	0.1351	0.6422	0.0484	0.0234
10	0.0106	0.0001	0.5553	0.0110
		probit		
2	0.0027	0.0009	0.0001	0.0614
3	0.0052	0.4908	0.0493	0.0172
4	0.1372	0.0000	0.0000	0.1025
5	0.0000	0.0062	0.0000	0.0000
6	0.0041	0.0000	0.0000	0.0053
7	0.0004	0.7805	0.0009	0.0001
8	0.3071	0.0009	0.0123	0.3987
9	0.7160	0.3453	0.0205	0.0546
10	0.0736	0.0000	0.5196	0.0259
		logit		
2	0.0116	0.0054	0.0048	0.0198
3	0.0135	0.1381	0.1598	0.0895
4	0.5481	0.0003	0.0000	0.3836
5	0.0000	0.3008	0.0001	0.0000
6	0.0004	0.0000	0.0000	0.0438
7	0.0000	0.7097	0.1274	0.0000
8	0.9698	0.0011	0.0041	0.1701
9	0.4127	0.3706	0.0130	0.1203
10	0.7687	0.0000	0.4983	0.0301

Notes: This table shows the pairwise test of the AUROC scores for the pseudo-real-time analysis. This is relatable to Figure 5.10. Each row of the table displays the p-value for testing the null hypothesis that the AUROC score obtained on the prediction day is statistically significantly different from the AUROC score on the previous prediction day. We have nine rows for each link function as we have 10 prediction days in total. The test uses bootstrapped standard errors.

BS

Table 5.11 presents the BS for the pseudo-real-time analysis and the figures reveal similar conclusions as earlier – i.e., (i) the BS are relatively closer to zero than one (ii) improvements are noticeable when compared with the BS from the benchmark model as reported in Table D.3 of Appendix D.2.1 (iii) there is a very low range of variation among different episodes and the link functions. Additionally, the sequence of BS exhibits signals of monotonicity – i.e., improvement of prediction accuracy indicated by a declining pattern of BS over the horizons as our model absorbs more information from newer data releases. Monotonicity was not evident from the analysis of AUROC scores previously.

KS

Analysing the results presented in Table 5.12, we find that KS varies more across choice of thresholds and episodes, but not much across link functions. Among the episodes, surges and flights show a better range of KS as compared to retrenchments and stops, over the sequence of prediction horizons under consideration. While the KS values are positive right from the start for flights and retrenchments, they become positive later on for stops and surges. Improvements are evident when compared to the KS of the predictions from the benchmark model, as reported in Table D.3 in Appendix D.2.1. Similar to BS, we also note a monotonic improvement of KS across all events.

Table 5.11: BS for Pseudo-Real-Time Analysis

Prediction Day	Surge	Stop	Retrench	Flight
		cloglog		
1	0.1590	0.1774	0.1731	0.1660
2	0.1599	0.1764	0.1713	0.1669
3	0.1592	0.1731	0.1697	0.1651
4	0.1607	0.1664	0.1636	0.1673
5	0.1593	0.1698	0.1689	0.1651
6	0.1618	0.1574	0.1584	0.1680
7	0.1614	0.1587	0.1602	0.1682
8	0.1621	0.1600	0.1602	0.1677
9	0.1612	0.1519	0.1557	0.1664
10	0.1555	0.1484	0.1529	0.1615
		probit		
1	0.1598	0.1727	0.1707	0.1665
2	0.1605	0.1713	0.1684	0.1663
3	0.1595	0.1669	0.1675	0.1647
4	0.1618	0.1621	0.1605	0.1672
5	0.1588	0.1667	0.1664	0.1647
6	0.1611	0.1535	0.1546	0.1675
7	0.1602	0.1563	0.1583	0.1663
8	0.1602	0.1580	0.1576	0.1667
9	0.1607	0.1467	0.1503	0.1665
10	0.1547	0.1416	0.1477	0.1605
		logit		
1	0.1597	0.1697	0.1666	0.1655
2	0.1600	0.1690	0.1665	0.1663
3	0.1597	0.1680	0.1650	0.1655
4	0.1601	0.1618	0.1600	0.1666
5	0.1581	0.1655	0.1639	0.1650
6	0.1611	0.1527	0.1541	0.1673
7	0.1594	0.1556	0.1565	0.1663
8	0.1596	0.1559	0.1575	0.1655
9	0.1589	0.1463	0.1501	0.1658
10	0.1559	0.1415	0.1471	0.1603

Notes: This table displays the BS for all the 10 prediction dates we consider in the pseudo-real-time analysis. The different link functions are grouped together in blocks for all of the four episodes.

Table 5.12: KS for Pseudo-Real-Time

(a) KS for Surges

Prediction Day	5%	25%	50%	75%	95%
			cloglog		
1	0.0431	0.0655	0.1271	0.2183	0.0493
2	0.0431	0.0919	0.0677	0.1721	0.0559
3	0.0431	0.0886	0.1535	0.1820	0.0658
4	0.0530	0.0787	0.1205	0.1622	0.0790
5	0.0497	0.1579	0.2030	0.1754	0.0592
6	0.0002	0.1051	0.1370	0.1193	0.0361
7	0.0497	0.1249	0.2096	0.1127	0.0361
8	0.0530	0.1315	0.2228	0.1391	0.0295
9	0.0497	0.1513	0.1700	0.1490	0.0460
10	0.0530	0.1711	0.1766	0.1523	0.0823
			probit		
1	0.0332	0.0490	0.1502	0.2150	0.0592
2	0.0530	0.0358	0.0776	0.1457	0.0460
3	0.0398	0.0919	0.1007	0.1952	0.0592
4	0.0167	0.0226	0.1271	0.1556	0.0559
5	0.0563	0.1480	0.2030	0.2051	0.0526
6	0.0332	0.1216	0.0974	0.1325	0.0526
7	0.0530	0.1282	0.2261	0.1589	0.0559
8	0.0530	0.1447	0.2426	0.1688	0.0559
9	0.0530	0.1381	0.1931	0.2150	0.0526
10	0.0596	0.1513	0.2294	0.2084	0.0823
			logit		
1	0.0332	0.0424	0.1370	0.2150	0.0493
2	0.0530	0.0193	0.1238	0.1820	0.0592
3	0.0431	0.1183	0.1238	0.1820	0.0460
4	0.0398	0.0721	0.1502	0.1787	0.0724
5	0.0563	0.1447	0.1700	0.2117	0.0592
6	0.0464	0.1348	0.1073	0.1226	0.0559
7	0.0563	0.1348	0.2294	0.1820	0.0658
8	0.0530	0.1249	0.2096	0.1688	0.0559
9	0.0497	0.1282	0.2096	0.2282	0.0592
10	0.0530	0.1612	0.1964	0.2117	0.0559

Notes: This table displays the KS for the prediction of surge episodes using a number of thresholds covering the distribution of predicted probabilities.

Table 5.12: KS for Pseudo-Real-Time

(b) KS for Stops

Prediction Day	5%	25%	50%	75%	95%
			cloglog		
1	-0.0961	-0.3176	-0.3142	-0.1392	-0.0391
2	-0.1181	-0.2006	-0.2412	-0.1465	-0.0354
3	-0.0413	-0.2043	-0.2010	-0.1355	-0.0281
4	-0.0998	-0.2299	-0.1169	-0.0624	0.0158
5	-0.0925	-0.2445	-0.1571	-0.0771	0.0267
6	-0.0633	-0.1568	-0.0548	0.0581	0.0486
7	-0.0523	-0.1605	-0.0438	0.0472	0.0596
8	-0.0961	-0.1714	-0.0073	-0.0076	0.0596
9	-0.0523	-0.0874	0.0512	0.0874	0.0559
10	0.0354	-0.0508	0.0548	0.1860	0.0267
			probit		
1	-0.1108	-0.2993	-0.2740	-0.1465	-0.0354
2	-0.1181	-0.1751	-0.2119	-0.1465	-0.0464
3	-0.0267	-0.2043	-0.1973	-0.1282	-0.0354
4	-0.0961	-0.2043	-0.1096	0.0070	0.0158
5	-0.0633	-0.2299	-0.1352	-0.0588	0.0267
6	-0.0559	-0.0947	-0.0548	0.0399	0.1144
7	-0.0450	-0.1568	-0.0219	0.0545	0.0596
8	-0.0377	-0.0947	-0.0256	0.0508	0.0706
9	-0.0158	-0.0070	0.0402	0.1678	0.0559
10	0.0354	0.0186	0.0877	0.1933	0.1254
			logit		
1	-0.0815	-0.3030	-0.2667	-0.1392	-0.0464
2	-0.1144	-0.1239	-0.2412	-0.1794	-0.0391
3	-0.0413	-0.2116	-0.1535	-0.1319	-0.0354
4	-0.0925	-0.2080	-0.1242	-0.0149	0.0194
5	-0.0961	-0.2335	-0.1535	-0.0624	0.0304
6	-0.0596	-0.1568	-0.0475	0.0399	0.1144
7	-0.0779	-0.1129	-0.0438	0.0545	0.0633
8	-0.0523	-0.0874	-0.0110	0.0508	0.0669
9	-0.0194	-0.0033	0.0438	0.1495	0.0559
10	-0.0121	0.0222	0.0658	0.2153	0.1034

Notes: This table displays the KS for the prediction of stop episodes using a number of thresholds covering the distribution of predicted probabilities.

Table 5.12: KS for Pseudo-Real-Time

(c) KS for Retrenchments

Prediction Day	5%	25%	50%	75%	95%
			cloglog		
1	-0.1067	-0.2977	-0.2533	-0.1726	-0.0319
2	-0.1468	-0.1592	-0.2169	-0.1398	-0.0428
3	-0.0775	-0.2503	-0.2388	-0.1252	-0.0209
4	-0.1140	-0.1701	-0.1112	-0.0778	0.0155
5	-0.1103	-0.2612	-0.1768	-0.0814	-0.0027
6	-0.0739	-0.1409	-0.1002	-0.0122	0.0301
7	-0.0848	-0.1810	-0.0893	0.0170	0.0556
8	-0.0702	-0.1810	-0.0820	0.0133	0.0520
9	-0.0666	-0.1446	-0.0091	0.0097	0.0593
10	0.0282	-0.1191	0.0310	0.0935	0.0228
			probit		
1	-0.1249	-0.2722	-0.2533	-0.1726	-0.0391
2	-0.1468	-0.1336	-0.2060	-0.1325	-0.0464
3	-0.0848	-0.2503	-0.2752	-0.1288	-0.0282
4	-0.1176	-0.1227	-0.1440	-0.0486	0.0155
5	-0.0702	-0.2357	-0.1914	-0.1033	0.0192
6	-0.0702	-0.0534	-0.0674	0.0316	0.0921
7	-0.0702	-0.1300	-0.0747	0.0133	0.0629
8	-0.0411	-0.0899	-0.1039	0.0170	0.0483
9	0.0027	-0.0790	-0.0273	0.0863	0.0593
10	0.0464	-0.1045	0.0091	0.1118	0.0775
			logit		
1	-0.0739	-0.2175	-0.2205	-0.1580	-0.0319
2	-0.1030	-0.1373	-0.2096	-0.1252	-0.0501
3	-0.0848	-0.2357	-0.2242	-0.1179	-0.0282
4	-0.1140	-0.1154	-0.1258	-0.0486	0.0228
5	-0.0848	-0.2175	-0.1732	-0.0997	-0.0136
6	-0.0739	-0.1045	-0.0930	-0.0122	0.0957
7	-0.0666	-0.1264	-0.0674	0.0206	0.0556
8	-0.0666	-0.1191	-0.0565	0.0133	0.0556
9	-0.0411	-0.0644	-0.0310	0.1008	0.0556
10	0.0282	-0.0826	0.0346	0.1081	0.0848

Notes: This table displays the KS for the prediction of retrenchment episodes using a number of thresholds covering the distribution of predicted probabilities.

Table 5.12: KS for Pseudo-Real-Time

(d) KS for Flights

Prediction Day	5%	25%	50%	75%	95%
			cloglog		
1	0.0222	0.0617	0.1578	0.1934	0.0575
2	0.0381	0.0266	0.1228	0.1679	0.0607
3	0.0286	0.0681	0.1483	0.1838	0.0480
4	0.0190	0.0585	0.1196	0.1742	0.0544
5	0.0477	0.1095	0.1770	0.2253	0.0544
6	0.0094	0.0713	0.1323	0.1392	0.0512
7	0.0477	0.1510	0.1865	0.1328	0.0703
8	0.0477	0.1382	0.1897	0.1392	0.0703
9	0.0445	0.1510	0.1993	0.1742	0.0639
10	0.0541	0.1574	0.2248	0.1838	0.1054
			probit		
1	0.0126	0.0458	0.1642	0.1519	0.0607
2	0.0381	0.0075	0.1036	0.1647	0.0639
3	0.0286	0.0617	0.1387	0.2189	0.0544
4	0.0349	0.0426	0.1164	0.1519	0.0512
5	0.0477	0.1191	0.1770	0.2093	0.0416
6	0.0413	0.0745	0.1323	0.1551	0.0448
7	0.0413	0.1191	0.1770	0.1902	0.0639
8	0.0445	0.1319	0.1961	0.1838	0.0607
9	0.0445	0.1478	0.1993	0.2380	0.0767
10	0.0541	0.1574	0.1961	0.2316	0.0703
			logit		
1	0.0126	0.0681	0.1578	0.1615	0.0575
2	0.0381	-0.0148	0.1068	0.1742	0.0448
3	0.0286	0.0745	0.1451	0.1774	0.0575
4	0.0254	0.0585	0.1291	0.1838	0.0607
5	0.0477	0.1191	0.1738	0.2093	0.0448
6	0.0413	0.1000	0.1451	0.1360	0.0352
7	0.0413	0.1414	0.1961	0.1902	0.0607
8	0.0445	0.1159	0.2152	0.2125	0.0416
9	0.0413	0.1414	0.2057	0.2285	0.0512
10	0.0541	0.1606	0.2089	0.2253	0.0830

Notes: This table displays the KS for the prediction of flight episodes using a number of thresholds covering the distribution of predicted probabilities.

5.5 Conclusion

In this chapter, we propose and estimate a novel binary choice model to predict the probabilities of extreme episodes in cross-border capital flows in a timely fashion. Our model is in a mixed-frequency panel framework and predicts the probabilities for the quarterly target events with monthly and daily predictors. To handle the mixed-frequency nature of the data, we used a non-linear MIDAS set-up with Almon lag polynomials. The model is estimated with a modified maximum likelihood technique which reduces the number of parameters. In the empirical application, the model generates predictions for 27 major countries from the IMF BoP database using high-frequency macro-financial predictors in full-information and pseudo-real-time setups. We rigorously evaluated predictions using formal forecast verification tools and statistical tests.

Our main findings indicate skilled model projections which can significantly outperform a random classifier and a naïve benchmark as by AUROC and complemented by BS and KS. There is no material difference between the three link functions we examined. Our pseudo-real-time version of the database resembles the actual publication lags. The predictions exhibit statistically significant forecast skill from the start of our prediction exercise which is 90 days prior to the beginning of the target quarter. The predictions change significantly when newer data releases become available. There are indications of monotonic improvement of accuracy, as seen from the declining BS and KS metrics. Overall, we conclude that accuracy remains steady and satisfactory, with negligible variations within a low range as new data releases are absorbed by the model.

Chapter 6

Conclusions and Outlook

To summarise, this thesis has made distinct contributions to four different areas of the panel forecasting literature. Firstly, we have extended the panel nowcasting literature by incorporating CSD in a MF-PVAR. Secondly, we augmented a panel bridge equation framework with a similar CSD structure. Thirdly, we have built up the panel GaR model with CSD factors. Finally, we have enhanced the panel discrete choice framework with CSD, ragged edges and a rigorous out-of-sample assessment. These models predict a number of important macroeconomic and environmental variables. In the linear setting, we modelled GDP growth, inflation and CO_2 emissions. In the quantile regression framework, we focused on GaR and finally we turn to non-linear models predicting extreme episodes of cross-border capital flows. Our datasets include international and regional panels. The following paragraphs sum up the core chapters of the thesis and highlight some of potential research ideas.

In Chapter 2 we proposed a method to incorporate CSD in panel nowcasting models with mixed-frequencies. CSD is well-recognised in large panels and has been explicitly modelled in previous causal studies. The model is applied to nowcast GDP and inflation – two of the key variables tracked for monetary policymaking – for large panels of countries. New information is added to the model as they become available and the predictions are updated. The series of predictions out-perform standard benchmarks and also improves monotonically as more information is incorporated.

The following research questions arise from this chapter. A natural progression of this work will be to implement the other forms of non-linear lag polynomials in the MIDAS part of the model. A further study could compare the results with the Dynamic Factor Model (DFM) which is widely applied in nowcasting studies. To enable this comparison, we would require an extension of the DFM to the panel data set-up. Another limitation we faced was the lack of harmony for published macroeconomic data among various countries. With more and more data being available for research, we hope that at some future point, we will be able to implement DFMs in panel frameworks. The CCE is one of the methods to approach CSD in panel data. It would be interesting to compare the results with the other methods of incorporating CSD such as in panel data models like that of Bai (2009) and related chapters. Another fruitful area for further work could be a fully-fledged non-linear panel extension to the MFVAR model with impulse response analysis. More broadly, future related studies could connect the forecasting literature with panel aggregation (such as Pesaran and Chudik 2014) for comprehensive predictions.

Chapter 3 develops and estimates a CSD panel bridge equation framework to predict state-level CO_2 emissions. Timely predictions of U.S. subnational CO_2 emissions can play a key role in the recent regional abatement policies as there are enormous publication lags. The bridge equation model predicts emissions with EC and in turn uses the quarterly real personal income to predict EC. The series of generated predictions show sizeable gains in prediction accuracy in select U.S. states as early as two years before the release of the official estimates. The overall accuracy improves remarkably once the model absorbs the actual releases of EC data.

Given the international recognition of the climate crisis, reducing greenhouse gases and decarbonisation have gained unprecedented priority in recent times across the globe. While the road to decarbonisation and achieving global climate goals has multiple challenges, future predictions could be an important tool in policymaking. The mixed-frequency panel model would be particularly useful in this case because policies need to focus on several layers such as sub-national, national, regional and

global. The methods developed here could be applied to other regions of the world. We have earlier mentioned possible applications for the prediction aggregation of firm-level emissions. Research on nowcasting CO_2 emissions is still very nascent and there are a lot of possibilities both in terms of choice of target of prediction and development of new econometric methods.

Chapter 4 proposes to incorporate CSD in a forward-looking panel GaR framework. The IMF introduced the concept of GaR modelling with quantile regressions, and it is now a well-accepted methodology to quantify macroeconomic tail–risks. The in-sample analysis of the model reveals a different nature of the relationship of GaR with a series of well-known vulnerability predictors, relative to existing studies. The predictions from the model turn out to be superior in out-of-sample comparison.

GaR is a key concept linking the real and the financial sectors of the economy and future research could have manifold implications for several policymakers including monetary policymaking, financial stability monitoring and others. Further studies need to be carried out to understand whether the panel GaR model excluding CSD was possibly misspecified. The present GaR methodology using quantile regression is a very data-intensive procedure and this very nature of the method restricts the framework to countries with a reasonably rich history of macro-financial data. Moving forward, a greater understanding of the phenomenon across a wider range of countries needs to be developed. Quantile regressions with shrinkage estimation could be one of the options to explore, which has not found applications in the GaR literature so far. The issue of timeliness of macroeconomic data also applies to the GaR framework. Higher-frequency or mixed-frequency set-ups have been proposed for GaR modelling for single time series such as the Euro Area (Ferrara et al. 2022) or the U.S. (Castelnuovo and Mori 2022). Panel extensions could be an area to explore and would be useful for policymakers from a risk-management perspective. International transmission of shocks is a key concern to policymaking and their explicit accounting in tail–risks modelling could be useful. Another aspect relevant to policy yet to be investigated is the link between national GaR and individual firm-level risk metrics which could be facilitated in aggregation in

a panel framework.

Chapter 5 proposes a mixed-frequency panel data model to predict the extreme episodes of cross-border capital flows in a timely fashion. Cross-border capital flows are volatile and can have extreme economic impacts. Although the existing literature recognises the episodic nature of these flows as well as their determinants and mitigating policies, surprisingly there is little focus on data release schedules and the timeliness of predictions. Therefore, the non-linear panel model makes provisions for the asynchronous calendars. The target of prediction is binary and indicates either the occurrence or the non-occurrence of the event. The model is updated on every release of relevant data and the sequence of predictions is seen to beat a standard benchmark much ahead of the event realisation.

Further research might explore different ways to include CSD in discrete choice panel models. Recently Gao et al. (2023) have provided a way to estimate similar models. Alternatively, the score-driven methods such as those of Creal et al. (2014) which have been used for credit risk modelling could be adapted. Methodologically, another important direction would be inference from mixed-frequency binary choice models. As noted in Ghysels et al. (2007) and more recently by Khalaf et al. (2021), inference for MIDAS models run into the well-known incidental parameter problem (for instance, see Davies 1977; Davies 1987; Andrews and Ploberger 1994; Hansen 1996; Teräsvirta et al. 2010; Hurn et al. 2016) and hence the usual inference using Wald or Score tests do not apply. Similarly, inference methods in this context also requires a way to deal with the incident parameter problem. There could be many interesting directions in empirical research as capital flows and extreme episodes can generate both extreme possibilities and distress and hence are keenly monitored by policymakers, especially when trying to attract steady streams of foreign investment. In this context, narrowing the focus of prediction down to particular types of flows or flows from and to specific regions could be of interest. Extending to multi-way panel models in the line of gravity models (such as that of Kapetanios et al. 2021) and expanding gravity models to include binary targets and mixed-frequencies could be interesting extensions

both methodologically and empirically.

In general, this thesis did not touch upon Bayesian estimation methods which have a long history and significant applications in panel VARs, and macroeconomics. These methods could be explored further in connection with the estimation of models discussed here. Overall, this thesis has attempted to extend the panel macroeconomic forecasting literature with distinct contributions. There remain numerous possibilities for future research as the challenges of forecasting for policymaking in an uncertain world are enormous.

Appendices

Appendix A

Appendix to Chapter 2

In support of Chapter 2, this appendix contains additional tables, figures, and derivations. The appendix is organised as follows. Section A.1 contains the derivations of the LCCE technique from the CCE method of Chudik and Pesaran (2015a). We present the additional results on the Monte Carlo simulations in Section A.2. Subsequently, further Monte Carlo results on different frequency mixes are included in the Section A.3 to complement the results presented earlier in the main chapter. Pseudo data release calendars in Section A.4 substantiate the main results of the chapter. Finally, we display a range of robustness results in Sections A.5 and A.6.

A.1 Details on Model Estimation and Derivation

In the main chapter we present the full mixed-frequency PMIDAS nowcasting model with a ragged edge. In this section, we go back and construct the PMIDAS model step-by-step in two phases, starting from the dynamic CSD panel data model of Chudik and Pesaran (2015a). As in the main chapter, we have a target variable of interest $y_{i,t}$ for the i^{th} cross-sectional unit and t^{th} time point, where $i = 1, 2, \ldots, N$ and $t = 1, 2, \ldots, T$. Let $x_{i,t}$ be a predictor which, for the sake of simplicity in this Appendix, we assume is a single variable. This is easily generalised to the case of many predictors as in the main text. In this first step we consider $x_{i,t}$ and $y_{i,t}$ to be of the same frequency. This allows us to directly modify the CCE estimation method of Chudik and Pesaran (2015a) to the lagged version, i.e. LCCE, which permits the model to be used for forecasting. In the second step, the model is further extended to incorporate the mixed-frequency data as in general nowcasting frameworks. Here the predictor variable $x_{i,t}$ is assumed to be of a higher frequency than that of the target $y_{i,t}$. Finally we add in the ragged edge where lag structures and model parameters depend on the nowcast day, v.

A.1.1 The Nowcasting Model: Single Frequency, no Ragged Edge

Set-up

The main framework for the dynamic heterogeneous panel model with multi-factor error structure follows the format of Chudik and Pesaran (2015a):

$$y_{i,t} = c_i + \phi_i y_{i,t-1} + \beta_{0i} x_{i,t} + \beta_{1i} x_{i,t-1} + u_{i,t} \tag{A.1a}$$

$$u_{i,t} = \gamma_i' f_t + \varepsilon_{i,t} \tag{A.1b}$$

$$x_{i,t} = \kappa_i + \alpha_i y_{i,t-1} + \Gamma_i' f_t + \epsilon_{i,t} \tag{A.1c}$$

In equations (A.1), c_i and κ_i are individual fixed effects. The term f_t is an $m \times 1$ vector of unobserved common factors which impact both the target and the predictor through loadings γ_i and Γ_i which are of orders $m \times 1$ respectively. The coefficient α_i characterises the relation between the predictor and lagged target variables, $\varepsilon_{i,t}$ represents the idiosyncratic errors and $\epsilon_{i,t}$ is assumed to follow a general linear covariance stationary process distributed independently of $\varepsilon_{i,t}$.

In the original formulation of the CCE approach, the common factors, f_t, are estimated using the cross-sectional averages of $z_{i,t} = (y_{i,t}, x_{i,t})'$. The presence of $y_{i,t}$ in the estimates of the factors clearly makes the model unsuitable for forecasting or nowcasting applications. Therefore, we propose the following modifications.

Estimation and Nowcasting

We define $z_{i,t}$ to contain lagged y and the current information on the predictor variable x, i.e.:

$$z_{i,t} = \begin{pmatrix} y_{i,t-1} \\ x_{i,t} \end{pmatrix}$$

Combining this with equations (A.1a), (A.1b) and A.1c we obtain:

$$A_{0i} z_{i,t} = c_{zi} + A_{1i} z_{i,t-1} + A_{2i} z_{i,t-2} + C_i F_t + e_{i,t} \tag{A.2a}$$

$$\implies z_{i,t} = K_{zi} + B_{0i} z_{i,t-1} + B_{1i} z_{i,t-2} + A_{0i}^{-1} C_i F_t + A_{0i}^{-1} e_{i,t} \tag{A.2b}$$

where:

$$c_{zi} = \begin{pmatrix} c_i \\ \kappa_i \end{pmatrix}, A_{0i} = \begin{pmatrix} 1 & 0 \\ -\alpha_i & 1 \end{pmatrix}, A_{1i} = \begin{pmatrix} \phi_i & \beta_{0i} \\ 0 & 0 \end{pmatrix}, A_{2i} = \begin{pmatrix} 0 & \beta_{1i} \\ 0 & 0 \end{pmatrix}$$

$$K_{zi} = A_{0i}^{-1} c_{zi},\ B_{0i} = A_{0i}^{-1} A_{1i},\ B_{1i} = A_{0i}^{-1} A_{2i}$$

$$C_i = \begin{pmatrix} 0 & \gamma_i' \\ \Gamma_i' & 0 \end{pmatrix} = \begin{pmatrix} C_{0i} & C_{1i} \end{pmatrix}\ C_{0i} = \begin{pmatrix} 0 \\ \Gamma_i' \end{pmatrix}$$

$$C_{1i} = \begin{pmatrix} \gamma_i' \\ 0 \end{pmatrix}, F_t = \begin{pmatrix} f_t \\ f_{t-1} \end{pmatrix} \text{ and } e_{i,t} = \begin{pmatrix} \varepsilon_{i,t-1} \\ \epsilon_{i,t} \end{pmatrix}$$

Assumption 1. *The eigenvalues of the following augmented matrix are less than one in absolute value:*

$$\begin{pmatrix} B_{0i} & B_{1i} \\ I & 0 \end{pmatrix}$$

Next, we derive the large-N representation of the factors, f_t, in terms of the cross-sectional averages of $z_{i,t}$. With Assumption 1, $z_{i,t}$ is an invertible covariance stationary process and can be written as:

$$(I - B_{0i}L - B_{1i}L^2) z_{i,t} = K_{zi} + A_{0i}^{-1} C_i F_t + A_{0i}^{-1} e_{i,t} \tag{A.3a}$$

$$\implies z_{i,t} = K_{1_{zi}} + \Psi_i(L) A_{0i}^{-1} C_i F_t + \Psi_i(L) A_{0i}^{-1} e_{i,t} \tag{A.3b}$$

$$\implies z_{i,t} - K_{1_{zi}} = \Psi_i(L) A_{0i}^{-1} C_i F_t + \Psi_i(L) A_{0i}^{-1} e_{i,t} \tag{A.3c}$$

where:

$$K_{1_{zi}} = (I - B_{0i}L - B_{1i}L^2)^{-1} K_{zi}$$

$$\Psi_{i0} = I, \Psi_{i1} = B_{0i}$$

$$\Psi_{iv} = B_{0i}\Psi_{i,v-1} + B_{1i}\Psi_{i,v-2}, v \geq 2$$

Assumptions 3–5 of Chudik and Pesaran (2015a) ensure that the $\Psi_i(L)$ coefficient matrices are independently distributed of each other and also over the cross-sections. We take weighted cross-sectional averages of equation (A.3c), using a weight vector $w = (\omega_1, \omega_2, \ldots, \omega_N)'$. Assuming the granularity conditions and using similar steps as in Chudik and Pesaran (2015a), the terms on the right-hand side (RHS) of equation (A.3c) give:

$$\begin{aligned}\sum_{i=1}^{N}\left[\sum_{l=0}^{\infty}\omega_i\Psi_{il}A_{0i}^{-1}C_iF_{t-l}\right] &= \sum_{l=0}^{\infty}E\left[\Psi_{il}A_{0i}^{-1}C_i\right]F_{t-l} + O_p(N^{-\frac{1}{2}}) \\ &= \Lambda(L)CF_t + O_p(N^{-\frac{1}{2}})\end{aligned} \tag{A.4a}$$

$$\text{and } \sum_{i=1}^{N}\left[\sum_{l=0}^{\infty}\omega_i\Psi_i(L)A_{0i}^{-1}e_{i,t}\right] = O_p(N^{-\frac{1}{2}}) \tag{A.4b}$$

where:

$$\Lambda(L) = \sum_{l=0}^{\infty}\Lambda_l L^l = \sum_{l=0}^{\infty}E\left[\Psi_{il}A_{0i}^{-1}\right]L^l$$

$$C = E[C_i] = E\begin{pmatrix}0 & \gamma_i' \\ \Gamma_i' & 0\end{pmatrix} = \begin{pmatrix}C_0 & C_1\end{pmatrix}$$

$$E(C_{0i}) = C_0 \text{ and } E(C_{1i}) = C_1$$

Assumption 2. *The inverse of the matrix* $\Lambda(L) = \sum_{l=0}^{\infty}\Lambda_l L^l = \sum_{l=0}^{\infty}E\left[\Psi_{il}A_{0i}^{-1}\right]L^l$ *exists and has exponentially decaying coefficients.*

Continuing from equation (A.4a) we have:

$$\sum_{i=1}^{N}\left[\sum_{l=0}^{\infty}\omega_i\Psi_{il}A_{0i}^{-1}C_iF_{t-l}\right] = \Lambda(L)\left[C_0 + C_1L\right]f_t + O_p(N^{-\frac{1}{2}}) \tag{A.5}$$

Defining the de-trended weighted cross-sectional averages from the left-hand side (LHS) of equation (A.3c) as $\widetilde{z}_{wt} = \sum_{i=1}^{N}\omega_i(z_{i,t} - K_{1_{zi}}) = \sum_{i=1}^{N}\omega_i z_{i,t} - \overline{c}_{zw}$, where $\overline{c}_{zw} = \sum_{i=1}^{N}\omega_i K_{1_{zi}}$, we obtain the following large-N representation of the detrended

cross-sectional averages $\widetilde{z}_{wt}$:

$$\widetilde{z}_{wt} = \Lambda(L)\left[C_0 + C_1 L\right] f_t + O_p(N^{-\frac{1}{2}}) \tag{A.6}$$

$$\implies \Lambda^{-1}(L)\widetilde{z}_{wt} = \left[C_0 + C_1 L\right] f_t + O_p(N^{-\frac{1}{2}}) \tag{A.7}$$

Assumption 3. *C_0 has full column rank.*

Assumption 4. *The eigenvalues of $(C_0'C_0)^{-1}C_0'C_1$ are less than unity in absolute value.*

Assumptions 3 and 4 are crucial for the estimation of the unit-specific coefficients. From equation (A.6) we have:

$$f_t = G(L)\widetilde{z}_{wt} + O_p(N^{-\frac{1}{2}}) \tag{A.8}$$

where:

$$G(L) = \left[I + (C_0'C_0)^{-1}C_0'C_1 L\right]^{-1}\left[C_0'C_0\right]^{-1}C_0'\Lambda^{-1}(L)$$

Substituting the large-N representation of the unobserved common factors from equation (A.8) into equation (A.1a), in a similar way to Chudik and Pesaran (2015a) we obtain an expression for $y_{i,t}$ as a function of the cross-sectional weighted averages $\overline{z}_{wt} = \sum_{i=1}^{N}\omega_i z_{i,t}$ as follows:

$$y_{i,t} = c_i^* + \phi_i y_{i,t-1} + \beta_{0i}x_{i,t} + \beta_{1i}x_{i,t-1} + \delta_i'(L)\overline{z}_{wt} + \varepsilon_{i,t} + O_p(N^{-\frac{1}{2}}) \tag{A.9a}$$

$$= c_i^* + \phi_i y_{i,t-1} + \beta_{0i}x_{i,t} + \beta_{1i}x_{i,t-1} + \sum_{l=0}^{p_T}\delta_{il}'\overline{z}_{w,t-l} + e_{i,t} \tag{A.9b}$$

where:

$$e_{i,t} = \varepsilon_{i,t} + \sum_{l=p_T+1}^{\infty}\delta_{il}'\overline{z}_{w,t-l} + O_p(N^{-\frac{1}{2}})$$

$$c_i^* = c_i - \delta_i'(1)\overline{c}_{zw}$$

and:

$$\delta_i(L) = \sum_{l=0}^{\infty} \delta_{il} L^l = \gamma_i' G(L) \tag{A.9c}$$

and p_T is the truncation used for the infinite lag polynomial of equation (A.9c).

The nowcasting approach is now based on least squares estimation of equation (A.9b), under Assumptions 1–4 and 7 of Chudik and Pesaran (2015a), in addition to the ones stated here. As in the main text, if one wishes to shut down parameter heterogeneity, the model can be estimated by pooled OLS. These steps show how the contemporaneous CCE estimation of the CSD panel models can be modified to LCCE which uses the lagged target variable and henceforth can be used for forecasting or nowcasting applications.

A.1.2 The Nowcasting Model: Mixed-Frequency, No Ragged Edge

Set-up

To extend the this nowcasting framework to include mixed-frequency data (though still no ragged edge, so no dependence on v), consider the single predictor variable to be of a higher frequency relative to the target variable. As in the main text, we take the example where $y_{i,t}$ is of quarterly frequency, and let the predictor variable be monthly and denoted by $x_{i,t}^M$. The ratio of frequencies can be easily generalised. We use the stacked high-frequency process $X_{i,t}^M$:

$$X_{i,t}^M = \begin{pmatrix} x_{i,t}^M \\ x_{i,t-\frac{1}{3}}^M \\ x_{i,t-\frac{2}{3}}^M \end{pmatrix}$$

which was defined in the main text in equation (2.1).

To extend the panel model to mixed-frequency, the lags of the high-frequency process

are directly included in equations (A.1a), (A.1b) and (A.1c) in line with UMIDAS-type models of Foroni et al. (2015) and others. Hence, we adapt the previous model to get the following mixed-frequency dynamic heterogeneous panel data model with multi-factor error structure:

$$y_{i,t} = c_i + \phi_i y_{i,t-1} + \beta_{0i} x^M_{i,t} + \beta_{1i} x^M_{i,t-\frac{1}{3}} + \beta_{2i} x^M_{i,t-\frac{2}{3}} + u_{i,t} \tag{A.10a}$$

$$u_{i,t} = \gamma_i' f_t + \varepsilon_{i,t} \tag{A.10b}$$

$$X^M_{i,t} = \kappa_i + \alpha_i y_{i,t-1} + \Gamma_i' f_t + \epsilon_{i,t} \tag{A.10c}$$

where we adopt the same notation as in the previous section for simplicity, noting that the parameters κ_i and α_i and the errors $\epsilon_{i,t}$ are now vectors and Γ_i is a matrix, in order to match the dimension of $X^M_{i,t}$ in the mixed-frequency set-up.

Equation (A.10a) is the panel equivalent of a UMIDAS model with no functional distributed lag polynomials. Foroni et al. (2015) conclude that UMIDAS performs better as compared to other functional lag MIDAS in case the difference in frequencies is not too high, particularly in the quarterly to monthly frequency mix, as in the empirical application later. This also suits the linear estimation framework of LCCE described earlier as UMIDAS models, unlike other MIDAS specifications, do not have to be estimated by non-linear least squares.

The entire system of equations can be cast into an MFVAR representation constructed using stacked skip-sampled processes (Ghysels 2016). In our case, the MFVAR is already in a reduced form, with restricted parameter space as in Ghysels (2018). Additionally, the MFVAR here is extended to the case of panel data (the MF-PVAR) and with a multi-factor error structure. To see this explicitly, construct the stacked compact expression of the equations (A.10a), (A.10b) and (A.10c) as below:

$$h_{i,t} = \begin{pmatrix} y_{i,t} \\ X^M_{i,t} \end{pmatrix}$$

$$K_{0i}h_{i,t} = c_i + K_{1i}h_{i,t-1} + C_i f_t + e_{i,t} \tag{A.11}$$

Equation (A.11) gives the panel extension of the reduced form MIDAS-VAR model. where:

$$K_{0i} = \begin{pmatrix} 1 & -\beta_{0i} & -\beta_{1i} & -\beta_{2i} \\ 0 & & I & \end{pmatrix}, \; c_i = \begin{pmatrix} c_i \\ \kappa_i \end{pmatrix}, \; K_{1i} = \begin{pmatrix} \phi_i & 0 \\ \alpha_i & 0 \end{pmatrix}$$

$$C_i = \begin{pmatrix} \gamma_i' \\ \Gamma_i' \end{pmatrix}, \; e_{i,t} = \begin{pmatrix} \varepsilon_{i,t} \\ \epsilon_{i,t} \end{pmatrix}$$

Estimation and Nowcasting

To estimate the factors in the mixed-frequency set-up, the process, in essence, remains quite similar to that in Section A.1.1. We redefine the stacked vector, $z_{i,t}^M$, of the lagged target variable and the stacked predictor variable, as well as the β parameters, as follows:

$$z_{i,t}^M = \begin{pmatrix} y_{i,t-1} \\ X_{i,t}^M \end{pmatrix} \quad \beta_i = \begin{pmatrix} \beta_{0i} \\ \beta_{1i} \\ \beta_{2i} \end{pmatrix}$$

Lagging equations (A.10a), and (A.10b) and writing the system in a stacked compact matrix notation:

$$\begin{aligned} \begin{pmatrix} 1 & 0 \\ -\alpha_{xi} & I \end{pmatrix} \begin{pmatrix} y_{i,t-1} \\ X_{i,t}^M \end{pmatrix} = \begin{pmatrix} c_i \\ \kappa_i \end{pmatrix} + \begin{pmatrix} \phi_i & \beta_i' \\ 0 & 0 \end{pmatrix} \begin{pmatrix} y_{i,t-2} \\ X_{i,t-1}^M \end{pmatrix} \\ + \begin{pmatrix} 0 & \gamma_i' \\ \Gamma_i' & 0 \end{pmatrix} \begin{pmatrix} f_t \\ f_{t-1} \end{pmatrix} + \begin{pmatrix} \varepsilon_{i,t-1} \\ \epsilon_{i,t} \end{pmatrix} \end{aligned} \tag{A.12}$$

This gives the reduced form MFVAR expression and rest of the estimation process can now be carried out as described in A.1.1 with the stacked skip-sampled high-frequency predictor variable $X_{i,t}^{M}$. The final mixed-frequency panel nowcasting equations are:

$$y_{i,t} = c_i^* + \phi_i y_{i,t-1} + \beta_i' X_{i,t}^{M} + \delta_i'(L)\overline{z}_{wt}^{M} + \varepsilon_{i,t} + O_p(N^{-\frac{1}{2}}) \tag{A.13a}$$

$$= c_i^* + \phi_i y_{i,t-1} + \beta_i' X_{i,t}^{M} + \sum_{l=0}^{p_T} \delta_{il}' \overline{z}_{t-l}^{M} + e_{i,t} \tag{A.13b}$$

where $\overline{z}_t^M = \sum_{i=1}^{N} \omega_i z_{i,t}^M$ is the equivalent cross-sectionally weighted average as in the previous section, this time modified for the mixed-frequency set-up. We note that, as in Chudik and Pesaran (2015a), an additional set of variables (for instance $g_{i,t}$) may be used in the cross-sectional averages to estimate the factors. The idea here is that the variables $g_{i,t}$ are also impacted by the same common factors. This is quite common in macroeconomic databases, where a handful of factors capture the information contained in large sets of indicators. Thus, the model can be further enriched by the information contained in other high-frequency macro-series, which do not enter the main nowcasting equation.

A.1.3 The Nowcasting Model: Mixed-Frequency, Ragged Edge

Finally, we now turn our attention to the main nowcasting approach with mixed-frequencies and the ragged edge, as outlined in the main text. As described there, the incorporation of country-level calendar effects requires additional notation:

1. The nowcast is performed on the v^{th} day of the nowcast quarter;
2. m_{iv}: The monthly lag available for the high-frequency variable for the cross-section i on the v^{th} day of the nowcast quarter;[1]
3. d_{iv}: The quarterly lag available for the high-frequency variable for the cross-section i on the v^{th} day of the nowcast quarter.

[1] Recall that, for simplicity, we use a single predictor variable in the model. With multiple predictors, m_{iv} would also potentially be different across variables.

The PMIDAS model equations (A.10a, A.10b and A.10c) in this set-up are then modified as follows (taking again the single variable case, unlike the multiple variable case in the main text), with a lag structure which depends on d_{iv} and m_{iv}, as well as model parameters that depend on v:

$$y_{i,t} = c_{vi} + \phi_{vi} y_{i,t-d_{iv}} + \beta'_{vi} X^M_{i,t-\frac{m_{iv}}{3}} + \gamma'_{vi} f_t + \varepsilon_{v,i,t} \tag{A.14a}$$

$$X^M_{i,t-\frac{m_{iv}}{3}} = \kappa_{vi} + \alpha_{vi} y_{i,t-d_{iv}} + \Gamma'_{vi} f_t + \epsilon_{v,i,t} \tag{A.14b}$$

where $X^M_{i,t}$, as before, is the stacked vector defined in equation (2.1) in the main text. Lagging equation (A.14a) by d_{iv} periods, and manipulating equation (A.14b) gives the following:

$$y_{i,t-d_{iv}} = c_{vi} + \phi_{vi} y_{i,t-2d_{iv}} + \beta'_{vi} X^M_{i,t-\frac{m_{iv}-d_{iv}}{3}} + \gamma'_{vi} f_{t-d_{iv}} + \varepsilon_{v,i,t-d_{iv}} \tag{A.15a}$$

$$-\alpha_{vi} y_{i,t-d_{iv}} + X^M_{i,t-\frac{m_{iv}}{3}} = \kappa_i + \Gamma'_{vi} f_t + \epsilon_{v,i,t} \tag{A.15b}$$

Stacking this into one system yields the following:

$$\begin{aligned} \begin{pmatrix} 1 & 0 \\ -\alpha_{vi} & I \end{pmatrix} \begin{pmatrix} y_{i,t-d_{iv}} \\ X^M_{i,t-\frac{m_{iv}}{3}} \end{pmatrix} &= \begin{pmatrix} c_{vi} \\ \kappa_{vi} \end{pmatrix} + \begin{pmatrix} \phi_{vi} & \beta'_{vi} \\ 0 & 0 \end{pmatrix} \begin{pmatrix} y_{i,t-2d_{iv}} \\ X^M_{i,t-\frac{m_{iv}}{3}-d_{iv}} \end{pmatrix} \\ &+ \begin{pmatrix} 0 & \gamma'_{vi} \\ \Gamma'_{vi} & 0 \end{pmatrix} \begin{pmatrix} f_t \\ f_{t-d_{iv}} \end{pmatrix} + \begin{pmatrix} \varepsilon_{v,i,t-d_{iv}} \\ \epsilon_{v,i,t} \end{pmatrix} \end{aligned} \tag{A.16}$$

Finally, we modify the stacked vector from before to get:

$$z^M_{i,t,v} = \begin{pmatrix} y_{i,t-d_{iv}} \\ X^M_{i,t-\frac{m_{iv}}{3}} \end{pmatrix} \tag{A.17}$$

as in equation (2.5) of the main text. So the MFVAR is written as:

$$A_{0i}z^M_{i,t,v} = c_{zi} + A_{1i}z^M_{i,t-d_{iv},v} + \left[C_{0i} + C_{1i}L^{d_{iv}}\right] f_t + e_{v,i,t} \tag{A.18a}$$

$$\implies z^M_{i,t,v} = K_{zi} + B_{0i}z^M_{i,t-d_{iv},v} + A^{-1}_{0i}\left[C_{0i} + C_{1i}L^{d_{iv}}\right] f_t + A^{-1}_{0i}e_{v,i,t} \tag{A.18b}$$

$$\implies (I - B_{0i}L^{d_{iv}})z^M_{i,t,v} = K_{zi} + A^{-1}_{0i}\left[C_{0i} + C_{1i}L^{d_{iv}}\right] f_t + A^{-1}_{0i}e_{v,i,t} \tag{A.18c}$$

where:

$$e_{v,i,t} = \begin{pmatrix} \varepsilon_{v,i,t-d_{iv}} \\ \epsilon_{v,i,t} \end{pmatrix}$$

and the rest of the matrices (A_{0i}, B_{0i} and others, suppressing dependence of these on v to avoid further notational clutter) have the similar definitions as earlier. Further manipulation yields:

$$z^M_{i,t,v} = K_{1_{zi}} + \Psi_i(L^{d_{iv}})A^{-1}_{0i}\left[C_{0i} + C_{1i}L^{d_{iv}}\right] f_t + \Psi_i(L^{d_{iv}})A^{-1}_{0i}e_{v,i,t} \tag{A.18d}$$

To estimate the factors, we take the weighted cross-sectional averages of equation (A.18d). The first term of the RHS gives:

$$\sum_{i=1}^{N}\left[\omega_i\Psi_i(L^{d_{iv}})A^{-1}_{0i}\left\{C_{0i} + C_{1i}L^{d_{iv}}\right\} f_t\right] = \sum_{l=0}^{\infty}\sum_{i=1}^{N}\omega_i\Psi_{il}A^{-1}_{0i}L^{ld_{iv}}\left[C_{0i} + C_{1i}L^{d_{iv}}\right] f_t \tag{A.18e}$$

The following generalised assumption replaces the Assumptions 2–4 stated earlier to estimate the factors using the cross-sectional averages of $z^M_{i,t,v}$ as defined in equation (2.5) – i.e., f_t can be approximated by a finite number of lags of $\sum_{i=1}^{N}\omega_i z^M_{i,t,v}$.

Assumption 5. *The weighted average of the lag polynomials on the RHS of equation*

(A.18e) *is invertible and the inverse polynomial has exponentially decaying coefficients:*

$$\sum_{l=0}^{\infty}\left[\sum_{i=1}^{N}\omega_i\Psi_{il}A_{0i}^{-1}\right]\left[C_{0i}+C_{1i}L^{d_{iv}}\right]L^{ld_{iv}}$$

Given that d_{iv} typically only takes on a handful of values, with $\{0,1,2\}$ being the exhaustive set in the GDP nowcasting example, we may have a weighted average of a maximum of two polynomials in Assumption 5. Taking the example of the U.S. and Germany, if we nowcast Q1 on the 2nd of February, d_{iv} takes values 1 and 2 respectively for the U.S. and Germany, i.e. $v = 33$, $d_{U.S.,33} = 1$, for the U.S. and $d_{GER,33} = 2$ for Germany. So, in this case, we have a weighted average of two lagged polynomials, which is assumed to be invertible by Assumption 5.

A.2 Additional Simulation Results $q = 3$

Figure A.1: Bias in ϕ – $q = 3$

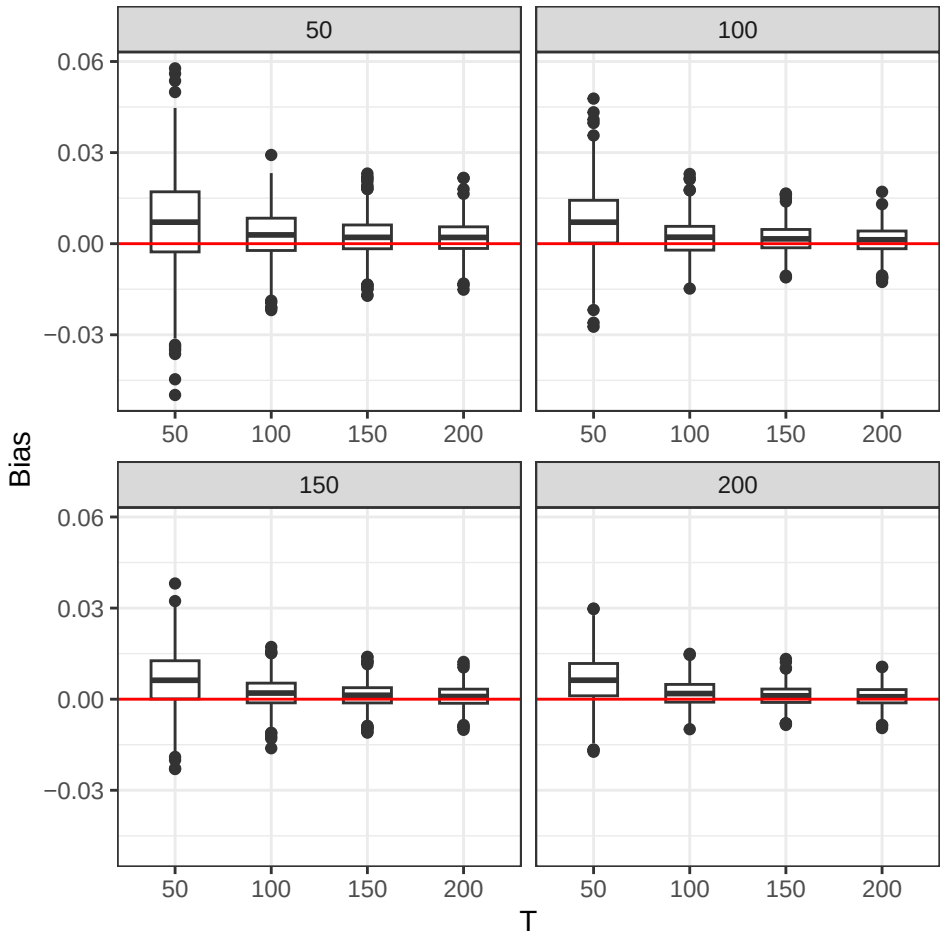

Notes: The panels display the distribution of the difference in absolute biases of the parameter ϕ for the estimation methods LCCE relative to CCE. Figures lower than zero mean that LCCE has lower absolute bias than CCE. The panel header shows the number of cross-sections.

Figure A.2: Bias Comparison in $\beta^{(0)}$ – $q = 3$

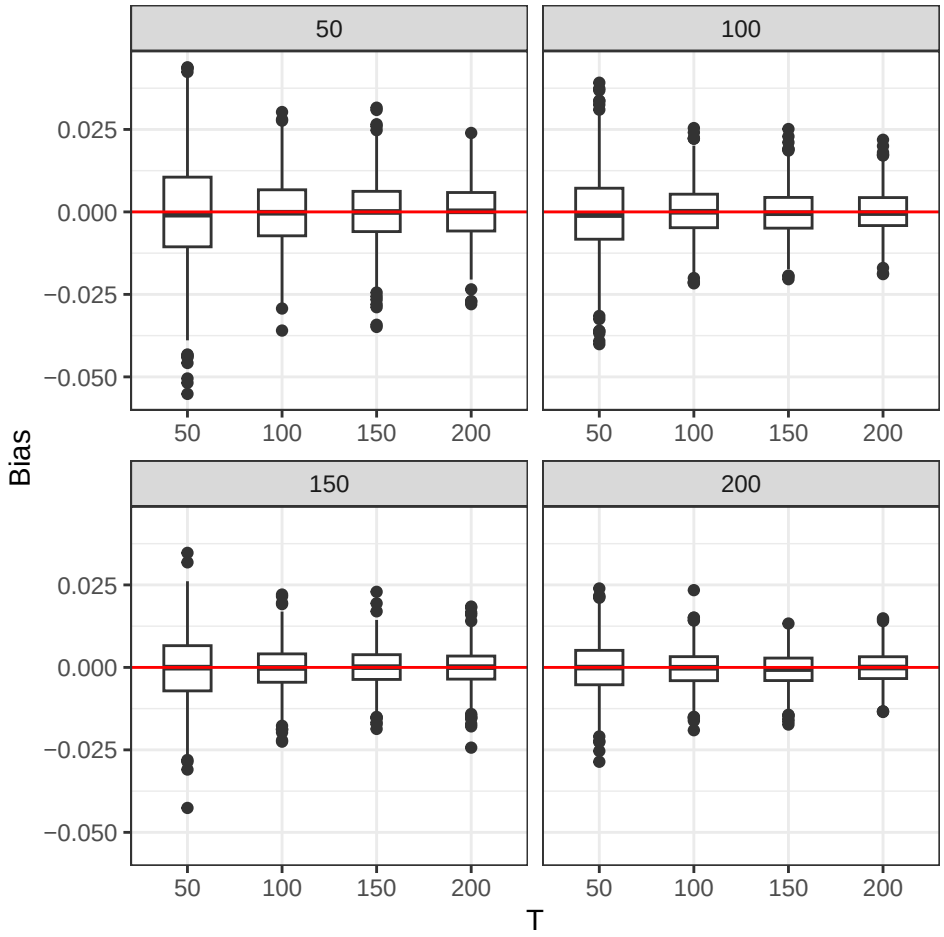

Notes: The panels display the distribution of the difference in absolute biases of the parameter $\beta^{(0)}$ for the estimation methods LCCE relative to CCE. Figures lower than zero mean that LCCE has lower absolute bias than CCE. The panel header shows the number of cross-sections.

Figure A.3: Bias Comparison in $\beta^{(1)}$ – $q = 3$

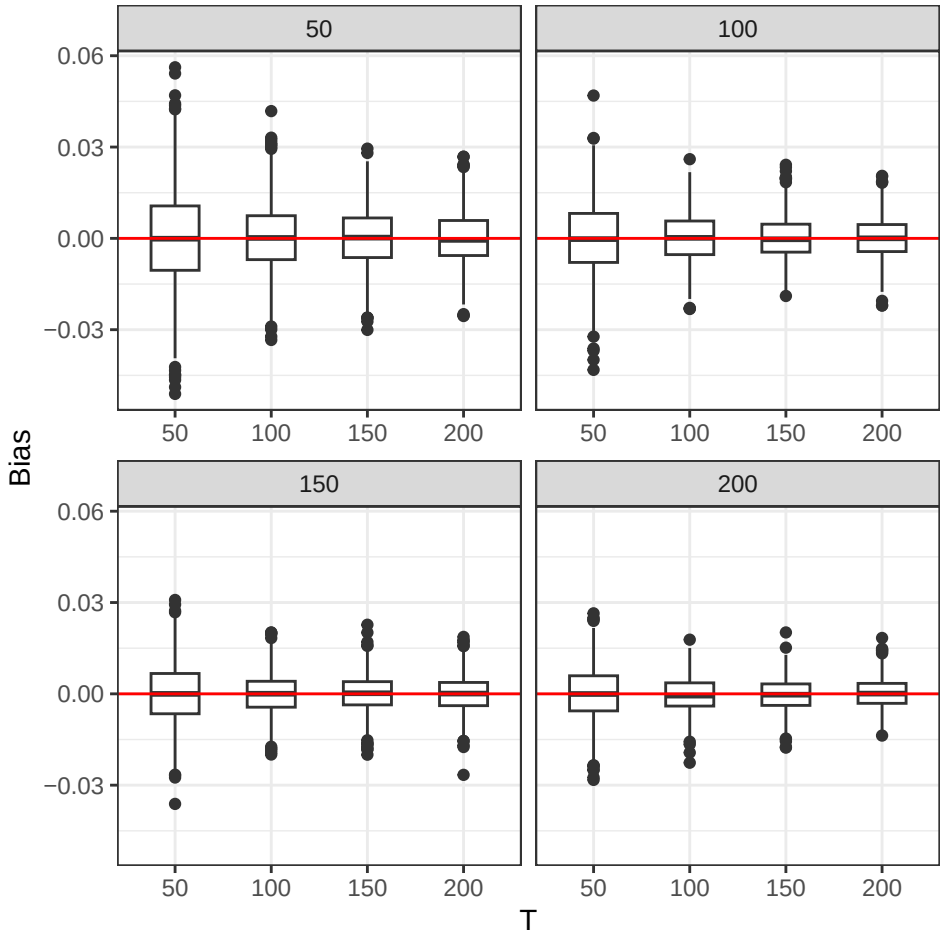

Notes: The panels display the distribution of the difference in absolute biases of the parameter $\beta^{(1)}$ for the estimation methods LCCE relative to CCE. Figures lower than zero mean that LCCE has lower absolute bias than CCE. The panel header shows the number of cross-sections.

Figure A.4: Bias Comparison in $\beta^{(2)}$ – $q = 3$

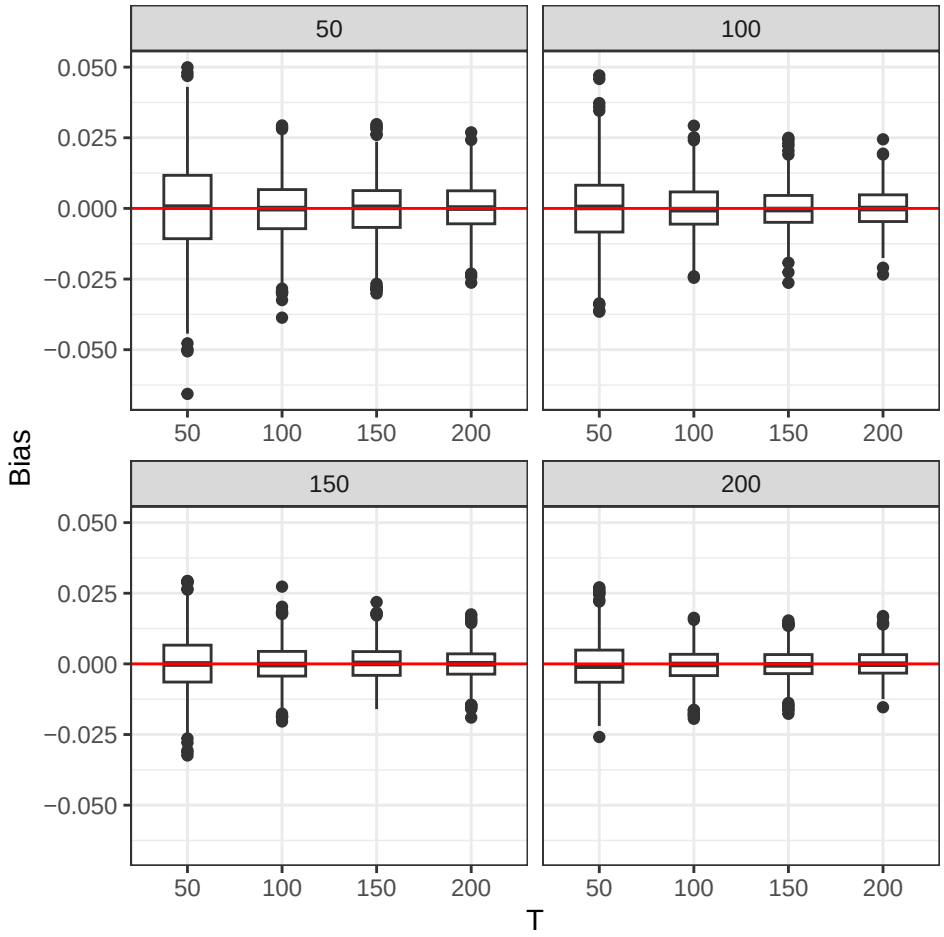

Notes: The panels display the distribution of the difference in absolute biases of the parameter $\beta^{(2)}$ for the estimation methods LCCE relative to CCE. Figures lower than zero mean that LCCE has lower absolute bias than CCE. The panel header shows the number of cross-sections.

A.3 Additional Monte Carlo Results: $q = 4$

In this section we present the additional Monte Carlo results when the frequency mix is changed from $q = 3$ to $q = 4$ which is relevant for annual-quarterly or monthly-weekly panel nowcasting exercises.

Table A.1: Simulation Results – Absolute Bias in LCCE and CCE ($q = 4$)

	CCE				LCCE			
N/T	**50**	**100**	**150**	**200**	**50**	**100**	**150**	**200**
				ϕ				
50	0.0638	0.0275	0.0185	0.0141	0.0545	0.0250	0.0175	0.0134
100	0.0641	0.0277	0.0177	0.0126	0.0557	0.0255	0.0163	0.0119
150	0.0646	0.0281	0.0175	0.0125	0.0565	0.0258	0.0161	0.0115
200	0.0648	0.0278	0.0177	0.0125	0.0563	0.0256	0.0164	0.0117
				$\beta^{(0)}$				
50	0.0262	0.0143	0.0106	0.0088	0.0237	0.0159	0.0125	0.0111
100	0.0183	0.0100	0.0075	0.0062	0.0171	0.0106	0.0085	0.0080
150	0.0149	0.0081	0.0061	0.0052	0.0140	0.0087	0.0071	0.0065
200	0.0124	0.0069	0.0054	0.0044	0.0118	0.0077	0.0065	0.0055
				$\beta^{(1)}$				
50	0.0259	0.0152	0.0114	0.0089	0.0243	0.0170	0.0133	0.0111
100	0.0177	0.0102	0.0076	0.0065	0.0168	0.0111	0.0089	0.0082
150	0.0150	0.0082	0.0063	0.0053	0.0140	0.0091	0.0074	0.0068
200	0.0123	0.0068	0.0054	0.0045	0.0120	0.0079	0.0064	0.0057
				$\beta^{(2)}$				
50	0.0257	0.0147	0.0109	0.0090	0.0242	0.0162	0.0132	0.0111
100	0.0181	0.0101	0.0076	0.0063	0.0173	0.0112	0.0089	0.0081
150	0.0144	0.0081	0.0064	0.0055	0.0138	0.0089	0.0077	0.0068
200	0.0125	0.0074	0.0057	0.0044	0.0116	0.0080	0.0066	0.0057
				$\beta^{(3)}$				
50	0.0267	0.0151	0.0113	0.0091	0.0261	0.0160	0.0130	0.0115
100	0.0178	0.0103	0.0078	0.0065	0.0171	0.0112	0.0094	0.0083
150	0.0145	0.0085	0.0062	0.0052	0.0137	0.0094	0.0075	0.0065
200	0.0125	0.0071	0.0055	0.0045	0.0118	0.0081	0.0063	0.0057

Notes: The numbers in this table are the absolute biases in the estimates of the key model parameters estimated using two methods, LCCE and CCE, across different sample sizes.

Figure A.5: Bias in $\phi - q = 4$

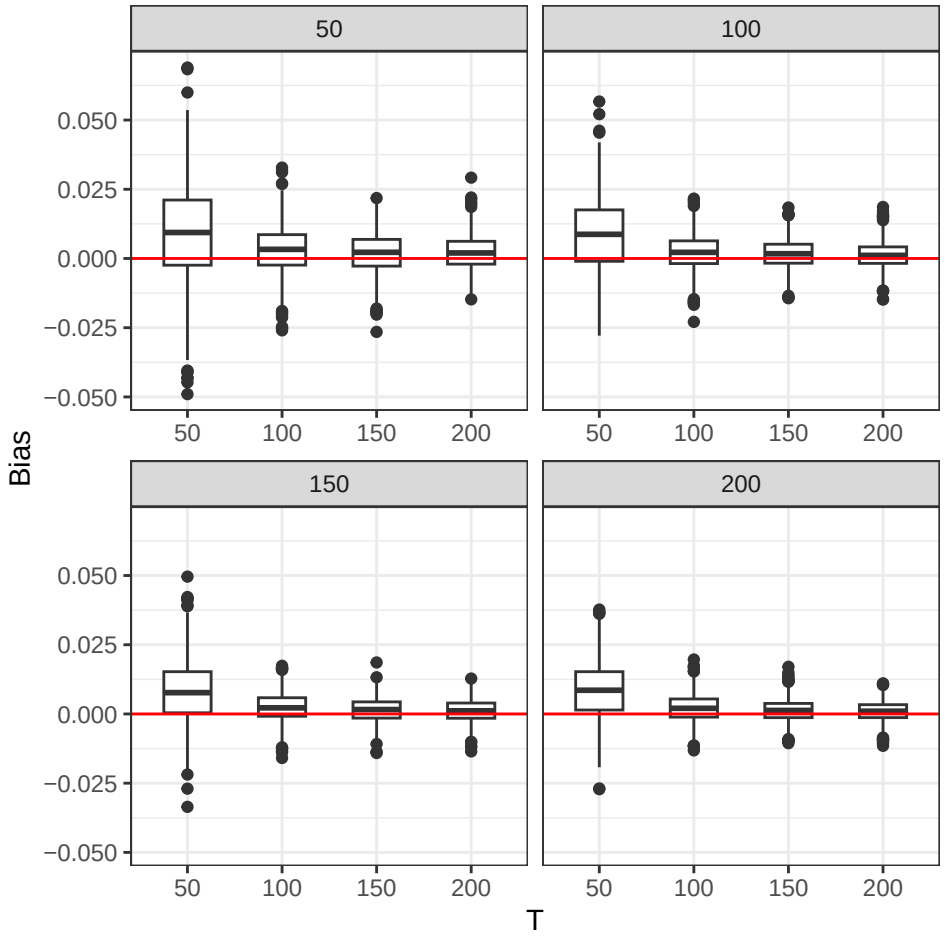

Notes: The panels display the distribution of the difference in absolute biases of the parameter ϕ for the estimation methods LCCE relative to CCE. Figures lower than zero mean that LCCE has lower absolute bias than CCE. The panel header shows the number of cross-sections.

Figure A.6: Bias Comparison in $\beta^{(0)}$ – $q = 4$

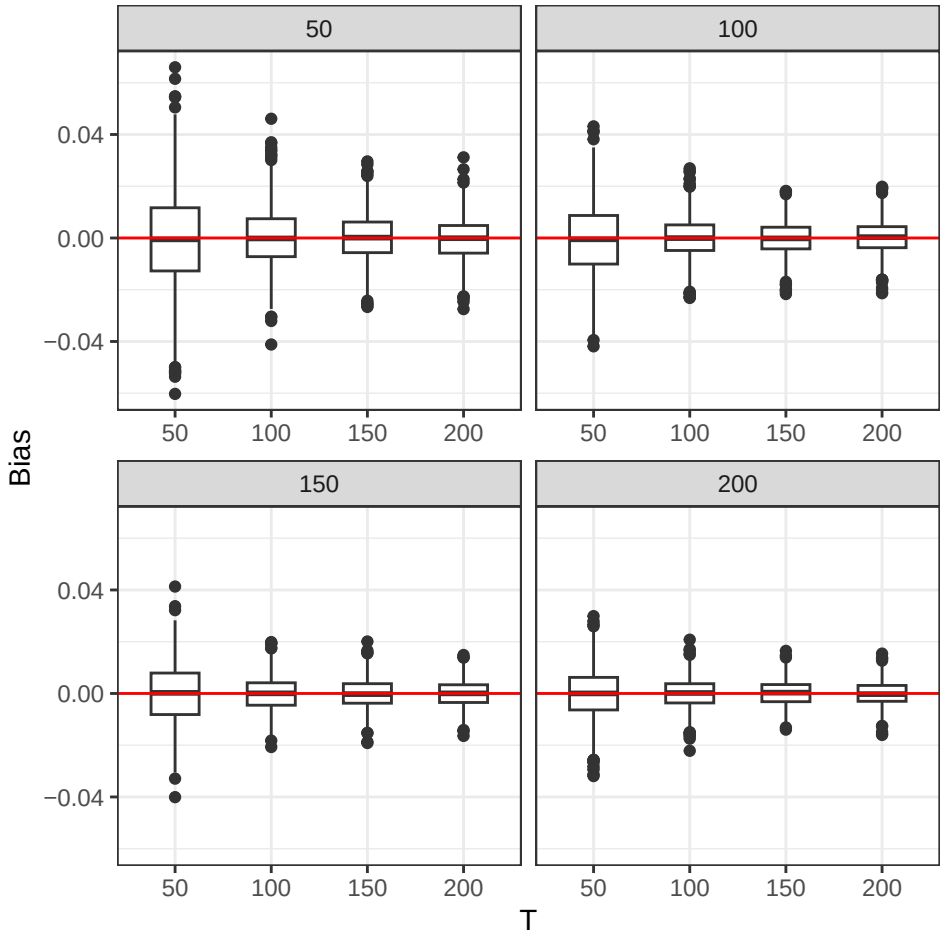

Notes: The panels display the distribution of the difference in absolute biases of the parameter $\beta^{(0)}$ for the estimation methods LCCE relative to CCE. Figures lower than zero mean that LCCE has lower absolute bias than CCE. The panel header shows the number of cross-sections.

Figure A.7: Bias Comparison in $\beta^{(1)}$ – $q = 3$

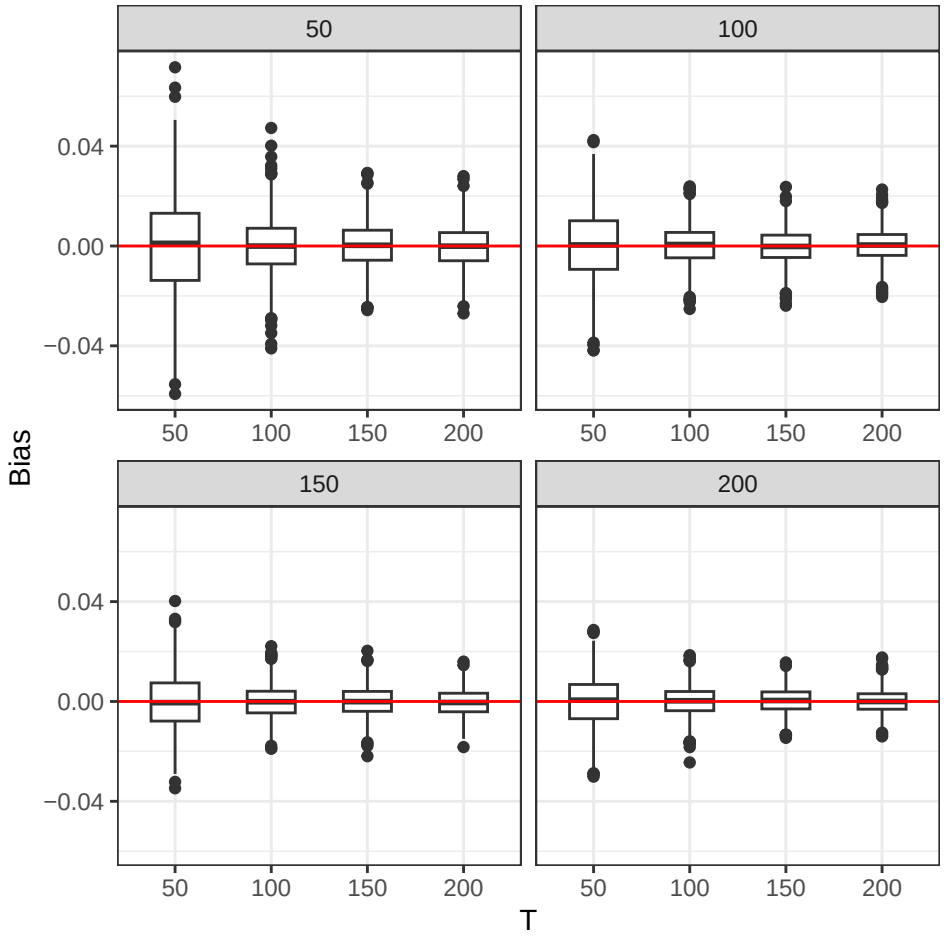

Notes: The panels display the distribution of the difference in absolute biases of the parameter $\beta^{(1)}$ for the estimation methods LCCE relative to CCE. Figures lower than zero mean that LCCE has lower absolute bias than CCE. The panel header shows the number of cross-sections.

Figure A.8: Bias Comparison in $\beta^{(2)}$ – $q = 4$

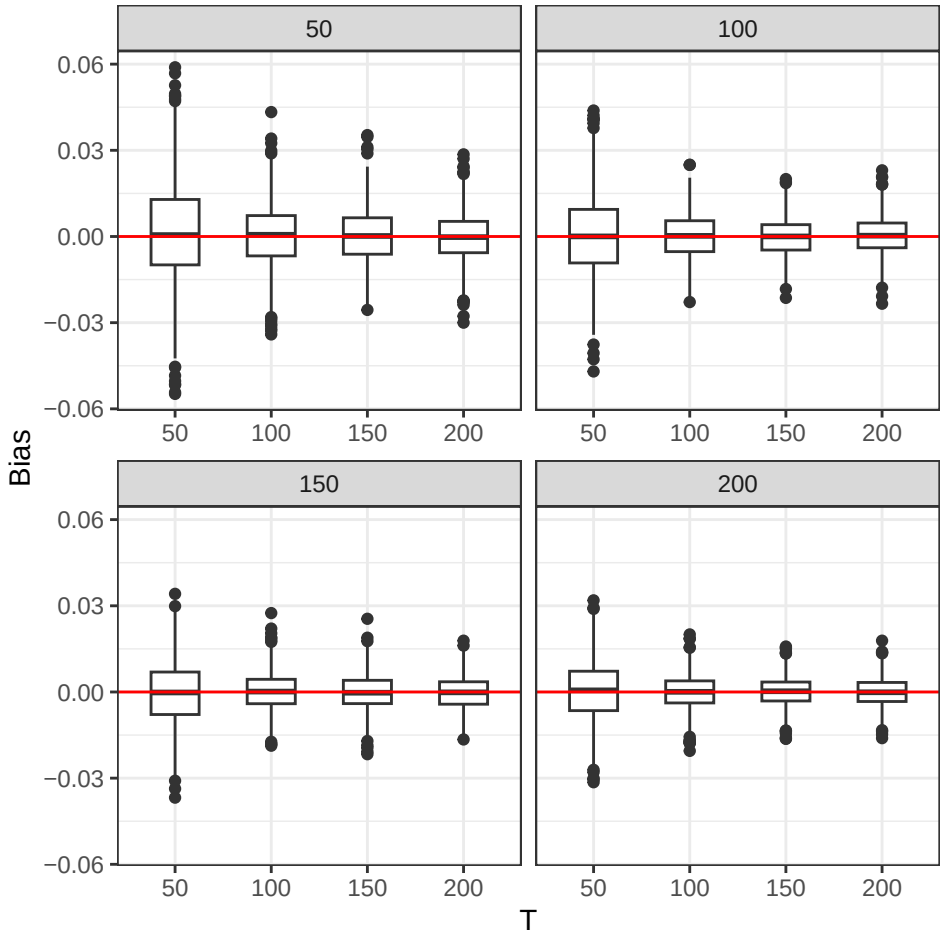

Notes: The panels display the distribution of the difference in absolute biases of the parameter $\beta^{(2)}$ for the estimation methods LCCE relative to CCE. Figures lower than zero mean that LCCE has lower absolute bias than CCE. The panel header shows the number of cross-sections.

Figure A.9: Bias Comparison in $\beta^{(3)}$ – $q = 4$

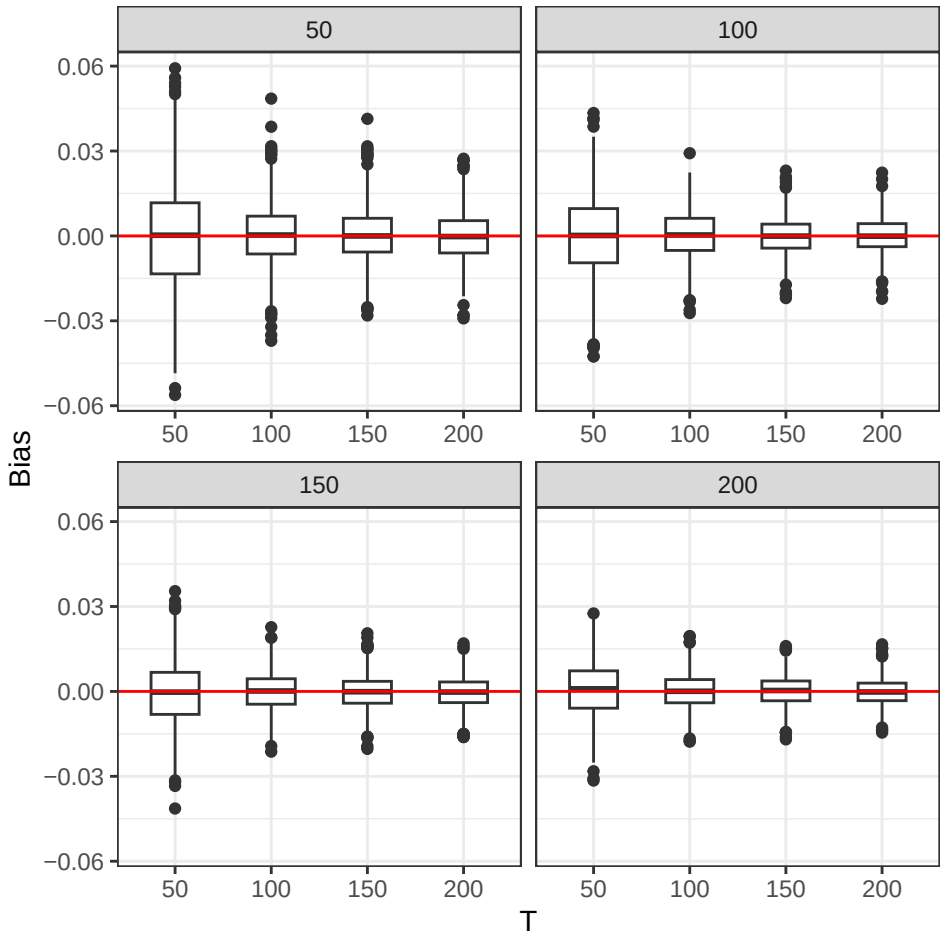

Notes: The panels display the distribution of the difference in absolute biases of the parameter $\beta^{(3)}$ for the estimation methods LCCE relative to CCE. Figures lower than zero mean that LCCE has lower absolute bias than CCE. The panel header shows the number of cross-sections.

Table A.2: Simulation Results – Forecast Accuracy of PMIDAS Relative to Benchmark, $q = 4$

	20%				**30%**				**50%**			
N/T	**50**	**100**	**150**	**200**	**50**	**100**	**150**	**200**	**50**	**100**	**150**	**200**
50	0.8937	0.7475	0.7132	0.6910	0.9336	0.7611	0.7146	0.6959	1.0186	0.7684	0.7197	0.7001
100	0.8946	0.7452	0.7127	0.6903	0.9372	0.7598	0.7135	0.6957	1.0180	0.7693	0.7183	0.6996
150	0.8928	0.7497	0.7148	0.6912	0.9348	0.7618	0.7155	0.6961	1.0139	0.7700	0.7204	0.7012
200	0.8936	0.7487	0.7117	0.6916	0.9357	0.7605	0.7132	0.6964	1.0173	0.7690	0.7187	0.7015

Notes: This table represents the relative RMSFE of the simulated mixed-frequency data, resembling a monthly to weekly (or annual to quarterly) frequency mix. Figures less than one indicate superior performance of the PMIDAS model, as compared to a time series AR(1) model. Results are shown for sample split ratios for P equal to 20, 30 and 50%.

A.4 Empirical Application I – Release Calendars

Figure A.10: Publication Lag Across Different Countries

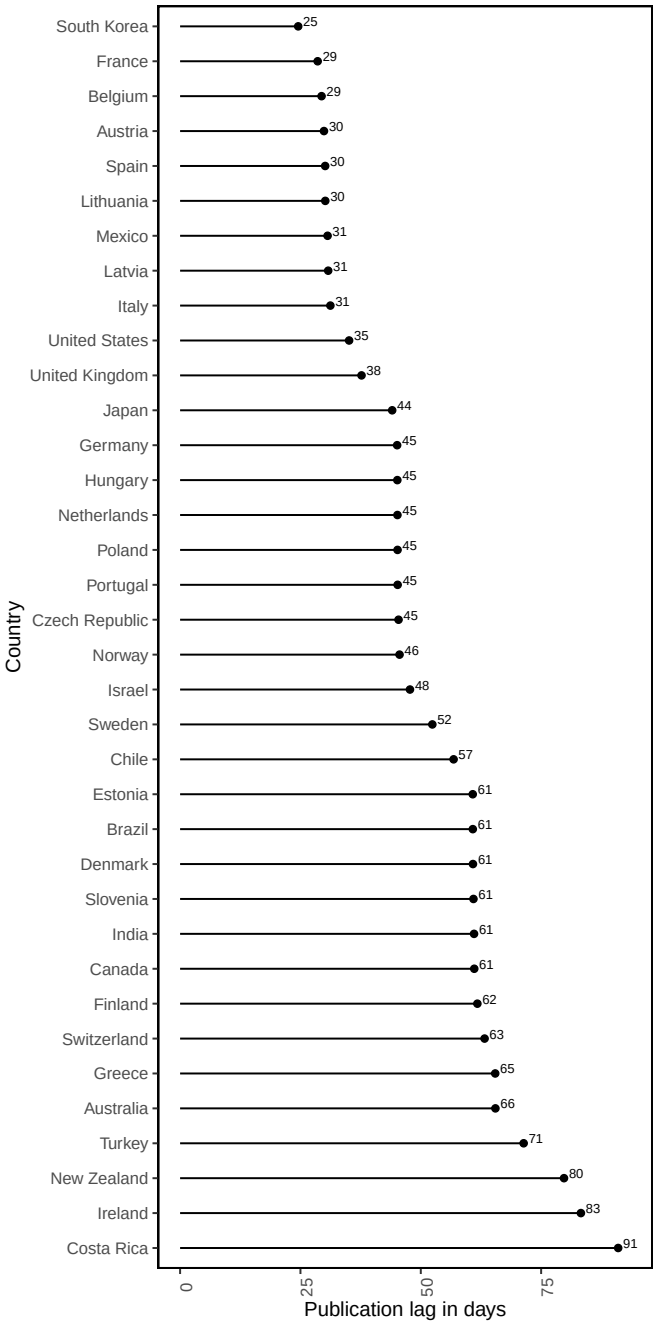

(a) Pseudo Calendar for the First Release of Quarterly GDP (Source: Bloomberg Finance L.P.).

Figure A.10: (cont'd) Publication Lag Across Different Countries

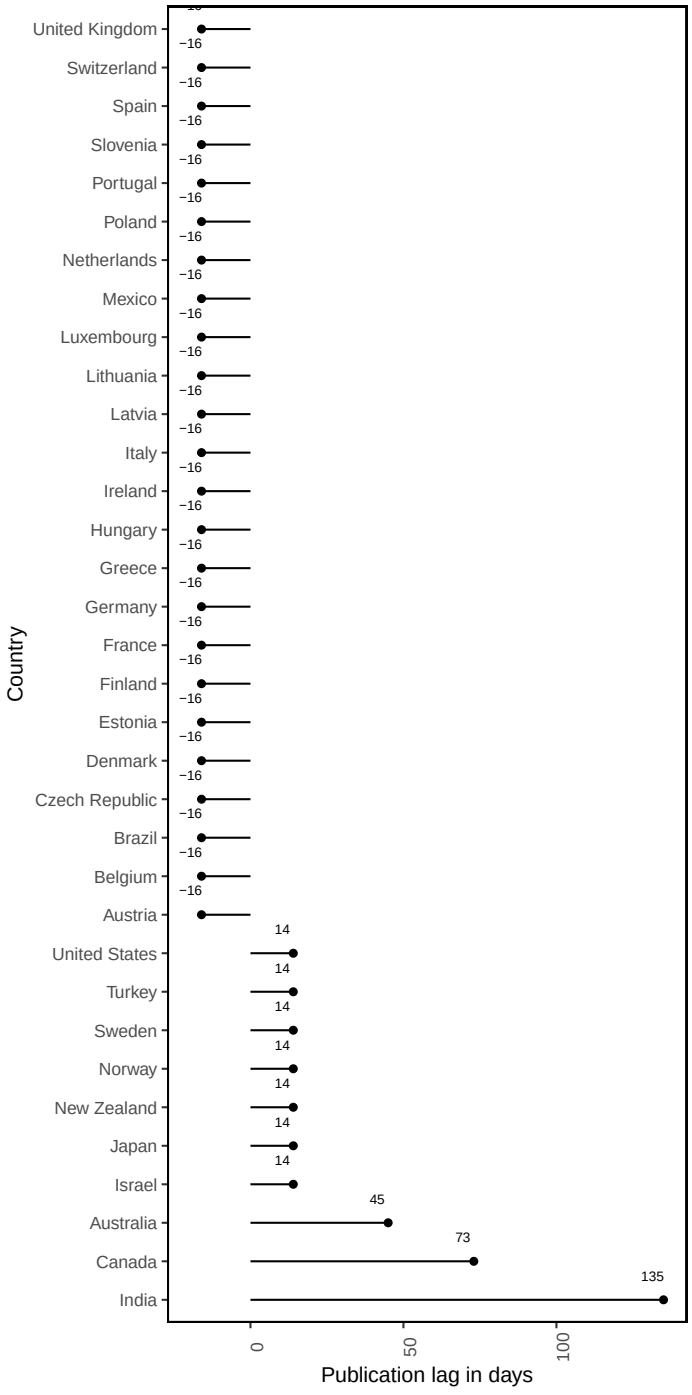

(b) Pseudo Calendar for BSM (Source: Macrobond)

[a]

[a]Negative lag indicates the data are available before the start of the month.

Figure A.10: (cont'd) Publication Lag Across Different Countries

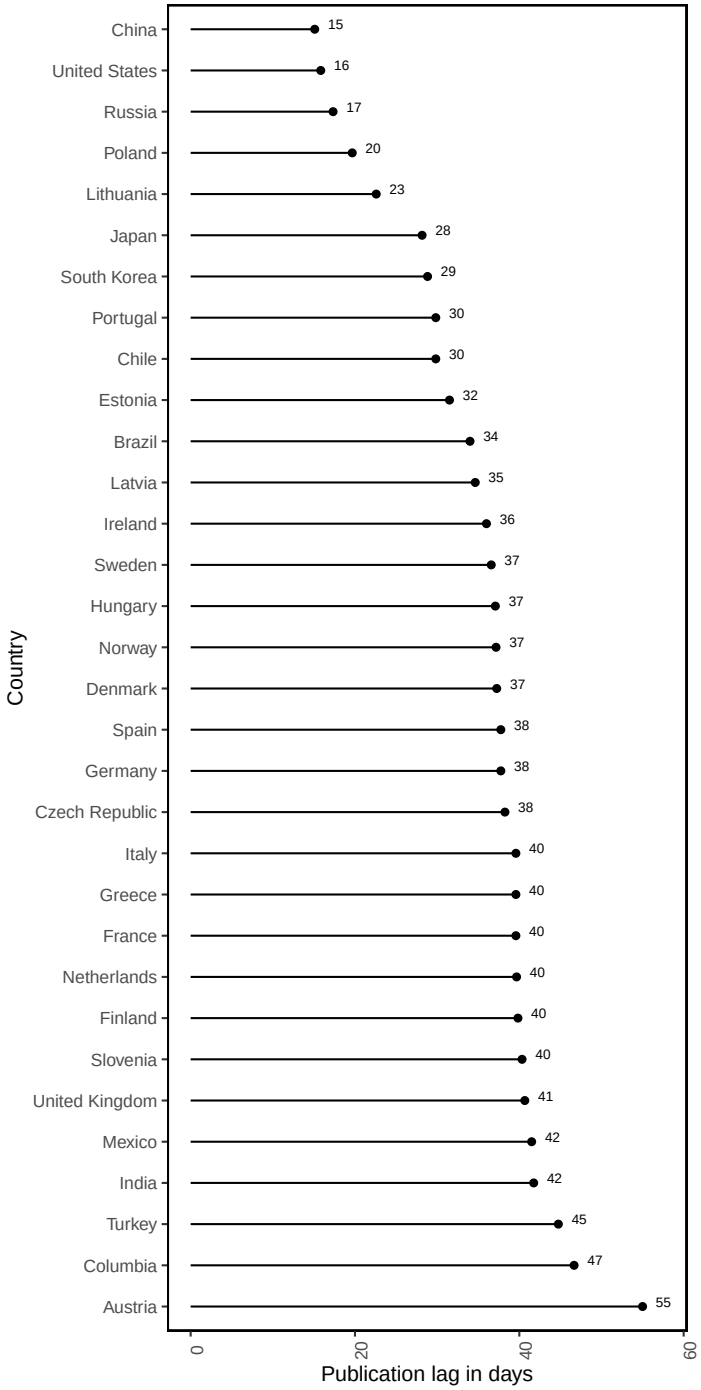

(c) Pseudo Calendar for IP (Source: Bloomberg Finance L.P.).

A.5 Empirical Application I: Robustness to Additional Predictor Results

Figure A.11: Additional Predictors – Target y-o-y

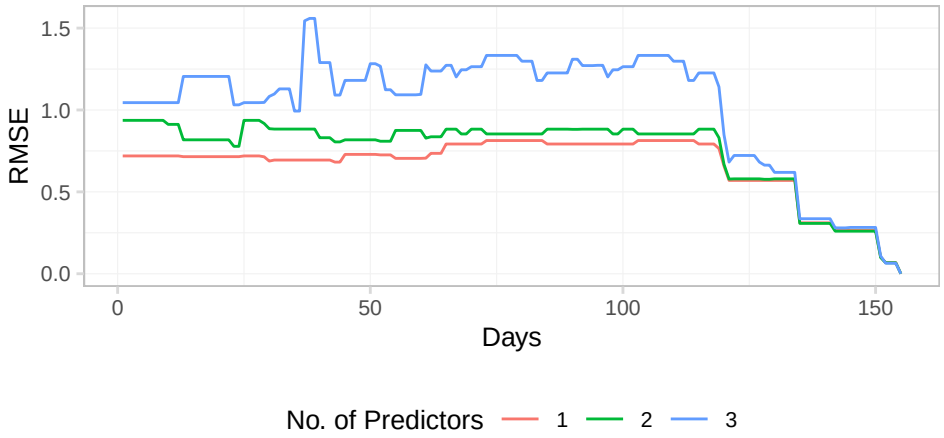

Notes: Each line represents the minimum RMSFE across all models with the specified number of predictors.

Figure A.12: Additional Predictors – Target q-o-q

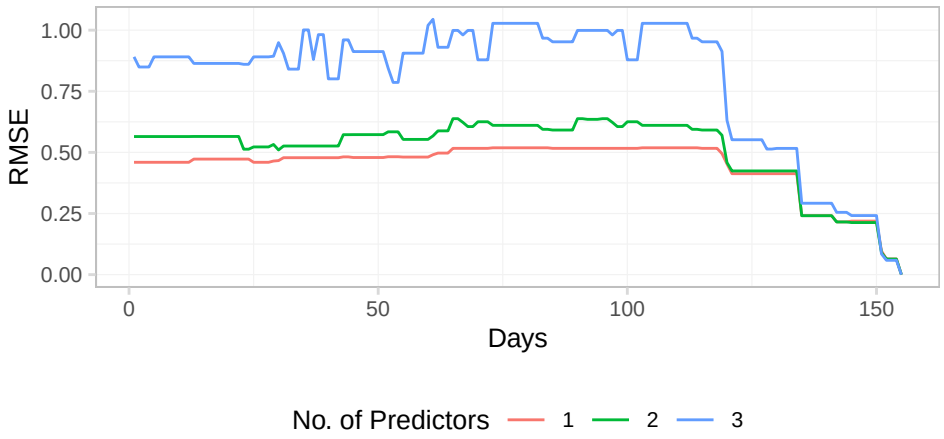

Notes: The same as for Figure A.11.

A.6 Empirical Application I: Robustness to Sample Split Results

Figure A.13: 20% Split – Target y-o-y

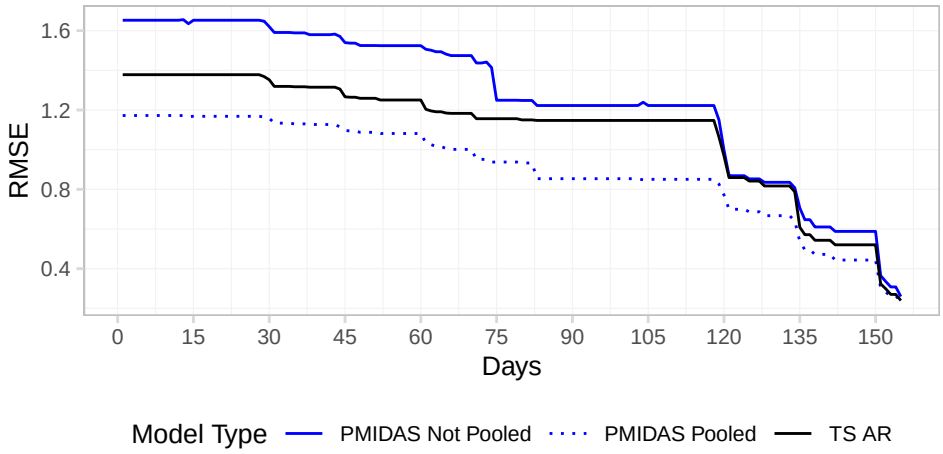

Figure A.14: 40% Split – Target y-o-y

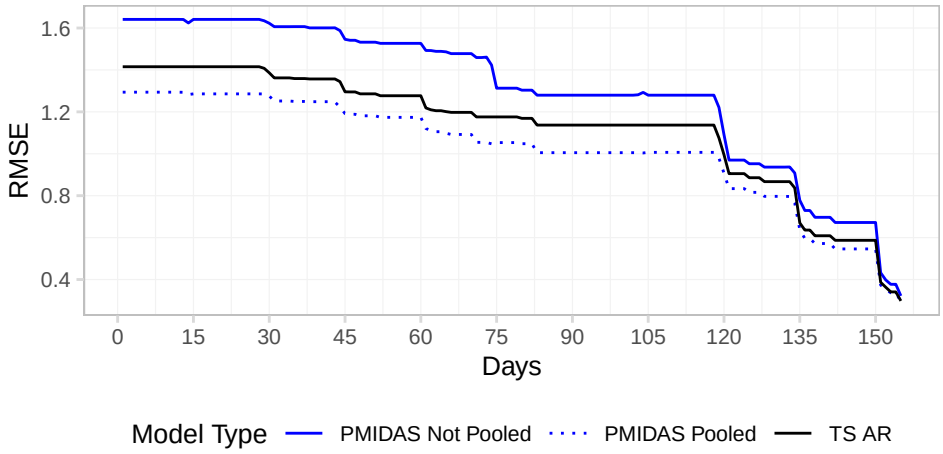

Figure A.15: 20% Split – Target q-o-q

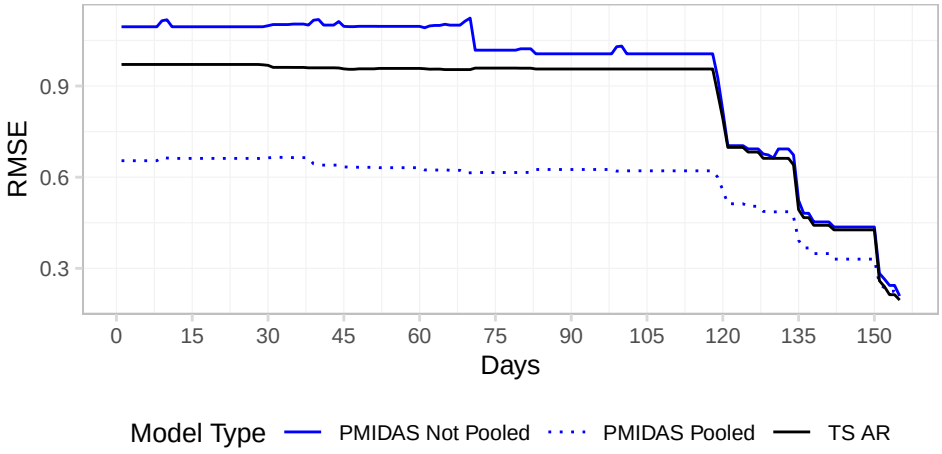

Notes: The same as for Figure 2.2.

Figure A.16: 40% Split – Target q-o-q

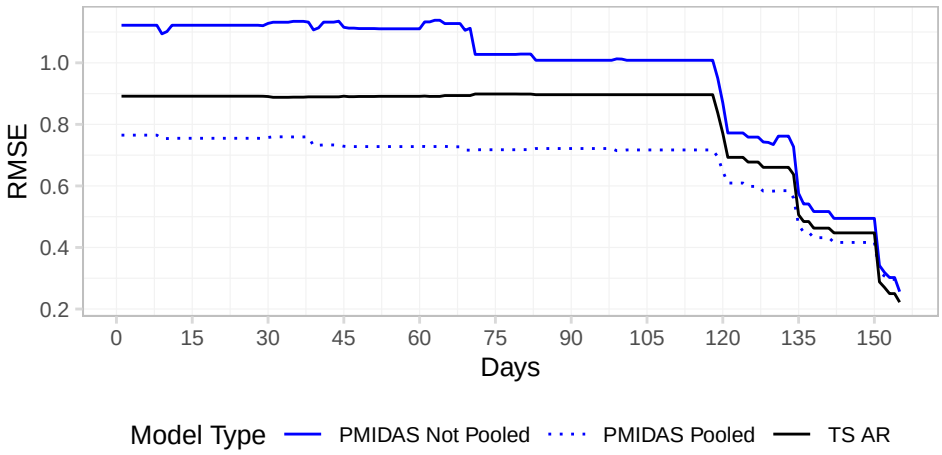

Notes: The same as for Figure 2.3.

Appendix B

Appendix to Chapter 3

This appendix contains additional plots to substantiate the results of Chapter 4. The appendix is organised as follows: Section B.1 contains the prediction results for per capita EC results and Section B.2 comprises of the results for per capita CO_2 prediction. Finally, Section B.3 presents a bunch of robustness results.

B.1 Per Capita EC Results

B.1.1 Per Capita EC Predictions with the Annual Data Flow

Overall Results

Figure B.1: Average RMSFE Across States – Per Capita EC, Annual Data Flow

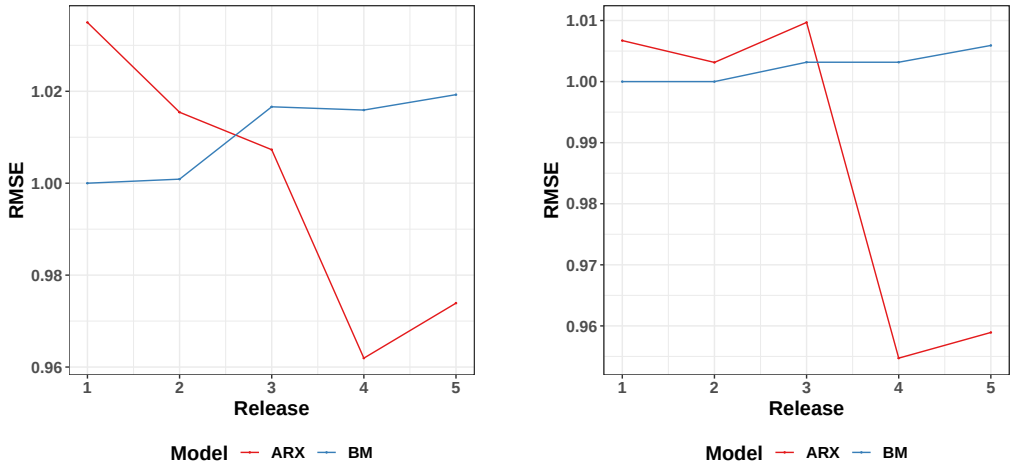

(a) Predictor: Per Capita GDP (b) Predictor: Per Capita PI

Notes: See Figure 3.1.

State-Level Results

Table B.1: Distribution of Relative RMSFE Across States – Per Capita EC, Annual Data Flow

Release	**10%**	**25%**	**50%**	**75%**	**90%**
1	0.9863	1.0121	1.0357	1.0671	1.0968
2	0.9832	0.9944	1.0167	1.0441	1.0614
3	0.9452	0.9590	0.9948	1.0133	1.0435
4	0.8578	0.8945	0.9369	0.9895	1.0358
5	0.8577	0.8949	0.9467	0.9984	1.0786

(a) Predictor – Per Capita GDP

Release	**10%**	**25%**	**50%**	**75%**	**90%**
1	0.9885	0.9970	1.0082	1.0167	1.0363
2	0.9693	0.9914	1.0031	1.0188	1.0348
3	0.9847	0.9946	1.0100	1.0175	1.0337
4	0.8169	0.9019	0.9560	0.9994	1.0500
5	0.8125	0.9090	0.9623	1.0004	1.0474

(b) Predictor – Per Capita PI

Notes: See Table 3.3.

B.1.2 Per Capita EC Predictions with the Quarterly Data Flow

Overall Results

Figure B.2: Average RMSFE Across States – Per Capita EC, Quarterly Data Flow

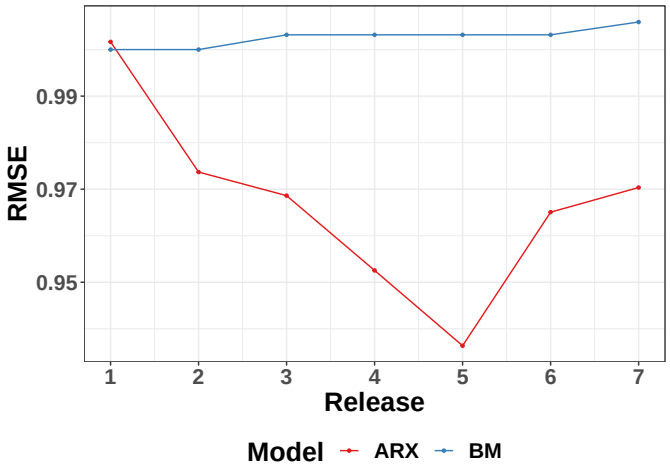

Notes: See Figure 3.2.

State-Level Results

Table B.2: Distribution of Relative RMSFE Across States – Per Capita EC, Quarterly Data Flow

Release	10%	25%	50%	75%	90%
1	0.9608	0.9734	0.9965	1.0195	1.0559
2	0.9220	0.9532	0.9746	1.0014	1.0267
3	0.8730	0.9209	0.9652	1.0109	1.0341
4	0.8257	0.9032	0.9478	0.9924	1.0635
5	0.8439	0.8919	0.9364	0.9772	1.0284
6	0.8519	0.9212	0.9747	1.0084	1.0559
7	0.8590	0.9357	0.9719	1.0079	1.0443

Notes: See Table 3.4.

B.2 Per Capita CO_2 Emissions Results

B.2.1 Per Capita CO_2 Predictions with the Annual Data Flow

Overall Results

Figure B.3: Average RMSFE Across States – Per Capita CO_2 Emissions, Annual Data Flow

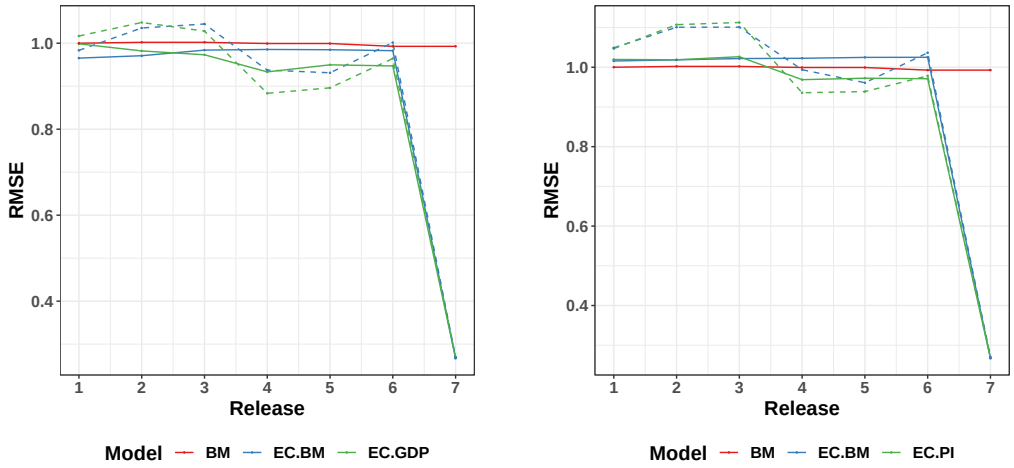

(a) Predictor: Per Capita GDP (b) Predictor: Per Capita PI

Notes: See Figure 3.3.

State-Level Results

Table B.3: Distribution of Relative RMSFE Across States – Per Capita CO_2 Emissions, Annual Data Flow (Predictor: GDP)

Release	**10%**	**25%**	**50%**	**75%**	**90%**
1	0.8979	0.9761	1.0059	1.0307	1.0691
2	0.9100	0.9357	0.9870	1.0177	1.0634
3	0.8706	0.9296	0.9766	1.0018	1.0496
4	0.8448	0.8858	0.9303	0.9744	1.0528
5	0.8390	0.8842	0.9476	1.0146	1.0756
6	0.8609	0.8933	0.9539	0.9955	1.0809
7	0.1754	0.2102	0.2693	0.3264	0.4007

(a) Model: EC.GDP

Release	**10%**	**25%**	**50%**	**75%**	**90%**
1	0.9243	0.9797	1.0286	1.0591	1.0881
2	0.9475	1.0054	1.0485	1.1001	1.1244
3	0.9401	0.9673	1.0267	1.0599	1.1276
4	0.7574	0.8176	0.8628	0.9369	1.0497
5	0.7486	0.8095	0.8936	0.9941	1.0850
6	0.8589	0.9130	0.9679	1.0283	1.1120
7	0.1820	0.2144	0.2641	0.3268	0.3976

(b) Model: EC.GDP with Factors

Notes: See Table 3.5.

Table B.3: (cont'd...)Distribution of Relative RMSFE Across States – Per Capita CO_2 Emissions, Annual Data Flow (Predictor: GDP)

Release	**10%**	**25%**	**50%**	**75%**	**90%**
1	0.8812	0.9303	0.9606	1.0091	1.0394
2	0.8885	0.9419	0.9735	1.0041	1.0349
3	0.8992	0.9528	0.9866	1.0088	1.0444
4	0.9231	0.9624	0.9893	1.0085	1.0577
5	0.9152	0.9647	0.9854	1.0129	1.0347
6	0.9290	0.9790	0.9912	1.0120	1.0333
7	0.1754	0.2102	0.2693	0.3264	0.4007

(c) Model: EC.BM

Release	**10%**	**25%**	**50%**	**75%**	**90%**
1	0.8900	0.9445	0.9779	1.0176	1.0925
2	0.9377	0.9956	1.0370	1.0723	1.1378
3	0.9398	0.9917	1.0517	1.0905	1.1452
4	0.8761	0.8992	0.9255	0.9893	1.0292
5	0.8288	0.8830	0.9307	0.9985	1.0439
6	0.9482	0.9917	1.0106	1.0325	1.0820
7	0.1820	0.2144	0.2641	0.3268	0.3976

(d) Model: EC.BM with Factors

Notes: See Table 3.5.

Table B.4: Distribution of Relative RMSFE Across States – Per Capita CO_2 Emissions, Annual Data Flow (Predictor: PI)

Release	**10%**	**25%**	**50%**	**75%**	**90%**
1	0.9739	0.9905	1.0123	1.0451	1.0756
2	0.9529	0.9945	1.0170	1.0370	1.0712
3	0.9490	0.9982	1.0223	1.0522	1.0954
4	0.8878	0.9276	0.9689	1.0239	1.0638
5	0.8867	0.9262	0.9698	1.0194	1.0753
6	0.9070	0.9462	0.9787	1.0118	1.0671
7	0.1754	0.2102	0.2693	0.3264	0.4007

(a) Model: EC.PI

Release	**10%**	**25%**	**50%**	**75%**	**90%**
1	0.9867	1.0118	1.0330	1.0735	1.1586
2	1.0153	1.0582	1.1081	1.1621	1.2123
3	0.9983	1.0670	1.1210	1.1642	1.2311
4	0.8358	0.8782	0.9326	0.9856	1.0974
5	0.8074	0.8772	0.9458	1.0041	1.1089
6	0.9095	0.9463	0.9923	1.0321	1.0540
7	0.1820	0.2144	0.2641	0.3268	0.3976

(b) Model: EC.PI with Factors

Notes: See Table 3.6.

Table B.4: Distribution of Relative RMSFE Across States – Per Capita CO_2 Emissions, Annual Data Flow (Predictor: PI)

Release	**10%**	**25%**	**50%**	**75%**	**90%**
1	0.9738	0.9864	1.0035	1.0255	1.0766
2	0.9710	0.9925	1.0042	1.0264	1.0673
3	0.9653	0.9940	1.0095	1.0354	1.0781
4	0.9871	0.9995	1.0084	1.0291	1.0824
5	0.9808	0.9994	1.0091	1.0381	1.0959
6	0.9949	1.0019	1.0130	1.0525	1.1055
7	0.1754	0.2102	0.2693	0.3264	0.4007

(c) Model: EC.BM

Release	**10%**	**25%**	**50%**	**75%**	**90%**
1	0.9814	1.0129	1.0345	1.0737	1.1460
2	1.0221	1.0581	1.1107	1.1518	1.1803
3	1.0192	1.0570	1.1071	1.1468	1.1967
4	0.9325	0.9517	0.9818	1.0306	1.0951
5	0.8902	0.9249	0.9606	1.0001	1.0388
6	1.0028	1.0133	1.0321	1.0691	1.0983
7	0.1820	0.2144	0.2641	0.3268	0.3976

(d) Model: EC.BM with Factors

Notes: See Table 3.6.

B.2.2 Per Capita CO_2 Predictions with the Quarterly Data Flow

Overall Results

Figure B.4: Average RMSFE Across States – Per Capita CO_2 Emissions, Quarterly Data Flow

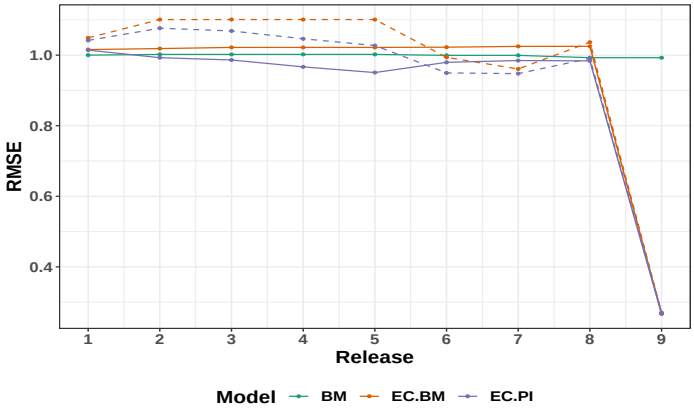

Notes: The same as for Figure 3.3.

State-Level Results

Table B.5: Distribution of Relative RMSFE Across States – Per Capita CO_2 Emissions, Quarterly Data Flow

Release	**10%**	**25%**	**50%**	**75%**	**90%**
1	0.9614	0.9846	1.0055	1.0284	1.0896
2	0.9203	0.9497	0.9851	1.0182	1.0677
3	0.9129	0.9321	0.9778	1.0181	1.0899
4	0.8793	0.8982	0.9670	1.0178	1.0720
5	0.8662	0.8944	0.9516	1.0001	1.0339
6	0.8877	0.9492	0.9844	1.0247	1.0691
7	0.9100	0.9532	0.9848	1.0288	1.0546
8	0.9255	0.9681	0.9963	1.0265	1.0478
9	0.1754	0.2102	0.2693	0.3264	0.4007

(a) Model: EC.PI

Release	**10%**	**25%**	**50%**	**75%**	**90%**
1	0.9743	0.9986	1.0313	1.0719	1.1342
2	0.9782	1.0364	1.0813	1.1273	1.1956
3	0.9636	1.0215	1.0667	1.1273	1.1909
4	0.9586	0.9872	1.0514	1.0932	1.1520
5	0.9431	0.9794	1.0229	1.0713	1.1414
6	0.8647	0.8958	0.9551	0.9980	1.0652
7	0.8246	0.8932	0.9432	1.0135	1.0959
8	0.9322	0.9723	1.0098	1.0346	1.0492
9	0.1820	0.2144	0.2641	0.3268	0.3976

(b) Model: EC.PI with Factors

Table B.5: (cont'd...)Distribution of Relative RMSFE Across States – Per Capita CO_2 Emissions, Quarterly Data Flow

Release	**10%**	**25%**	**50%**	**75%**	**90%**
1	0.9738	0.9864	1.0035	1.0255	1.0766
2	0.9710	0.9925	1.0042	1.0264	1.0673
3	0.9653	0.9940	1.0095	1.0354	1.0781
4	0.9653	0.9940	1.0095	1.0354	1.0781
5	0.9653	0.9940	1.0095	1.0354	1.0781
6	0.9871	0.9995	1.0084	1.0291	1.0824
7	0.9808	0.9994	1.0091	1.0381	1.0959
8	0.9949	1.0019	1.0130	1.0525	1.1055
9	0.1754	0.2102	0.2693	0.3264	0.4007

(c) Model: EC.BM

Release	**10%**	**25%**	**50%**	**75%**	**90%**
1	0.9814	1.0129	1.0345	1.0737	1.1460
2	1.0221	1.0581	1.1107	1.1518	1.1803
3	1.0192	1.0570	1.1071	1.1468	1.1967
4	1.0192	1.0570	1.1071	1.1468	1.1967
5	1.0192	1.0570	1.1071	1.1468	1.1967
6	0.9325	0.9517	0.9818	1.0306	1.0951
7	0.8902	0.9249	0.9606	1.0001	1.0388
8	1.0028	1.0133	1.0321	1.0691	1.0983
9	0.1820	0.2144	0.2641	0.3268	0.3976

(d) Model: EC.BM with Factors

Notes: The same as Table 3.5.

B.3 Further Results

B.3.1 Robustness to Sample Split

Figure B.5: Sample Split – Average RMSFE Across States – CO_2 Emissions, Quarterly Data Flow

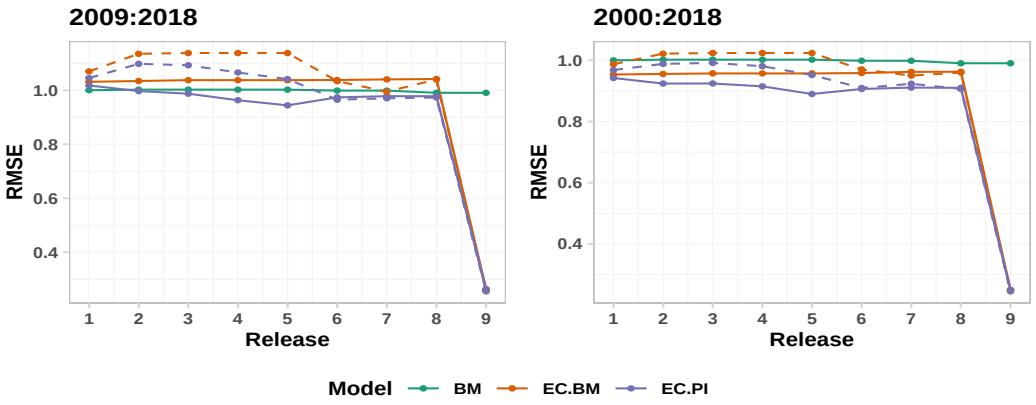

Notes: The same as for Figure 3.3.

B.3.2 Using the Philly Fed's State Coincident Indices (Quarterly)

Figure B.6: Average RMSFE Across States – CO_2 Emissions, Quarterly Data Flow

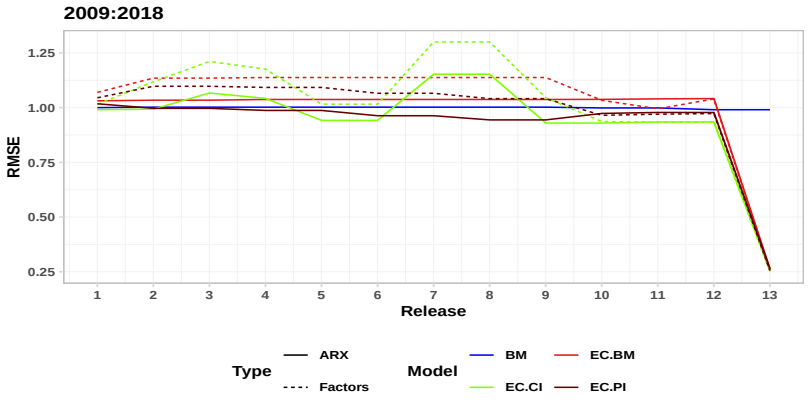

Notes: The same as Figure 3.4 with the addition of the model EC.CI which uses the Philly Fed's State Coincident index as a predictor.

B.3.3 Targeting CO_2 Emissions Directly Instead of Bridging

Figure B.7: Targeting CO_2 Emissions Directly – Average RMSFE Across States, Quarterly Data Flow

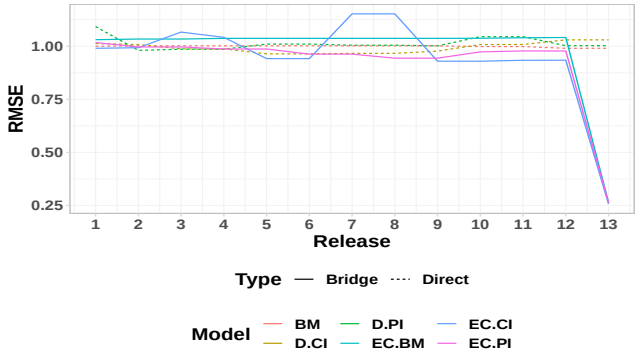

Notes: The same as Figure 3.4 with the addition of the models D.PI and D.CI which directly predict CO_2 using PI or Coincident index instead of through the bridging method.

B.3.4 Using Both GDP and PI in the Model (Annual Only)

Figure B.8: Average RMSFE Across States – CO_2 Emissions, Annual Data Flow

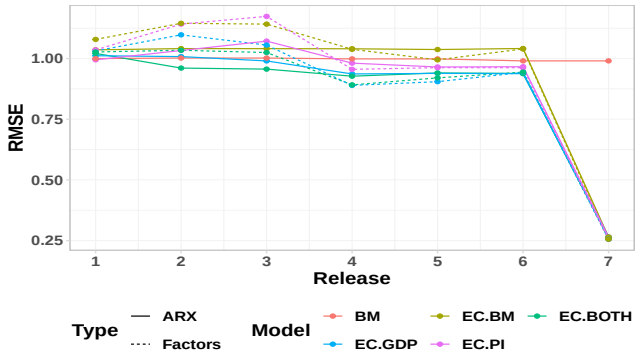

Notes: The same as Figure 3.3 with the addition of the model EC.BOTH which uses both PI and GDP in making the EC predictions for the bridge equation.

Appendix C

Appendix to Chapter 4

This appendix consists of a number of additional supportive tables and figures supporting Chapter 4. These primarily contain addition GaR levels and different prediction horizons to substantiate the results in the main chapter. Both in-sample and out-of-sample supplemental results along with predicted densities and prediction decomposition are included. The appendix is organised as follows: Section C.1 presents the in-sample results with two additional GaR levels for both assessing the significance of the coefficients and the goodness-of-fit; Section C.2 displays the out-of-sample validation, i.e. DQ tests and TL for the full sample and a subsample excluding the GFC; Section C.3 presents the time-series of estimated out-of-sample GaR for different prediction horizons; Section C.4 presents the entire predicted density for three different points in time that are distinct in terms of macroeconomic significance; Section C.5 consists of supplemental plots on predicted moment time series and finally Section C.6 presents substantiates the decomposition of the predicted GaR series.

C.1 In-Sample Analysis – Other Levels

C.1.1 Vulnerability Indicators

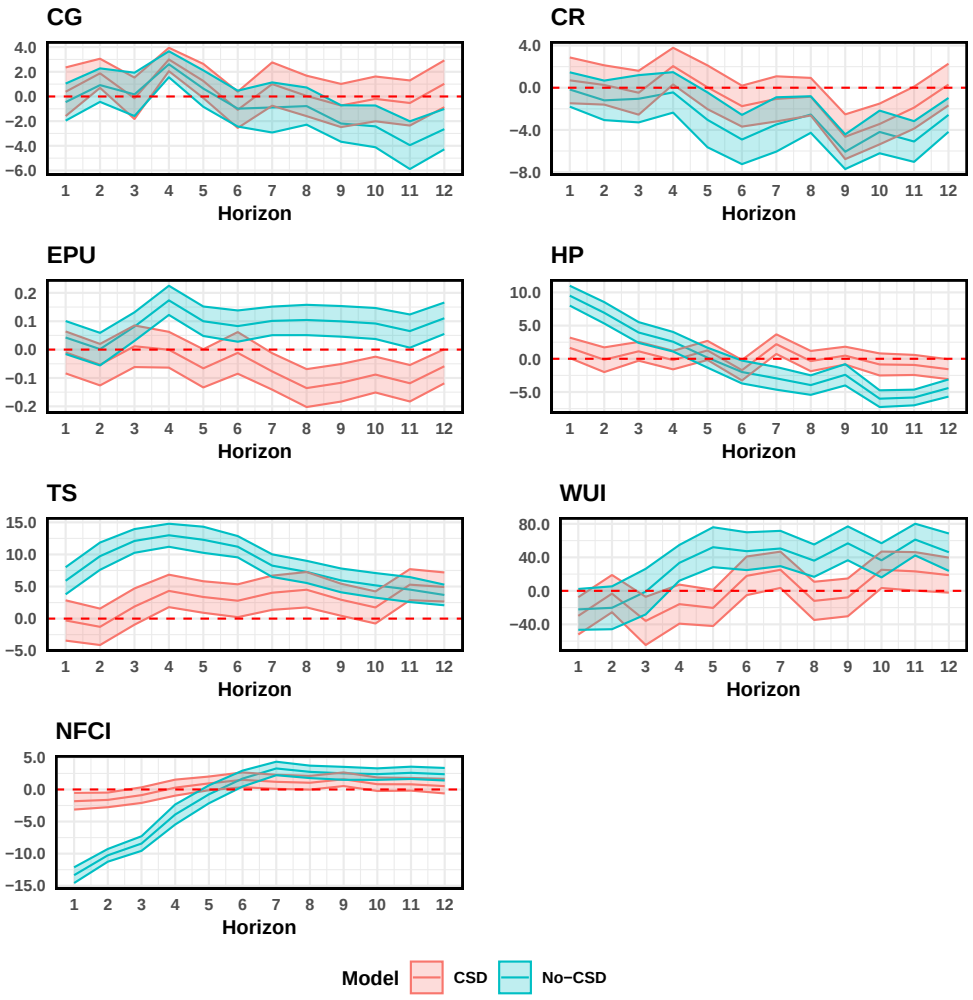

(a) Impact of Variables on 10% GaR

Notes: See Figure 4.2.

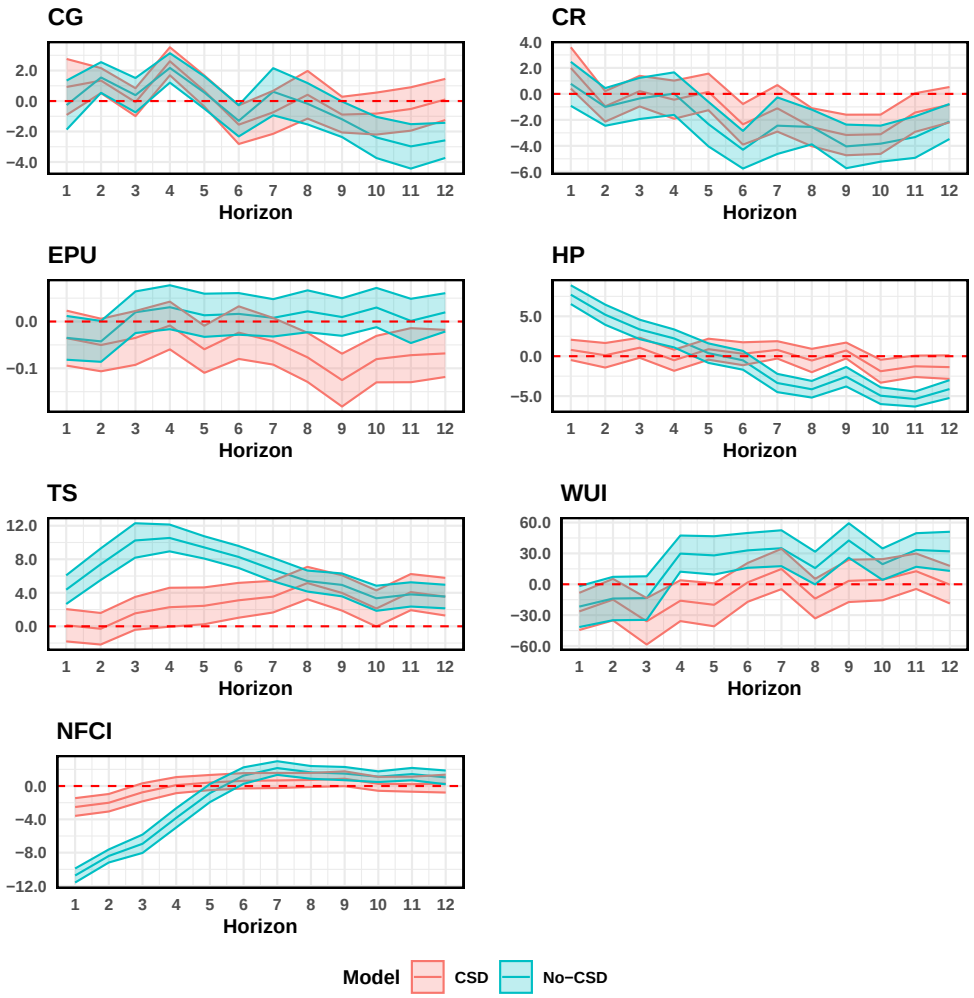

(b) Impact of Variables on 15% GaR

Notes: See Figure 4.2.

C.1.2 Goodness-of-Fit

Table C.1: R Squared

Indicator	Horizon											
	1	2	3	4	5	6	7	8	9	10	11	12
CSD 10% GaR												
CG	0.0705	0.0697	0.0654	0.0651	0.0611	0.0653	0.0662	0.0667	0.0663	0.0695	0.0699	0.0696
CR	0.0704	0.0713	0.0678	0.0653	0.0643	0.0643	0.0635	0.0623	0.0646	0.0637	0.0633	0.0645
EPU	0.0968	0.0988	0.1001	0.1009	0.1010	0.1018	0.1064	0.1091	0.1124	0.1075	0.1115	0.1123
EPU	0.0767	0.0698	0.0691	0.0650	0.0631	0.0695	0.0695	0.0693	0.0688	0.0688	0.0715	0.0710
TS	0.0840	0.0835	0.0758	0.0690	0.0690	0.0689	0.0684	0.0668	0.0655	0.0643	0.0648	0.0645
WUI	0.1486	0.1557	0.1594	0.1598	0.1618	0.1576	0.1570	0.1620	0.1660	0.1642	0.1664	0.1713
NFCI	0.1181	0.0864	0.0717	0.0648	0.0625	0.0624	0.0620	0.0625	0.0622	0.0603	0.0604	0.0619
No-CSD 10% GaR												
CG	0.0001	0.0002	0.0000	0.0017	0.0001	0.0008	0.0002	0.0002	0.0011	0.0012	0.0028	0.0011
CR	0.0000	0.0001	0.0004	0.0003	0.0023	0.0033	0.0023	0.0018	0.0064	0.0027	0.0031	0.0011
EPU	0.0001	0.0000	0.0011	0.0039	0.0015	0.0013	0.0012	0.0017	0.0007	0.0011	0.0008	0.0015
EPU	0.0139	0.0075	0.0022	0.0003	0.0001	0.0002	0.0005	0.0021	0.0006	0.0070	0.0076	0.0051
TS	0.0042	0.0097	0.0164	0.0170	0.0132	0.0098	0.0067	0.0059	0.0060	0.0052	0.0043	0.0030
WUI	0.0002	0.0001	0.0000	0.0025	0.0047	0.0080	0.0057	0.0045	0.0077	0.0048	0.0086	0.0065
NFCI	0.0507	0.0253	0.0091	0.0002	0.0005	0.0026	0.0035	0.0022	0.0016	0.0012	0.0013	0.0018

Table C.1: (cont'd...) R Squared

Horizon													
CCE 15% GaR													
CG	0.0629	0.0624	0.0588	0.0574	0.0551	0.0587	0.0589	0.0595	0.0587	0.0625	0.0628	0.0644	
CR	0.0644	0.0654	0.0625	0.0593	0.0589	0.0588	0.0573	0.0564	0.0573	0.0590	0.0580	0.0606	
EPU	0.0834	0.0842	0.0856	0.0852	0.0858	0.0875	0.0902	0.0916	0.0937	0.0907	0.0943	0.0944	
EPU	0.0692	0.0633	0.0607	0.0593	0.0569	0.0616	0.0614	0.0616	0.0615	0.0622	0.0646	0.0646	
TS	0.0752	0.0749	0.0692	0.0635	0.0632	0.0628	0.0628	0.0603	0.0598	0.0590	0.0591	0.0586	
WUI	0.1219	0.1277	0.1315	0.1310	0.1329	0.1284	0.1280	0.1315	0.1352	0.1332	0.1353	0.1387	
NFCI	0.1001	0.0723	0.0621	0.0576	0.0556	0.0553	0.0554	0.0560	0.0561	0.0552	0.0556	0.0561	
No-CSD 15% GaR													
CG	0.0000	0.0005	0.0000	0.0022	0.0002	0.0009	0.0000	0.0000	0.0003	0.0011	0.0013	0.0014	
CR	0.0001	0.0004	0.0001	0.0000	0.0012	0.0038	0.0013	0.0012	0.0022	0.0026	0.0014	0.0007	
EPU	0.0002	0.0003	0.0000	0.0004	0.0001	0.0001	0.0000	0.0001	0.0000	0.0000	0.0000	0.0003	
EPU	0.0120	0.0052	0.0017	0.0007	0.0001	0.0000	0.0007	0.0019	0.0006	0.0052	0.0073	0.0048	
TS	0.0023	0.0070	0.0112	0.0121	0.0109	0.0085	0.0057	0.0053	0.0053	0.0033	0.0036	0.0028	
WUI	0.0009	0.0002	0.0002	0.0017	0.0026	0.0051	0.0032	0.0015	0.0045	0.0021	0.0045	0.0042	
NFCI	0.0360	0.0189	0.0068	0.0006	0.0002	0.0013	0.0017	0.0011	0.0008	0.0005	0.0007	0.0004	

Notes: See Table 4.1.

C.2 Out-of-Sample Assessment

C.2.1 Coverage – Other Predictors

Figure C.2: Coverage

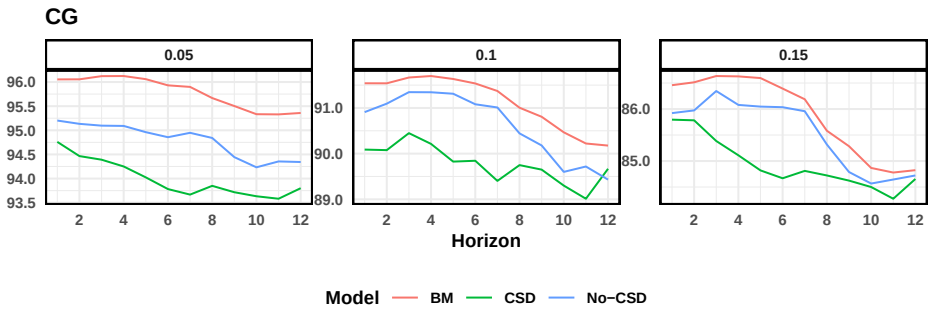

(a) CG

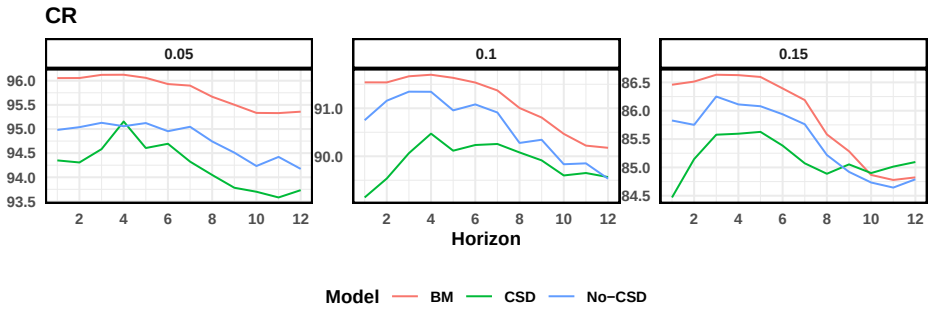

(b) CR

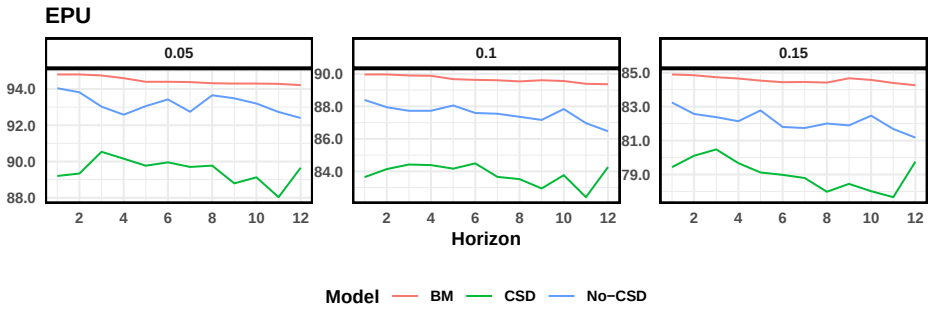

(c) EPU

Figure C.2: (cont'd...) Coverage

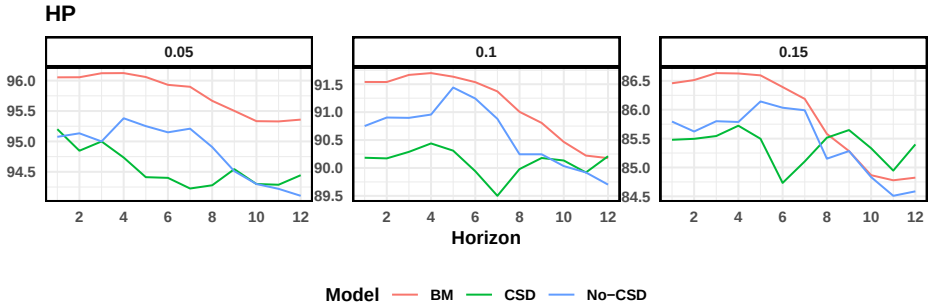

(d) HP

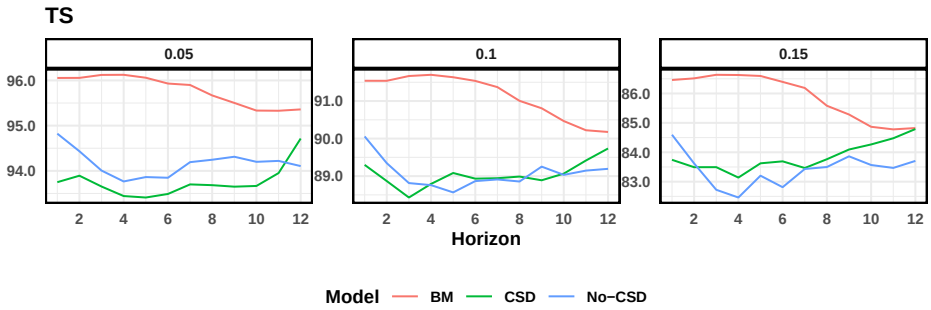

(e) TS

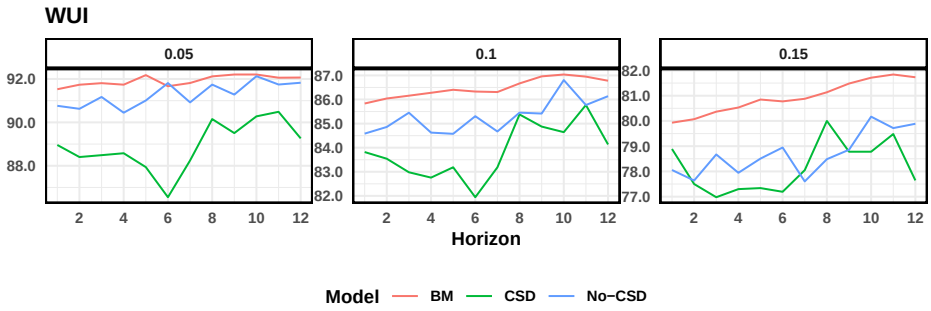

(f) WUI

Notes: These figures plot the coverage for the different models with different predictors considered over different prediction horizons. The GaR levels are indicated in the panel headers.

C.2.2 DQ Tests – Other Predictors

Table C.2: DQ Tests – CG

GaR	5%			10%			15%		
Horizon	BM	CSD	No-CSD	BM	CSD	No-CSD	BM	CSD	No-CSD
1	18	17	18	12	16	14	14	16	15
2	18	20	21	14	19	20	14	18	16
3	18	19	20	14	18	19	14	20	17
4	17	21	21	14	18	19	14	16	17
5	18	18	20	14	18	19	14	18	17
6	18	17	19	14	17	19	15	17	18
7	18	18	20	15	17	20	16	15	18
8	17	18	20	16	18	20	16	17	18
9	18	17	20	17	17	20	16	16	18
10	18	17	20	18	18	19	15	16	18
11	18	17	18	18	17	19	14	18	19
12	18	19	19	18	18	19	14	16	18

(a) Unconditional

GaR	5%			10%			15%		
Horizon	BM	CSD	No-CSD	BM	CSD	No-CSD	BM	CSD	No-CSD
1	8	12	9	6	9	5	6	9	5
2	18	18	16	15	16	13	7	9	12
3	21	17	20	13	19	16	13	17	14
4	21	18	19	18	18	18	13	20	17
5	21	19	21	18	16	19	17	14	18
6	20	18	21	20	13	18	17	18	16
7	21	17	21	19	19	20	17	18	16
8	22	20	21	19	20	20	17	14	15
9	19	19	21	21	20	18	14	19	16
10	19	20	22	22	18	21	21	17	19
11	19	20	21	20	17	21	17	19	20
12	19	21	20	21	17	19	18	16	22

(b) Hit

Notes: See Table 4.2.

Table C.2: DQ Tests – CR

GaR	5%			10%			15%		
Horizon	BM	CSD	No-CSD	BM	CSD	No-CSD	BM	CSD	No-CSD
1	18	17	18	12	16	14	14	14	15
2	18	20	20	14	19	20	14	17	17
3	18	20	20	14	18	19	14	19	17
4	17	20	20	14	18	19	14	19	16
5	18	20	20	14	18	19	14	17	17
6	18	19	20	14	17	20	15	18	18
7	18	19	20	15	17	20	16	19	17
8	17	18	20	16	18	20	16	17	18
9	18	19	20	17	18	19	16	16	18
10	18	19	20	18	18	20	15	19	20
11	18	18	19	18	17	19	14	18	18
12	18	20	19	18	18	19	14	17	18

(c) Unconditional

GaR	5%			10%			15%		
Horizon	BM	CSD	No-CSD	BM	CSD	No-CSD	BM	CSD	No-CSD
1	8	12	9	6	9	5	6	11	6
2	18	20	17	15	15	12	7	11	14
3	21	18	20	13	18	14	13	18	14
4	21	19	20	18	17	17	13	19	17
5	21	21	21	18	18	20	17	13	17
6	20	21	21	20	19	18	17	17	15
7	21	20	22	19	19	21	17	16	16
8	22	21	21	19	18	20	17	15	14
9	19	21	22	21	18	21	14	15	15
10	19	21	22	22	18	19	21	21	20
11	19	19	22	20	19	19	17	20	18
12	19	20	20	21	18	22	18	18	19

(d) Hit

Notes: See Table 4.2.

Table C.2: DQ Tests – EPU

GaR	5%			10%			15%		
Horizon	BM	CSD	No-CSD	BM	CSD	No-CSD	BM	CSD	No-CSD
1	19	9	20	13	11	18	10	14	17
2	21	14	21	18	15	20	13	17	22
3	21	15	21	18	14	20	13	18	21
4	21	17	21	18	14	20	13	17	21
5	20	15	21	18	15	20	13	15	21
6	20	17	22	18	15	20	13	15	21
7	20	16	20	19	16	21	14	15	21
8	20	14	22	19	16	21	17	16	20
9	20	15	22	19	16	21	17	14	21
10	20	14	21	19	16	21	17	16	20
11	20	14	19	19	14	21	17	15	19
12	20	14	20	19	15	20	17	16	20

(e) Unconditional

GaR	5%			10%			15%		
Horizon	BM	CSD	No-CSD	BM	CSD	No-CSD	BM	CSD	No-CSD
1	4	5	8	8	9	7	10	8	9
2	16	20	17	11	17	17	11	16	16
3	21	19	16	19	17	18	14	14	17
4	21	19	20	19	20	22	15	16	17
5	20	16	19	21	18	19	18	14	16
6	22	16	22	23	19	16	15	16	14
7	22	19	21	21	17	18	15	13	15
8	21	18	23	21	16	17	16	17	17
9	22	17	23	22	13	21	16	18	17
10	22	15	21	21	16	16	19	18	17
11	20	15	22	21	17	15	19	16	19
12	20	17	22	19	14	16	19	14	16

(f) Hit

Notes: See Table 4.2.

Table C.2: DQ Tests – HP

GaR	5%			10%			15%		
Horizon	BM	CSD	No-CSD	BM	CSD	No-CSD	BM	CSD	No-CSD
1	18	21	18	12	16	15	14	14	14
2	18	20	21	14	19	20	14	17	16
3	18	20	20	14	18	19	14	18	17
4	17	19	20	14	19	19	14	18	17
5	18	18	20	14	19	19	14	18	17
6	18	19	20	14	19	18	15	18	18
7	18	18	20	15	17	20	16	19	18
8	17	18	20	16	19	20	16	19	20
9	18	19	20	17	19	18	16	17	17
10	18	19	19	18	18	19	15	19	19
11	18	19	19	18	19	19	14	19	19
12	18	19	19	18	17	19	14	16	19

(g) Unconditional

GaR	5%			10%			15%		
Horizon	BM	CSD	No-CSD	BM	CSD	No-CSD	BM	CSD	No-CSD
1	8	14	11	6	8	5	6	8	5
2	18	20	17	15	17	15	7	14	11
3	21	18	20	13	13	14	13	17	13
4	21	19	22	18	16	15	13	17	13
5	21	21	21	18	18	19	17	15	18
6	20	20	21	20	14	19	17	14	16
7	21	20	21	19	18	20	17	15	16
8	22	19	20	19	16	20	17	16	18
9	19	22	20	21	18	20	14	18	19
10	19	23	21	22	21	17	21	19	19
11	19	22	18	20	18	21	17	19	20
12	19	21	21	21	21	19	18	19	18

(h) Hit

Notes: See Table 4.2.

Table C.2: DQ Tests – TS

GaR	5%			10%			15%		
Horizon	BM	CSD	No-CSD	BM	CSD	No-CSD	BM	CSD	No-CSD
1	18	16	18	12	13	14	14	16	17
2	18	19	20	14	18	19	14	20	17
3	18	20	20	14	18	19	14	18	20
4	17	20	20	14	17	18	14	18	18
5	18	18	20	14	16	18	14	18	17
6	18	18	19	14	17	18	15	17	18
7	18	20	19	15	18	19	16	18	19
8	17	19	20	16	18	19	16	16	18
9	18	19	20	17	18	19	16	19	18
10	18	17	20	18	18	19	15	15	18
11	18	18	19	18	17	19	14	18	18
12	18	19	19	18	17	19	14	16	17

(i) Unconditional

GaR	5%			10%			15%		
Horizon	BM	CSD	No-CSD	BM	CSD	No-CSD	BM	CSD	No-CSD
1	8	12	9	6	12	6	6	10	5
2	18	17	16	15	17	13	7	16	12
3	21	20	19	13	17	16	13	17	15
4	21	19	19	18	17	15	13	16	16
5	21	21	22	18	20	18	17	12	15
6	20	18	19	20	16	17	17	11	15
7	21	20	19	19	18	18	17	16	15
8	22	19	22	19	19	19	17	13	14
9	19	19	22	21	17	19	14	14	11
10	19	21	22	22	20	15	21	20	15
11	19	21	21	20	17	20	17	19	20
12	19	19	20	21	20	21	18	20	15

(j) Hit

Notes: See Table 4.2.

Table C.2: DQ Tests – WUI

GaR	5%			10%			15%		
Horizon	BM	CSD	No-CSD	BM	CSD	No-CSD	BM	CSD	No-CSD
1	19	12	18	14	16	17	12	14	15
2	19	16	21	18	17	22	14	17	20
3	19	14	23	17	17	22	14	15	20
4	20	16	22	17	17	19	14	15	19
5	21	15	22	18	16	21	15	16	20
6	19	10	23	18	12	22	15	15	22
7	20	16	20	18	16	20	15	16	20
8	21	20	23	17	21	23	15	19	21
9	22	18	21	18	21	20	16	20	20
10	22	19	23	18	19	23	16	18	21
11	22	18	23	18	21	22	15	19	22
12	22	17	23	19	22	22	17	19	22

(k) Unconditional

GaR	5%			10%			15%		
Horizon	BM	CSD	No-CSD	BM	CSD	No-CSD	BM	CSD	No-CSD
1	6	9	6	7	8	10	9	12	11
2	14	17	21	13	15	16	12	17	14
3	22	18	21	17	19	22	14	19	20
4	20	19	20	18	16	24	18	21	17
5	20	19	20	20	20	20	18	16	20
6	19	20	23	21	20	23	20	16	21
7	22	17	22	23	18	23	17	18	17
8	22	17	20	20	21	21	15	15	17
9	21	15	23	20	19	19	19	15	20
10	23	21	22	20	17	21	19	20	16
11	22	20	23	19	17	18	21	14	17
12	18	22	23	20	22	18	18	18	16

(l) Hit

Notes: See Table 4.2.

C.2.3 Tick-Loss – Other Predictors

Table C.3: TL – Other Predictors

	5%		10%		15%	
Horizon	**CSD**	**No-CSD**	**CSD**	**No-CSD**	**CSD**	**No-CSD**
1	6.68	3.16	3.66	1.81	2.12	1.09
2	6.24	2.68	3.85	1.65	2.52	1.28
3	6.36	2.87	4.21	2.03	2.46	1.41
4	5.57	2.52	4.60	1.26	3.31	0.98
5	5.97	3.81	4.69	2.13	3.81	1.18
6	7.14	3.33	5.59	2.14	4.45	1.81
7	7.21	3.50	5.57	2.21	4.57	1.67
8	5.97	3.62	5.62	2.30	4.06	1.58
9	5.69	3.94	5.17	2.44	3.70	1.55
10	4.80	3.50	4.84	2.24	3.88	1.77
11	5.50	3.46	4.46	2.50	3.61	1.74
12	5.52	3.19	4.25	2.07	4.13	1.52

(a) TL: CG

	5%		10%		15%	
Horizon	**CSD**	**No-CSD**	**CSD**	**No-CSD**	**CSD**	**No-CSD**
1	5.08	2.44	2.88	1.37	1.69	0.71
2	5.35	3.01	4.46	1.84	3.23	1.55
3	6.34	3.35	4.48	1.85	3.22	1.13
4	6.91	2.98	4.69	1.43	3.71	1.09
5	7.06	4.62	5.01	2.24	3.62	1.57
6	6.84	4.44	5.51	2.29	4.20	2.05
7	6.65	3.94	5.20	2.22	4.22	1.80
8	5.61	3.71	4.69	2.39	3.33	1.84
9	4.82	4.57	3.57	2.47	2.71	1.42
10	3.77	3.58	3.88	2.41	2.66	2.04
11	5.09	3.58	3.83	2.77	3.25	1.77
12	3.92	2.87	3.71	1.88	3.31	1.21

(b) TL: CR

Notes: See Table 4.3.

Table C.3: TL – Other Predictors

	5%		10%		15%	
Horizon	**CSD**	**No-CSD**	**CSD**	**No-CSD**	**CSD**	**No-CSD**
1	1.01	2.82	1.31	2.07	0.65	1.30
2	0.80	2.58	1.93	2.04	1.71	1.31
3	4.50	2.87	3.36	2.45	2.64	1.47
4	4.08	1.85	3.34	2.12	2.69	1.02
5	3.50	1.75	3.07	2.24	2.56	1.26
6	2.51	2.56	2.26	2.38	1.59	1.48
7	2.40	2.30	2.42	2.46	1.82	1.45
8	3.02	2.16	3.63	2.23	1.45	1.53
9	3.13	2.74	4.21	2.44	2.55	1.42
10	1.62	2.25	4.06	2.05	2.52	1.57
11	2.61	2.45	2.78	2.10	1.10	1.48
12	4.39	1.74	4.18	2.09	2.70	1.56

(c) TL: EPU

	5%		10%		15%	
Horizon	**CSD**	**No-CSD**	**CSD**	**No-CSD**	**CSD**	**No-CSD**
1	7.36	4.20	5.68	2.71	3.95	2.12
2	7.19	3.72	5.17	2.19	3.74	1.25
3	7.39	3.82	5.54	1.85	3.54	1.28
4	6.26	4.04	5.49	2.08	4.25	1.31
5	6.85	3.77	5.51	2.23	4.06	1.39
6	7.58	4.14	6.52	2.14	4.82	1.82
7	8.20	3.98	6.31	2.10	4.79	1.74
8	7.70	4.06	6.27	2.29	4.62	1.61
9	7.23	4.22	6.38	2.40	4.45	1.96
10	6.57	4.75	5.93	3.13	4.62	2.44
11	4.17	4.35	4.70	2.81	3.75	1.99
12	3.99	3.05	4.21	2.03	3.62	1.34

(d) TL: HP

Notes: See Table 4.3.

Table C.3: TL – Other Predictors

	5%		10%		15%	
Horizon	**CSD**	**No-CSD**	**CSD**	**No-CSD**	**CSD**	**No-CSD**
1	6.65	4.80	6.30	3.09	4.67	2.05
2	7.31	4.67	6.23	2.91	4.83	1.62
3	7.09	5.82	5.61	3.42	4.67	1.10
4	4.81	6.13	5.61	3.30	4.23	1.34
5	6.03	5.42	6.23	2.50	5.09	1.63
6	5.42	4.35	5.98	2.74	5.22	1.89
7	6.27	4.30	5.50	2.40	4.58	1.52
8	6.12	4.23	4.80	2.56	4.10	1.98
9	6.14	3.65	5.01	2.39	4.02	1.92
10	4.18	3.22	4.56	2.20	3.65	1.65
11	4.37	3.08	4.15	2.12	3.52	1.72
12	4.96	2.29	3.65	1.81	3.34	1.43

(e) TL: TS

	5%		10%		15%	
Horizon	**CSD**	**No-CSD**	**CSD**	**No-CSD**	**CSD**	**No-CSD**
1	1.85	1.22	4.73	4.33	4.24	3.41
2	2.88	1.72	4.76	3.95	2.88	2.96
3	6.89	0.81	5.59	3.87	3.35	3.63
4	7.02	-0.16	6.43	3.90	3.79	3.75
5	5.15	1.65	3.62	4.62	2.96	3.92
6	0.54	2.92	0.83	5.83	0.48	4.76
7	3.24	2.90	0.04	4.37	-1.28	3.46
8	10.29	4.49	6.96	6.65	4.10	4.81
9	7.60	2.56	5.74	5.29	4.65	4.41
10	9.90	2.75	7.70	5.79	4.95	5.07
11	8.03	2.32	8.13	6.14	5.41	4.96
12	6.59	1.95	5.46	5.70	3.67	5.03

(f) TL: WUI

C.2.4 Different Sub-sample – Q1:1990–Q4:2007

DQ Tests

Table C.4: Unconditional DQ Tests – Different Sub-samples

	5%			10%			15%		
Horizon	**BM**	**CSD**	**No-CSD**	**BM**	**CSD**	**No-CSD**	**BM**	**CSD**	**No-CSD**
1	24	22	23	14	17	14	16	16	18
2	24	22	23	15	15	15	17	17	17
3	24	22	23	15	16	15	17	18	18
4	24	22	23	15	16	14	17	18	18
5	24	22	23	15	15	16	17	17	18
6	24	22	23	15	15	16	17	17	18
7	24	21	23	15	14	17	17	16	18
8	22	20	23	15	15	16	17	17	18
9	22	20	23	15	15	16	17	17	17
10	22	22	23	15	15	15	17	16	18
11	22	21	22	15	17	15	17	17	18
12	22	20	22	15	15	16	17	19	18

(a) CG

	5%			10%			15%		
Horizon	**BM**	**CSD**	**No-CSD**	**BM**	**CSD**	**No-CSD**	**BM**	**CSD**	**No-CSD**
1	24	21	23	14	15	14	16	16	18
2	24	22	23	15	15	15	17	17	17
3	24	22	23	15	16	15	17	17	18
4	24	22	23	15	15	15	17	17	18
5	24	22	23	15	16	15	17	16	18
6	24	22	23	15	14	16	17	16	17
7	24	21	23	15	15	17	17	16	18
8	22	21	23	15	14	16	17	17	16
9	22	19	23	15	17	16	17	19	16
10	22	21	23	15	17	16	17	17	17
11	22	19	22	15	17	16	17	18	17
12	22	21	22	15	16	16	17	17	18

(b) CR

Notes: See Table 4.2.

Notes: See Table 4.3.

Table C.4: Unconditional DQ Tests – Different Sub-samples

	5%			10%			15%		
Horizon	**BM**	**CSD**	**No-CSD**	**BM**	**CSD**	**No-CSD**	**BM**	**CSD**	**No-CSD**
1	24	22	23	14	17	14	16	17	17
2	24	22	23	15	15	17	17	15	19
3	24	22	23	15	16	17	17	16	17
4	24	22	23	15	17	16	17	16	18
5	24	23	23	15	18	15	17	15	18
6	24	22	23	15	16	16	17	14	18
7	24	22	23	15	16	16	17	18	18
8	22	22	23	15	18	16	17	17	19
9	22	22	23	15	18	14	17	18	19
10	22	22	23	15	19	15	17	19	16
11	22	22	23	15	17	17	17	19	18
12	22	22	22	15	17	15	17	16	17

(c) HP

	5%			10%			15%		
Horizon	**BM**	**CSD**	**No-CSD**	**BM**	**CSD**	**No-CSD**	**BM**	**CSD**	**No-CSD**
1	24	22	23	14	16	13	16	15	16
2	24	22	23	15	17	14	17	19	17
3	24	22	22	15	17	16	17	19	19
4	24	22	22	15	17	18	17	18	19
5	24	22	22	15	15	19	17	17	16
6	24	22	21	15	16	17	17	15	20
7	24	21	21	15	15	16	17	16	18
8	22	22	22	15	14	16	17	15	18
9	22	23	22	15	16	16	17	17	17
10	22	22	23	15	17	15	17	17	18
11	22	22	22	15	17	15	17	17	16
12	22	23	22	15	16	16	17	17	17

(d) TS

Notes: See Table 4.2.

Table C.4: Unconditional DQ Tests – Different Sub-samples

	5%			10%			15%		
Horizon	**BM**	**CSD**	**No-CSD**	**BM**	**CSD**	**No-CSD**	**BM**	**CSD**	**No-CSD**
1	24	18	21	14	16	13	16	16	15
2	24	21	22	15	16	13	17	16	14
3	24	22	22	15	16	15	17	16	14
4	24	22	22	15	17	16	17	18	15
5	24	23	22	15	16	15	17	16	17
6	24	23	23	15	17	17	17	18	17
7	24	23	23	15	17	18	17	16	19
8	22	21	23	15	16	17	17	16	18
9	22	21	23	15	16	17	17	17	18
10	22	21	23	15	16	17	17	18	18
11	22	22	23	15	16	16	17	16	19
12	22	22	23	15	17	16	17	14	17

(e) NFCI

Notes: See Table 4.2.

Table C.5: DQ Tests Conditional on Lagged Hits – Different Sub-Samples

	5%			10%			15%		
Horizon	**BM**	**CSD**	**No-CSD**	**BM**	**CSD**	**No-CSD**	**BM**	**CSD**	**No-CSD**
1	8	10	11	17	17	14	16	18	18
2	11	12	12	15	16	17	15	16	16
3	10	15	15	15	13	18	18	17	16
4	8	13	11	16	14	16	17	19	16
5	8	15	13	16	15	17	18	16	18
6	10	12	15	17	16	17	16	15	18
7	11	14	14	17	16	17	18	18	20
8	12	14	15	16	17	17	18	14	21
9	14	17	16	17	17	17	16	19	19
10	14	14	17	17	18	16	18	17	17
11	14	16	16	18	18	16	19	17	19
12	13	15	16	16	17	17	18	17	17

(a) CG

	5%			10%			15%		
Horizon	**BM**	**CSD**	**No-CSD**	**BM**	**CSD**	**No-CSD**	**BM**	**CSD**	**No-CSD**
1	8	11	10	17	16	17	16	18	16
2	11	14	10	15	16	17	15	15	17
3	10	14	15	15	16	17	18	19	16
4	8	11	11	16	17	16	17	18	17
5	8	15	15	16	18	16	18	15	17
6	10	14	15	17	15	17	16	16	18
7	11	15	14	17	16	18	18	15	20
8	12	16	15	16	18	17	18	18	20
9	14	17	16	17	18	19	16	19	19
10	14	15	17	17	16	17	18	18	16
11	14	15	16	18	18	16	19	18	19
12	13	16	17	16	19	17	18	17	17

(b) CR

Notes: See Table 4.2.

Table C.5: DQ Tests Conditional on Lagged Hits

	5%			10%			15%		
Horizon	**BM**	**CSD**	**No-CSD**	**BM**	**CSD**	**No-CSD**	**BM**	**CSD**	**No-CSD**
1	8	11	10	17	16	14	16	15	18
2	11	16	12	15	18	16	15	15	16
3	10	15	15	15	17	16	18	17	16
4	8	17	14	16	16	14	17	18	16
5	8	16	15	16	20	16	18	18	16
6	10	14	14	17	15	16	16	14	18
7	11	13	13	17	16	19	18	20	19
8	12	15	14	16	14	18	18	18	20
9	14	15	14	17	17	15	16	20	19
10	14	15	17	17	15	17	18	16	17
11	14	16	15	18	18	16	19	18	18
12	13	15	17	16	18	18	18	18	16

(c) HP

	5%			10%			15%		
Horizon	**BM**	**CSD**	**No-CSD**	**BM**	**CSD**	**No-CSD**	**BM**	**CSD**	**No-CSD**
1	8	12	10	17	17	15	16	18	16
2	11	15	12	15	20	17	15	18	19
3	10	13	16	15	21	16	18	19	20
4	8	14	13	16	18	17	17	15	19
5	8	14	13	16	19	18	18	15	16
6	10	15	14	17	16	18	16	14	16
7	11	13	13	17	16	18	18	18	18
8	12	15	16	16	19	20	18	18	20
9	14	14	16	17	17	17	16	18	18
10	14	16	17	17	17	16	18	19	17
11	14	14	16	18	19	18	19	19	18
12	13	16	16	16	19	16	18	17	18

(d) TS

Notes: See Table 4.2.

Table C.5: DQ Tests Conditional on Lagged Hits

	5%			10%			15%		
Horizon	**BM**	**CSD**	**No-CSD**	**BM**	**CSD**	**No-CSD**	**BM**	**CSD**	**No-CSD**
1	8	9	10	17	11	13	16	13	16
2	11	15	13	15	15	16	15	19	15
3	10	17	15	15	17	17	18	18	16
4	8	16	13	16	17	15	17	18	18
5	8	16	13	16	16	17	18	15	17
6	10	16	13	17	18	17	16	15	19
7	11	14	12	17	18	17	18	17	20
8	12	13	14	16	16	17	18	17	21
9	14	16	16	17	19	17	16	17	19
10	14	15	17	17	17	16	18	19	18
11	14	17	16	18	20	16	19	19	20
12	13	17	17	16	19	17	18	18	17

(e) NFCI

Notes: See Table 4.2.

TL

Table C.6: TL for Different Sub-samples

	5%		10%		15%	
Horizon	**CSD**	**No-CSD**	**CSD**	**No-CSD**	**CSD**	**No-CSD**
1	0.1287	0.1289	0.1938	0.1933	0.2437	0.2387
2	0.1281	0.1293	0.1925	0.1945	0.2410	0.2397
3	0.1275	0.1292	0.1920	0.1931	0.2408	0.2389
4	0.1283	0.1314	0.1902	0.1949	0.2378	0.2394
5	0.1268	0.1289	0.1903	0.1938	0.2372	0.2397
6	0.1278	0.1283	0.1901	0.1932	0.2379	0.2387
7	0.1280	0.1279	0.1903	0.1919	0.2369	0.2380
8	0.1282	0.1272	0.1905	0.1908	0.2382	0.2379
9	0.1279	0.1266	0.1892	0.1900	0.2368	0.2380
10	0.1286	0.1264	0.1899	0.1898	0.2363	0.2377
11	0.1280	0.1257	0.1907	0.1896	0.2359	0.2371
12	0.1261	0.1261	0.1881	0.1903	0.2323	0.2375

(a) TL: CG

	5%		10%		15%	
Horizon	**CSD**	**No-CSD**	**CSD**	**No-CSD**	**CSD**	**No-CSD**
1	0.1296	0.1288	0.1964	0.1928	0.2446	0.2389
2	0.1291	0.1289	0.1941	0.1943	0.2413	0.2399
3	0.1280	0.1290	0.1924	0.1929	0.2409	0.2391
4	0.1269	0.1298	0.1918	0.1950	0.2397	0.2398
5	0.1263	0.1283	0.1906	0.1940	0.2373	0.2399
6	0.1277	0.1278	0.1888	0.1934	0.2373	0.2383
7	0.1283	0.1276	0.1895	0.1920	0.2375	0.2380
8	0.1266	0.1272	0.1904	0.1908	0.2379	0.2382
9	0.1268	0.1262	0.1918	0.1904	0.2388	0.2377
10	0.1288	0.1265	0.1921	0.1897	0.2400	0.2371
11	0.1283	0.1265	0.1935	0.1895	0.2400	0.2369
12	0.1287	0.1264	0.1934	0.1913	0.2393	0.2385

(b) TL: CR

Notes: See Table 4.3.

Table C.6: TL for Different Sub-samples

	5%		10%		15%	
Horizon	**CSD**	**No-CSD**	**CSD**	**No-CSD**	**CSD**	**No-CSD**
1	0.1271	0.1264	0.1914	0.1926	0.2395	0.2387
2	0.1281	0.1285	0.1916	0.1944	0.2394	0.2410
3	0.1258	0.1285	0.1900	0.1950	0.2388	0.2413
4	0.1260	0.1284	0.1894	0.1942	0.2372	0.2407
5	0.1271	0.1294	0.1903	0.1933	0.2375	0.2397
6	0.1263	0.1277	0.1882	0.1928	0.2369	0.2385
7	0.1248	0.1276	0.1895	0.1924	0.2365	0.2371
8	0.1252	0.1273	0.1888	0.1908	0.2353	0.2377
9	0.1257	0.1267	0.1883	0.1905	0.2351	0.2361
10	0.1264	0.1249	0.1886	0.1884	0.2352	0.2354
11	0.1279	0.1264	0.1897	0.1893	0.2358	0.2364
12	0.1265	0.1259	0.1885	0.1896	0.2339	0.2362

(c) TL: HP

	5%		10%		15%	
Horizon	**CSD**	**No-CSD**	**CSD**	**No-CSD**	**CSD**	**No-CSD**
1	0.1214	0.1222	0.1849	0.1852	0.2325	0.2301
2	0.1211	0.1206	0.1850	0.1841	0.2301	0.2288
3	0.1222	0.1197	0.1862	0.1847	0.2291	0.2303
4	0.1228	0.1201	0.1856	0.1850	0.2305	0.2292
5	0.1240	0.1218	0.1839	0.1866	0.2292	0.2290
6	0.1264	0.1244	0.1846	0.1858	0.2301	0.2286
7	0.1256	0.1248	0.1855	0.1866	0.2322	0.2295
8	0.1256	0.1248	0.1880	0.1865	0.2345	0.2314
9	0.1263	0.1255	0.1891	0.1871	0.2358	0.2328
10	0.1274	0.1261	0.1897	0.1876	0.2374	0.2347
11	0.1276	0.1266	0.1898	0.1882	0.2370	0.2347
12	0.1270	0.1262	0.1902	0.1890	0.2379	0.2356

(d) TL: TS

Notes: See Table 4.3.

Table C.6: TL for Different Sub-samples

	5%		10%		15%	
Horizon	**CSD**	**No-CSD**	**CSD**	**No-CSD**	**CSD**	**No-CSD**
1	0.1218	0.1212	0.1854	0.1861	0.2333	0.2331
2	0.1215	0.1227	0.1879	0.1891	0.2375	0.2352
3	0.1230	0.1239	0.1883	0.1890	0.2351	0.2352
4	0.1246	0.1260	0.1873	0.1904	0.2360	0.2367
5	0.1241	0.1278	0.1894	0.1921	0.2373	0.2377
6	0.1253	0.1281	0.1894	0.1920	0.2385	0.2385
7	0.1260	0.1288	0.1902	0.1933	0.2384	0.2391
8	0.1261	0.1273	0.1888	0.1913	0.2364	0.2385
9	0.1247	0.1275	0.1893	0.1910	0.2366	0.2388
10	0.1264	0.1267	0.1894	0.1898	0.2363	0.2377
11	0.1271	0.1274	0.1905	0.1904	0.2369	0.2383
12	0.1270	0.1266	0.1923	0.1914	0.2379	0.2383

(e) TL: NFCI

Notes: See Table 4.3.

C.3 Estimated GaR

Figure C.3: Estimated GaR (5%) at Different Horizons, Predictor – NFCI

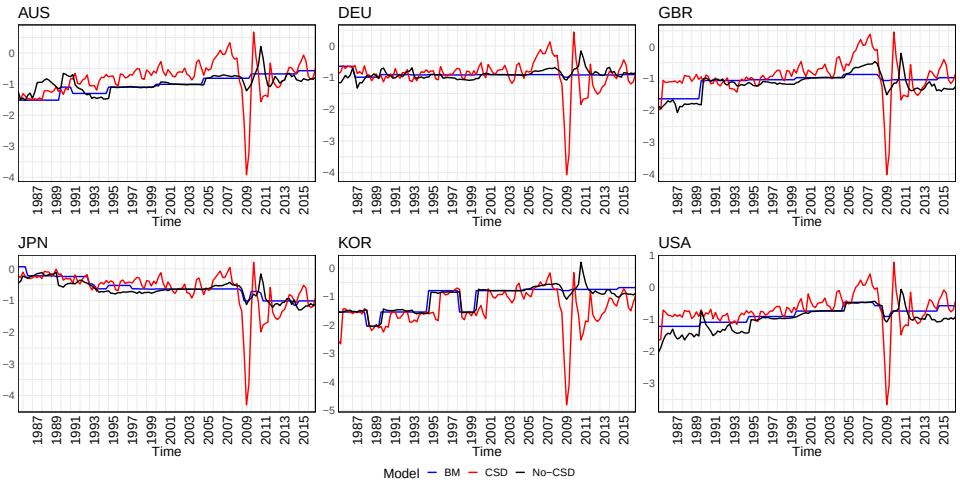

(a) 4–Quarter horizon

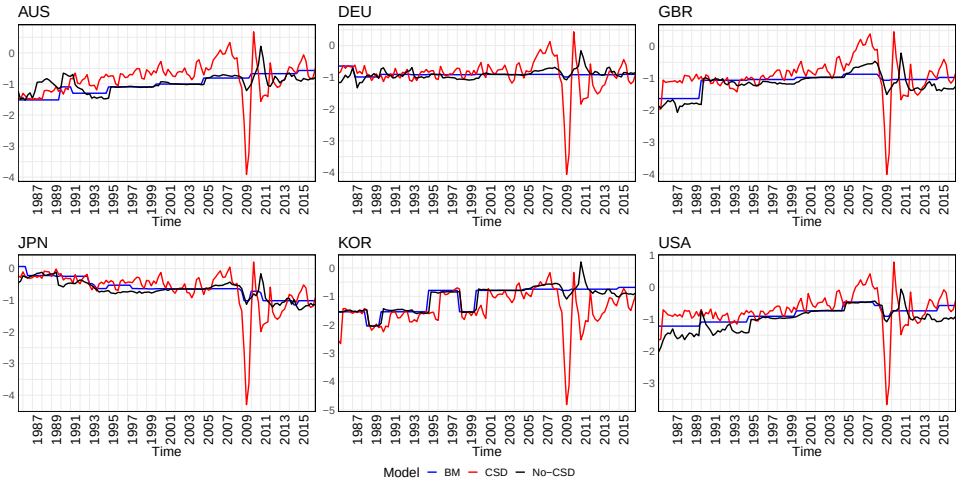

(b) 8 Quarter Horizon

Notes: See Figure 4.4.

C.4 Predicted Density

Figure C.4: Conditional Density

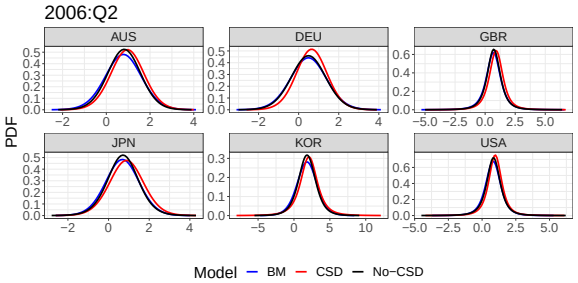

(a) Conditional Density – Q4:2006

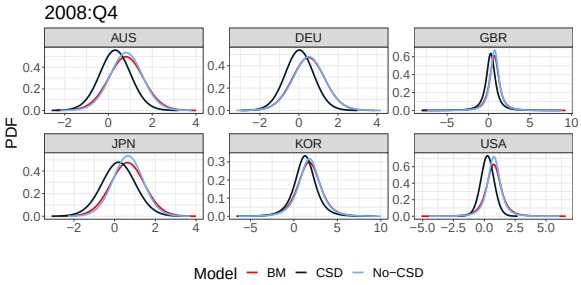

(b) Conditional Density – Q4:2008

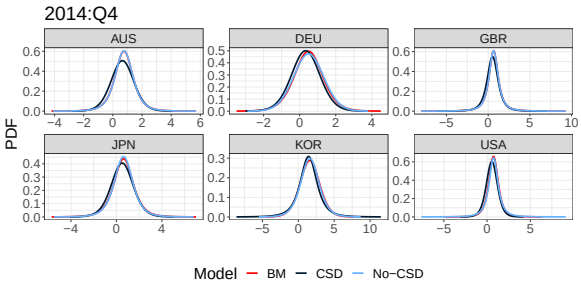

(c) Conditional Density – Q4:2014

Notes: The fitted skew-t distribution is conditional on the NFCI for the 12 quarter-ahead forecast horizon.

C.5 Moments

Figure C.5: Moments Conditional on NFCI; Prediction Horizon – 4 Quarter–Ahead

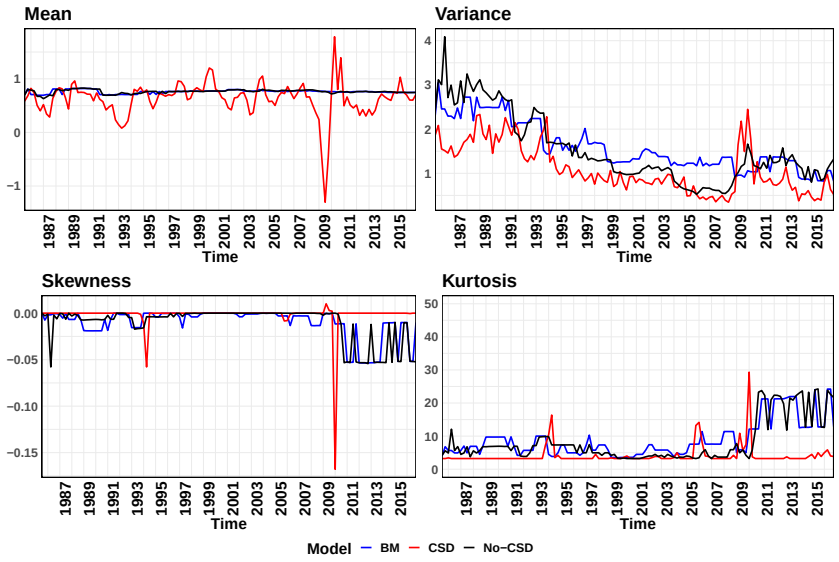

(a) Moments of AUS GDP; Conditional on NFCI

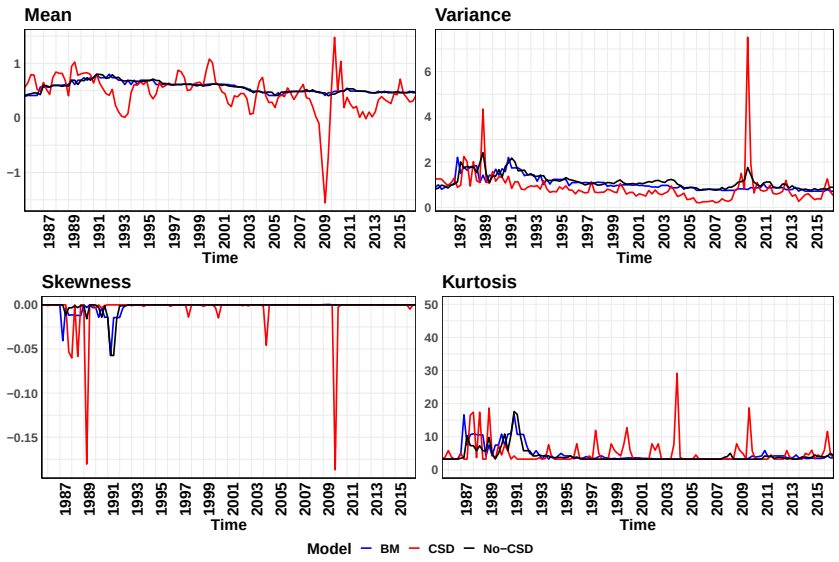

(b) Moments of DEU GDP

Notes: See Figure 4.5.

Figure C.5: (cont'd) Moments Conditional on NFCI; Prediction Horizon – 4 Quarter–Ahead

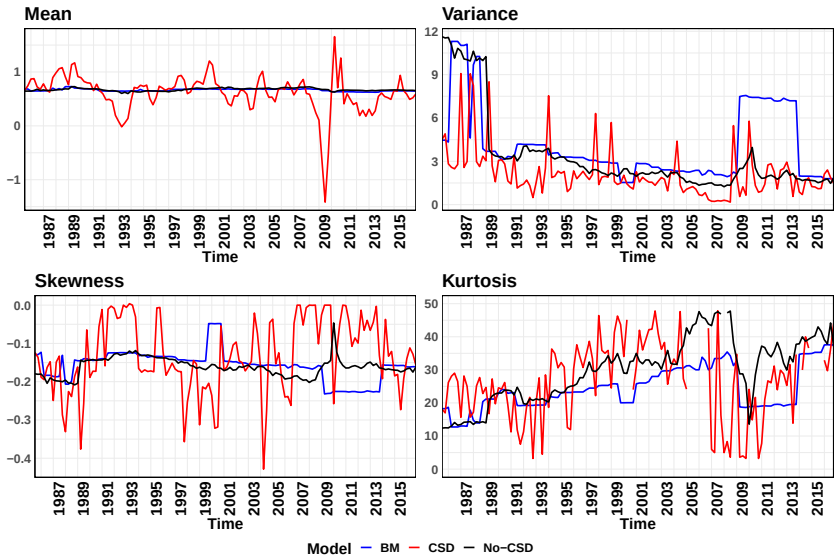

(c) Moments of GBR GDP

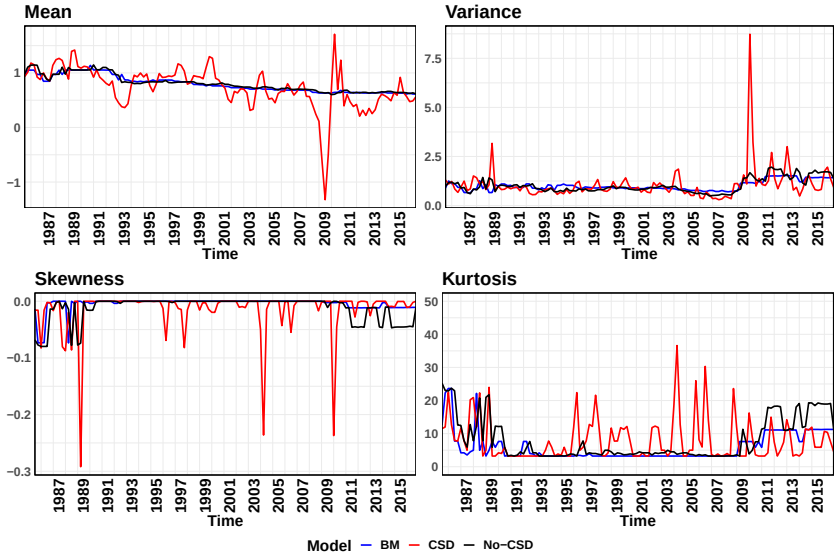

(d) Moments of JPN GDP

Notes: See Figure 4.5.

Figure C.5: (cont'd) Moments Conditional on NFCI; Prediction Horizon – 4 Quarter–Ahead

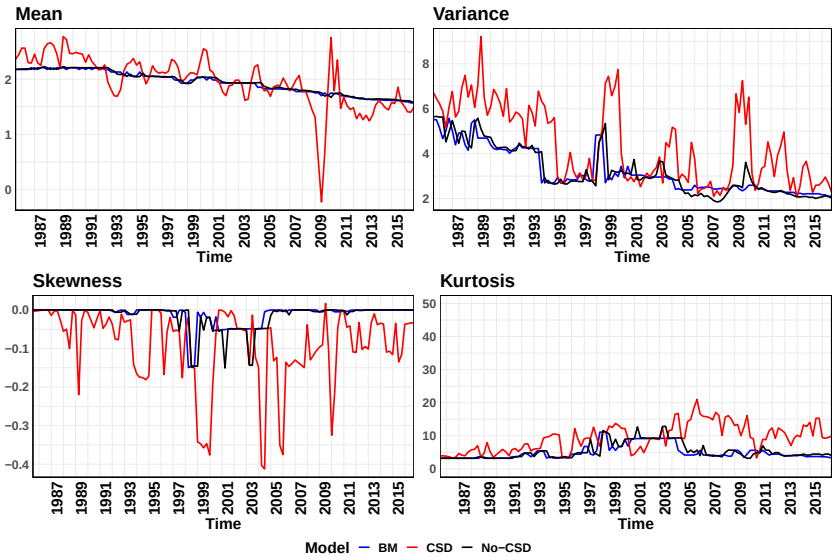

(e) Moments of KOR GDP

Notes: See Figure 4.5.

Figure C.6: Moments Conditional on NFCI; Prediction Horizon – 8 Quarter–Ahead

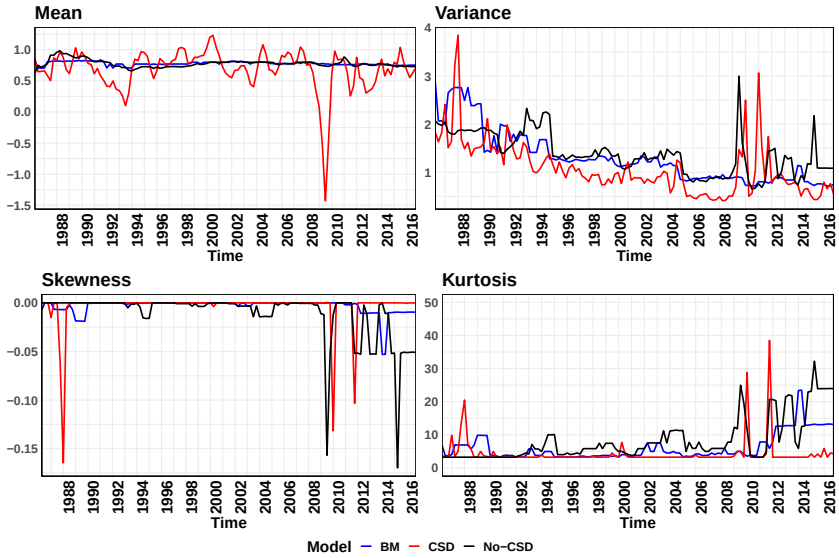

(a) Moments of AUS GDP

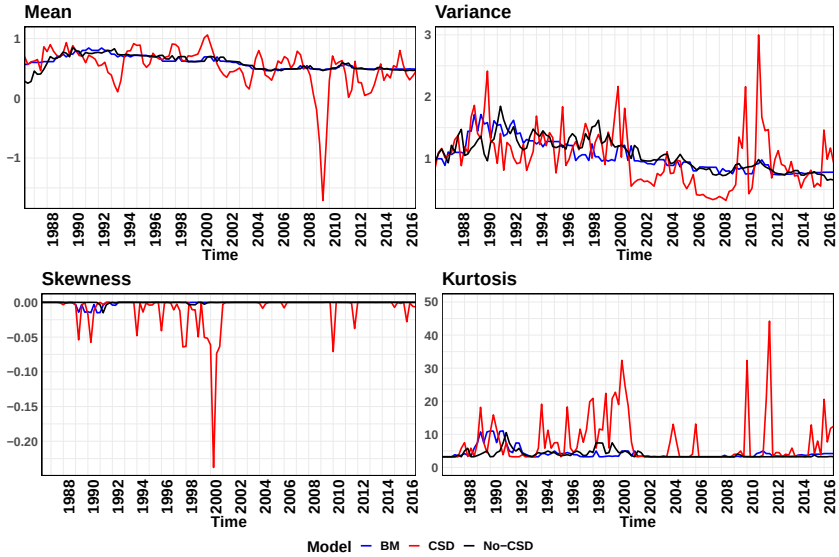

(b) Moments of DEU GDP

Notes: See Figure 4.5.

Figure C.6: (cont'd) Moments Conditional on NFCI; Prediction Horizon – 8–Quarters Ahead

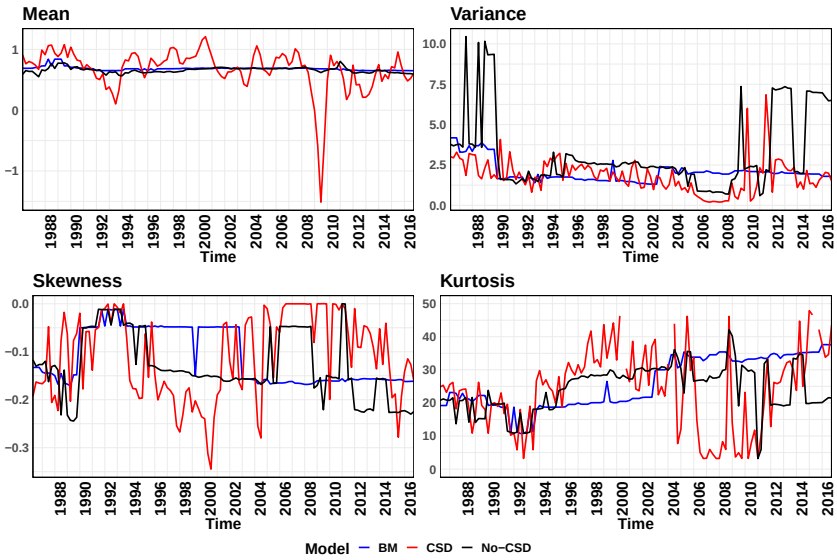

(c) Moments of GBR GDP

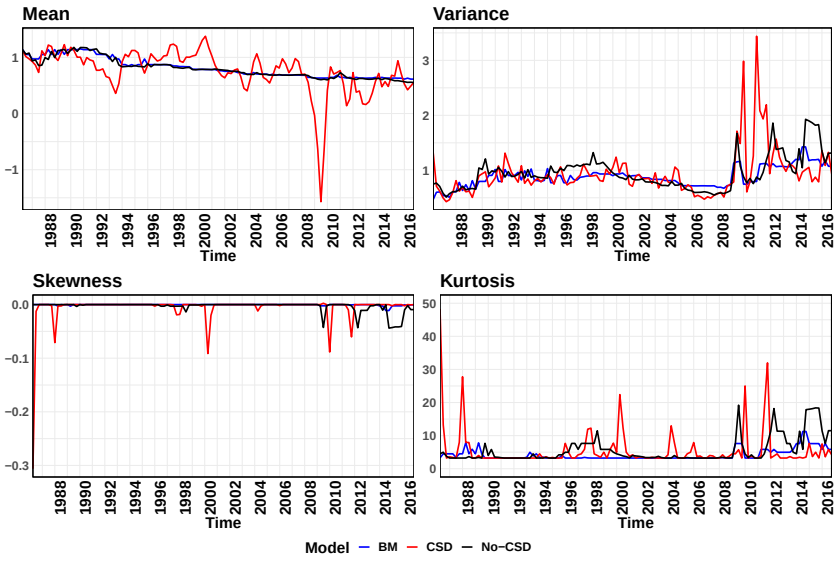

(d) Moments of JPN GDP

Notes: See Figure 4.5.

Figure C.6: (cont'd) Moments Conditional on NFCI; Prediction Horizon – 8–Quarters Ahead

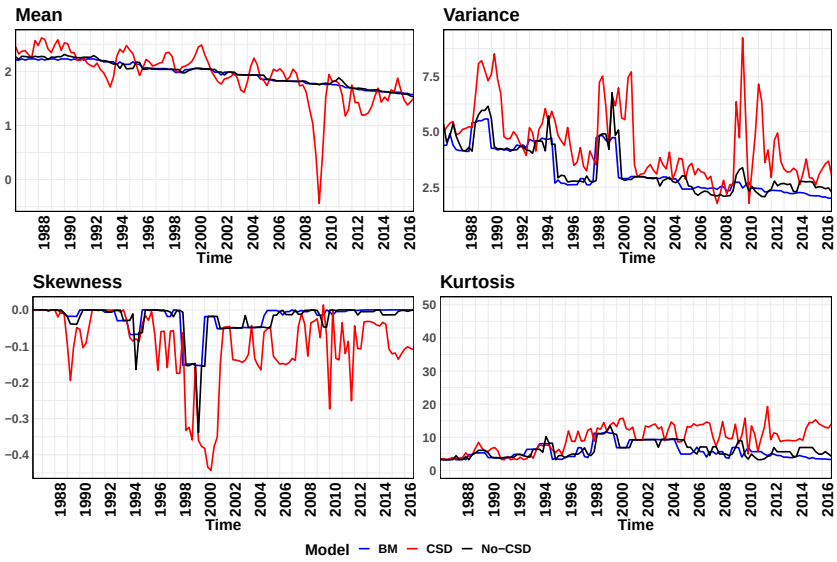

(e) Moments of KOR GDP

Figure C.7: Moments Conditional on NFCI; Prediction Horizon – 12 Quarter–Ahead

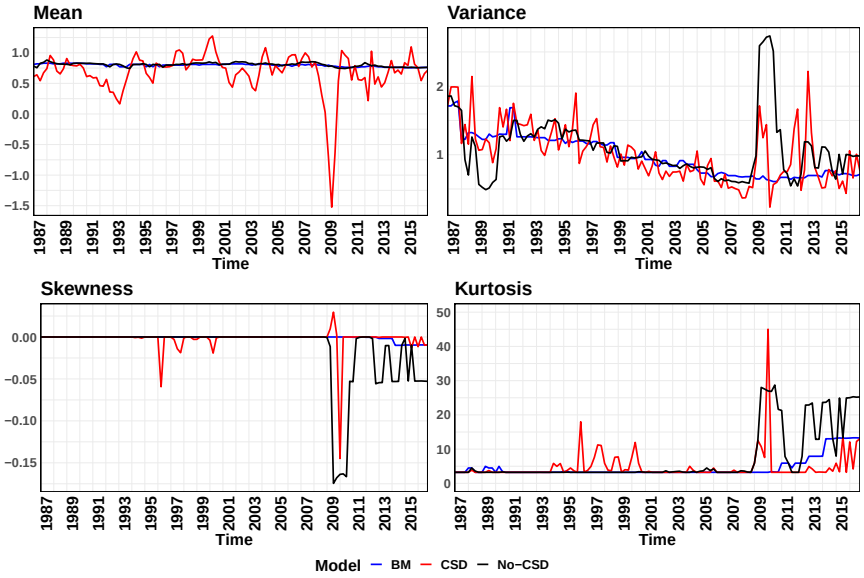

(a) Moments of AUS GDP; Conditional on NFCI

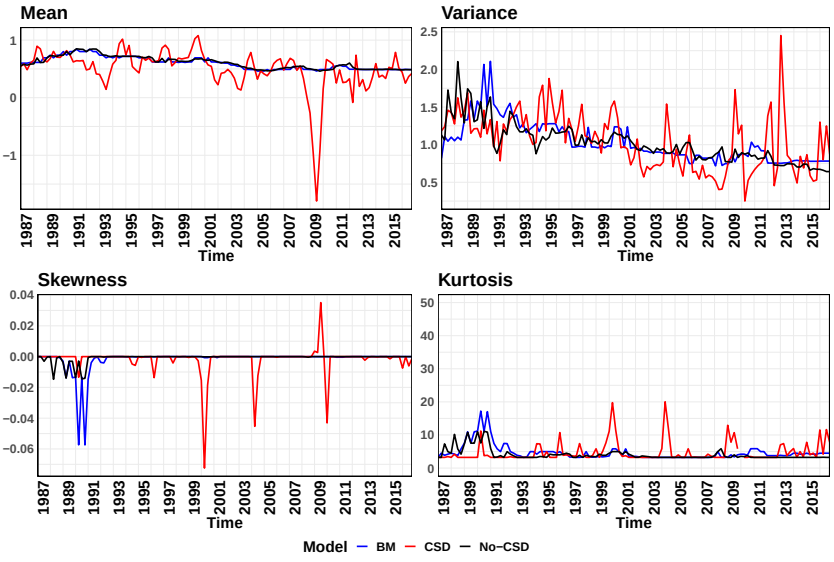

(b) Moments of DEU GDP

Notes: See Figure 4.5.

Figure C.7: (cont'd) Moments Conditional on NFCI; Prediction Horizon – 12 Quarter–Ahead

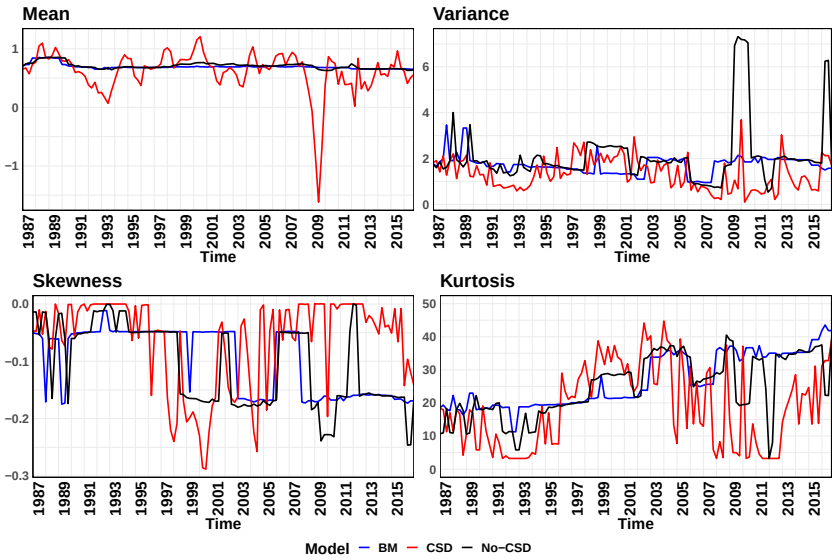

(c) Moments of GBR GDP

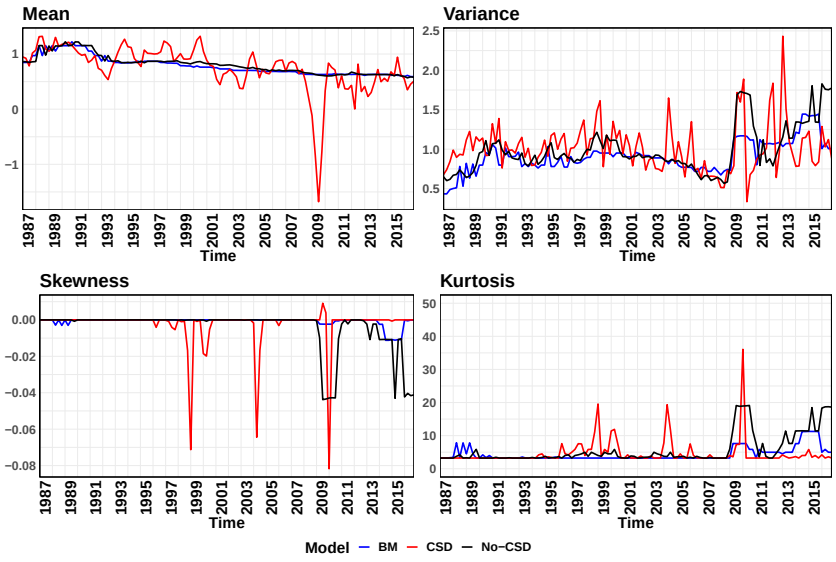

(d) Moments of JPN GDP

Notes: See Figure 4.5.

Figure C.7: (cont'd) Moments Conditional on NFCI; Prediction Horizon – 12 Quarter–Ahead

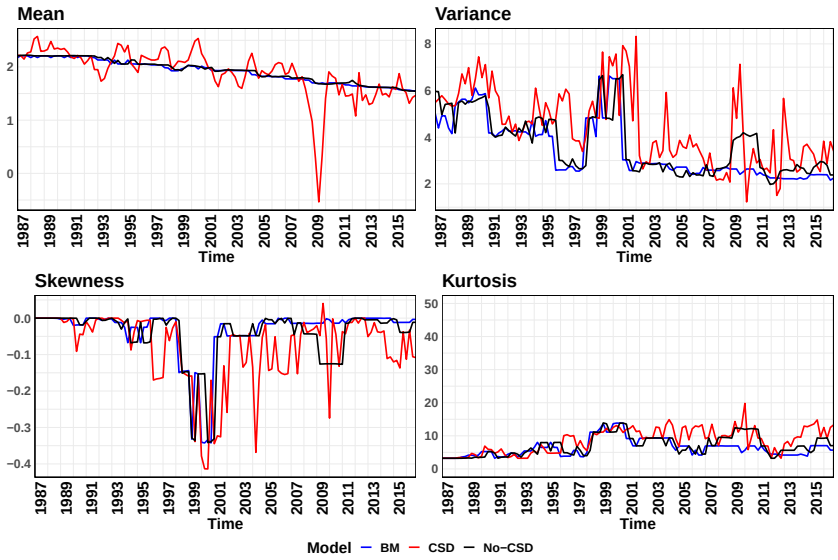

(e) Moments of KOR GDP; Conditional on NFCI

Notes: See Figure 4.5.

C.6 Forecast Decomposition – Different Horizons

Figure C.8: Decomposition of Predicted GaR(5%) – Predictor: NFCI

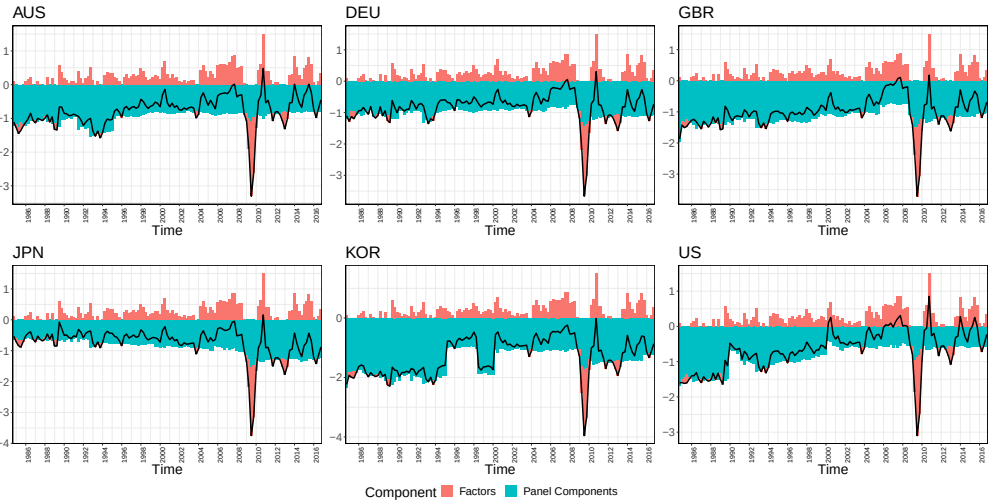

(a) 4 Quarter Horizon

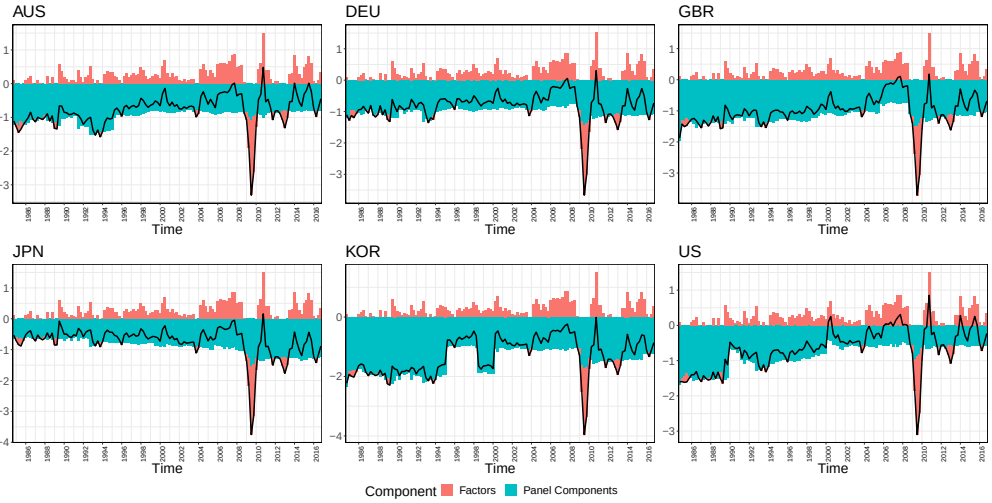

(b) 8 Quarter Horizon

Notes: See Figure 4.7.

Appendix D

Appendix to Chapter 5

This appendix consists of additional empirical results in support of the findings of Chapter 5 and is organised as follows: the full information results are corroborated in Section D.1 with additional results on the constant-only benchmark model, a model that omits the cross-sectional averages and a model augmented with a dummy for the GFC. The pseudo-real-time results are substantiated and contrasted in Section D.2 with the constant-only benchmark model and other alternatives as in Section D.1.

D.1 Additional results – Full Information

D.1.1 Constant-only BM

AUROC

Figure D.1: 95% CI for AUROC for Constant-only BM; Full Information

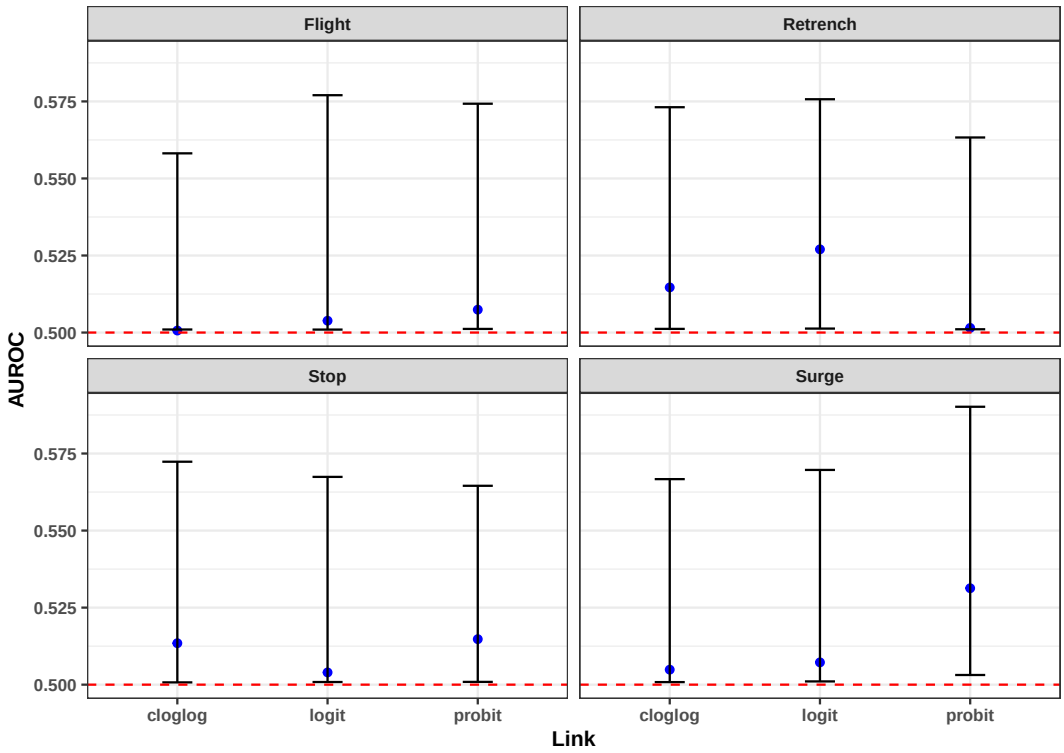

Notes: The figure presents the AUROC and the confidence intervals for a constant-only benchmark model which is equivalent to historical averages of the latent variable. See Figure 5.7 for more details.

BS

Table D.1: BS for Full-Information

Episodes	**cloglog**	**probit**	**logit**
Surge	0.3301	0.2436	0.2460
Stop	0.3397	0.2425	0.2450
Retrench	0.3388	0.2400	0.2466
Flight	0.3283	0.2417	0.2449

Notes: Same as Table 5.6

KS

Table D.2: KS for Full-Information

		Thresholds				
Episodes	**Link**	**5%**	**25%**	**50%**	**75%**	**95%**
Surge	cloglog	0.0155	-0.0016	-0.0095	-0.0016	-0.0027
Stop	cloglog	-0.0138	-0.0071	-0.0143	-0.0143	-0.0041
Retrench	cloglog	0.0005	-0.0071	-0.0463	-0.0178	-0.0076
Flight	cloglog	0.0180	0.0169	-0.0153	-0.0077	-0.0119
Surge	probit	-0.0227	-0.0271	-0.0350	-0.0334	-0.0155
Stop	probit	-0.0280	-0.0214	0.0000	-0.0143	-0.0183
Retrench	probit	0.0326	0.0107	-0.0143	-0.0107	-0.0112
Flight	probit	-0.0004	-0.0199	-0.0215	0.0261	0.0188
Surge	logit	-0.0164	-0.0302	0.0255	-0.0048	0.0036
Stop	logit	-0.0066	-0.0178	-0.0285	0.0392	0.0066
Retrench	logit	-0.0102	-0.0036	-0.0250	-0.0392	-0.0112
Flight	logit	0.0027	-0.0199	0.0153	-0.0015	0.0035

Notes: Same as Table 5.7

D.1.2 Excluding Cross-Sectional Averages

Figure D.2: 95% CI for AUROC – Excluding Cross-Sectional Averages; Full Information

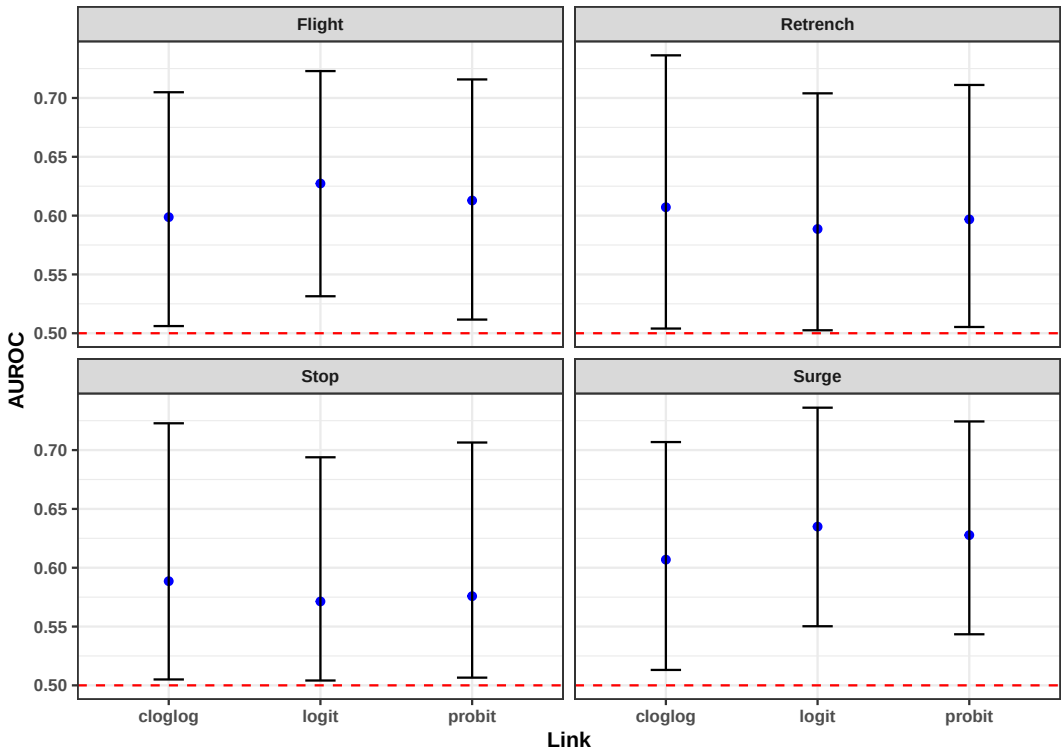

Notes: The figure presents the AUROC and the confidence intervals without modelling the cross-sectional averages. See Figure 5.7 for more details.

D.1.3 Including Dummy for the GFC

Figure D.3: 95% CI for AUROC – Including Dummy for the GFC; Full Information

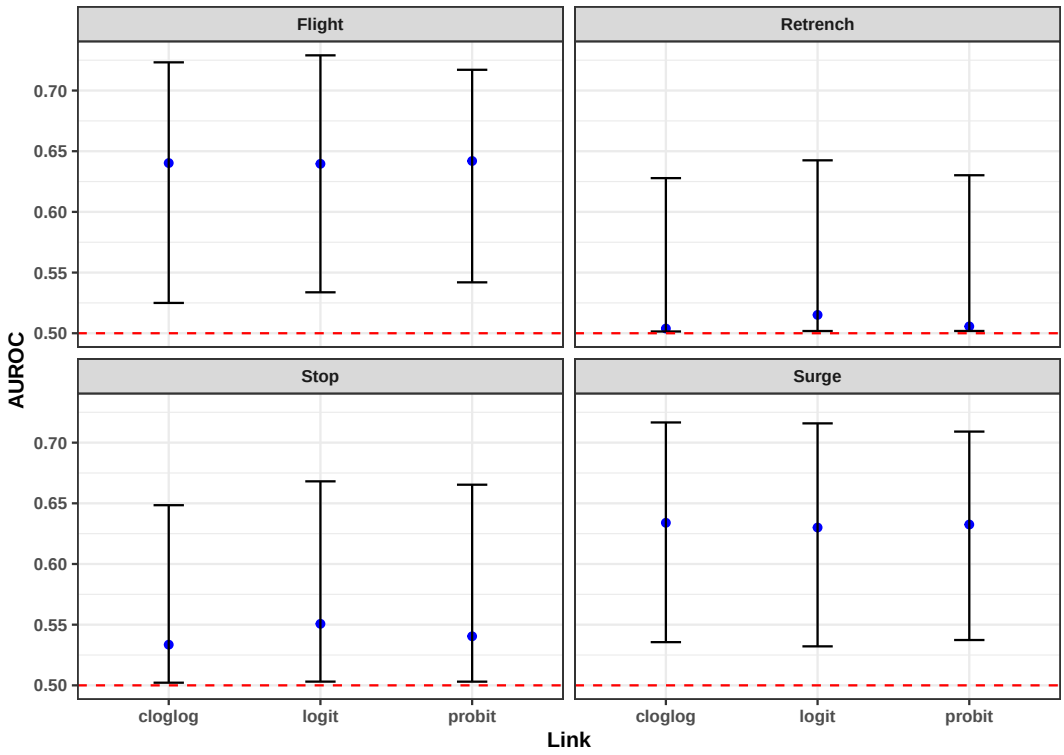

Notes: The figure presents the AUROC and the confidence intervals when we include dummies for the GFC, i.e. observations during and after 2009. See Figure 5.7 for more details.

D.2 Additional Results – Pseudo-Real-Time

D.2.1 Constant-only BM

AUROC

Figure D.4: 95% CI for AUROC – Constant-only BM; Pseudo-Real-Time

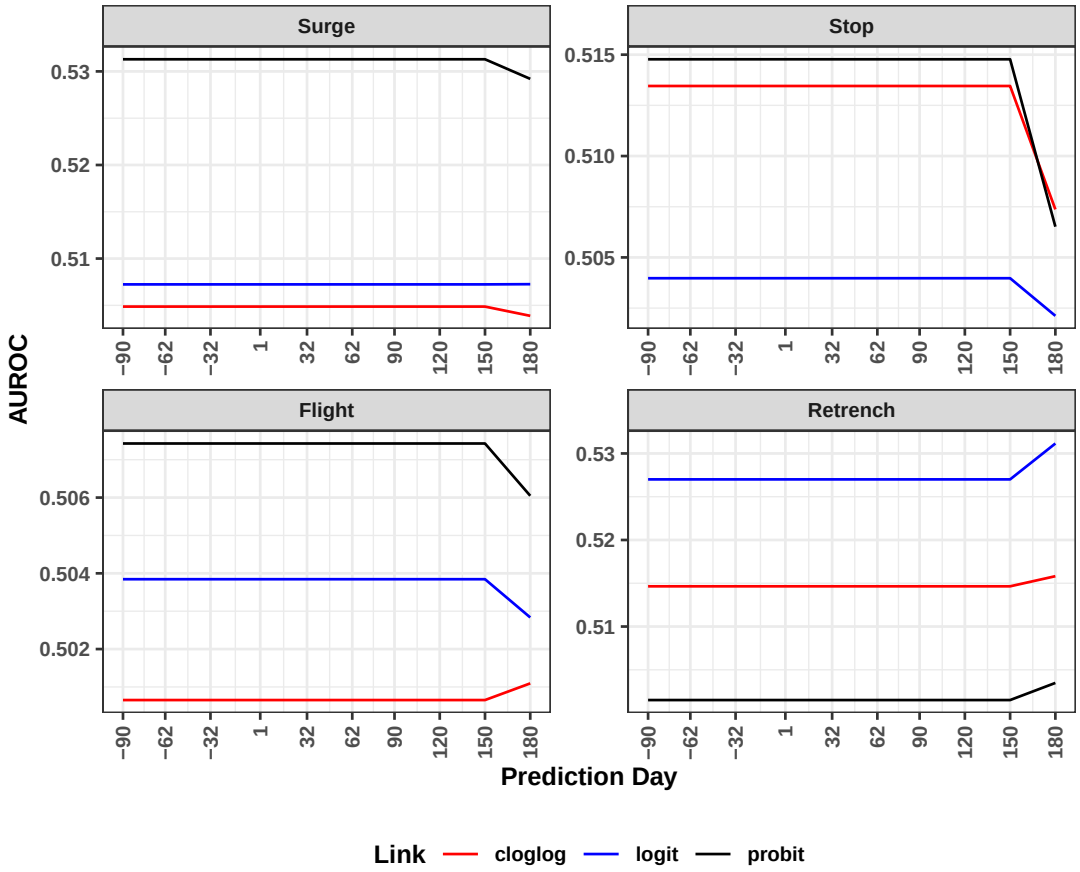

Notes: The figure presents the AUROC for the constant-only benchmark model which is equivalent to the averages of the latent variable. See Figure 5.10 for more details.

BS

Table D.3: BS for Pseudo-Real-Time

Prediction Day	Surge	Stop	Retrench	Flight
		cloglog		
1	0.3305	0.3388	0.3385	0.3289
2	0.3305	0.3388	0.3385	0.3289
3	0.3305	0.3388	0.3385	0.3289
4	0.3305	0.3388	0.3385	0.3289
5	0.3305	0.3388	0.3385	0.3289
6	0.3305	0.3388	0.3385	0.3289
7	0.3305	0.3388	0.3385	0.3289
8	0.3305	0.3388	0.3385	0.3289
9	0.3305	0.3388	0.3385	0.3289
10	0.3185	0.3267	0.3255	0.3166
		probit		
1	0.2434	0.2422	0.2399	0.2417
2	0.2434	0.2422	0.2399	0.2417
3	0.2434	0.2422	0.2399	0.2417
4	0.2434	0.2422	0.2399	0.2417
5	0.2434	0.2422	0.2399	0.2417
6	0.2434	0.2422	0.2399	0.2417
7	0.2434	0.2422	0.2399	0.2417
8	0.2434	0.2422	0.2399	0.2417
9	0.2434	0.2422	0.2399	0.2417
10	0.2340	0.2334	0.2313	0.2332
		logit		
1	0.2455	0.2448	0.2464	0.2457
2	0.2455	0.2448	0.2464	0.2457
3	0.2455	0.2448	0.2464	0.2457
4	0.2455	0.2448	0.2464	0.2457
5	0.2455	0.2448	0.2464	0.2457
6	0.2455	0.2448	0.2464	0.2457
7	0.2455	0.2448	0.2464	0.2457
8	0.2455	0.2448	0.2464	0.2457
9	0.2455	0.2448	0.2464	0.2457
10	0.2362	0.2364	0.2381	0.2376

KS

Table D.3: KS for Pseudo-Real-Time

(a) KS for Surges

Prediction Day	**5%**	**25%**	**50%**	**75%**	**95%**
		cloglog			
1	0.0134	-0.0005	-0.0083	-0.0094	-0.0002
2	0.0134	-0.0005	-0.0083	-0.0094	-0.0002
3	0.0134	-0.0005	-0.0083	-0.0094	-0.0002
4	0.0134	-0.0005	-0.0083	-0.0094	-0.0002
5	0.0134	-0.0005	-0.0083	-0.0094	-0.0002
6	0.0134	-0.0005	-0.0083	-0.0094	-0.0002
7	0.0134	-0.0005	-0.0083	-0.0094	-0.0002
8	0.0134	-0.0005	-0.0083	-0.0094	-0.0002
9	0.0134	-0.0005	-0.0083	-0.0094	-0.0002
10	0.0464	0.0424	0.0347	0.0203	0.0262
		probit			
1	-0.0163	-0.0302	-0.0314	-0.0358	-0.0200
2	-0.0163	-0.0302	-0.0314	-0.0358	-0.0200
3	-0.0163	-0.0302	-0.0314	-0.0358	-0.0200
4	-0.0163	-0.0302	-0.0314	-0.0358	-0.0200
5	-0.0163	-0.0302	-0.0314	-0.0358	-0.0200
6	-0.0163	-0.0302	-0.0314	-0.0358	-0.0200
7	-0.0163	-0.0302	-0.0314	-0.0358	-0.0200
8	-0.0163	-0.0302	-0.0314	-0.0358	-0.0200
9	-0.0163	-0.0302	-0.0314	-0.0358	-0.0200
10	0.0266	0.0160	-0.0050	0.0038	0.0130
		logit			
1	-0.0163	-0.0236	0.0413	0.0005	0.0031
2	-0.0163	-0.0236	0.0413	0.0005	0.0031
3	-0.0163	-0.0236	0.0413	0.0005	0.0031
4	-0.0163	-0.0236	0.0413	0.0005	0.0031
5	-0.0163	-0.0236	0.0413	0.0005	0.0031
6	-0.0163	-0.0236	0.0413	0.0005	0.0031
7	-0.0163	-0.0236	0.0413	0.0005	0.0031
8	-0.0163	-0.0236	0.0413	0.0005	0.0031
9	-0.0163	-0.0236	0.0413	0.0005	0.0031
10	0.0332	0.0028	0.0743	0.0335	0.0328

Notes: Same as Table 5.12

Table D.3: KS for Pseudo-Real-Time

(b) KS for Stops

Prediction Day	**5%**	**25%**	**50%**	**75%**	**95%**
		cloglog			
1	-0.0158	0.0040	-0.0073	-0.0003	-0.0025
2	-0.0158	0.0040	-0.0073	-0.0003	-0.0025
3	-0.0158	0.0040	-0.0073	-0.0003	-0.0025
4	-0.0158	0.0040	-0.0073	-0.0003	-0.0025
5	-0.0158	0.0040	-0.0073	-0.0003	-0.0025
6	-0.0158	0.0040	-0.0073	-0.0003	-0.0025
7	-0.0158	0.0040	-0.0073	-0.0003	-0.0025
8	-0.0158	0.0040	-0.0073	-0.0003	-0.0025
9	-0.0158	0.0040	-0.0073	-0.0003	-0.0025
10	0.0244	0.0332	0.0329	0.0435	0.0450
		probit			
1	-0.0194	-0.0253	0.0110	-0.0003	-0.0171
2	-0.0194	-0.0253	0.0110	-0.0003	-0.0171
3	-0.0194	-0.0253	0.0110	-0.0003	-0.0171
4	-0.0194	-0.0253	0.0110	-0.0003	-0.0171
5	-0.0194	-0.0253	0.0110	-0.0003	-0.0171
6	-0.0194	-0.0253	0.0110	-0.0003	-0.0171
7	-0.0194	-0.0253	0.0110	-0.0003	-0.0171
8	-0.0194	-0.0253	0.0110	-0.0003	-0.0171
9	-0.0194	-0.0253	0.0110	-0.0003	-0.0171
10	0.0244	0.0076	0.0621	0.0399	0.0158
		logit			
1	-0.0084	-0.0106	-0.0292	0.0362	0.0084
2	-0.0084	-0.0106	-0.0292	0.0362	0.0084
3	-0.0084	-0.0106	-0.0292	0.0362	0.0084
4	-0.0084	-0.0106	-0.0292	0.0362	0.0084
5	-0.0084	-0.0106	-0.0292	0.0362	0.0084
6	-0.0084	-0.0106	-0.0292	0.0362	0.0084
7	-0.0084	-0.0106	-0.0292	0.0362	0.0084
8	-0.0084	-0.0106	-0.0292	0.0362	0.0084
9	-0.0084	-0.0106	-0.0292	0.0362	0.0084
10	0.0464	0.0259	0.0146	0.0764	0.0450

Notes: Same as Table 5.12

Table D.3: KS for Pseudo-Real-Time

(c) KS for Retrenchments

Prediction Day	**5%**	**25%**	**50%**	**75%**	**95%**
		cloglog			
1	0.0027	-0.0061	-0.0456	-0.0158	-0.0100
2	0.0027	-0.0061	-0.0456	-0.0158	-0.0100
3	0.0027	-0.0061	-0.0456	-0.0158	-0.0100
4	0.0027	-0.0061	-0.0456	-0.0158	-0.0100
5	0.0027	-0.0061	-0.0456	-0.0158	-0.0100
6	0.0027	-0.0061	-0.0456	-0.0158	-0.0100
7	0.0027	-0.0061	-0.0456	-0.0158	-0.0100
8	0.0027	-0.0061	-0.0456	-0.0158	-0.0100
9	0.0027	-0.0061	-0.0456	-0.0158	-0.0100
10	0.0501	0.0267	-0.0164	0.0024	0.0155
		probit			
1	0.0282	0.0085	-0.0164	0.0061	-0.0100
2	0.0282	0.0085	-0.0164	0.0061	-0.0100
3	0.0282	0.0085	-0.0164	0.0061	-0.0100
4	0.0282	0.0085	-0.0164	0.0061	-0.0100
5	0.0282	0.0085	-0.0164	0.0061	-0.0100
6	0.0282	0.0085	-0.0164	0.0061	-0.0100
7	0.0282	0.0085	-0.0164	0.0061	-0.0100
8	0.0282	0.0085	-0.0164	0.0061	-0.0100
9	0.0282	0.0085	-0.0164	0.0061	-0.0100
10	0.0574	0.0523	0.0128	0.0389	0.0228
		logit			
1	-0.0046	-0.0024	-0.0237	-0.0304	-0.0100
2	-0.0046	-0.0024	-0.0237	-0.0304	-0.0100
3	-0.0046	-0.0024	-0.0237	-0.0304	-0.0100
4	-0.0046	-0.0024	-0.0237	-0.0304	-0.0100
5	-0.0046	-0.0024	-0.0237	-0.0304	-0.0100
6	-0.0046	-0.0024	-0.0237	-0.0304	-0.0100
7	-0.0046	-0.0024	-0.0237	-0.0304	-0.0100
8	-0.0046	-0.0024	-0.0237	-0.0304	-0.0100
9	-0.0046	-0.0024	-0.0237	-0.0304	-0.0100
10	0.0428	0.0195	-0.0018	-0.0049	0.0155

Notes: Same as Table 5.12

Table D.3: KS for Pseudo-Real-Time

(d) KS for Flights

Prediction Day	**5%**	**25%**	**50%**	**75%**	**95%**
		cloglog			
1	0.0222	0.0171	-0.0112	-0.0139	-0.0126
2	0.0222	0.0171	-0.0112	-0.0139	-0.0126
3	0.0222	0.0171	-0.0112	-0.0139	-0.0126
4	0.0222	0.0171	-0.0112	-0.0139	-0.0126
5	0.0222	0.0171	-0.0112	-0.0139	-0.0126
6	0.0222	0.0171	-0.0112	-0.0139	-0.0126
7	0.0222	0.0171	-0.0112	-0.0139	-0.0126
8	0.0222	0.0171	-0.0112	-0.0139	-0.0126
9	0.0222	0.0171	-0.0112	-0.0139	-0.0126
10	0.0509	0.0585	0.0399	0.0244	0.0225
		probit			
1	-0.0033	-0.0244	-0.0143	0.0276	0.0161
2	-0.0033	-0.0244	-0.0143	0.0276	0.0161
3	-0.0033	-0.0244	-0.0143	0.0276	0.0161
4	-0.0033	-0.0244	-0.0143	0.0276	0.0161
5	-0.0033	-0.0244	-0.0143	0.0276	0.0161
6	-0.0033	-0.0244	-0.0143	0.0276	0.0161
7	-0.0033	-0.0244	-0.0143	0.0276	0.0161
8	-0.0033	-0.0244	-0.0143	0.0276	0.0161
9	-0.0033	-0.0244	-0.0143	0.0276	0.0161
10	0.0317	0.0011	0.0207	0.0626	0.0512
		logit			
1	0.0030	-0.0212	0.0016	-0.0107	0.0001
2	0.0030	-0.0212	0.0016	-0.0107	0.0001
3	0.0030	-0.0212	0.0016	-0.0107	0.0001
4	0.0030	-0.0212	0.0016	-0.0107	0.0001
5	0.0030	-0.0212	0.0016	-0.0107	0.0001
6	0.0030	-0.0212	0.0016	-0.0107	0.0001
7	0.0030	-0.0212	0.0016	-0.0107	0.0001
8	0.0030	-0.0212	0.0016	-0.0107	0.0001
9	0.0030	-0.0212	0.0016	-0.0107	0.0001
10	0.0509	0.0075	0.0367	0.0308	0.0384

Notes: Same as Table 5.12

D.2.2 Dummy for GFC

Figure D.5: AUROC – GFC Dummies; Pseudo-Real-Time

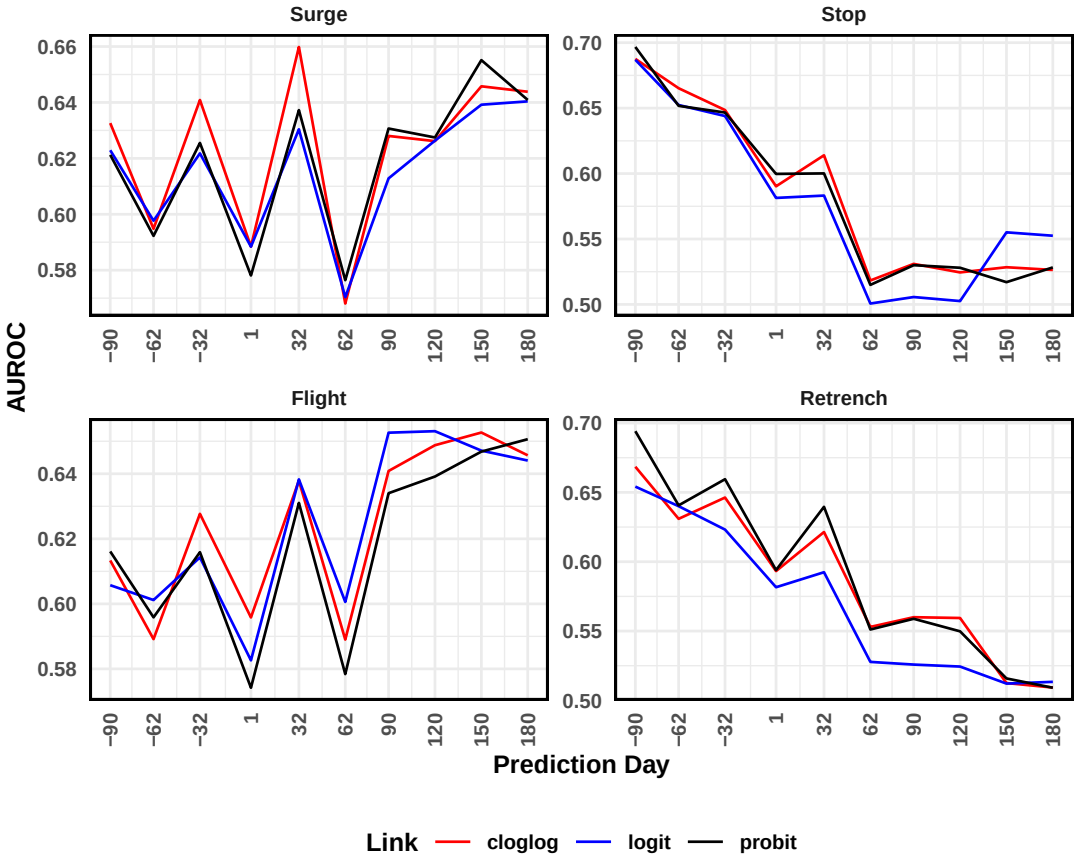

Notes: The figure presents the AUROC for the model including an additional dummy variable for the GFC. See Figure 5.10 for more details.

D.2.3 Excluding Cross-sectional Averages

Figure D.6: AUROC – Excluding Cross-sectional Averages – Pseudo-Real-Time

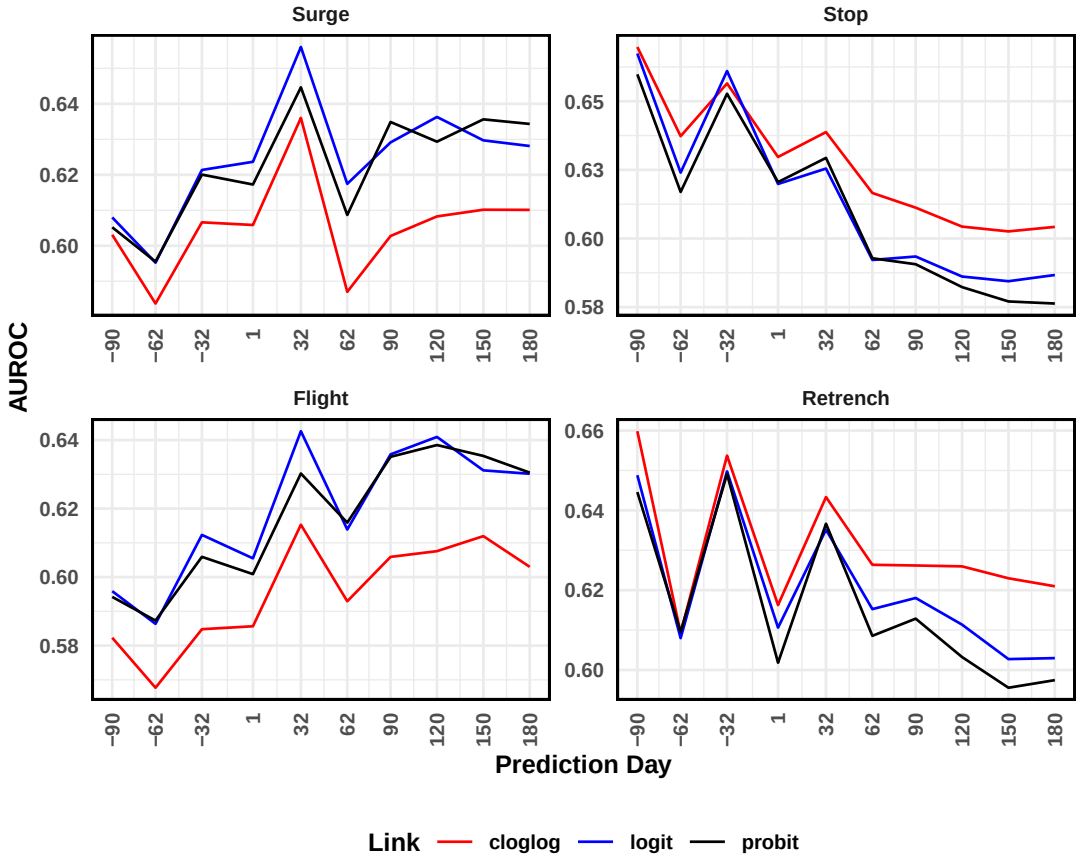

Notes: The figure presents the AUROC for the model excluding cross-sectional averages. See Figure 5.10 for more details.

Bibliography

Aastveit, K. A., Gerdrup, K. R., Jore, A. S. and Thorsrud, L. A. (2014). 'Nowcasting GDP in real time: A density combination approach'. *Journal of Business and Economic Statistics* 32 (1), pp. 48–68.

Adams, P. A., Adrian, T., Boyarchenko, N. and Giannone, D. (2021). 'Forecasting macroeconomic risks'. *International Journal of Forecasting* 37 (3), pp. 1173–1191.

Adrian, T., Boyarchenko, N. and Giannone, D. (2019a). 'Vulnerable growth'. *American Economic Review* 109 (4), pp. 1263–1289.

Adrian, T., Estrella, A. and Shin, H. S. (2019b). 'Risk-taking channel of monetary policy'. *Financial Management* 48 (3), pp. 725–738.

Adrian, T., Grinberg, F., Liang, N. and Malik, S. (2018). *The term structure of growth-at-risk*. Working Papers 18/180. International Monetary Fund. URL: https://www.imf.org/en/Publications/WP/Issues/2018/08/02/The-Term-Structure-of-Growth-at-Risk-46150 [Last accessed: 10/08/2020].

Adrian, T., Grinberg, F., Liang, N., Malik, S. and Yu, J. (2022). 'The Term Structure of Growth-at-Risk'. *American Economic Journal: Macroeconomics* 14 (3), pp. 283–323.

Ahir, H., Bloom, N. and Furceri, D. (2018). *The World Uncertainty Index*. Mimeo. URL: http://www.policyuncertainty.com/media/http://www.policyuncertainty.com/media/EPU_BBD_Mar2016.pdf [Last accessed: 18/12/2021].

Ahmed, R. (2023). 'Flights-to-safety and macroeconomic adjustment in emerging markets: The role of U.S. monetary policy'. *Journal of International Money and Finance* 133 (102827), pp. 1–31.

Aikman, D., Bridges, J., Hoke, S. H., Neill, C. O. and Raja, A. (2019). *Credit, capital and crises: a GDP-at-risk approach*. Staff Working Paper 284. Bank of England. URL: https://www.bankofengland.co.uk/working-paper/2019/credit-capital-and-crises-a-gdp-at-risk-approach [Last accessed: 04/07/2023].

Alter, A. and Mahoney, E. M. (2020). *Household debt and house Prices-at-risk: A tale of two countries*. Working Papers 20/42. International Monetary Fund. URL: https://www.imf.org/en/Publications/WP/Issues/2020/02/28/Household-Debt-and-House-Prices-at-risk-A-Tale-of-Two-Countries-49054 [Last accessed: 04/07/2023].

Ando, T. and Bai, J. (2020). 'Quantile Co-Movement in Financial Markets: A Panel Quantile Model With Unobserved Heterogeneity'. *Journal of the American Statistical Association* 115 (529), pp. 266–279.

Andrews, D. W. K. and Ploberger, W. (1994). 'Optimal Tests when a Nuisance Parameter is Present Only Under the Alternative'. *Econometrica* 62 (6), pp. 1383–1414.

Anesti, N., Galvao Galvão, A. B. and Miranda-Agrippino, S. (2022). 'Uncertain Kingdom: nowcasting GDP and its revisions'. *Journal of Applied Econometrics* 37 (1), pp. 42–62.

Arregui, N., Elekdag, S., Gelos, R., Lafarguette, R. and Seneviratne, D. (2018). *Can countries manage their financial conditions amid globalization?* Working Papers 18/15. URL: https://www.imf.org/en/Publications/WP/Issues/2018/01/24/Can-Countries-Manage-Their-Financial-Conditions-Amid-Globalization-45581 [Last accessed: 04/07/2023].

Audrino, F., Kostrov, A. and Ortega, J. P. (2019). 'Predicting U.S. bank failures with MIDAS logit models'. *Journal of Financial and Quantitative Analysis* 54 (6), pp. 2575–2603.

Azzalini, A. and Capitanio, A. (2003). 'Distributions generated by perturbation of symmetry with emphasis on a multivariate skew t-distribution'. *Journal of the Royal Statistical Society: Series B (Statistical Methodology)* 65 (2), pp. 367–389.

Babii, A., Ball, R. T., Ghysels, E. and Striaukas, J. (2020). *Machine learning panel data regressions with an application to nowcasting price earnings ratios*. Working Paper. URL: https://arxiv.org/abs/2005.14057 [Last accessed: 08/12/2020].

Baffigi, A., Golinelli, R. and Parigi, G. (2004). 'Bridge models to forecast the Euro Area GDP'. *International Journal of Forecasting* 20 (3), pp. 447–460.

Bai, J. (2009). 'Panel data models with interactive fixed effects'. *Econometrica* 77 (4), pp. 1229–1279.

Bai, J. and Ng, S. (2002). 'Determining the number of factors in approximate factor models'. *Econometrica* 70 (1), pp. 191–221.

Baker, S. R., Bloom, N. and Davis, S. J. (2016). 'Measuring economic policy uncertainty'. *The Quarterly Journal of Economics* 131 (4), pp. 1593–1636.

Baltagi, B. H. (2008). 'Forecasting with panel data'. *Journal of Forecasting* 27 (2), pp. 153–173.

Bańbura, M., Giannone, D., Modugno, M. and Reichlin, L. (2013). *Now-casting and the real-time data flow*. Working Paper Series 1564. European Central Bank. URL: https://www.ecb.europa.eu/pub/pdf/scpwps/ecbwp1564.pdf [Last accessed: 13/05/2021].

Bańbura, M., Giannone, D. and Reichlin, L. (2012). 'Nowcasting'. In: *The Oxford Handbook of Economic Forecasting*, pp. 1–61.

Bennedsen, M., Hillebrand, E. and Koopman, S. J. (2021). 'Modeling, forecasting, and nowcasting US CO2 emissions using many macroeconomic predictors'. *Energy Economics* 96 (105118), pp. 1–17.

Berge, T. J. and Jordà, Ò. (2011). 'Evaluating the classification of economic activity into recessions and expansions'. *Journal: Macroeconomics* 3 (2), pp. 246–277.

BIS (2010). *Guidance for national authorities operating the countercyclical capital buffer*. Basel Commitee of Banking Supervision. URL: https://www.bis.org/publ/bcbs187.htm [Last accessed: 04/07/2023].

— (2021). *Changing patterns of capital flows*. Report prepared by a Working Group co-chaired byGerardo García López (Bank of Mexico) and Livio Stracca(European

Central Bank), pp. 1–90. URL: https://www.bis.org/publ/qtrpdf/r_qt2212g.htm [Last accessed: 18/07/2023].

Bloom, N. (2014). 'Fluctuations in uncertainty'. *Journal of Economic Perspectives* 28 (2), pp. 153–176.

Bok, B., Caratelli, D., Giannone, D., Sbordone, A. M. and Tambalotti, A. (2018). 'Macroeconomic nowcasting and forecasting with big data'. *Annual Review of Economics* 10 (1), pp. 615–643.

Bouallègue, Z. B., Haiden, T. and Richardson, D. S. (2018). 'The diagonal score: Definition, properties, and interpretations'. *Quarterly Journal of the Royal Meteorological Society* 144 (714) (714), pp. 1463–1473.

Bragoli, D. and Fosten, J. (2018). 'Nowcasting Indian GDP'. *Oxford Bulletin of Economics and Statistics* 80 (2), pp. 259–282.

Breitung, J. (2015). 'The analysis of macroeconomic panel data'. In: *The Oxford Handbook of Panel Data*. Oxford University Press, pp. 453–492.

Brier, G. W. (1950). 'Verification of Forecasts Expressed in Terms of Probability'. *Monthly weather review* 78 (1), pp. 1–3.

Broner, F., Didier, T., Erce, A. and Schmukler, S. L. (2013). 'Gross capital flows: Dynamics and crises'. *Journal of Monetary Economics* 60 (1), pp. 113–133.

Brownlees, C. and Souza, A. B. (2021). 'Backtesting global growth-at-risk'. *Journal of Monetary Economics* 118, pp. 312–330.

Ca' Zorzi, M., Dedola, L., Jarociński, M., Stracca, L. and Strasser, G. (2020). *Monetary policy and its transmission in a globalised world*. Working Paper Series 2407. Frankfurt am Main: European Central Bank. URL: https://www.ecb.europa.eu/pub/pdf/scpwps/ecb.wp2407~586c50e03f.en.pdf [Last accessed: 03/07/2023].

Canay, I. A. (2011). 'A simple approach to quantile regression for panel data'. *The Econometrics Journal* 14 (3), pp. 368–386.

Canova, F. and Ciccarelli, M. (2004). 'Forecasting and turning point predictions in a Bayesian panel VAR model'. *Journal of Econometrics* 120 (2), pp. 327–359.

Carriero, A., Clark, T. E. and Marcellino, M. (2020). *Nowcasting tail risks to economic activity with Many indicators*. Working Paper 20-13R2. Federal Reserve Bank of Cleveland. URL: https://www.clevelandfed.org/publications/working-paper/wp-2013r2-capturing-macroeconomic-tail-risks-with-bayesian-vector-autoregressions [Last accessed: 16/04/2022].

Cascaldi-Garcia, D., Ferreira, T. R., Giannone, D. and Modugno, M. (2023). 'Back to the present: Learning about the euro area through a now-casting model'. *International Journal of Forecasting*. In Press, Corrected Proof. URL: https://doi.org/10.1016/j.ijforecast.2023.04.005 [Last accessed: 11/08/2023].

Caselli, F., Grigoli, F., Lafarguette, R. and Wang, C. (2020). *Predictive density aggregation: A model for global GDP growth*. Working Paper 20/78. International Monetary Fund. URL: https://www.imf.org/en/Publications/WP/Issues/2020/05/29/Predictive-Density-Aggregation-A-Model-for-Global-GDP-Growth-49441 [Last accessed: 04/07/2023].

Castelnuovo, E. and Mori, L. (2022). *Uncertainty, skewness, and the business cycle through the MIDAS lens*. Working Paper 10062. CESifo Group Munich. URL: https://papers.ssrn.com/sol3/papers.cfm?abstract_id=4273436 [Last accessed: 03/07/2023].

Cepni, O., Güney, I. E. and Swanson, N. R. (2019). 'Nowcasting and forecasting GDP in emerging markets using global financial and macroeconomic diffusion indexes'. *International Journal of Forecasting* 35 (2), pp. 555–572.

Chen, S. and Ranciere, R. (2019). 'Financial information and macroeconomic forecasts'. *International Journal of Forecasting* 35 (3), pp. 1160–1174.

Chernozhukov, V., Fernández-Val, I. and Weidner, M. (2020). 'Network and panel quantile effects via distribution regression'. *Journal of Econometrics*. In Press, Corrected Proof. URL: https://doi.org/10.1016/j.jeconom.2020.08.009 [Last accessed: 04/07/2023].

Choi, I. (2001). 'Unit root tests for panel data'. *Journal of International Money and Finance* 20 (2), pp. 249–272.

Chudik, A., Grossman, V. and Pesaran, H. M. (2016). 'A multi-country approach to forecasting output growth using PMIs'. *Journal of Econometrics* 192 (2), pp. 349–365.

Chudik, A., Mohaddes, K., Pesaran, H. M. and Raissi, M. (2017). 'Is there a debt-threshold effect on output growth?' *The Review of Economics and Statistics* 99 (1), pp. 135–150.

Chudik, A. and Pesaran, H. M. (2015a). 'Common correlated effects estimation of heterogeneous dynamic panel data models with weakly exogenous regressors'. *Journal of Econometrics* 188 (2), pp. 393–420.

— (2015b). 'Large panel data models with cross-sectional dependence'. In: *The Oxford Handbook of Panel Data*. Oxford University Press, pp. 3–45.

Claessens, S., Kose, M. A. and Terrones, M. E. (2012). 'How do business and financial cycles interact?' *Journal of International Economics* 87 (1), pp. 178–190.

Clements, M. P. and Galvão, A. B. (2008). 'Macroeconomic forecasting with mixed-frequency data: Forecasting output growth in the United States'. *Journal of Business and Economic Statistics* 26 (4), pp. 546–554.

— (2009). 'Forecasting US output growth using leading indicators: An appraisal using MIDAS models'. *Journal of Applied Econometrics* 24 (7), pp. 1187–1206.

Clements, M. P., Galvão, A. B. and Kim, J. H. (2008). 'Quantile forecasts of daily exchange rate returns from forecasts of realized volatility'. *Journal of Empirical Finance* 15 (4), pp. 729–750.

Creal, D., Schwaab, B., Koopman, S. J. and Lucas, A. (2014). 'Observation-driven mixed-measurement dynamic factor models with an application to credit risk'. *Review of Economics and Statistics* 96 (5), pp. 898–915.

Crescenzio, A. de and Lepers, E. (2021). *Extreme capital flow episodes from the global financial crisis to COVID-19*. Working Papers on International Investment 2021/05. OECD. URL: https://www.oecd-ilibrary.org/finance-and-investment/extreme-capital-flow-episodes-from-the-global-financial-crisis-

to-covid-19_d557b9c4-en?crawler=true&mimetype=application/pdf [Last accessed: 04/07/2023].

Dahlhaus, T., Guénette, J.-D. and Vasishtha, G. (2017). 'Nowcasting BRIC+M in real time'. *International Journal of Forecasting* 33 (4), pp. 915–935.

Davies, R. B. (1977). 'Hypothesis Testing When a Nuisance Parameter is Present Only Under the Alternative'. *Biometrika* 64 (2), pp. 247–254.

Davies, R. B. (1987). 'Hypothesis Testing when a Nuisance Parameter is Present Only Under the Alternatives'. *Biometrika* 74 (1), p. 33.

Delle-Monache, D., De-Polis, A. and Petrella, I. (2020). *Modelling and forecasting macroeconomic downside risk*. Discussion Paper DP15109. CEPR. URL: https://cepr.org/publications/dp15109 [Last accessed: 04/07/2023].

Drehmann, M., Borio, C. and Tsatsaronis, K. (2011). 'Anchoring countercyclical capital buffers: The role of credit aggregates'. *International Journal of Central Banking* 7 (4), pp. 189–240.

Drehmann, M. and Juselius, M. (2014). 'Evaluating early warning indicators of banking crises: Satisfying policy requirements'. *International Journal of Forecasting* 30 (3), pp. 759–780.

Eguren-Martin, F. and Sokol, A. (2022). 'Attention to the Tail(s): Global Financial Conditions and Exchange Rate Risks'. *IMF Economic Review* 70 (3), pp. 487–519.

Eickmeier, S. and Ng, T. (2011). 'Forecasting national activity using lots of international predictors: An application to New Zealand'. *International Journal of Forecasting* 27 (2), pp. 496–511.

Engle, R. F. and Manganelli, S. (2004). 'CAViaR'. *Journal of Business and Economic Statistics* 22 (4), pp. 367–381.

Ferrara, L. and Marsilli, C. (2019). 'Nowcasting global economic growth: A factor-augmented mixed-frequency approach'. *World Economy* 42 (3), pp. 846–875.

Ferrara, L., Mogliani, M. and Sahuc, J.-G. (2022). 'High-frequency monitoring of growth at risk'. *International Journal of Forecasting* 38 (2), pp. 582–595.

Forbes, K. J. and Warnock, F. E. (2012). 'Capital flow waves: Surges, stops, flight, and retrenchment'. *Journal of International Economics* 88 (2), pp. 235–251.

— (2021). 'Capital flow waves – or ripples? Extreme capital flow movements since the crisis'. *Journal of International Money and Finance* 116 (102394), pp. 1–24.

Foroni, C. and Marcellino, M. (2014). 'A comparison of mixed frequency approaches for nowcasting Euro area macroeconomic aggregates'. *International Journal of Forecasting* 30 (3), pp. 554–568.

Foroni, C., Marcellino, M. and Schumacher, C. (2015). 'Unrestricted mixed data sampling (MIDAS): MIDAS regressions with unrestricted lag polynomials'. *Journal of the Royal Statistical Society. Series A: (Statistics in Society)* 178 (1), pp. 57–82.

Fosten, J. and Greenaway-McGrevy, R. (2022). 'Panel data nowcasting'. *Econometric Reviews* 41 (7), pp. 675–696.

Fosten, J. and Gutknecht, D. (2018). 'Testing nowcast monotonicity with estimated factors'. *Journal of Business and Economic Statistics* 38 (1), pp. 107–123.

Friedrich, C. and Guérin, P. (2020). 'The dynamics of capital flow episodes'. *Journal of Money, Credit and Banking* 52 (5), pp. 969–1003.

Galvao, A. F. and Wang, L. (2015). 'Efficient minimum distance estimator for quantile regression fixed effects panel data'. *Journal of Multivariate Analysis* 133, pp. 1–26.

Galvão, A. B. and Owyang, M. T. (2022). 'Forecasting low-frequency macroeconomic events with high-frequency data'. *Journal of Applied Econometrics* 37 (7), pp. 1314–1333.

Gao, J., Liu, F., Peng, B. and Yan, Y. (2023). 'Binary response models for heterogeneous panel data with interactive fixed effects'. *Journal of Econometrics* 235 (2), pp. 1654–1679.

Garcia Alvarado, F. (2020). 'Detecting crisis vulnerability using yield spread interconnectedness'. *International Journal of Finance and Economics* 27 (4), pp. 3864–3880.

Garnitz, J., Lehmann, R. and Wohlrabe, K. (2019). 'Forecasting GDP all over the world using leading indicators based on comprehensive survey data'. *Applied Economics* 51 (54), pp. 5802–5816.

Garratt, A. and Petrella, I. (2022). 'Commodity prices and inflation risk'. *Journal of Applied Econometrics* 37 (2), pp. 392–414.

Gavin, W. T. and Theodorou, A. T. (2005). 'A common model approach to macroeconomics: Using panel data to reduce sampling error'. *Journal of Forecasting* 24 (3), pp. 203–219.

Gelos, G., Gornicka, L., Koepke, R., Sahay, R. and Sgherri, S. (2022). 'Capital flows at risk: Taming the ebbs and flows'. *Journal of International Economics* 134 (103555), pp. 1–23.

Ghosh, A. R., Ostry, J. D. and Qureshi, M. S. (2016). 'When do capital inflow surges end in tears?' *American Economic Review* 106 (5), pp. 581–585.

Ghysels, E. (2016). 'Macroeconomics and the reality of mixed frequency data'. *Journal of Econometrics* 193 (2), pp. 294–314.

— (2018). 'Mixed frequency models'. In: *Oxford Research Encyclopedia of Economics and Finances*.

Ghysels, E. and Qian, H. (2019). 'Estimating MIDAS regressions via OLS with polynomial parameter profiling'. *Econometrics and Statistics* 9, pp. 1–16.

Ghysels, E., Sinko, A. and Valkanov, R. (2007). 'MIDAS Regressions: Further Results and New Directions'. *Econometric Reviews* 26 (1), pp. 53–90.

Giannone, D., Reichlin, L. and Small, D. (2008). 'Nowcasting: The real-time informational content of macroeconomic data'. *Journal of Monetary Economics* 55 (4), pp. 665–676.

Greenaway-McGrevy, R. (2019). 'Asymptotically efficient model selection for panel data forecasting'. *Econometric Theory* 35 (4), pp. 842–899.

Gregory, K. B., Lahiri, S. N. and Nordman, D. J. (2018). 'A smooth block bootstrap for quantile regression with time series'. *The Annals of Statistics* 46 (3), pp. 1138–1166.

Hansen, B. E. (1996). 'Inference When a Nuisance Parameter Is Not Identified Under the Null Hypothesis'. *Econometrica* 64 (2), p. 413.

Hansen, P. and Timmermann, A. (2012). *Choice of sample split in out-of-sample forecast evaluation*. Economics Working Papers ECO2012/10. European University Institute. URL: https://cadmus.eui.eu/handle/1814/21454 [Last accessed: 29/07/2020].

Hantzsche, A., Lopresto, M. and Young, G. (2018). 'Using NiGEM in uncertain times: introduction and overview of NiGEM'. *National Institute Economic Review* 244 (1), R1–R14.

Harding, M. and Lamarche, C. (2014). 'Estimating and testing a quantile regression model with interactive effects'. *Journal of Econometrics* 178 (Part 1), pp. 101–113.

Harding, M., Lamarche, C. and Pesaran, H. M. (2020). 'Common correlated effects estimation of heterogeneous dynamic panel quantile regression models'. *Journal of Applied Econometrics* 35 (3), pp. 294–314.

Hultman, N. E., Clarke, L., Frisch, C., Kennedy, K., McJeon, H., Cyrs, T., Hansel, P., Bodnar, P., Manion, M., Edwards, M. R. et al. (2020). 'Fusing subnational with national climate action is central to decarbonization: the case of the United States'. *Nature Communications* 11 (1), pp. 1–10.

Hurn, A. S., Silvennoinen, A. and Teräsvirta, T. (2016). 'A Smooth Transition Logit Model of The Effects of Deregulation in the Electricity Market'. *Journal of Applied Econometrics* 31 (4), pp. 707–733.

Im, K. S., Pesaran, H. M. and Shin, Y. (2003). 'Testing for unit roots in heterogeneous panels'. *Journal of Econometrics* 115 (1), pp. 53–74.

IMF (2002). *Global financial stability report: market developments and issues*. March. International Monetary Fund.

— (2012). *World economic outlook: Coping with high debt and sluggish growth*. October. International Monetary Fund.

— (2013a). *World economic outlook: Hopes, realities, risks*. April. International Monetary Fund.

IMF (2013b). *World economic outlook: Transition and tensions*. October. International Monetary Fund.

— (2017). 'Financial conditions and Growth at Risk'. In: *Global Financial Stability Report: Is Growth at Risk?* October. International Monetary Fund. Chap. 1, pp. 91–118.

— (2020). 'Emerging and frontier markets'. In: *Global Financial Stability Report*. October. International Monetary Fund. Chap. 3, pp. 47–65.

— (2021). *World economic outlook: Recovery during a pandemic. Health concerns, supply disruptions, and price pressures*. October. International Monetary Fund.

Iseringhausen, M. (2023). 'A time-varying skewness model for Growth-at-Risk'. *International Journal of Forecasting*. In Press, Corrected Proof. URL: https://doi.org/10.1016/j.ijforecast.2023.02.006 [Last accessed: 11/08/2023].

Jo, S. and Sekkel, R. (2019). 'Macroeconomic uncertainty through the lens of professional forecasters'. *Journal of Business and Economic Statistics* 37 (3), pp. 436–446.

Jordà, Ò. (2005). 'Estimation and inference of impulse responses by local projections'. *American Economic Review* 95 (1), pp. 161–182.

Jordà, Ò., Schularick, M. and Taylor, A. M. (2013). 'When credit bites back'. *Journal of Money, Credit and Banking* 45 (s2), pp. 3–28.

— (2015). 'Leveraged bubbles'. *Journal of Monetary Economics* 76 (Supplement), S1–S20.

— (2016). 'The great mortgaging: housing finance, crises and business cycles'. *Economic Policy* 31 (85), pp. 107–152.

Kaminsky, G. L. (2019). *Boom-bust capital flow cycles*. Working Paper 25890. National Bureau of Economic Research. URL: https://www.nber.org/papers/w25890 [Last accessed: 03/07/2023].

Kapetanios, G. (2008). 'A bootstrap procedure for panel data sets with many cross-sectional units'. *Econometrics Journal* 11 (2), pp. 377–395.

Kapetanios, G., Serlenga, L. and Shin, Y. (2021). 'Estimation and inference for multi-dimensional heterogeneous panel datasets with hierarchical multi-factor error structure'. *Journal of Econometrics* 220 (2), pp. 504–531.

Khalaf, L., Kichian, M., Saunders, C. J. and Voia, M. (2021). 'Dynamic panels with MIDAS covariates: Nonlinearity, estimation and fit'. *Journal of Econometrics* 220 (2), pp. 589–605.

Kilian, L. (2009). 'Not all oil price shocks are alike: Disentangling demand and supply shocks in the crude oil market'. *American Economic Review* 99 (3), pp. 1053–1069.

Kilian, L. and Zhou, X. (2018). 'Modeling fluctuations in the global demand for commodities'. *Journal of International Money and Finance* 88, pp. 54–78.

Kindberg-Hanlon, G. and Sokol, A. (2018). 'Gauging the globe: the Bank's approach to nowcasting world GDP'. *Bank of England Quarterly Bulletin* 58 (3), pp. 21–30.

Knotek, E. S. and Zaman, S. (2017). 'Nowcasting US headline and core inflation'. *Journal of Money, Credit and Banking* 49 (5), pp. 931–968.

Koenker, R. (2004). 'Quantile regression for longitudinal data'. *Journal of Multivariate Analysis* 91 (1), pp. 74–89.

Koenker, R. and Bassett, G. (1978). 'Regression quantiles'. *Econometrica* 46 (1), pp. 33–50.

Koenker, R. and Machado, J. A. F. (1999). 'Goodness of fit and related inference processes for quantile regression'. *Journal of the American Statistical Association* 94 (448), pp. 1296–1310.

Koepke, R. (2019). 'What drives capital flows to emerging markets? A survey of the empirical literature'. *Journal of Economic Surveys* 33 (2), pp. 516–540.

Koepke, R. and Paetzold, S. (2022). 'Capital flow data – A guide for empirical analysis and real-time tracking'. *International Journal of Finance & Economics*, pp. 1–21.

Koop, G., McIntyre, S. and Mitchell, J. (2020). 'UK regional nowcasting using a mixed frequency vector auto-regressive model with entropic tilting'. *Journal of the Royal Statistical Society: Series A (Statistics in Society)* 183 (1), pp. 91–119.

Krishnamurthy, A. and Muir, T. (2017). *How Credit Cycles across a Financial Crisis*. Working Paper 23850. National Bureau of Economic Research. URL: https://www.nber.org/papers/w23850 [Last accessed: 04/07/2023].

Kuzin, V., Marcellino, M. and Schumacher, C. (2011). 'MIDAS vs. mixed-frequency VAR: Nowcasting GDP in the euro area'. *International Journal of Forecasting* 27 (2), pp. 529–542.

Lamarche, C. (2010). 'Robust penalized quantile regression estimation for panel data'. *Journal of Econometrics* 157 (2), pp. 396–408.

Larson, W. D. and Sinclair, T. M. (2022). 'Nowcasting unemployment insurance claims in the time of COVID-19'. *International Journal of Forecasting* 38 (2), pp. 635–647.

Lee, Y. and Phillips, P. C. (2015). 'Model selection in the presence of incidental parameters'. *Journal of Econometrics* 188 (2), pp. 474–489.

Levin, A., Lin, C.-F. and Chu, C.-S. J. (2002). 'Unit root tests in panel data: asymptotic and finite-sample properties'. *Journal of Econometrics* 108 (1), pp. 1–24.

Liu, W. and Moench, E. (2016). 'What predicts US recessions?' *International Journal of Forecasting* 32 (4), pp. 1138–1150.

Lloyd, S., Manuel, E. and Panchev, K. (2023). 'Foreign Vulnerabilities, Domestic Risks: The Global Drivers of GDP-at-Risk'. *IMF Economic Review*.

Manzan, S. (2015). 'Forecasting the distribution of economic variables in a data-Rich environment'. *Journal of Business & Economic Statistics* 33 (1), pp. 144–164.

Marcellino, M., Porqueddu, M. and Venditti, F. (2016). 'Short-term GDP forecasting with a mixed-frequency dynamic factor model with stochastic volatility'. *Journal of Business and Economic Statistics* 34 (1), pp. 118–127.

Marcellino, M. and Schumacher, C. (2010). 'Factor MIDAS for nowcasting and forecasting with ragged-edge data: A model comparison for German GDP'. *Oxford Bulletin of Economics and Statistics* 72 (4), pp. 518–550.

Martin, F. E., O'Neill, C., Sokol, A. and Berge, L. von dem (2020). *Capital flows-at-risk: Push, pull and the role of policy*. Staff Working Papers 881. Bank of England. URL:

https://www.bankofengland.co.uk/working-paper/2020/capital-flows-at-risk-push-pull-and-the-role-of-policy [Last accessed: 04/07/2023].

Mason, S. J. and Graham, N. E. (2002). 'Areas beneath the relative operating characteristics (ROC) and relative operating levels (ROL) curves: Statistical significance and interpretation'. *Quarterly Journal of the Royal Meteorological Society* 128 (584 Part B), pp. 2145–2166.

McCracken, M. W., McGillicuddy, J. T. and Owyang, M. T. (2022). 'Binary conditional forecasts'. *Journal of Business and Economic Statistics* 40 (3), pp. 1246–1258.

Modugno, M. (2011). *Nowcasting inflation using high frequency data*. Working Paper Series 1324. European Central Bank. URL: https://www.ecb.europa.eu/pub/pdf/scpwps/ecbwp1324.pdf [Last accessed: 03/07/2023].

— (2013). 'Now-casting inflation using high frequency data'. *International Journal of Forecasting* 29 (4), pp. 664–675.

Murphy, A. H. (1988). 'Skill scores Based on the mean square error and their relationships to the correlation coefficient'. *Monthly Weather Review* 116 (12), pp. 2417–2424.

Nordhaus, W. D. (1992). 'An optimal transition path for controlling greenhouse gases'. *Science* 258 (5086), pp. 1315–1319.

OECD (2020). *OECD share in world GDP stable at around 50% in PPP terms in 2017*. URL: https://www.oecd.org/sdd/prices-ppp/oecd-share-in-world-gdp-stable-at-around-50-per-cent-in-ppp-terms-in-2017.htm [Last accessed: 04/07/2023].

Patton, A. J., Ziegel, J. F. and Chen, R. (2019). 'Dynamic semiparametric models for expected shortfall (and Value-at-Risk)'. *Journal of Econometrics* 211 (2), pp. 388–413.

Pesaran, H. M. (2006). 'Estimation and inference in large heterogeneous panels with a multifactor error structure'. *Econometrica* 74 (4), pp. 967–1012.

— (2016). *Time series and panel data econometrics*. Oxford University Press.

Pesaran, H. M. and Chudik, A. (2014). 'Aggregation in large dynamic panels'. *Journal of Econometrics* 178 (Part 2), pp. 273–285.

Peterson, W., Birdsall, T. and Fox, W. (1954). 'The theory of signal detectability'. *Transactions of the IRE Professional Group on Information Theory* 4 (4), pp. 171–212.

Plagborg-Moller, M., Reichlin, L., Ricco, G. and Hasenzagl, T. (2020). 'When is Growth at risk?' *Brookings Papers on Economic Activity* (Spring), pp. 167–229.

Prasad, A., Elekdag, S., Jeasakul, P., Lafarguette, R., Alter, A., Xiaochen Feng, A. and Wang, C. (2019). *Growth at risk: Concept and application in IMF country surveillance*. Working Papers 19/36. International Monetary Fund. URL: https://www.imf.org/en/Publications/WP/Issues/2019/02/21/Growth-at-Risk-Concept-and-Application-in-IMF-Country-Surveillance-46567 [Last accessed: 03/07/2023].

Reichlin, L., Ricco, G. and Hasenzagl, T. (2020). *Financial variables as predictors of real growth vulnerability*. Discussion Paper 05/2020. Deutsche Bundesbank. URL: https://www.bundesbank.de/en/publications/research/discussion-papers/financial-variables-as-predictors-of-real-growth-vulnerability-827682 [Last accessed: 04/07/2023].

Rennert, K., Prest, B. C., Pizer, W. A., Newell, R. G., Anthoff, D., Kingdon, C., Rennels, L., Cooke, R., Raftery, A. E. and Ševčiková, H. (2021). 'The social cost of carbon: Advances in long-term probabilistic projections of population, GDP, emissions, and discount rates'. *Brookings Papers on Economic Activity* (2) (Fall), pp. 223–275.

Robin, X., Turck, N., Hainard, A., Tiberti, N., Lisacek, F., Sanchez, J.-C. and Müller, M. (2011). 'pROC: an open-source package for R and S+ to analyze and compare ROC curves'. *BMC Bioinformatics* 12, p. 77.

Rudebusch, G. D. and Williams, J. C. (2009). 'Forecasting recessions: The puzzle of the enduring power of the yield curve'. *Journal of Business and Economic Statistics* 27 (4), pp. 492–503.

Scheubel, B., Stracca, L. and Tille, C. (2019). 'Taming the global financial cycle: What role for the global financial safety net?' *Journal of International Money and Finance* 94, pp. 160–182.

Schorfheide, F. and Song, D. (2015). 'Real-time forecasting with a mixed-frequency VAR'. *Journal of Business and Economic Statistics* 33 (3), pp. 366–380.

Schularick, M. and Taylor, A. M. (2012). 'Credit Booms Gone Bust: Monetary Policy, Leverage Cycles, and Financial Crises, 1870–2008'. *American Economic Review* 102 (2), pp. 1029–1061.

Schumacher, C. (2010). 'Factor forecasting using international targeted predictors: The case of German GDP'. *Economics Letters* 107 (2), pp. 95–98.

— (2016). 'A comparison of MIDAS and bridge equations'. *International Journal of Forecasting* 32 (2), pp. 257–270.

Siliverstovs, B. (2017). 'Short-term forecasting with mixed-frequency data: a MIDASSO approach'. *Applied Economics* 49 (13), pp. 1326–1343.

Stock, J. H. and Watson, M. W. (2002). 'Forecasting using principal components from a large number of predictors'. *Journal of the American Statistical Association* 97 (460), pp. 1167–1179.

Teräsvirta, T., Tjøstheim, D. and Granger, W. J. (2010). 'Testing linearity against parametric alternatives'. In: *Modelling Nonlinear Economic Time Series*. Oxford University Press. Chap. 5, pp. 65–91.

Wang, W., Zhang, X. and Paap, R. (2019). 'To pool or not to pool: What is a good strategy for parameter estimation and forecasting in panel regressions?' *Journal of Applied Econometrics* 34 (5), pp. 724–745.

West, K. D. (1996). 'Asymptotic inference about predictive ability'. *Econometrica* 64 (5), pp. 1067–1084.

Wilks, D. (2010). 'Sampling distributions of the Brier score and Brier skill score under serial dependence'. *Quarterly journal of the Royal Meteorological Society* 136 (653), pp. 2109–2118.

Wilks, D. S. (2019). 'Forecast Verification'. In: *Statistical Methods in the Atmospheric Sciences (Fourth Edition)*. Ed. by D. S. Wilks. Fourth Edition. Elsevier. Chap. 9, pp. 369–483.

WMO (2017). *Guidelines for Nowcasting Techniques*. Technical Report 1198. World Metereological Organization. URL: https://public.wmo.int/en/resources/bulletin/nowcasting-guidelines-%E2%80%93-summary#:~:text=Keith%20Browning%20first%20defined%20nowcasting,local%20detail,%20by%20any%20method, [Last accessed: 15/05/2023].

Xu, Q., Zhuo, X., Jiang, C., Liu, X. and Liu, Y. (2018). 'Group penalized unrestricted mixed data sampling model with application to forecasting US GDP growth'. *Economic Modelling* 75, pp. 221–236.

Index

CO_2 Carbon Dioxide.

AE Advanced Economy.

AR Autoregressive.

ARX Autoregressive with an exogenous regressor.

AUROC Area Under Receiver Operating Characteristic Curve.

BCBS Basel Committee of Banking Supervision.

BEA Bureau of Economic Analysis.

BM Benchmark.

BoP Balance of Payments.

BS Brier Score.

BSM Business Survey Manufacturing.

BSS Business Survey Services.

CBOE Chicago Board Options Exchange.

CCE Common Correlated Effects.

cdf cumulative density function.

CG Credit to GDP Gap.

CI Confidence Interval.

COP Conference of Parties.

CR Credit to GDP Growth.

CSD Cross-sectional Dependence.

DFM Dynamic Factor Model.

DICE Dynamic Integrated Climate-Economy model.

DQ Dynamic Quantile.

EC Energy Consumption.

EIA Energy Information Administration.

EME Emerging Market Economy.

EPFR Emerging Portfolio Fund Research.

EPU Economic and Polictical Uncertainty.

ES Expected Shortfall.

GaR Growth-at-Risk.

GDP Gross Domestic Product.

GFC Global Financial Crisis.

GVAR Global Vector Autoregression.

HICP Harmonised Index of Consumer Prices.

HP House Prices.

i.i.d. independently and indentically distributed.

IIF Institute of International Finance.

IMF International Monetary Fund.

IP Industrial Production.

KS Kuiper's Score.

LASSO Least Absolute Shrinkage and Selection Operator.

LCCE Lagged Common Correlated Effects.

LHS left-hand side.

MEI Main Economic Indicators.

MF-PVAR Mixed-Frequency Panel Vector Autoregression.

MFVAR Vector Autoregression.

MIDAS Mixed Data Sampling.

m-o-m month-on-month.

NFCI National Financial Conditions Index.

OECD Organisation of Economic Cooperation and Development.

OLS Ordinary Least Squares.

pdf probability density function.

PI Personal Income.

PMIDAS Panel Mixed Data Sampling.

q-o-q quarter-on-quarter.

RGGI Regional Greenhouse Gas Initiative.

RHS right-hand side.

RMSFE Root Mean Square Forecast Error.

ROC Receiver Operating Characteristic Curve.

SEDS State Energy Data System.

TL Tick-Loss.

TMT telecom-media-technology.

TS Term Spread.

UMIDAS Unrestricted Mixed Data Sampling.

VAR Vector Autoregression.

VIX CBOE Volatility Index.

WOB Weekly Oil Bulletin.

WTI West Texas Intermediate.

WUI World Uncertainty Index.

y-o-y year-on-year.